



THE HONG KONG
POLYTECHNIC UNIVERSITY

香港理工大學

Pao Yue-kong Library

包玉剛圖書館

Copyright Undertaking

This thesis is protected by copyright, with all rights reserved.

By reading and using the thesis, the reader understands and agrees to the following terms:

1. The reader will abide by the rules and legal ordinances governing copyright regarding the use of the thesis.
2. The reader will use the thesis for the purpose of research or private study only and not for distribution or further reproduction or any other purpose.
3. The reader agrees to indemnify and hold the University harmless from and against any loss, damage, cost, liability or expenses arising from copyright infringement or unauthorized usage.

If you have reasons to believe that any materials in this thesis are deemed not suitable to be distributed in this form, or a copyright owner having difficulty with the material being included in our database, please contact lbsys@polyu.edu.hk providing details. The Library will look into your claim and consider taking remedial action upon receipt of the written requests.

The Hong Kong Polytechnic University

School of Optometry

*A new approach to early glaucomatous diagnosis
by multifocal electroretinogram:
Luminance-modulation of the global flash
stimulation paradigm*

Patrick Ho-Wai Chu

**A thesis submitted in partial fulfillment of the
requirements for the Degree of Doctor of Philosophy**

September 2008

CERTIFICATE OF ORIGINALITY

I hereby declare that this thesis is my own work and that, to the best of my knowledge and belief, it reproduces no material previously published or written, nor material that has been accepted for the award of any other degree or diploma, except where due acknowledgement has been made in the text.

_____ (Signed)

Patrick Ho-Wai Chu

(Name of student)

ABSTRACT

Early recognition and accurate assessment of glaucomatous functional loss is a major goal for clinicians and researchers. Ganglion cells lost due to glaucomatous damage cannot be regenerated, but early and appropriate treatment is effective for preventing further retinal ganglion cell death. Early detection is essential to prevent the progression of glaucomatous damage, thus a more sensitive diagnostic technique is very important for early treatment.

Electrophysiological tests are objective tools for measuring the functional responses of the visual system. The multifocal electroretinogram (mfERG) has been developed to study and diagnose diseases of the human retina. Using this advanced technique, localized retinal damage can be detected; however, currently unresolved problems with the mfERG are the extent to which the inner retina contributes to the response and how to create an appropriate technique for measuring this contribution. By improving the sensitivity of the mfERG measurement, the functional changes of the inner retina due to glaucomatous damage can be detected in an earlier stage, hopefully before nerve fiber loss. In an attempt to improve the efficacy of the mfERG in detecting inner retinal activity, a modification of a stimulus protocol previously employed by Fortune and his colleagues (Fortune et al., 2002a) was used in this study; the new mfERG protocol allowed early detection of glaucoma.

Objectives

1. To investigate the variation of retinal functions in glaucoma by using a global flash mfERG stimulation with different stimulus contrast levels of the multifocal flashes, in an attempt to maximise inner retinal contributions.
2. To use the global flash mfERG stimulation in subjects with unilateral glaucoma to determine whether retinal function is affected in fellow eyes without glaucomatous visual field defects.
3. To investigate the association of the luminance-modulation global flash mfERG and other retinal assessments for subsets of subjects at high risk of developing glaucomatous damage.
4. To use global flash mfERG stimulation and a pharmacologic dissection method in an animal eye model to help understand the basis of damage produced in glaucoma.

Methods

In experiment 1, the global flash mfERG was assessed with a new stimulation paradigm in steps of four video frames, which consisted of 103 hexagonal elements followed by a dark frame, global flash, and dark frame. The localized luminance-difference was set at 96%, 65%, 49% or 29% stimulus contrast as different

luminance-modulation levels. Thirty subjects with glaucoma and 30 age-matched normal subjects were recruited for visual field and mfERG measurements.

In experiment 2, 40 normal subjects and 12 subjects with unilateral glaucoma were recruited for visual field and mfERG measurement. The mfERG was assessed by using a global flash stimulation paradigm with luminance-modulation as in experiment 1.

In experiment 3, 42 subjects (75 eyes) with unilateral glaucoma, ocular hypertension (OHT), family history of glaucoma and large optic disc cupping were examined in this three-year study of visual field, optical coherence tomography (OCT) and global flash mfERG measurements with luminance-modulation. Four complete ophthalmic examinations were scheduled, one every 12 months.

In experiment 4, global flash mfERG responses using the 4-frame luminance-modulation paradigm were recorded from 14 eyes of 10 six-week-old Yorkshire pigs in control conditions and after suppression of inner retinal responses with inhalation of isoflurane (ISO), and injections of tetrodotoxin (TTX) and N-methyl-D-aspartic acid (NMDA). ON- and OFF-pathway responses were isolated by injection of 2-amino-4-phosphonobutyric acid (APB) and cis-2,3-piperidinedicarboxylic acid (PDA).

Results

The global flash stimulation paradigm induces complex local first-order responses with an early direct component (DC) and a later induced component (IC). The luminance-modulated response functions of the DC and IC responses showed markedly different behavior. The peripheral IC showed a linear dependence on luminance-difference, whereas the peripheral DC was saturated at higher levels of luminance-difference. This saturation became less obvious in glaucoma subjects mostly because of greater reduction of the response amplitude in the mid luminance-difference level. An “adaptive index” was calculated from the luminance-difference dependence of the peripheral DC, and it showed good sensitivity (93%) and specificity (95%) for differentiating normal from glaucomatous eyes, and also had a good correlation ($r = 0.58$) with the glaucomatous visual field defect. Furthermore, in better (fellow) eyes with normal visual fields of unilateral glaucoma subjects, the amplitude of the IC was significantly reduced, and the adaptive index was also reduced by a factor of almost 10 ($p < 0.0001$). The adaptive index in the fellow eyes was similar to the index in the glaucoma eyes and they did not show a statistically significant difference.

In the longitudinal experiment, there was significant thinning of the retinal nerve fiber layer (RNFL) thickness ($p < 0.05$) over the course of the study for the fellow

eyes with unilateral glaucoma or the eyes with OHT which initially had an abnormal adaptive index; such eyes showed a thinning rate of -3.02 and -3.54 $\mu\text{m}/\text{year}$ respectively. However, thinning was not found in eyes which initially had a normal adaptive index.

The pig eye was chosen as the animal model and the porcine global flash mfERG also consisted of an early DC and a late IC. ISO and TTX removed inner retinal contributions to the IC; NMDA application further abolished the oscillatory wavelets in the DC and removed the residual IC waveform. The inner retina contributed regular oscillating wavelets (W1, W2 and W3) to the DC and shaped the IC. After removing the inner retinal contributions, the porcine global flash mfERG waveform becomes comparable to that obtained with conventional mfERG stimulation. The remaining waveform (smoothed DC) was mainly formed by contributions of the ON- and OFF-bipolar cells, as revealed after APB or PDA injection. Photoreceptors contributed a small signal to the leading edge of N1. The luminance-modulated response function of the DC was shown to be contributed by the inner retinal oscillation wavelets.

Conclusions

The peripheral DC luminance-modulated response function is altered by the

adaptive mechanism that is induced by the global flash; the reduction of the adaptive index may thus relate to an abnormal adaptive mechanism, presumably due to inner retinal damage. Glaucoma appears to cause a large reduction of the adaptive index which correlates with field defects. In addition, the significant reduction of the adaptive index in the fellow eyes in subjects with unilateral glaucoma shows impaired adaptive mechanism(s) in these eyes. This implies that although eyes with high risk factors may have functionally normal visual acuity (VA) and visual fields, they are likely to have abnormal adaptive mechanisms. Furthermore, the adaptive index calculated from the measurement of luminance-modulated global flash mfERG may be useful for predicting glaucomatous progression, especially in subjects with high risk factors. The abnormal adaptive index follows from change in fast-adaptive mechanisms and may indicate the risk of developing glaucoma.

The DC of the porcine global flash mfERG was shown to be composed mainly of contributions from photoreceptors, and ON- and OFF-bipolar cells, where inner retinal activity partially shapes the DC with superimposed regular oscillations. In addition, the IC is dominated by inner retinal activity. The luminance-modulated response function of the DC consisted of both outer retinal response and oscillation wavelets of the inner retinal response. IC and DC responses show different characteristics under various luminance-modulation levels, where the changes of W2

(second oscillating wavelet) of the inner retinal response seem independent of luminance-modulation, but the outer retinal response seems to depend on luminance-modulation. The DC luminance-modulated response feature depends mainly on the relative contribution of inner retinal activities; the impairment of inner retinal activity may alter the DC luminance-modulated response function, making it tend toward linearity. This may explain why glaucoma patients show loss of independence of the luminance-modulated response function under luminance-modulation in global flash mfERG responses.

PUBLICATIONS ARISING FROM THE THESIS

- 1) Chu, P.H., Chan, H.H., and Brown, B. (2006). Glaucoma detection is facilitated by luminance modulation of the global flash multifocal electroretinogram. *Invest Ophthalmol Vis Sci*, 47 (3), 929-37.
- 2) Chu, P.H., Chan, H.H., and Leat, S.J. (2006). Effects of unsteady fixation on multifocal electroretinogram (mfERG). *Graefes Arch Clin Exp Ophthalmol*, 244 (10), 1273-82.
- 3) Chu, P.H., Chan, H.H., and Brown, B. (2007). Luminance-modulated adaptation of global flash mfERG: fellow eye losses in asymmetric glaucoma. *Invest Ophthalmol Vis Sci*, 48 (6), 2626-33.
- 4) Chu, P.H., Chan, H.H., Ng, Y.F., Brown, B., Siu, A.W., Beale, B.A., Gilger, B.C., and Wong, F. (2008). Porcine global flash multifocal electroretinogram: possible mechanisms for the glaucomatous changes in contrast response function. *Vision Res*, 48 (16), 1726-34.

Conference Presentation

- 1) Chu, H.W. and Chan, H.L. (2003). New approach in detecting the inner retinal activity by mfERG. Presented at the 41st International Society for Clinical Electrophysiology of Vision Symposium, Nagoya, Japan.
- 2) Chu, H.W., Chan, H.L. and Brown, B. (2004). New protocol in evaluation of the inner retinal activity in glaucoma by multifocal ERG. Presented at the 8th International meeting of American Academy of Optometry, Global-Pacific Rim, Honolulu, Hawaii.
- 3) Chu, H.W., Chan, H.L. and Brown, B. (2005). Luminance-modulated adaptive characteristics of global flash multifocal electroretinogram (mfERG) paradigm. Presented at the 43rd International Society for Clinical Electrophysiology of Vision Symposium, Glasgow, UK.
- 4) Chu, H.W., Chan, H.L. and Brown, B. (2006). Changes of luminance-modulated adaptive characteristic of global flash mfERG stimulation in unilateral glaucoma. Presented at the 44th International Society for Clinical Electrophysiology of Vision Symposium, Fontveraud, France.
- 5) Chan, H.L., Chu, P.H.W., Ng, Y.F., Siu, A.W., Beale, B.A., Gilger, B.C. and Wong, F. (2007). Cellular contributions of the global flash multifocal ERG. Presented at the 16th Asia-Pacific Optometric Congress, Asia-Pacific Council of Optometry, Goa, India.

ACKNOWLEDGEMENTS

I would like to take this opportunity to express my most sincere thanks to all people who contributed in one way or another to the completion of this work. With reverence and humbleness, I first and foremost thank God for his many blessings and guide in the writing of this thesis. Without him, I would not have had the wisdom or the physical ability to do so.

I am greatly in debt to my chief supervisor, Dr. Henry Chan who's outstanding knowledge and interest in issues related to electrophysiology enabled him to give me the professional guidance and also provided me with much needed motivation and numerous novel research ideas. I was privileged to under the supervision with him, and he has also guided me through the whole writing process with great patience and provided helpful advices necessary to complete my thesis.

I am also grateful to my co-supervisor, Prof. Brian Brown, for devoting much time for reviewing my manuscripts over and over again and gave me many helpful suggestions on my research studies. I am particularly indebted to Prof. Fulton Wong who provided me with insights and advices about the animal study, and I would also like to thank Prof. Brian Gilger and Dr. Brady Beale for helping me in many technique issues

throughout the animal study. I am especially like to thank Mr. Brian Choi for his valuable advice on the statistical analysis, and my thanks also go to all my superb colleagues in our research term for their friendship and support.

Finally, I have to thank my family especially my wife who provides me with unconditional emotional support and continuous caring.

TABLE OF CONTENTS

CERTIFICATE OF ORIGINALITY.....	I
ABSTRACT.....	II
PUBLICATIONS ARISING FROM THE THESIS.....	IX
ACKNOWLEDGEMENTS.....	X
TABLE OF CONTENTS.....	XII
LIST OF FIGURES, TABLES AND ABBREVIATIONS.....	XV
PART I – INTRODUCTION & LITERATURE REVIEW.....	1
Chapter 1 – Introduction.....	2
Chapter 2 - What is Glaucoma?.....	7
2.1 Prevalence of glaucoma.....	7
2.2 Primary open-angle glaucoma.....	9
2.2.1 Risk factors for primary open-angle glaucoma.....	10
2.2.2 Pathogenesis of primary open-angle glaucoma.....	11
2.2.2.1 Mechanical theory.....	12
2.2.2.2 Vascular theory.....	13
2.2.2.3 Apoptosis.....	15
Chapter 3 - Retinal Ganglion Cell Loss in Glaucoma.....	17
3.1 Retinal ganglion cell topography.....	17
3.2 Major types of retinal ganglion cell.....	18
3.3 Selective loss of ganglion cell in glaucoma.....	19
Chapter 4 - Diagnosis of Glaucoma.....	21
4.1 Cost-effectiveness of early detection.....	21
4.2 Intraocular pressure.....	24
4.3 Optic disc appearance.....	24
4.4 Nerve fiber layer thickness.....	25
4.5 Automated perimetry.....	28
4.5.1 Visual field defect in glaucoma.....	28
4.5.2 Sensitivity of automated perimetry.....	29
4.6 Other psychophysical tests.....	30
4.6.1 Tests target on M-pathway.....	31
4.6.2 Tests target on P/K-pathway.....	32
4.6.3 Comparison of the new tests.....	33
Chapter 5 - Electrophysiological Tools for Diagnosing Glaucoma.....	35
5.1 Electrophysiological examination.....	36
5.2 Possible electrophysiological techniques for early diagnosis of glaucoma.....	37
5.3 Current electrophysiological technique for early diagnosis of glaucoma.....	42
Chapter 6 - Multifocal Electroretinogram (mfERG).....	43
6.1 Basic technique of mfERG recording.....	43
6.2 Multifocal binary kernels.....	46
6.3 Differences between mfERG and full-field flash ERG.....	48
6.4 Origins of the human mfERG.....	49
6.5 Characteristics of mfERG in normal subjects.....	51
6.6 Clinical application of mfERG.....	52
6.7 The mfERG responses in glaucoma patients.....	54
6.8 Inner retinal contribution in mfERG.....	56
6.8.1 Evidence of inner retinal contribution in non-human primate mfERG.....	57
6.8.2 Evidence of inner retinal contribution in human mfERG.....	58
6.8.2.1 The optic nerve head component.....	59
6.8.2.2 The low contrast mfERG.....	61

6.8.2.3	The slow-sequence mfERG.....	62
6.8.2.4	The global flash mfERG.....	64
6.8.2.5	Future approaches.....	69

PART II – EXPERIMENTS

Chapter 7 - Experiment I - Glaucoma Detection Is Facilitated by Luminance-Modulation of the Global flash mfERG.....	71
Abstract.....	72
Introduction.....	74
Methods.....	78
Subjects.....	78
Stimulus conditions.....	79
Recording conditions.....	82
Data analysis.....	83
Results.....	84
Responses from six concentric rings.....	84
Summed peripheral responses.....	87
Peripheral quadrant responses.....	90
Discussion.....	97
Chapter 8 - Experiment II - Luminance-Modulated Adaptation of Global Flash mfERG: Fellow Eye Losses in Unilateral Glaucoma.....	103
Abstract.....	104
Introduction.....	106
Methods.....	109
Subjects.....	109
Stimulus conditions.....	112
Recording conditions.....	112
Data analysis.....	113
Results.....	114
Discussion.....	127
Chapter 9 - Experiment III - Luminance-Modulated Adaptation of Global Flash mfERG: A potential indicator of early changes in high risk glaucoma patients.....	133
Abstract.....	134
Introduction.....	136
Methods.....	140
Subjects.....	140
Stimulus and recording conditions.....	143
Follow up visits.....	144
Subject consent.....	145
Data analysis.....	145
Results.....	149
Discussion.....	158
Chapter 10 - Experiment IV - Porcine Global Flash mfERG: Possible Mechanisms for the Glaucomatous Changes in Luminance-Modulated Response Function.....	164
Abstract.....	165
Introduction.....	167
Methods.....	171
Animals.....	171
Stimulus conditions.....	172
Recording conditions.....	173
Intravitreal injections.....	175
Data analysis.....	177
Results.....	178
Control recordings.....	178
Effects of ISO, TTX and NMDA.....	178
Effects of PDA and APB.....	183
Effect of luminance-modulation.....	186
Discussion.....	191
Contributions from the inner retina.....	192

Contributions from the outer retina.....	195
Luminance-modulated response function.....	197
Chapter 11 - Conclusions and Suggestions for Future Research.....	200
11.1 Possible glaucoma retinal mechanism(s).....	210
11.2 Suggestions for future research.....	214
PART III – APPENDIX	
Chapter 12 – Appendix I - Effects of Unsteady Fixation on the mfERG.....	218
Abstract.....	219
Introduction.....	221
Methods.....	223
Subjects.....	223
Stimulus conditions.....	223
Recording conditions.....	224
Data analysis.....	226
Results.....	228
Responses from six concentric rings.....	228
Localized responses from the ring-2 hexagons.....	232
Depth of depression at the blind spot region.....	235
Discussion.....	238
REFERENCES.....	244

LIST OF FIGURES, TABLES AND ABBREVIATIONS

List of Figures

- Figure 6.1** Stimulus pattern with 103 scaled hexagons.
- Figure 6.2** Schematic explanation for the signal derivation of **(a)** the first-order kernel, and **(b)** the first slice of second-order kernels of the mfERG (Adopted from figures in (Sutter and Bearnse, 1999)).
- Figure 6.3** The proposed model of human mfERG based on the pharmacological dissection results from the monkey's mfERG response. (Adapted from figure in (Hood et al., 2002)).
- Figure 6.4** Left column of traces: The RC extracted from the first-order waveforms of the second ring. Right column of traces: The ONHC extracted from the first order waveforms of the second ring. (Adopted from figure in (Sutter and Bearnse, 1999)).
- Figure 6.5** Schematic comparison for the signal derivation of **(a)** the first slice of second-order kernels of the conventional mfERG and **(b)** the first-order kernels of the global flash mfERG (Adapted from figures in (Sutter and Bearnse, 1999)).
- Figure 7.1** **(a)** The stimulus sequence (one element of the m-sequence) contains four frames. The initial frame (multifocal flashes) alternates between light and dark according to a pseudorandom binary m-sequence with a preset contrast level. After each initial frame of the four-frame set, a global flash ($2.16 \text{ cd}\cdot\text{s}/\text{m}^2$; frame 3) was applied, separated by a pre- and post-dark frame ($0.04 \text{ cd}\cdot\text{s}/\text{m}^2$; frames 2 and 4). As the number of flashing elements in frame 1 involved half of the total number of hexagons, the average luminance in the global flash (frame 3) is twice as bright as frame 1. **(b)** The luminance-difference between the brighter luminance hexagons and the dimmer luminance hexagons ($L_{\max} - L_{\min}$) of the multifocal flashes in four stimulus contrast settings are denoted 2.12, 1.42, 1.08, and $0.62 \text{ cd}\cdot\text{s}/\text{m}^2$.
- Figure 7.2** **(a)** An example of the averaged concentric ring responses from a $2.12 \text{ cd}\cdot\text{s}/\text{m}^2$ luminance-difference stimulation using the global flash

stimulus paradigm from one typical subject. Ring 1 is the macular response; where ring 6 is the most peripheral averaged response. All the averaged ring responses contain two components: DC and IC. P1 to P4 represent four major peaks obtained in the responses from the central and peripheral regions. Measurement of the peak-to-peak amplitudes of the two components is illustrated, where P1 and P3 are the peaks that were used for the analyses of DC and IC, respectively. **(b)** Localized responses of 103 traces are also demonstrated.

Figure 7.3 The luminance-modulated response functions of the DC and the IC from different ring analyses are illustrated. Ring 1 is the macular response and ring 6 is the most peripheral averaged response. Lines: second-order best-fitting curves. Error bars, ± 1 SD.

Figure 7.4 The modified luminance-modulated response function (with four points instead of six points, with selection guided by the results from experiment 1a) of the peripheral grouped **(a)** DC and **(b)** IC responses (ring 4 to ring 6) from normal subjects and those with glaucoma. Lines: second-order best-fitting curves. Error bars, ± 1 SD.

Figure 7.5 **(a)** The peripheral mfERG response amplitudes were averaged into four spatial quadrants in corresponding visual field quadrants. The central 10° region was omitted. The response amplitudes of **(b)** DC and **(c)** IC are plotted against the visual field MD according to the visual field quadrants. The box plots at the right of each graph show normal values: middle line, the mean; top and bottom box edges, one SD; top and bottom bars, the range; solid lines, the best-fit line of the points showing the relationship between the mfERG amplitude and the visual field MD. (*) Correlation coefficients are statistically significance, but both are negative and of little clinical significance.

Figure 7.6 **(a)** Shaded area: the adaptive index of the DC response. It is calculated as the difference between the area under the curve (plotted using the second-order best-fit curve of the responses) and the area under the line (plotted joining the two values at the points at 2.12 and 0.62 $\text{cd}\cdot\text{s}/\text{m}^2$ luminance-difference). **(b)** The adaptive indices from all quadrants plotted against the visual field MD in corresponding visual field quadrants. Box plot at the right: normal values; solid line: the

best-fit line of the points showing a statistically significant correlation ($r = 0.58$) between the adaptive index and the visual field MD and this correlation is also clinically significant; dotted line: the cutoff value of the adaptive index based on the ROC curve in Figure 7.7 (adaptive index = 1.5).

Figure 7.7 ROC plot derived from different cutoffs of the adaptive index. The adaptive index cutoff of 1.5 provides the best differentiation between the normal and glaucoma groups, and gives a sensitivity of 93% with specificity of 95%.

Figure 8.1 Typical grouped responses from three normal (A-C) and three subjects with unilateral glaucoma (D-F) for the 2.12 cd·s/m² luminance-difference of the multifocal flashes.

Figure 8.2 The luminance-modulated response function of the peripheral grouped DC responses (rings 4 - 7) from the normal eyes of the control subjects and the affected and fellow eyes of the subjects with glaucoma. Lines represent the second-order, best fitting curves. Error bars, ± 1 SD.

Figure 8.3 Statistical results of the adaptive index from the three groups shown as box plots. There was a statistically significant reduction (*) of the adaptive index in both the affected and fellow eyes of the subjects with glaucoma when compared with the control group ($p < 0.05$). Dotted line: best cutoff point of the adaptive index (1.5) for glaucoma differentiation; middle line: the mean; top and bottom box edges: ± 1 SD; top and bottom bars: the range. (♦) The individual values from fellow and affected eyes of subjects with unilateral glaucoma.

Figure 8.4 The adaptive indices from all quadrants from fellow (upper panel) and affected (lower panel) eyes of the subjects with unilateral glaucoma plotted against visual field MD values in corresponding visual field quadrants. Vertical dotted lines: mean MD for each group. Solid line: the best-fitting line of the points showing a statistically significant correlation ($r = 0.37$ and $r = 0.44$) between adaptive index and visual field MD of fellow eyes (top) and affected eyes (bottom).

Figure 8.5 The IC response amplitude elicited for the 2.12 cd·s/m²

luminance-difference of the multifocal flashes. **Top:** Central IC in the control group and the fellow eyes of subjects with glaucoma. No statistically significant difference was found. **Bottom:** Peripheral IC in the control group and the fellow eyes of subjects with glaucoma. There was a statistically significant reduction (*) in the peripheral IC amplitude in the fellow eyes when compared with the control group ($p < 0.05$). The box plot indications are as in Figure 8.4. (♦) Individual values from fellow eye; the mean and ± 1 SD are shown.

Figure 8.6 Statistical results of the DC slope grouped in central and peripheral region from the three groups (Control, Fellow eye, Glaucomatous eye). The DC slope is calculated as the slope of the DC response amplitude at the two lowest luminance-difference levels. Black diamonds: individual values from fellow eyes; Grey diamonds: individual values from glaucomatous eyes. The box plot is as described in [Figure 8.3](#). (*) represents statistically significant differences compared with the appropriate control group.

Figure 8.7 ROC plot derived from different cutoff values of the peripheral DC slope (**top**). The peripheral slope cutoff of 4.7 provides the best differentiation between the normal and glaucoma groups and gives a sensitivity of 75% with specificity of 80%. The ROC plot of the adaptive index (**bottom**) shows that the cutoff of 1.5 provides the best differentiation between the normal and glaucoma groups and gives a sensitivity of 82% with specificity of 91%.

Figure 9.1 (a) The global flash mfERG responses from the four peripheral rings were grouped as the peripheral responses, which were further averaged into visual field quadrants shown for analysis. (b) The peripheral global flash mfERG responses were divided into superior and inferior field for comparison with the corresponding optic nerve head sectors from the OCT assessment.

Figure 9.2 The adaptive index for different high risk groups in the first visit. Dotted line: best cutoff point of the adaptive index (1.5) for glaucoma differentiation; middle line: the mean; top and bottom box edges: ± 1 SD. (♦) The individual values from subjects with different high risk groups.

- Figure 9.3** The variations of adaptive index with the grouped initially normal adaptive index (grey) and the grouped initially abnormal adaptive index (black) among different high risk groups were plotted over the four visits. Bars indicate ± 1 SD and result marked with (*) showed significant reduction.
- Figure 9.4** The visual field MD from subjects in different high risk groups were divided into two groups based on the initial adaptive index value. Both the MD with abnormal initial adaptive index value (black) and those with initially normal adaptive index (grey) revealed no significant changes over the course of the study. Bars indicate ± 1 SD and \triangle indicate rate of change.
- Figure 9.5** The RNFL thickness measured by OCT from subjects with (a) unilateral glaucoma; (b) OHT; (c) abnormal optic disc cupping; and (d) family history of glaucoma were divided into two groups based on the initial adaptive index value. The RNFL thickness with abnormal initial adaptive index value (black) showed a significant thinning (*) at the last visit in both OHT and unilateral glaucoma groups, while there was no significant thinning of the RNFL thickness for subjects with normal initial adaptive index value (grey). Bars indicate ± 1 SD and \triangle indicate rate of change.
- Figure 10.1** (a) Each stimulus sequence contains four frames. The initial frame (multifocal flash) alternated between bright and dark according to a pseudo-random binary m-sequence with a preset stimulus contrast level. (b) The luminance-difference between the brighter hexagons and the dimmer hexagons ($L_{\max} - L_{\min}$) of the multifocal flashes in four stimulus contrast settings are denoted 1.87, 1.23, 0.93 and 0.55 $\text{cd}\cdot\text{s}/\text{m}^2$.
- Figure 10.2** A typical mfERG result from a porcine eye. (a) Three-dimensional field-view topography across the retina from a left porcine eye at 99% stimulus contrast level, where the optic nerve head and the visual streak are shown. (b) Localized responses of 103 traces are also demonstrated. (c) The typical global flash mfERG response of first-order kernel (K1) contains two components: the DC and the IC. The measurements of peak-to-peak amplitudes of the two components

are illustrated (P1 represents the DC amplitude and N3 represents the IC amplitude). **(d)** Superimposed comparisons of the averaged responses grouped from the visual streak (dark trace) and the para-visual streak region (grey trace).

Figure 10.3 Superimposed comparisons of the typical averaged responses from the visual streak of one porcine eye. **(a)** The K1 waveforms of global flash mfERG under the influence of ISO (dark trace) and the control response (grey dotted trace). **(b)** The K1 waveforms of global flash mfERG under the effect of ISO+TTX (dark trace) and the control response (grey dotted trace).

Figure 10.4 Superimposed comparisons of the typical averaged responses from the visual streak of one of the porcine eyes. **(a)** The K1 waveforms of global flash mfERG under the influence of ISO+TTX+NMDA (dark trace) and the control response (grey dotted trace). **(b)** The dark trace is an estimation of inner retinal activity suppressed by ISO+TTX+NMDA. (The amplitude of the oscillation-like wavelets indicated by the red lines was measured from the first trough (base line) to the peak of W1, W2 and W3, respectively.)

Figure 10.5 The grey dotted traces are the mfERG waveforms under effect of ISO+TTX+NMDA from two different porcine eyes. **(a)** The left dark trace shows the typical effect of APB on the global flash mfERG from one eye and the right dark trace estimates the ON-bipolar contributions isolated by APB. **(b)** The left dark trace shows the typical effect of PDA on the global flash mfERG from another eye and the right dark trace estimates the OFF-bipolar contributions isolated by PDA.

Figure 10.6 **(a)** The main contributions of the outer retinal response to the global flash mfERG are demonstrated, where the photoreceptor response (grey trace) obtained after APB+PDA is injected, the estimated ON-bipolar response (thick dark trace) and the estimated OFF-bipolar response (thin dark trace). **(b)** The approximate outer retinal response (grey trace) and the estimated inner retinal response (dark trace) are believed to shape the porcine global flash mfERG response.

Figure 10.7 The luminance-modulated response functions of the grouped DC

responses (P1) and the grouped IC responses (N3) from the visual streak (upper panels) and the para-visual streak area (lower panels) for control data. Lines represent the second-order best-fitting curves which provide better fit with higher value of R^2 than straight lines (Error bars = ± 1 SEM).

Figure 10.8 The typical mfERG waveform at the visual streak under different luminance-difference levels from one of the porcine eyes **(a)** Estimated outer retinal responses isolated with ISO+TTX+NMDA under different luminance-difference levels of the multifocal flash. **(b)** Estimated inner retinal responses obtained by subtraction of responses under ISO+TTX+NMDA from the control response with four different luminance-difference levels of the multifocal flash. (1.87 cd·s/m²: thick dark trace, 1.23 cd·s/m²: thin dark trace, 0.93 cd·s/m²: grey trace and 0.55 cd·s/m²: grey dotted trace)

Figure 10.9 **(a)** The luminance-modulated response functions of the P1 amplitude of the DC from the estimated outer retinal response. **(b)** The estimated luminance-modulated response functions of the P1 amplitude of the ON-bipolar, OFF-bipolar and photoreceptors and **(c)** the estimated luminance-modulated response functions of W1, W2 and W3 amplitudes from the inner retinal response. Fitted lines are the best-fitting second-order curves that provide better fit with higher value of R^2 than straight lines (Error bars = ± 1 SEM).

Figure 12.1 Pattern of voluntary eye movements used to mimic involuntary unsteady fixation. Subjects were required to shift their fixation every 2s starting from the center and following the fixation sequence shown. A pre-set timer was used to remind the subjects to move their fixations. Subjects were asked to shift the whole pattern as clockwise (from 1 to 7) for every segment. This pattern of fixation was used (about 15 s), but with clockwise 90° phase shift for each recording segment in order to distribute the different recording time at different ends of the fixation cross equally.

Figure 12.2 Responses from 103 stimulus hexagons were grouped into six concentric rings (left) for analysis and localized responses from the ring-2 hexagons (right) were also investigated.

- Figure 12.3** Statistical results of N1 and P1 implicit times (ms) in ring response under four conditions: steady fixation, 2° unsteady fixation, 4° unsteady fixation and 6° unsteady fixation. There was no statistically significant difference ($p > 0.05$) between the central fixation and any unsteady fixation conditions at any eccentricity. Error bars indicate ± 1 SD of means.
- Figure 12.4** Amplitude values (nV/deg²) in ring responses of N1 and P1 under four conditions: steady fixation, 2° unsteady fixation, 4° unsteady fixation and 6° unsteady fixation. (*) indicates statistical significantly difference ($p < 0.05$) compared with the steady fixation condition at the particular eccentricity. Error bars indicate ± 1 SD of means.
- Figure 12.5** Amplitude values (nV/deg²) of ring-2 hexagons responses of N1 and P1 under four conditions: steady fixation, 2° unsteady fixation, 4° unsteady fixation and 6° unsteady fixation. (*) indicates statistical significantly difference ($p < 0.05$) compared with the steady fixation condition at ring-2. Error bars indicate ± 1 SD of means.
- Figure 12.6** Implicit time (ms) of ring-2 hexagons responses of N1 and P1 under four conditions: steady fixation, 2° unsteady fixation, 4° unsteady fixation and 6° unsteady fixation. There was no statistically significant difference ($p > 0.05$) between the central fixation and any unsteady fixation conditions at ring-2. Error bars indicate ± 1 SD of means.
- Figure 12.7** Concentric ring responses (left) and three-dimensional plots (right) under four conditions from a typical subject: steady fixation, 2° unsteady fixation, 4° unsteady fixation and 6° unsteady fixation (top to bottom, respectively).
- Figure 12.8** Effects of unsteady fixation on the depth of depression at the blind spot region by calculating the depth ratio of the blind spot were shown. (*) indicates there was statistical significantly difference ($p < 0.05$) compared with the steady fixation condition. Error bars indicate ± 1 SD of means.

List of Tables

- Table 7.1** The statistical analytic result of the response (peak-to-peak) amplitudes of (a) DC and (b) IC in the periphery between the glaucoma group and normal group at the four luminance-difference levels.
- Table 8.1** Clinical data of unilateral glaucoma subjects. The eyes shaded in grey are glaucoma eyes with abnormal GHT values; GHT index of fellow eyes were normal except for borderline GHT values found in fellow eyes of subjects 1 and 3 (*).
- Table 8.2** Grouped peripheral response (peak-to-peak) amplitudes of DC for the three groups at four luminance-difference levels, with statistical comparisons.
- Table 9.1** Clinical data of unilateral glaucoma subjects. The eyes shaded in grey are glaucoma eyes with abnormal GHT values; GHT index of fellow eyes were normal except for borderline GHT values found in fellow eyes of subjects 8 and 10 (*).
- Table 9.2** The visual field and the OCT data for different high risk groups in the first visit were divided into two categories according to whether the initial adaptive index was above or below 1.5. Quadrants in the field with adaptive index below 1.5 were considered as abnormal.
- Table 10.1** Mean of amplitude and implicit time with ± 1 SEM of the global flash mfERG features from the visual streak area. Statistical comparisons (ANOVA with Bonferroni *post-hoc* test) were done with the control data; ** (p<0.01) and *** (p<0.001) indicate levels of significant difference from the control group.
- Table 10.2** Mean of amplitude and implicit time with ± 1 SEM of the global flash mfERG features from the visual streak area. Statistical comparisons (ANOVA with Bonferroni *post-hoc* test) were done with the data under ISO+TTX+NMDA; * (p<0.05), ** (p<0.01) and *** (p<0.001) indicate levels of significant difference from the control group. Values marked with (Nil) represent no such parameters could be measured.

Abbreviations

AGIS	Advanced Glaucoma Intervention Study
ARM	Age-related maculopathy
APB	2-amino-4-phosphonobutyric acid
ACG	Angle-closure glaucoma
CIGTS	Collaborative Initial Glaucoma Treatment Study
CRT	Cathode ray tube
DTL	Dawson-Trick-Litzkow
DC	Direct component
EMGT	Early Manifest Glaucoma Trial
EOG	Electrooculogram
ERG	Electroretinogram
FDT	Frequency-doubling technology
GEE	Generalized estimating equations
GHT	Glaucoma hemifield test
HRT	Heidelberg retina tomograph
IC	Induced component
ISCEV	International society for clinical electrophysiology of vision
IOP	Intraocular pressure
ISO	Isoflurane
K	Koniocellular
LGN	Lateral geniculate nucleus
LogMAR	Logarithm of the minimum angle of resolution
M	Magnocellular
MD	Mean defect
mfERG	Multifocal electroretinogram
NMDA	N-methyl-D-aspartic acid
NTG	Normal tension glaucoma
OHT	Ocular hypertension
OHTS	Ocular Hypertension Treatment Study
OAG	Open-angle glaucoma
ONHC	Optic nerve head component
OCT	Optical coherence tomography
OPs	Oscillatory potentials
P	Parvocellular
PERG	Pattern electroretinogram

PhNR	Photopic negative response
PDA	cis-2,3-piperidinedicarboxylic acid
PRL	Preferred retinal locus
POAG	Primary open-angle glaucoma
ROC	Receiver operating characteristic
RC	Retinal component
RNFL	Retinal nerve fiber layer
RPE	Retinal pigment epithelium
SLP	Scanning laser polarimetry
STR	Scotopic threshold response
SWAP	Short wavelength automated perimetry
TTX	Tetrodotoxin
VA	Visual acuity
VEP	Visual evoked potential

PART I
INTRODUCTION & LITERATURE
REVIEW

Chapter 1 - Introduction

It is well known that the severe stages of glaucoma cause blindness. Glaucoma affects primarily the inner retina, specifically the ganglion cells, most likely with unremarkable signs and symptom in the early stages. The damage to the inner retina results in visual field constriction and ultimately in loss of central vision. The most common technique for detecting this abnormal change is visual field testing. Unfortunately, it is found that glaucoma patients may suffer more than 25% loss of retinal ganglion cell axons before a visual field defect is evident (Quigley et al., 1989; Harwerth et al., 1999). Since the nerve fibers cannot be regenerated and the glaucomatous damage cannot be recovered, current testing is not ideal for detecting or diagnosing glaucoma before extensive loss of nerve fibers.

A number of reports have shown that electrophysiological tools can detect early functional changes of the retina and it is possible that early functional changes are detectable before significant fiber loss occurs. Several studies have demonstrated that the pattern electroretinogram (PERG) is abnormal in glaucoma patients (Weinstein et al., 1988; O'Donaghue et al., 1992). However, the PERG has limitations, in that it gives only the average electrical potential change from inner retina over the stimulation area, so that details of localized change in different retinal regions cannot be obtained.

The multifocal electroretinogram (mfERG) technique was developed by Sutter and Tran in 1992. It allows multiple local retinal responses to be recorded in a visual field of about 50 degrees within a short time period, and it is thus believed that it can be a tool for both diagnosing and studying diseases of the human retina (Sutter and Tran, 1992). With the use of the mfERG, local retinal damage can be detected; however, currently unresolved problems are the extent to which the inner retina contributes to the human mfERG and how to build an appropriate protocol for measuring this contribution. Improving the sensitivity of the mfERG measurement will allow the functional changes of the inner retina due to the glaucomatous damage to be detected in an earlier stage before loss of nerve fibers. The usefulness of the technique will depend on its ability to detect changes in the mfERG responses from particular retinal layers.

Recently, a number of studies have used the mfERG to access the physiological response of the ganglion cells in order to look for signs of glaucomatous damage in terms of amplitude (Chan and Brown, 1999), implicit time or waveform (Hasegawa et al., 2000), but one other study did not find any changes reflecting glaucomatous field defects even for the second-order kernel mfERG response (Sakemi et al., 2002), although the poor signal-to-noise ratio of higher-order kernels may affect the results, its validity of reflecting the function of the ganglion cells was questioned. The most

important study is that of Sutter and Bearnse, who presented evidence for a response generated from the optic nerve head and found that glaucomatous damage can reduce this optic nerve head component (ONHC) (Sutter and Bearnse, 1999). Moreover, altering the stimulus by interposing a global flash frame between the m-sequence can also enhance the naso-temporal asymmetric characteristic of the ONHC which is affected by glaucoma (Fortune et al., 2002a). This recent approach of using the mfERG with the global flash technique was introduced to evoke a large non-linear mfERG component, which is provoked by the interaction between a focal flash and a global flash. These authors make an argument that ganglion cells actually contribute to the human mfERG. However, the mfERG procedure is still not sensitive to detect activity from the inner retina and modified paradigms are necessary to develop in order to improve the sensitivity of the technique.

A clear demonstration of the inner retinal contribution to the mfERG is provided by studies in the monkey where the mfERG was recorded before and after intra-vitreous injections of N-methyl-D-aspartic acid (NMDA) and tetrodotoxin (TTX) (Hood et al., 1999b; Frishman et al., 2000). TTX blocks the sodium-based-action potentials of ganglion cells and NMDA depolarizes the postsynaptic membranes of ganglion and amacrine cells. These studies suggest that the mfERG waveform from monkeys exhibits a significant naso-temporal variation and this variation can be

removed by TTX. In other words, it is the spiking activity of the inner retinal neurons that appears to cause the variable waveform across the retina. Hood and his colleagues showed similar naso-temporal variation in the human mfERG, and this variation is more obvious if the stimulus contrast is decreased to 50% (Hood et al., 1999b). This is an important observation as naso-temporal variations in waveform have been hypothesized to be due to ganglion cell activity; contrast attenuation of the stimulus is reported to increase the proportion of the responses from the inner retina in the mfERG (Bears and Sutter, 1998). In an attempt to improve the mfERG response from the inner retina for detecting local functional changes, Hood and his colleagues set the stimulus for the mfERG to a contrast of 50% to measure glaucomatous retinal changes (Hood et al., 2000a). They found that the mfERG waveform with this contrast stimulus is similar to the mfERG waveform in the monkey, with a trough followed by a double-peak component. For subjects with glaucoma, the second peak seems to be reduced in amplitude. However, these changes are not detectable in some patients, and in others, the changes in the mfERG are not related to the local field losses, hence it was explained that this effect may only be seen if and only if a sufficient number of ganglion cells was being damaged. Thus, it is not effective in detecting local or early glaucomatous damage.

Nevertheless, the evidence for a ganglion cell contribution to both the monkey

(Hood et al., 1999b) and human mfERG (Sutter and Bearse, 1999) is still a very important finding. These findings provide the motivation for this study, in attempting to enhance the response from the inner retina. The human mfERG contains a component (ONHC) contributed from ganglion cell activity (Sutter and Bearse, 1999; Fortune et al., 2002a). Furthermore, Hood and his colleagues found that the contribution of outer retina outweighs that of the inner retina in human mfERG with 100% contrast stimulus, while the proportion contributed by the inner retina becomes larger with contrast attenuation (Hood et al., 1999b). Thus, in an attempt to improve the efficacy of the mfERG in detecting the inner retinal activity, a new mfERG stimulus protocol was designed in this study; it was based on the framework provided by Fortune's study (Fortune et al., 2002a), with different levels of contrast stimulation. If the new approach can measure the activity of the inner retina, clinical assessments for detecting glaucoma can be enhanced by this new method. Furthermore, the functional changes of the inner retina due to glaucomatous damage can then be detected and the disease can be controlled at an early stage.

Chapter 2 - What is Glaucoma?

Glaucoma is an eye disease that can cause irreversible blindness in the advanced stage. It refers a group of eye diseases with characteristic pattern of optic neuropathy involving loss of retinal ganglion cells. The atrophic change of nerve fibers is accompanied by characteristic alterations in the appearance of the optic nerve head, such as increase cupping of the disc and notching at the retinal neural rim, and subsequent visual field loss (Khaw et al., 2004). Glaucoma is a major health concern throughout the world because it is one of the leading preventable causes of blindness in the world. It is the second leading cause of blindness globally, causing around 12% of all cases of total blindness (Resnikoff et al., 2004). It is the major cause of blindness in Hong Kong and is the third leading cause of blindness among the Hong Kong elderly population (Michon et al., 2002).

2.1 Prevalence of glaucoma

According to the World Health Organization, there are now more than 4 million people who are currently blind due to glaucoma (WHO, 1997; Resnikoff et al., 2004). Quigley in 2006 used prevalence models constructed by age, sex and ethnicity to estimate the number of people who will have glaucoma in 2010 (Quigley and Broman, 2006). The number of people worldwide who will have glaucoma by the year 2010

was estimated at about 60.5 million, and over 8.4 million people will suffer from bilateral blindness due to primary glaucoma. China was identified as the region with largest number of glaucoma case in the world, followed by Europe (Quigley and Broman, 2006). This may be due to the large adult population in China (around 1.2 billion). However, regardless of the total number, Africa had the highest ratio of glaucoma sufferers in the adult population. Besides, based on different glaucoma type, the greatest number of people with open-angle glaucoma (OAG) was in Europe, while the absolute number of people with angle-closure glaucoma (ACG) was the highest in China in 2010. Both incidence and prevalence of glaucoma are increasing worldwide, particularly with the rapid growth of the elderly population (Quigley and Broman, 2006).

In Hong Kong, from the statistical report given by the Hong Kong Hospital Authority and the Department of Health in 2005, about 2% of the population suffer from glaucoma and about 2000 people were hospitalized due to glaucoma in that year. The incidence of glaucoma has risen about 15% in the past 5 years, and it has become the major cause of blindness in Hong Kong. There are about 90 registrations of blindness due to glaucoma every year and it is around 23% of all causes of total blindness.

Visual loss from glaucoma is irreversible, thus individual awareness and

knowledge of glaucoma are important for diagnosis and prevention. Nevertheless, even in developed countries, public health knowledge of glaucoma is still poor. In the United States, only half of the people with glaucoma may be aware that they have the disease (Whitaker et al., 1999), and only 30% of Germans had heard about glaucoma (Pfeiffer and Krieglstein, 1993). Although nearly 80% Hong Kong adults were aware of glaucoma, only 10% could describe its symptoms correctly and more than 70% of the population were not familiar with appropriate treatments (Lau et al., 2002). This is similar to Australia, where about 80% of the population were aware of glaucoma, but only 20% had correct understanding of the disease (Livingston et al., 1998). The proportional increase in glaucoma will challenge social resources. As the scanty knowledge of the disease and dramatically increase in the number of suffering from the disease around the world, advancement of diagnostic and therapeutic techniques for glaucoma management is an urgent need that would effectively reduce the disability caused by glaucoma.

2.2 Primary open-angle glaucoma

Primary open-angle glaucoma (POAG), also referred as chronic glaucoma which is a disorder characterized by open iridocorneal angles, is the major primary type of glaucoma in most populations worldwide (Quigley, 1996; Quigley and Broman,

2006). The estimated prevalence of OAG worldwide in 2010 was 1.96% (Quigley and Broman, 2006). POAG is generally bilateral but its severity is not necessarily symmetrical (Harbin et al., 1976; Kass et al., 1976; Susanna et al., 1978).

2.2.1 Risk factors for primary open-angle glaucoma

There are several risk factors for developing POAG. It is more common in elderly people, and the risk increases with increasing age (Bengtsson, 1981; Tielsch et al., 1991); it is unusual for POAG to be diagnosed in a patient younger than 40 years. POAG is significantly more common (Quigley, 1996) and more severe in blacks than in whites. It has been suggested that black people are 16 times more likely than whites to develop POAG-associated visual impairment (Munoz et al., 2000), and are more likely to become blind than are white people (Hiller and Kahn, 1975; Grant and Burke, 1982; Wilson et al., 1985). In addition to ocular hypertension (OHT), a family history of POAG and myopic refractive error are also associated with greater glaucomatous damage. There is a strong familial association in POAG, which was found in 13 to 25% of glaucoma patients (Biro, 1951; Kellerman and Posner, 1955). Myopia may coexist in about 17% of patients with glaucoma (Mastropasqua et al., 1992). Long-term steroid use will also increase the chance of suffering glaucoma, and there is also close association between glaucoma and diabetes mellitus (Becker, 1971) and both systemic hypertension and hypotension (Leighton and Phillips, 1972; Leske

et al., 1995; Tielsch et al., 1995). Chronic hypertension may cause retinal ischemia, resulting in cell and axonal damage, mainly due to increased resistance of blood flow after retinal vessels damaged, and low systolic blood pressure may reduce the local perfusion of the optic nerve head, especially when intraocular pressure (IOP) is elevated.

Patients with POAG are usually asymptomatic in the early stages of glaucoma and do not usually have any visual complaints until late in the course of the disease, when a significant loss of visual field has occurred. Furthermore, as the initial glaucomatous field loss has most likely occurred in the nasal Bjerrum area (Caprioli and Spaeth, 1985) the field loss can be compensated by the fellow eye; thus most patients will only seek for help in the advanced stage.

2.2.2 Pathogenesis of primary open-angle glaucoma

The development of the field loss in glaucoma is caused by the progressive damage to retinal nerve fibers. However, the patho-physiology of this complex disease is still not well understood. The chance of damage, the rate of progression and the response to treatment show wide variation between individuals even those of similar age, race and risk factors. Glaucoma commonly affects primarily the inner retina, specifically the ganglion cells (Quigley et al., 1989; Glovinsky et al., 1991; Hare et al., 1999), most likely with unremarkable signs and symptoms in the early

stage. Most patients even with advanced glaucomatous damage sometimes still can perform well in daily visual tasks. Therefore, patients may suffer considerable damage before they seek a professional opinion. Unfortunately, the damage to the inner retina results in visual field constriction and ultimately in loss of central vision (Wilson et al., 2002).

Nevertheless, the pathology of POAG cannot be simply explained by a single mechanism and it appears to be multifactorial in etiology. The most prevalent explanations for glaucomatous optic neuropathy are the direct mechanical theory and the vascular theory (Bathija, 2000).

2.2.2.1 Mechanical theory

The mechanical theory emphasizes the structural damage to the optic nerve head at the level of the lamina cribrosa, caused by the elevated IOP. The nonmyelinated retinal nerve fiber axons pass through the sclera at the lamina cribrosa. The lamina cribrosa provides a fibroelastic platform for axon bundles, and principally consists of astrocytes which synthesize the extracellular matrix (Hernandez, 2000). Astrocytes, which provide cellular support functions to the axons, are the major glial cell type in the nonmyelinated optic nerve head. However, elevated IOP exerts a posterior force on the lamina cribrosa (Fechtner and Weinreb, 1994), where it is the weakest part of the sclera, and may lead to extensive remodeling. In addition, the astrocytes are

subject to the same force and respond to the elevated IOP (Hernandez, 2000). The important function of astrocytes is to preserve the integrity of neural tissues following injury; reactive astrocytes thus form a barrier around the injured neural area isolating intact neural tissues from further lesions. However, this redistribution and migration of reactive astrocytes into the nerve bundles in the lamina cribrosa and the up-regulation of cell surface adhesion molecules in the repair process (Hernandez, 2000) may alter fascicular support of the lamina cribrosa.

Furthermore, reactive astrocytes also remodel the extracellular matrix and there are marked changes in elastic fibers at the level of the lamina cribrosa. Both elastotic degeneration and new synthesis of elastin are found in response to elevated IOP (Hernandez, 2000). In addition, the changes in elastic fibers are also accompanied by changes in the collagen network and these extensive changes in the extracellular matrix may alter the biomechanical properties in response to mechanical tension with an adverse impact on the matrix to respond normally to pressure. This may change the compliance of the optic disc and make it more susceptible to collapse under elevated pressure (Hernandez, 2000).

2.2.2.2 Vascular theory

Glaucomatous damage in POAG may also occur without elevation of IOP, and thus the mechanical theory alone is not sufficient as an explanation. The vascular

theory suggests that eyes with poor vascular supply to the optic nerve head cause tissue ischemia and are more predisposed to glaucomatous damage. Indeed, glaucomatous optic neuropathy can occur due to the compromise of vascular circulation of the axon in the optic nerve head. The major causes include loss of capillaries, low perfusion pressure, as well as alteration and failure of regulation in capillary blood flow (Flammer et al., 2002).

Retinal and optic nerve circulation are autoregulated within a certain flow range which is independent of perfusion pressure (Dumskyj et al., 1996). Besides myogenic regulation, endothelial cells play a major role in local regulation (Haefliger et al., 2001) by releasing vasodilating factors such as nitric oxide or the vasoconstrictor endothelin-1 (Haefliger et al., 1992) in order to maintain a constant oxygen concentration. However, this regulatory mechanism may fail in patients with glaucoma (Chung et al., 1999), and the average ocular blood flow is decreased in some glaucoma patients especially in normal tension glaucoma (NTG) patients (Flammer et al., 2002). In addition, the failure of the regulatory mechanism may also affect the ability to adapt to the elevated IOP or the decreased blood pressure as a consequence of insufficient blood supply, which finally prones to glaucomatous damage.

2.2.2.3 Apoptosis

Glaucomatous injury ultimately results in cell death through apoptosis regardless of the mechanism to retinal ganglion cell damage in glaucoma. Apoptosis is a genetically programmed cell death pathway designed to cull damaged cells through self-destruction. Retinal ganglion cell apoptosis in glaucoma could be triggered by neurotrophic factor deprivation, nitric oxide generation after ischemia or by glutamate excitotoxicity.

In experimental glaucoma, elevated IOP impairs the axonal transport at the level of the lamina cribosa (Minckler et al., 1977), and this reversible blockage has been observed within hours of IOP elevation (Quigley and Anderson, 1976). Disruption of axoplasmic flow may alter the normal functioning of retinal ganglion cells as several neurotrophins have been shown to be essential for retinal ganglion cell survival following injury. Brain-derived neurotrophic factor is one of the growth factors provided to the retinal ganglion cells by way of axonal transport. Its insufficient delivery to the retina has been suggested to have a direct impact on retinal ganglion cell death in glaucoma (Ko et al., 2001), and thus withdrawal of neurotropic factors may lead to apoptotic cell death.

Under conditions of retinal ischemia, production of a vasodilator, such as an increase in nitric oxide, will alter ocular blood flow regulation (Haefliger et al., 1992).

However, excessive levels of nitric oxide may cause retinal ganglion cell death by apoptosis (Becquet et al., 1997). In particular, nitric oxide levels are elevated in the retina under experimental glaucoma (Siu et al., 2002), and inhibition of nitric oxide production can prevent the loss of retinal ganglion cells (Neufeld et al., 2002). These findings suggest that excessive production of nitric oxide may play an important role in ganglion cells loss in glaucoma.

Glutamate is a major neurotransmitter in the retina for photoreceptor-bipolar cell and bipolar cell-retinal ganglion cell synaptic transmission. However, excessive levels of glutamate may cause neuronal death as a result of excitotoxicity (Kwong and Lam, 2000); even chronic mild elevation in glutamate level can be toxic to ganglion cells (Vorwerk et al., 1996). The proposed role of excitotoxicity in glaucoma is further confirmed by the elevation of vitreal glutamate level which has been detected in glaucoma patients (Dreyer et al., 1996); however, more recent studies have failed to support this in both human glaucoma patients (Honkanen et al., 2003) or in an animal glaucoma model (Wamsley et al., 2005). The role of glutamate excitotoxicity in glaucoma thus remains unclear.

Chapter 3 - Retinal Ganglion Cell Loss in Glaucoma

Retinal ganglion cells and their axons are believed to be the major affected ocular structures in glaucoma; evidence for this comes from both human studies (Anderson and O'Brien, 1997; Klistorner and Graham, 1999a) and experimental studies in animals (Glovinsky et al., 1991; Desatnik et al., 1996). However, retinal ganglion cells consist of different subtypes with specific functional and morphological features, and there have been conflicts over the location of damage, and to which retinal nerve fiber or visual pathway it occurs in glaucoma.

3.1 Retinal ganglion cell topography

There are more than one million ganglion cells in the retina and approximately 50% of the ganglion cells are located within 16° of the foveal center (Curcio and Allen, 1990). Interestingly, the distribution of the ganglion cells in the vertebrate retina is non-uniform. In non-human primates, there is higher cell density in nasal than temporal retina (Perry and Cowey, 1985); human ganglion cell topography also exhibits a similar characteristic (Curcio and Allen, 1990), with greater ganglion cell density in nasal retina than in temporal retina and with greater ganglion cell density in the superior retina compared with the inferior retina. This naso-temporal asymmetrical distribution is quite similar to that of the human cone distribution,

however the overall density is much lower than that of the cones suggesting the presence of retinal convergence for neural processing (Curcio et al., 1990).

3.2 Major types of retinal ganglion cell

Retinal ganglion cells with larger receptive field, larger fiber diameter and higher conduction velocity project to the magnocellular (M) layers of the lateral geniculate nucleus (LGN). They represent only about 10% of the total ganglion cell population (Perry et al., 1984) and are sensitive to high temporal and low spatial frequency information as well as the achromatic or luminance information. Therefore, they are thought to be involved in conveying motion and high frequency flicker information (Livingstone and Hubel, 1987; Livingstone and Hubel, 1988). On the other hand, retinal ganglion cells with smaller fiber diameter, smaller receptive fields and slower conductive velocity project to the parvocellular (P) layers of the LGN. They tend to be responsive to high spatial frequency information, low temporal frequency and chromatic information. They are thought to be involved in the processing of color, form and spatial acuity information (Blessing et al., 2004). The smallest koniocellular (K) neurons located within and between the principal layers of the primate LGN, which receive input mostly from the blue-ON retinal ganglion cells (Martin et al., 1997), and are believed to be involved in blue-yellow color processing.

3.3 Selective loss of ganglion cell in glaucoma

Previous evidence has shown that in chronic glaucoma, cells with larger axons tend to be affected in early glaucoma (Quigley et al., 1987). Since both the superior and inferior poles of the optic nerve head contain more larger fibers, those regions seem to be damaged earlier as seen in human glaucoma eyes (Lee and Mok, 1999). Furthermore, at least two studies of experimental glaucoma have supported the hypothesis that larger axons are more susceptible in glaucoma (Glovinsky et al., 1991; Glovinsky et al., 1993), and concluded that M-ganglion cells are preferentially lost in early glaucoma. There have also been reports of selective reduction of M-fibers at the level of the LGN in glaucoma (Dandona et al., 1991; Chaturvedi et al., 1993).

However, the rationale of selectively lost of ganglion cells in early glaucoma has been refuted by more recent evidence indicating that the number of neurons in the M- and P-layers of LGN also show a tendency to decrease with increasing optic nerve fiber loss (Yucel et al., 2000). Evidence based on psychophysical evaluation is also consistent with the hypothesis that there is no selective damage of ganglion cells in early glaucoma (Ansari et al., 2002).

Recent studies have argued that the identification of specific retinal ganglion cell type loss in glaucoma depending on size alone may not be reliable, since larger diameter optic nerve fibers are not exclusively for M-ganglion cell fibers. In addition

to being determined by ganglion cell type, the size of fibers is eccentricity dependent and some eccentric P-ganglion cell axons may be larger than those M-ganglion cell axons in the central retina. However, morphological change of retinal ganglion cells can occur, (including body size reduction and axon diameter reduction) usually prior to cell death (Morgan et al., 2000; Yucel et al., 2001; Morgan, 2002). These authors have also shown that both P- and M-retinal ganglion cells undergo shrinkage before cell death in glaucoma, and these changes are likely to affect the physiological behavior of these cells. Most recent studies oppose the hypothesis that selective loss of M-retinal ganglion cells occurs in early glaucoma and suggested that the apparent selective loss of large ganglion cells in early glaucoma may be merely shrinkage of these cells.

Chapter 4 - Diagnosis of Glaucoma

The ganglion cells lost due to glaucomatous damage cannot be regenerated, but some loss is manageable and appropriate treatment is effective for preventing further degeneration and cell death. Early detection becomes essential to prevent the progression of glaucomatous damage, thus sensitive diagnostic techniques are very important to allow early commencement of glaucoma treatment.

4.1 Cost-effectiveness of early detection

Glaucoma suspect is a clinical situation for those patients who have suspicious functional or structural changes but without satisfying the diagnosis of glaucoma or for those who are at high risk for developing glaucoma with one or more risk factors. However, there are a number of risk factors for developing POAG and the prevalence of glaucoma is higher in some subsets of the population. Patients with unilateral glaucomatous visual field loss are believed to constitute a high risk group for developing glaucomatous damage in the fellow eye (Harbin et al., 1976; Kass et al., 1976; Olivius and Thorburn, 1978; Susanna et al., 1978; Poinosawmy et al., 1998), since POAG is generally a bilateral but asymmetric disease. In additions, OHT is defined as elevated IOP without the visual field abnormalities which characterize glaucoma. Although elevated IOP is not always an indicator of glaucoma, it is a major

risk factor in glaucomatous optic neuropathy (Kass et al., 2002; Keltner et al., 2006).

The risk of developing glaucoma is approximately 1% in those with IOP below 20 mmHg, and may be six times higher in those with IOP greater than 24 mmHg (Leske, 1983). Indeed, about 7.2% of fellow eyes in patients with unilateral POAG progress to glaucomatous visual field loss five years after initial diagnosis (Chen and Park, 2000). Other studies have reported that 24 – 43% of fellow eyes in patients with unilateral POAG develop glaucomatous visual field loss over 3 to 7 years (Harbin et al., 1976; Kass et al., 1976; Olivius and Thorburn, 1978; Susanna et al., 1978). In addition, the conversion rate from untreated OHT to glaucoma is about 1% per year and the conversion rate possibly decreases to half for treated OHT (Kass et al., 2002).

Actually, both the Ocular Hypertension Treatment Study (OHTS) and the Early Manifest Glaucoma Trial (EMGT) found that early IOP reduction could probably delay or prevent the glaucomatous progression. According to the OHTS, reduction of IOP by 20% or more and to reach an IOP of 24 mm Hg or less in those OHT patients can decrease the conversion rate to glaucoma from 9.5% to 4% in 5 years (Kass et al., 2002). The EMGT also pointed out that 25% IOP reduction can reduce the progression of glaucoma from 62% to 45% in 6 years (Heijl et al., 2002). Another study, the Advanced Glaucoma Intervention Study (AGIS), reported that low IOP is associated with reduced progression of visual field defect, supporting evidence

from other studies that lowering IOP has a protective role in slowing the visual field deterioration (The AGIS Investigators, 2000).

Various studies have shown that both direct and indirect costs increase with severity of POAG (Chou et al., 2003; Lee et al., 2006), where direct costs in glaucoma including the medical and surgical treatments, hospitalizations and the examinations, indirect costs including the expenses of social benefit, and some associated effects on caregivers. Lee and colleagues (2006) reported that the annual direct costs of glaucoma management for glaucoma suspects was US\$623 per year compared with US\$2511 per year for those with end-stage disease, so the resource used and direct cost of glaucoma management increase with worsening disease severity. Thus, the overall costs for managing glaucoma can be reduced by preventing disease progression as soon as possible.

Although early detection and treatment seems to be effective to reduce the related costs due to glaucoma (Peeters et al., 2008), it is not so cost-effective for treating all patients who are at high risk for developing glaucoma (Kymes et al., 2006; Stewart et al., 2008). Thus, the goal for early detection is necessary to identify those patients who are at risk of glaucoma and will potentially have early stage of glaucomatous damage before visual field losses occur, while sparing patients who only have risks but will not show any progression of disease. Thus a sensitivity

clinical test that can predict the progression of glaucoma is very important, as therapy can be applied before irreversible retinal nerve fiber damage has occurred.

4.2 Intraocular pressure

IOP is one of the conventional measurements for glaucoma assessment. The higher the IOP value, the higher the risk for suffering glaucoma. Although OHT is usually considered as the primary risk factor for glaucoma, it is not definitely correct that all glaucoma patients have higher IOP value than normal, and not all subjects with OHT will develop glaucoma. Indeed, measurement of IOP can become a supplementary assessment for glaucoma and can be used to predict the risk of suffering glaucoma, but cannot be used for diagnosing glaucoma alone.

4.3 Optic disc appearance

In glaucoma, retinal nerve fibers will gradually be lost, and the optic nerve head, a region that collects the entire fiber bundles from the retina, should have certain changes related to the severity of the disease (Quigley, 1985). The increase of cup-to-disc ratio and notching should occur if a certain amount of nerve fibers have degenerated. The observation of these abnormal optic nerve head changes is widely used clinically for glaucoma assessment, however, diagnosing early glaucoma based

on the evaluation of optic nerve head appearance is highly subjective and observer dependent (Azuara-Blanco et al., 2003). Recently, computerized scanning laser ophthalmoscopy has been developed for objective evaluation of the optic nerve head, and has become widely used for measuring glaucomatous optic nerve head changes (Uchida et al., 1996). The Heidelberg Retina Tomograph (HRT) is a confocal scanning laser ophthalmoscope providing rapid and reproducible measurement (Rohrschneider et al., 1994) for assessing the topographic image of the optic disc; it can be used for monitoring topographical changes (Chauhan et al., 2001). It also automatically calculates a series of optic nerve head parameters, such as cup area and cup-to-disc ratio, for helping to classify the topography of the glaucomatous optic disc (Trick et al., 2006). Although studies have raised the problem of inter-observer variation (Iester et al., 2001), this advanced technology is still useful for monitoring the progression of glaucomatous changes at the optic disc.

4.4 Nerve fiber layer thickness

A direct measurement of the retinal nerve fiber layer (RNFL) thickness has been claimed to be effective on early diagnosis of glaucoma, and thinning of the RNFL thickness was found to precede detectable visual field loss in glaucoma patients (Matsumoto et al., 2003). Scanning laser polarimetry (SLP) is an objective laser

scanning device developed for quantitative measurement of peripapillary RNFL thickness based on the birefringence property of the RNFL. However, the cornea and the crystalline lens are also polarizing structures that vary among individuals (Greenfield et al., 2000), and which may alter the retardation of the measuring laser beam. The current version of the SLP with variable cornea compensator (GDx-VCC) incorporates a function for estimating the anterior segment birefringence for each measurement (Trick et al., 2006), and this increases the discriminating power in detection of early to moderate glaucoma (Greenfield et al., 2002). The high reflectivity of any peripapillary chorioretinal atrophy in myopic patients (Bozkurt et al., 2002) may also affect the reliability of this technique.

Optical coherence tomography (OCT), is a non-contact technology that allows cross-sectional imaging of the retina by the use of a coherent near-infrared light beam (Trick et al., 2006). RNFL thickness measurements made with OCT are not affected by the axial length of the eye, or light transmission changes, except in cases of severe nuclear sclerosis (Carpineto et al., 2003). OCT imaging is similar to B-scan ultrasound and presents a two-dimensional pseudo-color image of the retinal section based on different reflective properties of the retinal layers. OCT allows a direct measure of RNFL thickness, and has high diagnostic ability in glaucoma (Sihota et al., 2006). This enables early detection of glaucoma and thinning of RNFL thickness

measured from OCT has proven useful in predicting glaucomatous changes (Lalezary et al., 2006). There is also a strong association between RNFL thickness measured by OCT and visual field loss detected by automated visual field analyzer (Kanamori et al., 2003). The reproducibility of OCT is high either in children (Wang et al., 2007) or in adults (Blumenthal et al., 2000b). This technique, although, has been reported with higher sensitivity than SLP (Bowd et al., 2001) the large inter-subject variation resulting from different optic disc sizes (Carpineto et al., 2003) and the underestimation of RNFL thickness (Jones et al., 2001) still need to be refined.

Despite the good diagnostic value of RNFL thickness and optic nerve head topographic measurement in glaucoma, imaging instruments with quantitative outputs, including the confocal scanning laser ophthalmoscope, the SLP and the OCT provide only structural assessment for glaucoma diagnosis. However, the functional changes in glaucoma should also be considered because the loss of retinal ganglion cells is characterized by specific patterns of progressively decreasing retinal sensitivity which reflects the patient's visual performance, and indicating real visual malfunction. Exploring the diagnostic ability of the combination of structural and functional tests should improve test sensitivity with only a limited decrease in specificity compared with the assessment of structural parameters alone in early glaucoma diagnosis (Shah et al., 2006).

4.5 Automated perimetry

In the last decade, automated perimetry as a functional assessment tool has been improved dramatically, and static white-on-white threshold perimetry has become the standard procedure for the assessment of many ocular diseases especially for glaucoma (Johnson, 1996). The major reason for the success of perimetry in glaucoma diagnosis is that it is a psychophysical assessment and the damage of the retinal nerve fiber due to glaucoma has a characteristic visual field defect. Since the distribution of the axons across the retina has a particular pattern, the degeneration of such axons due to glaucoma causes a particular defect and can be discriminated from other ocular diseases.

4.5.1 Visual field defect in glaucoma

In the early stage of glaucoma, visual field defects such as paracentral scotoma, arcuate scotoma and nasal step are commonly found. With the progress of disease, further axonal loss causes these defects to enlarge. Typically, one-half of the visual field (either superior or inferior field) is extensively damaged before the second-half becomes involved, and at the end stage of glaucoma, only the central portion remains (Quigley et al., 1996).

These field defects seem to provide a straightforward diagnosis, but many of the results with automated perimetry are in the 'grey area'. Additional techniques, relying

on the fact that one half of the field, either superior or inferior field, is damaged first in glaucoma, have been developed for enhancement of glaucoma diagnosis (Asman and Heijl, 1992a). Such techniques have used several sectors in the visual field and are believed to be more closely matched with the distribution of the retinal nerve fiber layer bundle and able to be compared with its mirror sector on the other half. This glaucoma hemifield test (GHT) is performed automatically and attempts to find shallow visual field loss between sectors by stratifying the results into “outside normal limits”, “borderline” and “within normal limits”. However, this technique cannot be applied to cases with glaucomatous visual field defects in both superior and inferior fields.

4.5.2 Sensitivity of automated perimetry

Threshold automated perimetry is a way to test the visual sensitivity. In a glaucomatous eye, the reduction of visual sensitivity is a result of retinal ganglion cell loss (Harwerth et al., 2002) and the areas with greater loss of sensitivity suffer from a more significant degeneration of retinal ganglion cells. However, there is no precise relationship between reduction in visual sensitivity and local losses in retinal ganglion cells (Quigley et al., 1989; Harwerth et al., 1999; Kerrigan-Baumrind et al., 2000) because a certain number of ganglion cells must be lost before significant visual field defects can be detected by standard perimetry. An initial 5 dB loss in sensitivity has

been reported with 25% of retinal ganglion cells lost (Kerrigan-Baumrind et al., 2000). However, with greater degree of cell loss, the visual field defects were more correlated to the ganglion cell loss, with about 4.2 dB sensitivity loss for each ten per cent of cells loss (Harwerth et al., 1999). Recently, Spry and co-workers also showed that standard automated perimetry significantly overestimates the true value of visual sensitivity, especially on damaged field areas (Spry et al., 2003). Although automated perimetry provides a relatively good diagnosis of glaucoma and is currently used as a gold standard for clinical evaluation, its sensitivity for detection of early glaucomatous changes is still doubtful, and attention thus has been directed toward developing a more advanced and sensitive test.

4.6 Other psychophysical tests

The poor sensitivity of standard automated perimetry has been explained by its lack of stimulus specificity for the mechanisms affected in early glaucoma (Porciatti et al., 1997). For further development of perimetry, it is necessary to focus the tests on specific type of ganglion cell. Since there is still no definite answer as to whether certain nerve fiber types are more susceptible to damage in glaucoma, some recent psychophysical tests have been designed based on the function of different visual pathways and can be divided into two categories: M-pathway and P/K-pathway.

4.6.1 Tests target on M-pathway

Perimetry using frequency-doubling technology (FDT) is a newly developed psychophysical test designed to favor the measurement of M-pathway activity (Fujimoto and Adachi-Usami, 2000). The stimulus in FDT uses black and white sinusoidal gratings of low spatial frequency (0.25 cycle/degree) undergoing counter phase flickering at a rapid temporal frequency (25 Hz), and presented randomly in one of 17 target locations. This technique is based on a frequency-doubling illusion where the perception of spatial frequency from the target appears to be double under low spatial and high temporal frequencies in counter phase flickering (Kelly, 1981). The FDT stimulus predominately stimulates the M-ganglion cell pathway (Maddess et al., 1998), which are presumed to be lost early in glaucoma. As a glaucoma diagnostic technique, studies have been reported reasonable sensitivity (Wall et al., 2002) and specificity (Horn et al., 2003) of the FDT test when compared with standard automated perimetry. Some investigations also describe reliable test results of FDT screening even in OHT (Sample et al., 2000) or in suspected glaucoma eyes (Paczka et al., 2001).

Motion automated perimetry is another technique designed to specifically stimulate the M-pathway by motion perception (Silverman et al., 1990). This technique employs a dynamic random dot display that contains varying degrees of a

coherent motion signal within a background of random motion noise. The testing points are localized in areas where defects are likely to occur in glaucoma. The visual field defects in glaucoma patients identified by motion perimetry and conventional perimetry are similar but the extent of field losses was larger if depicted by motion perimetry suggesting early glaucomatous damage affecting motion perception occurred in these extended area (Shabana et al., 2003). However, due to the poor correlation with the field defect on conventional perimetry in the central vision, the motion perimetry was suggested only as a diagnostic tool for assessing localized defect at eccentricities of more than 15 degrees (Shabana et al., 2003).

4.6.2 Tests target on P/K-pathway

Generally speaking, short wavelength automated perimetry (SWAP) is a modified visual field test which is designed to measure particular P-pathway visual function. The SWAP used a narrow-band, short wavelength stimulus (440 nm) on a bright yellow background which was claimed to adapt the rods as well as the middle and long wavelength sensitive cones. Only the short wavelength sensitive cones, sensitive to the blue stimulus, are working optimally to detect the target, and the responses are most likely mediated by the blue-yellow retinal ganglion cells (Sample, 2000). Therefore, it was now considered that SWAP possibly isolates the K-pathway that is involved in blue-yellow chromatic processing (Martin et al., 1997).

The SWAP has been shown to be useful to predict the development of glaucomatous visual field loss. It was also reported that, even in terms of the sensitivity (Girkin et al., 2000; Qi and Jiang, 2002) and the area or depth of the field defect detected (Qi and Jiang, 2002), SWAP is often superior to standard automated perimetry. Therefore, SWAP has been suggested for both diagnosing and follow-up of suspected glaucoma (Larrosa et al., 2000). However, the large long-term variability of SWAP makes it difficult to analyze the progression of the field defect (Blumenthal et al., 2000a). In addition, there is a potential age-related effect from yellowing of the crystalline lens which contaminates long term measurements.

4.6.3 Comparison of the new tests

Although each of the above new tests, which target a specific visual pathway, have been shown to be superior to the conventional visual field test for early glaucoma assessment (Sample et al., 2000), each test has its own advantages over the others. In addition to the lower test-retest variability than standard automated perimetry (Chauhan and Johnson, 1999), FDT has the shortest testing time due to the smaller number of test location used, and is less affected by blurred vision and pupil size (Sample et al., 2000; Delgado et al., 2002). Therefore, it seems to be better than SWAP which shows a higher test-retest variability and is more sensitive to media opacities (Delgado et al., 2002), although SWAP has been used for evaluating early

glaucoma for some years. Motion perimetry, on the other hand, showed the greatest variability and this makes it less ideal for monitoring over time (Sample et al., 2000). Based on these results, a combination of two or more visual functional tests has been suggested to improve the detection of functional loss (Sample et al., 2000). However, this is time consuming and, usually only one kind of visual field test is commonly applied in a general clinic for the monitoring of the progression of visual field defects.

Chapter 5 – Electrophysiological Tools for Diagnosing Glaucoma

Early recognition and accurate assessment of the functional losses produced by glaucoma are major goals for clinicians and researchers. Many psychophysical tests are available for assessment of visual function and have been reported to provide high sensitivity in glaucoma diagnosis. However, a major problem of most psychophysical tests is the high false-positive rate especially when the test is first performed (Graham et al., 1996). This is because all of the psychophysical tests require learning and inappropriate responses will add noise to the response set. Electrophysiological tests on the other hand are objective tools for measuring the functional response of the visual system. The principle of these tests is to measure the electrical impulse generated from the neurons after certain stimuli have been applied.

The nervous system is one of the major systems in our body and acts as a network designed to receive and transmit information. The major function of the nervous system is to detect and transform the information from the external environment into electrical impulses in order to communicate and coordinate the activities between different organs or systems in the body. The neuron is one type of cell in the nervous system and it is designed to transmit electrical signals rapidly from one area to another area through a long fiber-like structure called the axon. When the neurons receive a threshold amount of stimulation, an action potential occurs; the

membrane potential is temporarily disrupted, and this change of potential is transmitted along the axon to the terminal (synapse) where another neuron is connected and will be stimulated.

5.1 Electrophysiological examination

Electrophysiological examinations of the visual system are tests which directly measure the electrical activities of the visual system. These tests can provide objective functional information regarding the visual pathways, which is effective for the diagnosis and management of eye diseases (Corbett et al., 1995). There are different tests where the strategies are designed to examine particular parts of the visual pathway. The common tests for the examination of visual function include the following:

Electrooculogram (EOG), which is a measurement of the function of the retinal pigment epithelium (RPE), and the interaction between the RPE and the photoreceptors (Marmor, 1998);

Electroretinogram (ERG) is a summed electrical activity of different cells and structure within the retina as it reacts to light stimulation. The ERG records mainly the function of the photoreceptors and the bipolar cells;

Pattern electroretinogram (PERG) is related to the macular photoreceptors as

well as the inner retinal cell function (Bach et al., 2000);

Visual evoked potential (VEP), examines the electrical activities of the visual cortex, where the intracranial visual pathways, particularly the optic nerves and the optic chiasm, can be assessed.

5.2 Possible electrophysiological techniques for early diagnosis of glaucoma

Theoretically, glaucoma occurs when the ganglion cell bodies shrink, either because of mechanical or vascular impairment, and the communication via the cells may be affected. Ultimately, the ganglion cells degenerate, while it is suggested that the remaining bipolar cells as well as the photoreceptors are normal. With a better understanding of the patho-physiology of this disease, researchers have started to use different visual electrophysiological tools in detecting glaucoma and have proposed some ideas for early diagnosis of glaucoma.

The flash ERG is a mass electrical response of the retina to light stimulation. The early a-wave reflects mainly the activity from the photoreceptors whereas the b-wave is contributed by the middle retinal layers. The oscillatory potentials (OPs) on the leading edge of the b-wave are generally thought to arise from the activity of the inner plexiform layer. However the exact origin and mechanism of generation of the OPs still not well understood. There is no significant retinal ganglion cell contribution

to these conventional ERG components, thus the response has been regarded as without value in early diagnosis of glaucoma. Some investigators have reported normal flash ERG responses in monkeys with laser-induced glaucoma (Marx et al., 1986). However, others have shown abnormality of flash ERG responses in glaucoma patients (Fazio et al., 1986). In some studies, the OPs from the flash ERG response were also found to be altered in glaucoma patients and experimental glaucoma either in amplitude (Gur et al., 1987; Vaegan et al., 1991) or latency (Holopigian et al., 2000). These findings may indicate that glaucomatous damage is not only localized in the ganglion cells, but that additional more widespread retinal damage has occurred (Kielczewski et al., 2005; Zhou et al., 2007). Such findings indicate that the conventional flash ERG may not be an ideal test for early glaucoma assessment.

A further flash ERG component called scotopic threshold response (STR), which is the lowest detectable response under scotopic conditions, was suggested to originate in the proximal retina (Bui and Fortune, 2004). It has been found that reduction of the STR indicates retinal ganglion cell injury in rodent models of experimental glaucoma (Fortune et al., 2004; Li et al., 2006), and the STR has been used in the assessment of functional changes in a monkey OHT model (Frishman et al., 1996). However, the STR is less effective for early glaucoma assessment in humans (Korth et al., 1994). A negative response component following the b-wave,

the photopic negative response (PhNR), was also recently suggested to be a sensitive indicator of experimental glaucoma damage (Viswanathan et al., 1999). The PhNR was greatly reduced in experimental glaucoma eyes even when the a- or b-wave of the ERG response was unchanged; it is thought that this response may arise from the retinal ganglion cells and their axons (Viswanathan et al., 1999). PhNR amplitudes are greatly reduced in POAG patients (Viswanathan et al., 2001), even in patients with mild visual field sensitivity losses. The PhNR losses correlate well with visual field losses. There is a potential role for the PhNR in early detection of glaucomatous damage. Recently, it was also found that the reduction of scotopic negative response in rat OHT model could be another useful parameter for measuring inner retinal activity (Li et al., 2006).

The electrode activity of the brain in response to sensory stimulation is referred to as an evoked potential. The VEP, elicited by visual stimulation, is measured at the level of the occipital cortex as the objective measurement of visual function, any dysfunction of the visual pathway can interrupt the signals to the visual cortex and thus generates abnormal responses. VEP measurement has been proven to be an effective assessment method for optic nerve damage due to glaucoma (Towle et al., 1983). Besides, multifocal VEP can provide localized responses of the visual cortex and this test has been suggested as an objective functional visual field measurement

(Klistorner et al., 1998). Usually, a reversing black and white checkerboard is adopted as the multifocal VEP stimulus, and recent studies have also asserted that multifocal VEP is valuable in diagnosing glaucoma where it is possible to demonstrate losses of response in localized scotoma area in visual field (Hood et al., 2000b; Klistorner et al., 2000; Hood et al., 2003b). The sensitivity of the multifocal VEP to a field defect was reported to be as small as 5 degrees in diameter (Chan et al., 2003) and it can also objectively identify the extent of glaucomatous damage which could detect abnormal changes before conventionally measured visual field loss occurs (Graham et al., 2000). However, the VEP responses are highly variable (Johnson et al., 1989) since the placement of the electrodes can considerably affect the response across the field topography. Commonly, most of the investigators use theinion as the reference point for placing the active electrodes (Klistorner et al., 1998; Hood et al., 2000b; Hood et al., 2003b). However, the position of the visual cortex relative to the inion is in proportion to the size of the head and so is different among humans (Odom et al., 2004); this may be part of why the variation in VEP measurements is large. These large amplitude variations between individuals limit the application of this technique as an objective perimetry (Klistorner and Graham, 1999b).

Although vary electrode placement may help to decrease the inter-subject variability of the multifocal VEP (Klistorner et al., 1998), Hood and co-workers

further improved its sensitivity by inter-ocular comparison within a subject and comparison of the multifocal VEP responses from corresponding points in the visual field of both eyes, this inter-ocular analysis allowed accurate and quantitative measurement of localized damage due to glaucoma (Hood et al., 2000b). However, this analysis raises problem in measurement if bilateral glaucomatous damages occur in the corresponding points in the visual field.

Recently, a new blue-on-yellow multifocal VEP in the detection of early glaucoma has been reported (Klistorner et al., 2007). The test targets a blue-and-yellow subset of the visual pathway and it appears to detect early glaucomatous visual field defects with high accuracy. With this advanced stimulation modality, more extensive field defects were noted on blue-on-yellow multifocal VEP compared with achromatic stimulation. A high correspondence between field defects and amplitude changes of blue-on-yellow multifocal VEP was observed. This test may make better detection of glaucomatous field loss possible, thereby leading to early detection of glaucoma; however as with the SWAP, there is still the potential problem of crystalline lens yellowing, which will affect the results over time, thus making interpretation difficult.

5.3 Current electrophysiological technique for early diagnosis of glaucoma

PERG is the response of the central retina triggered by a reversing black and white checkerboard or grating stimulus. It allows both diagnosing the macular function as well as evaluation of the retinal ganglion cell function. The PERG contains two main components: P50 which is affected in macular disease (Holder, 1987), while N95 is the second trough likely derived from inner retina and is a direct indicator of ganglion cell function (Bach, 2001). As a result, it becomes the most common electrophysiological test for diagnosing glaucoma and studies have been reported that PERG amplitude have a significant reduction in glaucoma patients (Graham et al., 1996; Bach, 2001; Drasdo et al., 2002; Toffoli et al., 2002). Study has also reported a correlation between PERG amplitude and visual field sensitivity (Garway-Heath et al., 2002). It was suggested as a useful technique for eliciting the inner retina response and is particularly good at detecting optic nerve disease (Hitchings, 1997). However, it gives an average electrical potential change of the inner retina from an overall stimulus area, the localized change in different localized retinal regions thus is difficult to obtain.

Chapter 6 - Multifocal Electroretinogram (mfERG)

The VERIS mfERG technique was developed by Sutter and Tran (Sutter and Tran, 1992); it allows for recording multiple local retinal responses in a field of about 50 degrees diameter within a period of minutes. It can act as a tool for both diagnosing and studying retinal diseases (Sutter and Tran, 1992), and can be used to investigate retinal temporal processing mechanisms (Smith et al., 2002). Generally, the electrical response from the mfERG is recorded by a corneal electrode similar to those used for traditional full-field ERG recording, but due to computer control of the stimulus pattern and response analysis, the topography of retinal responses can be obtained.

6.1 Basic technique of mfERG recording

As with full-field ERG recording, the pupil should usually be dilated in order to obtain a high and constant retinal illumination for measurement. An active electrode used in mfERG recording should have good contact with the cornea and a reference electrode should be placed near the orbital rim of the corresponding eye unless a bipolar electrode is used; a ground electrode is usually placed either on the forehead or on the ear lobe (Marmor et al., 2003).

The stimulus is most commonly delivered by a cathode ray tube (CRT) monitor

at a frame rate of 75 Hz. The luminance of the stimulus in the 'on' state should be around 100 – 200 cd/m² and should be less than 1 cd/m² in the 'off' state in order to maintain the needed contrast between the bright and the dark hexagons at more than 90%; the recommended background luminance should be equal to the mean luminance of the stimulus (Marmor et al., 2003). A grounded hood with internal dull black surface may be used in front of the monitor to avoid stray light and to reduce the electromagnetic noise which may be picked up by the electrodes, and may be synchronous with the stimulus.

The stimulus hexagonal elements are usually scaled with eccentricity according to the density of cone distribution (Sutter and Tran, 1992). Thus the central hexagon is the smallest, while the peripheral hexagons are the largest (Figure 6.1). Stable fixation is necessary during mfERG recording (Chu et al., 2006b); usually a cross is made available for central fixation, and the fixation cross should be kept as small as possible. The overall stimulus pattern should subtend a visual angle of 40-60 degrees (Marmor et al., 2003), and the number of hexagons used depends on the resolution required. The stimulations, which are black-white transitions of the hexagons, are presented according to a pseudo-random binary m-sequence. This m-sequence controls the order of flickering in the hexagonal elements and controls the length of the entire recording. M-sequences have a length of $2^n - 1$ transitions; the higher

m-sequences produce longer recording times and have better signal-to-noise ratios.

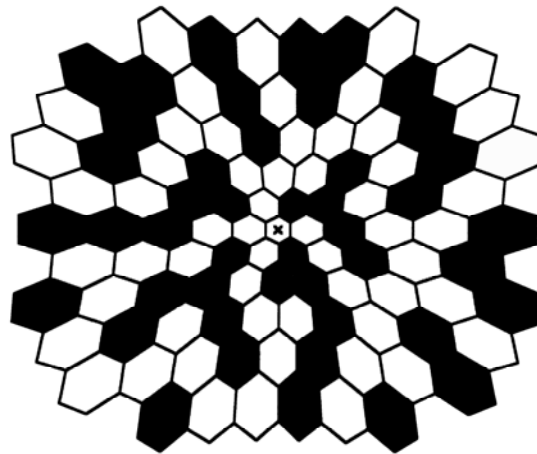


Figure 6.1 Stimulus pattern with 103 scaled hexagons.

The generated signals are small and amplifiers with a gain setting of 100,000 or 200,000 are most widely used. The gain however should produce a recognizable signal without saturating the amplifier, and also avoid any extraneous electrical noise. In addition, a bandpass filter range of 3-300 or 10-300 is advised (Marmor et al., 2003). Blinking or eye movement can distort the recorded waveform; these artifacts are eliminated in the VERIS system by monitoring the incoming signal and re-recording contaminated signal segments. VERIS has an inbuilt artifact rejection system which can be used only after a complete signal record has been accumulated (Sutter and Tran, 1992). Sutter and Tran (1992) also recommend smoothing individual waveforms and reducing some noise by averaging responses (by a specifiable percentage) with those from adjacent elements; this procedure may be

repeated a number of times if needed. However, the averaging program can affect the clarity of the margin of localized lesions and thus it should be used with caution. The data can be displayed as an array of traces from different retinal regions or averaged together with any number of traces for comparing (for example) quadrants or successive eccentric rings from center to periphery. Three-dimensional topographic response density plots can also be used to show an overview of retinal responses.

6.2 Multifocal binary kernels

The VERIS mfERG presents its stimulus (bright or dark) based on the m-sequence. By performing a cross-correlation of the output signals with the input binary pattern, it is possible to extract the local retinal contribution of different binary kernels (Sutter, 2000; Sutter, 2001). Imagine that a series of identical flashes with a high frequency of flickering is used as stimuli, the first flash will generate a signal similar to that produced by a single flash. However, the signal generated by the following flashes will have different amplitudes and shapes because of the interaction with responses to the preceding flashes. This is the so called nonlinear response.

Mathematically, first-order kernel can be obtained by adding all records which follow a bright flash to a hexagon and subtracting all records which follow a dark presentation to the same hexagon; the response of that hexagon is then built up while

the contributed responses from other hexagons will be eliminated (Figure 6.2a).

The second-order kernel measures how responses are influenced by adaptation to successive flashes. The first slice of the second-order kernel response shows the effect of a following flash, the second slice shows the effect of the flash which is two frames away, and so on. In other words, it is obtained by adding all the records following a change from either bright to dark or dark to bright and subtracting all records with no change in the stimulus (Figure 6.2b). The third-order kernel then is the response to a third stimulus that depends on the two previous stimuli.

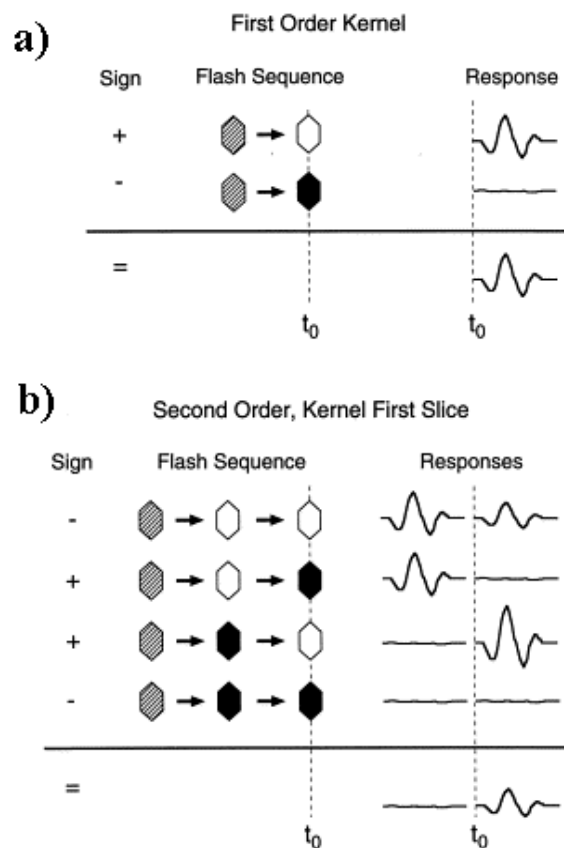


Figure 6.2 Schematic explanation for the signal derivation of (a) the first-order kernel, and (b) the first slice of second-order kernels of the mfERG (Adopted from figures in (Sutter and Bearse, 1999)).

6.3 Differences between mfERG and full-field flash ERG

Although the mfERG is usually measured under photopic conditions, the waveform of the mfERG is different from the photopic full-field flash ERG even when all the localized mfERG responses are summed together. This is not surprising as the full-field flash ERG measures a global retinal response with successive flashes and more than one second is allowed between flashes for recovery of the retina. However, the mfERG responses are mathematically derived through cross correlation, and its fast flickering stimulation induces temporal interaction in the retina as the flashes are closely spaced in time; these temporal interactions probably lead to the difference.

In order to minimize the paradigm difference between the mfERG and full-field flash ERG, the sequence of multifocal flashes was slowed down by interposition of 7 blank frames (7F) with the background intensity between consecutive flashes (Hood et al., 1997). These flashes were separated by more than 106 ms at a frame rate of the monitor of 75 Hz. Under these conditions the waveform of the summated mfERG appeared to be the same as that of the photopic full-field flash ERG, although the response amplitude was much smaller, as the summated mfERG covered only the central region of the retina. Increasing the number of inserted background frames did not significantly change the first negative component of the mfERG, but the implicit

time of the main positive component decreased and the oscillatory components along its leading edge become more prominent. Thus it was believed that the mfERG response shows a certain amount of adaptation in the normal stimulation mode. As the number of inserted frames did not affect the first negative component of the mfERG, it was suggested that this component originated from the same components of the a-wave in the photopic full-field flash ERG (Hood et al., 1997).

6.4 Origins of the human mfERG

As with the traditional full-field ERG, the mfERG reflects contributions from various retinal cell types. The overall shape of the human mfERG response is attributed mainly to bipolar cell contributions combined with smaller contributions from photoreceptors; this analysis is based on the pharmacological dissection of the monkey's mfERG (Figure 6.3) (Hood et al., 2002). The human mfERG is significantly different from that recorded from the monkey (Frishman et al., 2000). However once the inner retinal components are removed from the monkey's mfERG responses, the mfERG waveform of the monkey becomes similar to that from humans (Hood et al., 1999b; Frishman et al., 2000). Based on these findings, a proposed model of human mfERG was deduced and this model suggests that the contribution to the human mfERG is mainly from the outer retina (Hood et al., 2002).

Hood et al. (2002) proposed that the onset (hyperpolarization) of the OFF-bipolar cell starts just before the depolarization of the ON-bipolar cell, thus the leading edge of the N1 is generated by the hyperpolarization of the OFF-bipolar cell with small contribution from the photoreceptors. The shape of N1 is then altered by the onset of the ON-bipolar response and the recovery of the OFF-bipolar response occurs slightly after the peak of N1; thus the leading edge of the P1 contains both the recovery of the OFF-response and the depolarization of the ON-bipolar cell. The peak of P1 occurs at the time when the recovery of the OFF-response has reached its positive peak and the contribution of the ON-bipolar has also reached its peak. The recovery of the ON-response mainly forms the trailing edge of P1.

This proposed model of the retinal origins of the human mfERG is based on monkey studies. Although the monkey has a retinal structure similar to that of humans, the different species may have different retinal physiologies that produce differences in the origins of monkey and human mfERG. Other clues to the origin of different components of the human mfERG can be evaluated by studying the effect of different retinal diseases on the mfERG (Hood, 2000).

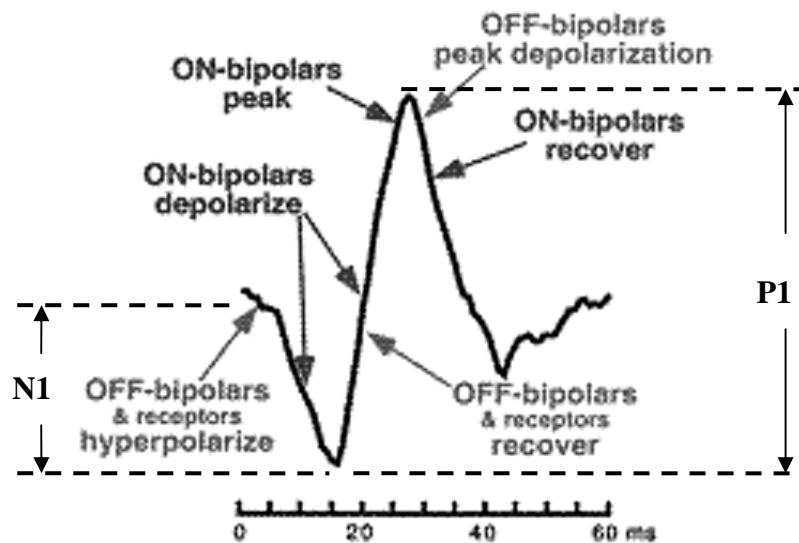


Figure 6.3 The proposed model of human mfERG based on the pharmacological dissection results from the monkey's mfERG response. (Adapted from figure in (Hood et al., 2002)).

6.5 Characteristics of mfERG in normal subjects

The mfERG is able to reflect visual function objectively. As would be expected, the response density decreases with eccentricity and the reduction rate is slightly less in the nasal retina due to the higher cone density in the nasal retina (Sutter and Tran, 1992). Changes of mfERG response density with eccentricity were shown to be well-correlated with the cone density.

As with other visual function assessment tools, ageing significantly affects the mfERG responses (Nabeshima et al., 2002). It was suggested that the most central mfERG responses exhibited the greatest decline with age (Fortune and Johnson, 2002;

Gerth et al., 2002; Jackson et al., 2002). The averaged peak-to-peak amplitude decline rate is about 10.5% per decade (Seiple et al., 2003), and it is believed that optical factors contribute most to the loss of function (Fortune and Johnson, 2002). A recent study found that neural factors start to significantly influence the mfERG topography after the age of 70 years since these older subjects show significantly increased latency (Tam et al., 2006).

6.6 Clinical application of mfERG

With the development of this multi-input technology, a physiological topography of retinal response became possible, which can enhance traditional behavioural visual field testing (Brown and Yap, 1996). It gives an objective and quantifiable result which can be compared from visit to visit or compared to standard data sets. This technique stimulates multiple retinal areas and shows retinal responses for each of these retinal areas (Sutter and Tran, 1992), thus localized reduction in response in the mfERG topography according to the dysfunctional areas can be revealed (Bears and Sutter, 1996). However, when using the mfERG with 103 hexagon stimulus it is difficult to detect a visual field defect of less than 5 degrees diameter, and the sensitivity in the detection of localized defects would be lower if a small defect is located over two hexagonal stimulus elements (Yoshii et al., 1998). Actually, the

sensitivity of the mfERG in the detection of a small scotoma would be higher if a higher resolution stimulus pattern (e.g. 241 hexagons) was used (Marmor et al., 2002). However, long recording time and poor signal-to-noise ratio are the drawbacks of using a high resolution stimulus pattern in recording the mfERG. After optimizing the conditions, 103 hexagon stimulus is recommended for clinical use.

Data from clinical cases have been used to demonstrate that retinal functional losses due to outer retinal disorders can be described by this technique and that the defect pattern of mfERG activity is similar to the pattern of the visual field defect (Kretschmann et al., 2000). Previous studies have evaluated this system for clinical application and have found that it is sensitive in detecting diseases such as retinitis pigmentosa (Chan and Brown, 1998; Hood et al., 1998; Seeliger et al., 1998). This system also allows accurate topographical mapping of focal areas of retinal dysfunction due to age-related macular degeneration (Li et al., 2001), retinal vascular occlusion (Wildberger and Junghardt, 2002) and retinal detachment (Sasoh et al., 1998). It has also been demonstrated that in some patients with diabetic retinopathy that the mfERG responses are reduced and delayed (Palmowski et al., 1997); the mfERG can reveal local retinal dysfunction in diabetic eyes before retinopathy is evident (Fortune et al., 1999). It has been suggested that the second-order response components are more sensitive for detection of early changes in retinal function of

diabetes than the commonly used first-order kernel response (Palmowski et al., 1997). However, for retinal diseases where the disorder is restricted to the inner retina (especially the ganglion cell layer), there is no simple correlation between the mfERG and the visual field defect (Kretschmann et al., 2000). This raises questions about how the ganglion cells contribute to the human mfERG and what is the best method to measure this response.

6.7 The mfERG responses in glaucoma patients

Glaucoma is an eye disease which initially damages the inner retina, specifically the ganglion cells (Quigley et al., 1989; Glovinsky et al., 1991; Hare et al., 1999). With the development of the multi-input mfERG technology, attempts have been made to obtain a better assessment of glaucoma in terms of topographical mapping of the field defect. However, it has been shown that the first-order kernel response is derived mainly from the outer retina, especially the ON- and OFF-bipolar responses (Hood et al., 2002), and that the second-order kernel response reflects the mechanisms of temporal interactions in the retina. Retinal processing involves different levels of adaptation processing, and these adaptation mechanisms start in the photoreceptor layer followed by post-receptor feedback mechanisms. It has been believed that the non-linear mechanisms in the retina arise predominantly from the

inner retinal layer (Sutter et al., 1999). However, there is still conflict over the hypothesis that the second-order kernel response components reflect the activities of the retinal ganglion cells (Vaegan and Sanderson, 1997; Yoshii et al., 2001).

Nevertheless, a number of studies have used the mfERG to access the physiological response of the (presumably damaged) ganglion cells in order to detect the signs of glaucomatous damage in terms of amplitude (Chan and Brown, 1999) and implicit time (Hasegawa et al., 2000). In addition, the amplitude changes have been found to affect primarily the central retina (Chan and Brown, 1999), where the latency of mfERG responses showed significant negative correlation with the mean sensitivity value (dB) of static perimetry (Hasegawa et al., 2000). It has been found that the amplitude of the mfERG response is also decreased even in patients with OHT (Chan and Brown, 2000) and the second-order kernel is also abnormal even in glaucoma patients or glaucoma suspects with normal visual field responses (Bears et al., 1996). However, Sakemi and colleagues found that neither the first- nor the second-order kernels of the mfERG showed any changes correlated with glaucomatous visual field abnormalities, and questioned its relationship with inner retinal responses even for the second-order kernel (Sakemi et al., 2002). In fact, outer retinal activity also makes a contribution to second-order responses (Hare and Ton, 2002), and this contribution may complicate interpretation of the retinal changes in

glaucoma. Sakemi and co-workers also reported no difference in the second-order kernel of the mfERG between eyes in glaucoma subjects who only had unilateral visual field abnormalities (Sakemi et al., 2002). This would not be surprising if inner retinal function of eyes with normal visual fields from subjects with unilateral glaucoma were compromised already. Hence, studies could possibly report abnormality in the second-order responses (Chan and Brown, 1999) where it was believed mainly to originate from the inner retinal cells.

Even though the latency changes were found to be more sensitive than amplitude changes in showing glaucomatous visual field defects (Hasegawa et al., 2000), it has been emphasized that mfERG still cannot provide a more sensitive way to detect visual field defects in glaucoma patients than static perimetry, as the loss of sensitivity in visual field occurs before the mfERG latency becomes abnormal (Hasegawa et al., 2000). In conclusion, using the mfERG as an objective method to detect glaucomatous visual field defects still needs further investigation and advancement.

6.8 Inner retinal contribution in mfERG

The mfERG was introduced more than 15 years ago. However, currently unresolved is the extent to which the inner retina contributes to the human mfERG or

the best technique for measuring this contribution. Functional changes of the inner retina due to glaucomatous damage could be detected in an earlier stage before significant loss of retinal nerve fibers if the sensitivity of the mfERG was to be improved.

6.8.1 Evidence of inner retinal contribution in non-human primate mfERG

Experimental ocular hypertensive glaucoma results in a loss of retinal ganglion cells, and this retinal nerve fiber damage results in a marked attenuation of both the first- and second-order primate mfERG responses (Hare et al., 2001); mfERG amplitudes are highly correlated with the density of surviving retinal ganglion cells. These results support the view that mfERG responses reflect the contribution from the ganglion cells. Indeed, the waveform of the mfERG response from monkey is actually quite different from that in humans even for the first-order kernel response. The monkey response has large naso-temporal variation with double peaks in the waveform (Hood et al., 2002). These differences indicate that the cellular contribution of the monkey's mfERG is largely influenced by the inner retina.

A clear demonstration that the inner retina contributed to the monkey mfERG was provided by recording before and after intra-vitreous injections of NMDA and TTX (Hood et al., 1999a; Frishman et al., 2000). TTX blocks the sodium-based-action potentials of ganglion and amacrine cells, and substantially

alters the mfERG from monkeys (Hare and Ton, 2002). TTX also removes the significant naso-temporal variation in the mfERG waveform from monkeys (Hood et al., 1999a). Additional treatment with NMDA demonstrates the amacrine cell component and feedback components since it depolarises the postsynaptic membranes of ganglion and amacrine cells. Another study on monkeys also showed that the effects of experimental glaucoma on the first-order responses and the first slice of second-order responses in mfERG were similar to the effects of TTX and NMDA (Frishman et al., 2000). In addition, the naso-temporal variation and OPs also disappeared in the experimental glaucoma eyes. In other words, the spiking activity of the inner retinal neurons appears to be the cause of the naso-temporal variation across the retina. Although both first- and second-order kernels in primate mfERG have contributions from both outer and inner retina, the inner retina has a relatively greater input to the primate second-order mfERG response (Hare and Ton, 2002). Therefore, in the laser induced experimental glaucoma model, the second-order responses were found to be more sensitive to glaucomatous changes (Raz et al., 2003).

6.8.2 Evidence of inner retinal contribution in human mfERG

Conventionally, most studies have applied the fast stimulation and high contrast mfERG protocol to test for glaucomatous dysfunction (Chan and Brown, 1999; Chan and Brown, 2000). However, no simple correlation of the topographical changes of

the mfERG and the retinal dysfunction observed in field defect has been found when using high contrast mfERG stimulation (Fortune et al., 2001; Sakemi et al., 2002), and the nature of the contribution from the inner retina to the conventional mfERG stimulation is less clear. Thus, different advanced stimulation paradigms have been proposed for glaucoma assessment.

6.8.2.1 The optic nerve head component

The recent most important study was done by Sutter and Bearnse, who demonstrated evidence of the human mfERG response containing a component attributable to ganglion cell activity. As the latency of this component increases in proportion to the estimated length of ganglion cell axons from the site of stimulation to the optic nerve head, it was speculated that this optic nerve head component (ONHC) originated from the axons near the optic nerve head (Sutter and Bearnse, 1999). They found that glaucomatous damage can reduce the magnitude of this component (Sutter and Bearnse, 1999). Although this component exists in the mfERG, it is difficult to observe in most records because it must be extracted from the signal with a complex mathematical algorithm. Sutter and Bearnse also suggested that the human mfERG also consists another component, a retinal component (RC), which has an invariant latency. Within a ring of the same eccentricity around the fovea, the ONHC varies in latency around the ring while the RC is relatively constant in latency.

The latency variation of the ONHC depends on the length of the unmyelinated axons for the transmission of action potentials between the stimulated area and the optic nerve head (Sutter and Bearnse, 1995) (Figure 6.4). It is believed that this causes the naso-temporal variations in the mfERG waveform. It was also found that the response of the ONHC was larger when the active electrode was referenced to the other eye (Sutter and Bearnse, 1999).

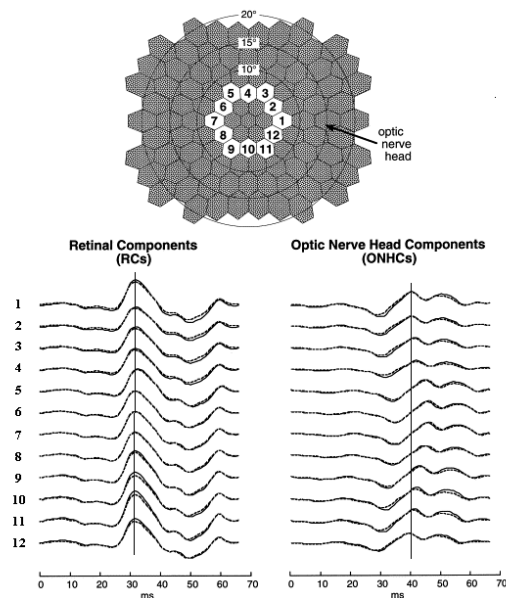


Figure 6.4 Left column of traces: The RC extracted from the first-order waveforms of the second ring. Right column of traces: The ONHC extracted from the first-order waveforms of the second ring. (Adopted from figure in (Sutter and Bearnse, 1999)).

This ONHC theory was also supported by data from the monkey (Hood et al., 2001), where the TTX sensitive component from the mfERG waveform was similar

to the ONHC (Hood et al., 2001). This suggested that this TTX sensitive component was likely to be related to ganglion cell activity. In addition, the marked naso-temporal variation of monkey mfERG was eliminated by pharmacological suppression of inner retinal activity (Frishman et al., 2000) suggesting that the primate ONHC derives from ganglion cells.

6.8.2.2 The low contrast mfERG

Naso-temporal variation also appears in the human mfERG, and this variation is more obvious if the contrast of the stimulus is decreased by 50% (Hood et al., 1999b). This is an important observation as naso-temporal variations in waveform have been hypothesized to be due to ganglion cell activity; this finding indicates that contrast attenuation of the stimulus can increase the relative proportion of the responses coming from the inner retina in the human mfERG (Bears and Sutter, 1998). In addition, under the varied contrast stimulations, the ONHC saturates at a contrast of about 60% while the RC shows a more linear behaviour (Bears and Sutter, 1998).

Therefore, in an attempt to improve the mfERG response from the inner retina for detecting local functional changes, mfERG recordings have been obtained with reduced stimulus contrast (50%) in order to detect glaucomatous retinal changes (Hood et al., 2000a). At this contrast level, the mfERG waveform is similar to that of the monkey with a trough followed by a double-peak. Additionally, for subjects with

glaucoma, the second peak seems to be reduced in amplitude (Hood et al., 2000a; Chan, 2005). Nevertheless, it is not detectable in all OAG patients, and in others with clear changes in the mfERG waveform, the changes are not correlated to the localized visual field losses. Although the first-order response shows changes in OAG with recordings obtained at low stimulus contrast (Palmowski et al., 2000), sensitivity may not be sufficiently increased to detect inner retinal disease under these conditions.

6.8.2.3 The slow-sequence mfERG

In the conventional mfERG, the stimulus is usually displayed on an achromatic monitor with a frame rate of 75 Hz, which means that the time period between two successive stimuli is about 13.3 ms. Recently, a new wavelet in the mfERG has been found when the m-sequence presentation is slowed (slow-sequence mfERG) by interleaving three blank frames between the presentations (Sano et al., 2002), where the time period between two successive frames was increased by four times. The luminance of the hexagon elements in the interval was reduced to a level (appeared grey) and at which the contrast of this luminance level to the white light was equivalent to 50% contrast.

This study reported that a positive wavelet appeared on the trailing edge of the first positive peak of the slow-sequence mfERG. This newly discovered wavelet is more obvious and the amplitude of this new wavelet increased significantly with

introduction of 30 further blank frames between m-sequence frames. Furthermore, the amplitude of this unmasking wavelet obtained from the nasal retina was significantly larger than those from the temporal retina and this naso-temporal variation is also related to the distance from the optic nerve head. The characteristic of this small wavelet, the so-called s-wave, was not observed in eyes with optic neuritis at mfERG recording at any presentation rate. However, it was observed in unaffected eyes in all patients with unilateral optic neuritis. This wavelet reappeared with recovery from the disease and the recovery of the wavelet significantly correlated with the recovery of visual acuity (VA) and the central critical fusion frequency. Thus, these findings support the idea that the new wavelet originates from the ganglion cells (Sano et al., 2002).

OPs in human full-field flash ERGs have long been believed to have an inner retinal origin. Recently, it was found that a slow-sequence mfERG stimulation with three dark frames interleaved between m-sequence presentations would also enhance a small induced response component with high frequency wavelets resembling OPs following the dominant component of the first-order response. This component was believed to result from the response to the following stimulus, similar to the first slice of the second-order kernel response (Bears et al., 2000). Under this condition, major changes of the OPs were observed in glaucoma patients. The OPs reduced

significantly in the central field and in the nasal field for patients with normal tension glaucoma, allowing 85% sensitivity for differentiation from control subjects (Palmowski-Wolfe et al., 2006). Additionally, mfERG waveforms can be made similar to those of the full-field flash ERG by slowing the presentation (Hood et al., 1997). The OPs become prominent and can be divided into fast (143 Hz) and slow OPs (77 Hz) (Rangaswamy et al., 2006). In monkey, the fast OPs are significantly larger in temporal than nasal retina (Rangaswamy et al., 2003; Rangaswamy et al., 2006) and they are reduced in experimental glaucoma with moderate correlation with local visual field sensitivity (Rangaswamy et al., 2006). This was suggested to be most likely related to the activity of retinal ganglion cells (Zhou et al., 2007).

6.8.2.4 The global flash mfERG

Most of the earlier glaucoma studies have used the standard multifocal flickering stimulation. However, some reports have indicated that it can detect human glaucomatous dysfunction (Chan and Brown, 1999; Hasegawa et al., 2000), while others have not (Sakemi et al., 2002). Studies also tried to analyze the changes of the second-order kernel response of glaucomatous dysfunction (Chan and Brown, 1999). Since the inner retina is assumed to contribute to the adaptation mechanism(s) (Sutter et al., 1999), dysfunction of the inner retina may alter the adaptation mechanism(s). However, unlike the first-order kernel responses, the second-order kernel responses

depend on the effect of the preceding flash, which is obtained by adding all the records following a change from either white to black or black to white and subtracting all records with no change in stimulus. Nonetheless, the signal-to-noise ratio is usually poor for the higher-order kernel responses. Some recent approaches using the mfERG paradigm with global flash technique, the interaction between a focal flash and a global flash, have been introduced to evoke a large non-linear mfERG component (Sutter et al., 1999). The hypothesis here is that if the global flash does not produce any adaptive effect, it would not contribute to the mfERG response, as its contribution would be cancelled when the focal responses were extracted (Figure 6.5).

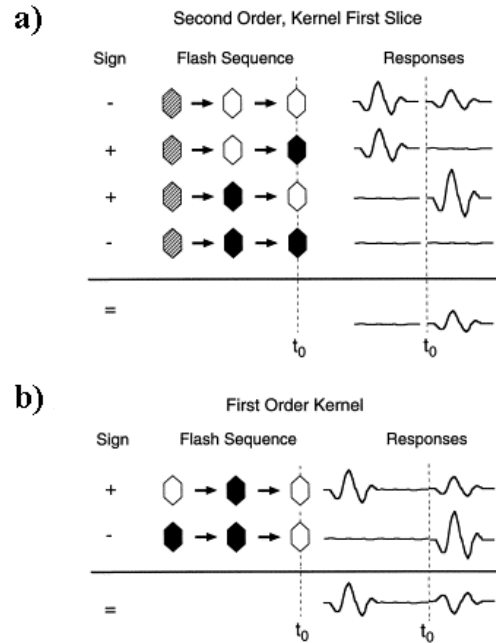


Figure 6.5 Schematic comparison for the signal derivation of (a) the first slice of second-order kernels of the conventional mfERG and (b) the first-order kernels of the global flash mfERG (Adapted from figures in (Sutter and Bearnse, 1999)).

There are two response components to the global flash mfERG stimulation: a direct component (DC) and an induced component (IC). The DC is analogous to a conventional mfERG response, while the IC is the change in the response to the global flash produced by the prior local flash. This non-linear component represents the adaptive changes in the response and it is also believed that it is generated by the inner retina (Sutter et al., 1999). There are different approaches for enhancing these non-linear retinal responses and most studies have used the simplest paradigm, interposing only one periodic global flash between the two multifocal flashes

(Shimada et al., 2001; Fortune et al., 2002a; Feigl et al., 2005; Shimada et al., 2005; Chen et al., 2006); others use multifocal flash stimulation with two (Palmowski-Wolfe et al., 2007), or three periodic global flashes (Palmowski et al., 2002). The global flash technique, although with different protocols, has been claimed to exhibit a large ONHC (Sutter et al., 1999; Sutter et al., 2001a), and the naso-temporal response asymmetries are more easily observed in the IC of the human global flash mfERG (Fortune et al., 2002a). It has also been shown that the loss of the ONHC in glaucoma is more apparent with this technique (Fortune et al., 2002a), and that the IC is affected in glaucoma (Palmowski et al., 2002; Palmowski-Wolfe et al., 2007). Although, the IC amplitude in the nasal retinal response has been found to be most affected in glaucoma (Palmowski et al., 2002), a small oscillation in the temporal retinal IC response was also found to be sensitive in glaucoma detection (Fortune et al., 2002a). A more recent study found that the IC of the superior temporal retinal response is the most sensitive parameter for glaucoma differentiation (Palmowski-Wolfe et al., 2007). The different outcomes may possibly be due to the different global flash protocols used that may elicit different adaptation activities.

The receiver operating characteristic (ROC) illustrates the balance between sensitivity and specificity for the discrimination of glaucoma subjects from normal subjects; the IC response can provide a sensitivity of 85% in detection of POAG

patients with a specificity of 80% under a “two global flash” paradigm (Palmowski-Wolfe et al., 2007). This result compares well with another study using “one global flash” stimulation protocol, allowing glaucoma subjects to be identified with a sensitivity of 75% and a specificity of 83% (Fortune et al., 2002a). The IC response in the human mfERG seems to provide high sensitivity in detecting glaucomatous retinal dysfunction, but the correlation with the corresponding visual field parameters is not yet well defined (Fortune et al., 2002a; Palmowski et al., 2002). The large intersubject variation of the IC (Shimada et al., 2001) has limited the possibility for the assessment of localized glaucomatous damage in individual patients.

In contrast, only a few studies have been conducted to investigate the characteristics of the DC. So far, the DC has been suggested to be sensitive to early changes in age-related maculopathy (Feigl et al., 2005) or diabetic retinopathy (Shimada et al., 2001), and it may also show certain optic nerve head response contributions (Sutter et al., 1999). Indeed, the global flash paradigm actually provides an interaction between the multifocal flashes and the periodic global flash. Although it has been pointed out that the DC is analogous to a mfERG response using the conventional flickering protocol (Sutter et al., 1999), the DC is also believed to reflect a certain level of light adaptation produced by the periodic global flashes (Shimada et

al., 2005). In addition, since the shape of the DC response is different from that obtained with conventional mfERG stimulation (Fortune et al., 2002a), it may also reflect certain nonlinear retinal activity.

6.8.2.5 Future approaches

The mfERG has been applied in an attempt to detect early glaucomatous dysfunction for a number of years, and its sensitivity has increased dramatically over the past years with better knowledge of its cellular components and the nonlinear mechanisms that shape the mfERG waveform. While the inner retinal contribution to the mfERG has been enhanced by modifying the stimulus parameters, a reliable quantitative measurement for early discrimination of glaucomatous damage has not been developed. If the sensitivity of the mfERG could be further increased, the application of mfERG in the early diagnosis of glaucoma should be possible. An alternative approach with advanced exploration of mfERG paradigms will be necessary to improve the sensitivity and specificity of the mfERG, where the possibility for the assessment of localized glaucomatous damage in individual patient should also be improved. Therefore, a new approach in mfERG measurement by consolidation of the models previously reviewed will help to further enhance the assessment of the inner retinal contribution in mfERG responses for early diagnosis of glaucoma.

The aim of this study is to combine the luminance-modulation effect (variation of contrast level) in the global flash mfERG stimulation in order to investigate if this new protocol can help in glaucoma assessment, especially the early detection of the glaucomatous functional damage. We hypothesize that this stimulation can further enhance the inner retinal contribution in the human mfERG which is a major component usually influenced by glaucomatous changes.

PART II

EXPERIMENTS

Chapter 7

Experiment I

**Glaucoma Detection is Facilitated by
Luminance-Modulation of the Global Flash mfERG**

(Invest Ophthalmol Vis Sci. 2006; 47 (3):929-37)

Abstract

Purpose

To investigate the variation of retinal electrophysiological function in glaucoma by using the global flash mfERG stimulation with altered differences in the stimulus luminance of the multifocal flashes, in an attempt to alter the levels of inner retinal contributions.

Methods

The mfERG was assessed with a visual stimulus in steps of four video frames, which consisted of 103 hexagonal elements followed by a dark frame, global flash, and dark frame. The localized luminance-difference was set at 96%, 65%, 49% or 29% stimulus contrast. Thirty subjects with glaucoma and 30 age-matched normal subjects were recruited for visual field and mfERG measurements.

Results

This stimulus induces complex local first-order responses with an early DC and a later IC. The luminance-modulated response functions of the DC and IC responses showed markedly different behavior. The central DC, central and peripheral IC showed a linear dependence on luminance-difference, whereas the peripheral DC was saturated for higher luminance-differences. This saturation became less obvious in subjects with glaucoma mostly because of greater reduction of the response amplitude

in the mid luminance-difference level. An “adaptive index” was calculated from the luminance-difference dependence of the peripheral DC, and it showed a sensitivity of 93%, with a specificity of 95% for differentiating normal from glaucomatous eyes, and also had a significant correlation ($r = 0.58$) with the glaucomatous visual field defect.

Conclusions

The peripheral DC luminance-modulated response function is altered by the adaptive mechanism that is induced by the global flash; the reduction of the adaptive index may relate to an abnormal adaptive mechanism, presumably due to inner retinal damage. Glaucoma appears to produce large reductions of the adaptive index which correlate with field defects.

Introduction

The mfERG has been developed to study and diagnose diseases of the human retina (Sutter and Tran, 1992) and to investigate retinal processing mechanisms (Smith et al., 2002). Recent studies have found that human first-order mfERG responses with the conventional m-sequence protocol are mainly generated from distal retinal layers (photoreceptors and bipolar cells) (Hood et al., 2002). It was suggested that functional disorders of the outer retinal layers can be described by this technique and that defective patterns of mfERG responses may be similar to patterns of visual field defects (Kretschmann et al., 2000).

For retinal diseases restricted to the inner retinal layers, there appears to be no simple correlation between the mfERG and visual field defects (Kretschmann et al., 2000). There are conflicts in the literature regarding the early detection of glaucoma (Quigley et al., 1989; Glovinsky et al., 1991; Hare et al., 1999). Findings in some studies support (Chan and Brown, 1999; Chan and Brown, 2000; Hasegawa et al., 2000), whereas those in other studies fail to support (Sakemi et al., 2002), the use of the mfERG to detect glaucoma. Changes in the mfERG are not easily detected in all patients with glaucoma, whereas in others, these changes are not related directly to the visual field losses (Hood et al., 2000a). Different stimulation and analysis techniques in mfERG measurement probably contribute to this disagreement.

However, evidence has been presented for a response generated from the ganglion cell fibers near the optic nerve head, and it has been shown that glaucoma can affect this ONHC (Sutter and Bearnse, 1999). Hood and his colleagues (2001) essentially replicated this in the monkey (Hood et al., 2001). Unfortunately, the commonly used mfERG m-sequence stimulus elicits an ONHC with a relatively poor signal-to-noise ratio and the ONHC must be extracted from mfERG signals by the use of complex processing.

To enhance the contribution of the ONHC to the mfERG, an alternative stimulus mode has been developed that is thought to elicit a relatively larger inner retinal response. A paradigm including global flashes has been introduced to evoke a large nonlinear component (Sutter et al., 1999; Bearnse et al., 2001b; Shimada et al., 2001; Sutter et al., 2001b; Fortune et al., 2002a; Palmowski et al., 2002). Fortune and his colleagues (2002a) showed that the loss of the ONHC in glaucoma was more apparent, even by use of the simple global flash stimulation sequence (multifocal flash, dark frame, global flash, dark frame, and so forth).

There are two response components (DC and IC) in the mfERG waveform from this global flash paradigm. The IC is the change in the response to the global flash produced by the prior local flash. It appears to be a nonlinear response, which is thought to originate predominantly from the inner retina (Sutter et al., 1999).

However, the large intersubject variability of the IC (Shimada et al., 2001) and the poor correlation between the localized IC responses and the visual field defects (Fortune et al., 2002a) has prevented so far the localized assessment of glaucomatous damage in individual patients.

Only a few studies have been conducted to investigate the characteristics of the DC, although it has been suggested to be sensitive to early changes in diabetic retinopathy (Shimada et al., 2001), and it may show certain optic nerve head response contributions (Sutter et al., 1999). The global flash paradigm actually provides an interaction between the multifocal flashes and the periodic global flash. Although it has been pointed out that the DC is analogous to a standard mfERG response (with conventional flickering protocol) (Sutter et al., 1999), the DC is also believed to reflect certain light adaptation produced by the periodic global flashes (Shimada et al., 2005). In addition, because the shape of the DC is different from that obtained with a conventional mfERG stimulation (Fortune et al., 2002a), it is likely to contain a nonlinear response component.

The magnitude of the ONHC response saturates at approximately 60% contrast (Bears and Sutter, 1998) and a reduction in stimulus contrast to 50% has been attempted to increase the relative contribution of ONHC to the mfERG response (Hood et al., 2000a; Palmowski et al., 2000). Hence, in this experiment, patients with

glaucoma and age-matched control subjects were examined by application of the global flash mfERG stimulation with altered stimulus luminance-difference in the multifocal flashes, in an attempt to measure the inner retinal signals at different luminance adaptation levels.

Methods

Subjects

Thirty normal Chinese subjects age ranged from 23 to 56 years (mean, 36.9 ± 12.2 years), without any reported systemic or ocular diseases were recruited. All had best corrected VA of logMAR (logarithm of the minimum angle of resolution) 0.0 or better (Range of refractive errors: between +1.0 and -4.0 DS and less than -1.0 DC). An eye examination was performed to exclude ocular abnormalities. All subjects had cup-to-disc ratios < 0.4 with normal neural rim appearance and similar optic discs in both eyes. Intraocular pressures were less than 21 mmHg (Goldmann tonometer: Haag-Streit AG, Bern, Switzerland). All subjects had open anterior angles, no family history of any eye diseases, and no visual field defects detected by the central 30-2 threshold visual field test (Visual Field Analyser: Humphrey; Carl Zeiss Meditec, Inc., Dublin CA). One eye of each subject was randomly selected for testing.

Thirty Chinese POAG patients, age ranged from 19 to 53 years (mean, 39.4 ± 11.5 years), without any systemic diseases were also recruited. All had diagnosed glaucoma of more than 2 years' duration. Their both eyes were being treated with either latanoprost (Pfizer Corp., New York) or timolol maleate (Alcon, Ltd., Fort Worth, TX) which were prescribed by their own ophthalmologists. An eye examination was performed to exclude ocular abnormalities in addition to glaucoma.

One eye of each patient was randomly selected for testing. Patients had long-standing binocular glaucomatous visual field loss as measured by the central 30-2 threshold test (Humphrey; Carl Zeiss Meditec, Inc.), and one or more quadrants of the field of the tested eye was involved in the defect (mean defect [MD] = -7.79 ± 5.76 dB). The best corrected VA of the tested eye was 0.1 logMAR or better (Range of refractive errors: between +1.0 and -4.0 DS and less than -1.0 DC). The cup-to-disc ratios of the tested eyes were greater than 0.65.

All research procedures adhered to the tenets of the Declaration of Helsinki and were approved by the ethics committee of The Hong Kong Polytechnic University. All subjects were fully informed of the possible risks and gave written, voluntary consent.

Stimulus conditions

Experiment 1a. Ten normal subjects participated in this experiment. The stimulus pattern was presented on an RGB 19-inch monitor (model GDM-500PS; Sony, Tokyo, Japan); and a computer (Macintosh G3, Apple Computer, Cupertino, CA) was used to run an mfERG program (VERIS 4.1; EDI, San Mateo, CA). The working distance was 30 cm where the hexagonal stimulus pattern subtended 42° vertically and 48° horizontally. The mfERG was measured using the global flash paradigm of

Fortune et al. (2002a) with modification. The pattern consisted of 103 hexagons, scaled with eccentricity and each m-sequence of the stimulus contained four video frames (each frame lasts 13.3 ms with a 75 Hz frame rate). During the stimulation with multifocal flashes, each hexagon was either bright or dark, according to the binary m-sequence, and the stimulus contrast of the display was set at 96%, 79%, 65%, 49%, 40%, or 29%. In addition to the multifocal flashes, the global flash paradigm contains a dark frame, a full screen global flash, and a second dark frame between successive m-sequence stimulations (Figure 7.1). This modified global flash paradigm is actually set up to measure the adaptive changes in the retina using luminance-modulation; thus, the luminance-difference of the multifocal flashes should be denoted 2.12, 1.74, 1.42, 1.08, 0.86 and 0.62 $\text{cd}\cdot\text{s}/\text{m}^2$. The average luminance of the multifocal flashes was approximately 1.11 $\text{cd}\cdot\text{s}/\text{m}^2$, and the background was also set to this luminance. After the multifocal flashes, the entire stimulus pattern was dark ($0.04 \text{ cd}\cdot\text{s}/\text{m}^2$) for one frame and then there was a global flash ($2.16 \text{ cd}\cdot\text{s}/\text{m}^2$) followed by a dark frame. The recording time for each stimulation cycle was approximately 8 minutes with a 2^{13} binary m-sequence. The recording process was divided into 16 slightly overlapping recording segments, and a rest period was allowed between segments. The order of the six stimulus conditions across subjects was randomized.

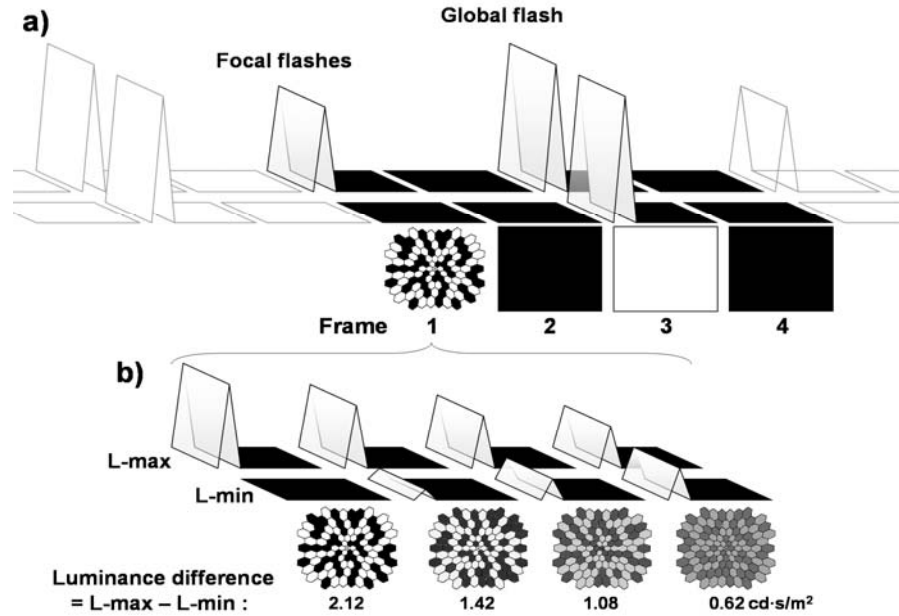


Figure 7.1 (a) The stimulus sequence (one element of the m-sequence) contains four frames. The initial frame (multifocal flashes) alternates between light and dark according to a pseudorandom binary m-sequence with a preset contrast level. After each initial frame of the four-frame set, a global flash ($2.16 \text{ cd}\cdot\text{s}/\text{m}^2$; frame 3) was applied, separated by a pre- and post-dark frame ($0.04 \text{ cd}\cdot\text{s}/\text{m}^2$; frames 2 and 4). As the number of flashing elements in frame 1 involved half of the total number of hexagons, the average luminance in the global flash (frame 3) is twice as bright as frame 1. (b) The luminance-difference between the brighter luminance hexagons and the dimmer luminance hexagons ($L_{\max} - L_{\min}$) of the multifocal flashes in four stimulus contrast settings are denoted 2.12, 1.42, 1.08, and $0.62 \text{ cd}\cdot\text{s}/\text{m}^2$.

Experiment 1b. Thirty normal subjects and 30 subjects with glaucoma participated in this modified experiment. The stimulus was the same scaled

103-hexagon pattern that was displayed on the same monitor as in experiment 1a. Viewing parameters and luminance of the stimuli were as for experiment 1a. According to the result from experiment 1a, mfERG responses were recorded with four stimulus luminance-difference conditions of the multifocal flashes set at 2.12, 1.42, 1.08 and 0.62 cd·s/m². The recording time for each stimulation cycle was approximately 8 minutes and a 2¹³ binary m-sequence was also used. In other respects the recording process was the same as for experiment 1a.

Recording conditions

Before testing, the pupil of the tested eye was fully dilated, to at least 7 mm diameter, with 1% tropicamide (Alcon, Fort Worth, TX). DTL electrodes were used as the active electrode and gold-cup surface electrodes were used for both reference (located 10 mm lateral to the outer canthus of the test eye) and ground (located at the central forehead). During the mfERG recording, the untested eye was occluded. The refractive error of the tested eye was fully corrected with a 70mm diameter uncut ophthalmic lens for the viewing distance, where the optical center of the lens was aligned with the pupil center. The signal was amplified using an amplifier (band pass: 10 to 300 Hz; gain: x100,000; model P511K; Grass-Telefactor, West Warwick, RI). The measurement was monitored using the signal shown online by mfERG program

(VERIS; EDI); any recording segments contaminated with blinks or small eye movements were rejected and immediately re-recorded.

Data analysis

First-order kernels were analysed using with the system software (VERIS 4.1; EDI). In experiment 1a, the mfERG findings were presented using a peak-to-peak response amplitude measurement; the responses from different stimulus conditions were plotted as a function of luminance-difference. In experiment 1b, the way in which these functions varied from the normal response in subjects with glaucoma was observed. These response functions were also compared with the visual field defect by quadrants.

Results

Responses from six concentric rings

The traces in [Figure 7.2a](#) are typical normal ring responses grouped according to retinal eccentricity. To facilitate the comparison of waveforms, normalized responses with equal root-mean-square amplitudes were used. The DC in the central region contained a main trough at 15 ms and a main peak at 35 ms, with a very small peak at ~45 ms, similar to the photopic full-field flash ERG responses. In the periphery, the DC still shows a double-peak with faster latency, P1 at 30 ms and P2 at 40 ms. The IC waveforms from central to peripheral regions are similar and contain two peaks (P3 at 55 ms and P4 at 65 ms; faster latencies are seen in the periphery) with a triphasic shape, which is quite similar to the second-order kernel response recorded from the conventional mfERG stimulation.

There is an obvious difference in the P1 waveform between central and peripheral regions. A delayed N1 seems to be observed in the peripheral region and this happens even in localized responses ([Figure 7.2b](#)). All the responses from various luminance-difference stimulus conditions, either from normal subjects or those with glaucoma show similar wave patterns and have a good signal-to-noise ratio.

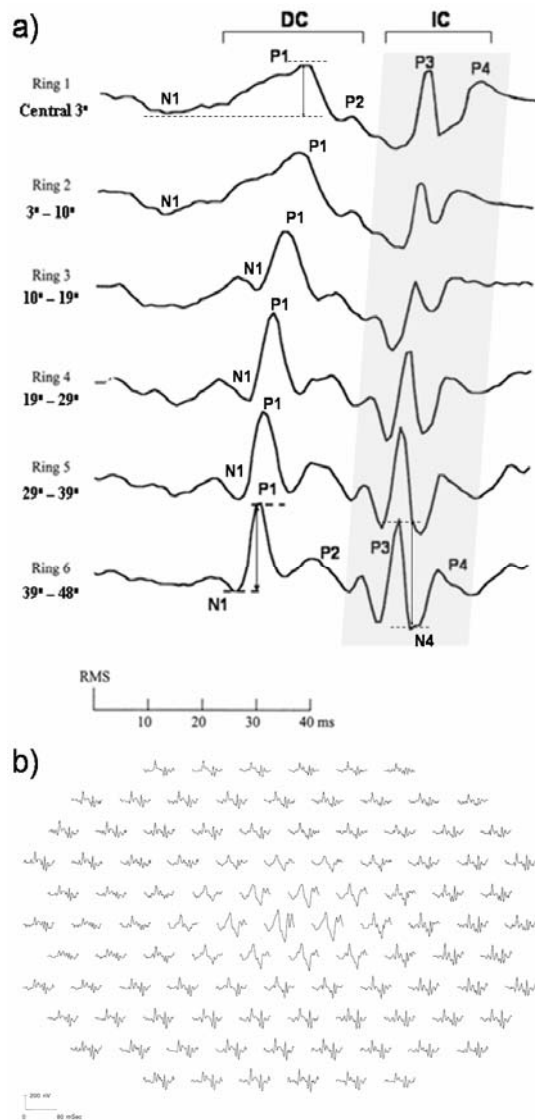


Figure 7.2 (a) An example of the averaged concentric ring responses from a 2.12 $\text{cd}\cdot\text{s}/\text{m}^2$ luminance-difference stimulation using the global flash stimulus paradigm from one typical subject. Ring 1 is the macular response; where ring 6 is the most peripheral averaged response. All the averaged ring responses contain two components: DC and IC. P1 to P4 represent four major peaks obtained in the responses from the central and peripheral regions. Measurement of the peak-to-peak amplitudes of the two components is illustrated, where P1 and P3 are the peaks that were used for the analyses of DC and IC, respectively. (b) Localized responses of 103 traces are also demonstrated.

The luminance-modulated response functions of the amplitude of the DC and IC response (measured as N1-P1 and P3-N4 as shown in [Figure 7.2a](#)) from ring analysis showed markedly different behaviors ([Figure 7.3](#)). The DC responses from the central two rings show a linear function with increasing luminance-difference, whereas the DC responses from the peripheral three rings seem independent of the luminance-difference beyond $1.1 \text{ cd}\cdot\text{s}/\text{m}^2$ luminance-difference and become relatively steady in their responses. Ring 3 appears to be a region of transition between the central and peripheral regions. In contrast to the independence of the luminance-difference shown in the peripheral DC response, the IC responses increase linearly with increased luminance-difference for all six rings.

Luminance-modulated response function of DC and IC in different ring responses

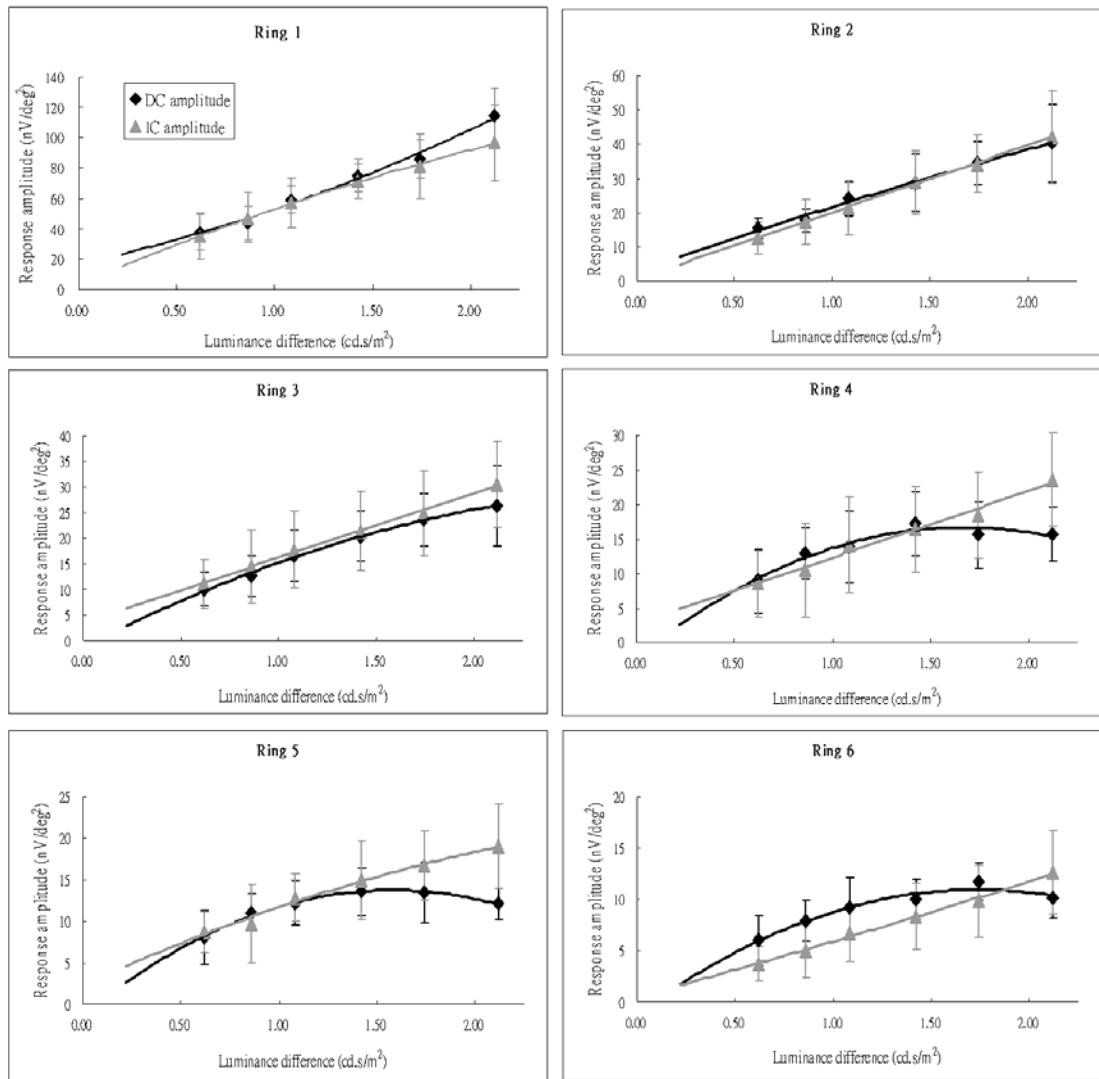


Figure 7.3 The luminance-modulated response functions of the DC and the IC from different ring analyses are illustrated. Ring 1 is the macular response and ring 6 is the most peripheral averaged response. Lines: second-order best-fitting curves. Error bars, ± 1 SD.

Summed peripheral responses

Because the glaucomatous visual field defects occurred in the Bjerrum area, the peripheral mfERG responses were analyzed in this experiment. The responses from

the three peripheral rings were grouped due to their similarities in waveform and latency, as well as their similar characteristics in the luminance-modulated response function. **Figure 7.4** shows the modified luminance-modulated response function obtained from both normal and subjects with glaucoma. Subjects with glaucoma showed a statistically significant decrease in peripheral DC response amplitude at all luminance-difference levels compared with the control subjects (**Figure 7.4a; Table 7.1**). The largest decreases in response amplitudes are at the mid luminance-difference levels that make the response function show a loss of the luminance-difference independence characteristic seen in normal subjects.

Subjects with glaucoma also show a statistically significant decrease in peripheral IC responses at all luminance-difference levels compared with the control subjects. The largest differences are at the high luminance-difference levels. The luminance-modulated response function in subjects with glaucoma increases linearly with increasing luminance-difference level but with a lower slope than does the control subject group (**Figure 7.4b; Table 7.1**).

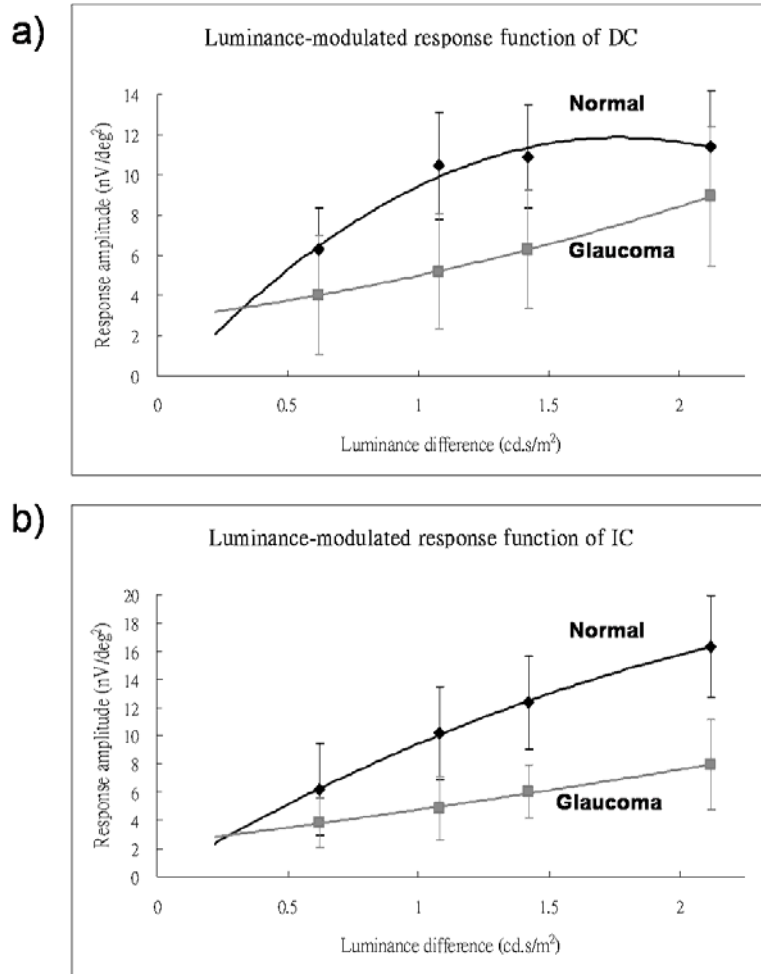


Figure 7.4 The modified luminance-modulated response function (with four points instead of six points, with selection guided by the results from experiment 1a) of the peripheral grouped **(a)** DC and **(b)** IC responses (ring 4 to ring 6) from normal subjects and those with glaucoma. Lines: second-order best-fitting curves. Error bars, ± 1 SD.

a) Direct component

Luminance-difference level	2.12 cd·s/m ²	1.42 cd·s/m ²	1.08 cd·s/m ²	0.62 cd·s/m ²
Normal (nV/deg ²)	11.44 ± 2.79	10.90 ± 2.52	10.46 ± 2.63	6.31 ± 2.02
Glaucoma (nV/deg ²)	8.88 ± 3.53	6.29 ± 2.98	5.25 ± 2.87	4.02 ± 3.04
One-way repeated measures ANOVA	F = 33.321			
	df = (7, 239)			
	p < 0.0001			
<i>Post-hoc</i> test (Bonferroni)	t = 3.679	t = 6.643	t = 7.498	t = 3.290
	p < 0.01	p < 0.001	p < 0.001	p < 0.01

b) Induced component

Luminance-difference level	2.12 cd·s/m ²	1.42 cd·s/m ²	1.08 cd·s/m ²	0.62 cd·s/m ²
Normal (nV/deg ²)	16.31 ± 3.63	12.36 ± 3.29	10.19 ± 3.30	6.20 ± 3.25
Glaucoma (nV/deg ²)	7.96 ± 3.15	6.06 ± 1.88	4.82 ± 2.27	3.85 ± 1.74
One-way repeated measures ANOVA	F = 67.330			
	df = (7, 239)			
	p < 0.0001			
<i>Post-hoc</i> test (Bonferroni)	t = 11.447	t = 8.642	t = 7.353	t = 3.226
	p < 0.001	p < 0.001	p < 0.001	p < 0.01

Table 7.1 The statistical analytic result of the response (peak-to-peak) amplitudes of (a) DC and (b) IC in the periphery between the glaucoma group and normal group at the four luminance-difference levels.

Peripheral quadrant responses

The relationship between the peripheral mfERG response amplitude and the visual field defect was evaluated by comparing the measurements averaged within each quadrant. The peripheral mfERG response amplitudes were averaged into four

quadrants, and the MD of the visual field thresholds were also averaged by corresponding quadrants, but only the points beyond 10° were included in order to provide similar field dimension for comparison (Figure 7.5a). Figure 7.5 shows the response amplitudes for the DC (Figure 7.5b) and the IC (Figure 7.5c) for all four stimulus conditions plotted against the MD in every quadrant. The normal results (DC or IC) for all four quadrants were similar for each stimulus condition (one-way repeated measures ANOVA; $p > 0.05$, for all four stimulus conditions).

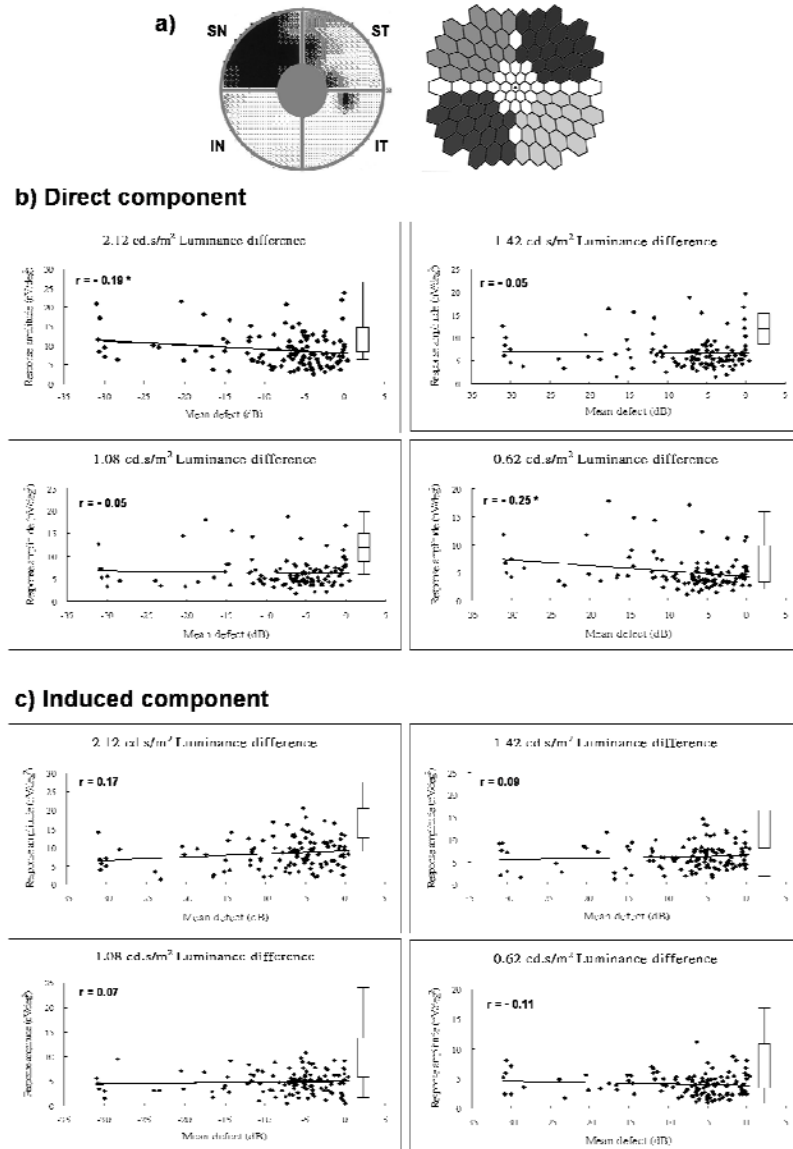


Figure 7.5 (a) The peripheral mfERG response amplitudes were averaged into four spatial quadrants in corresponding visual field quadrants. The central 10° region was omitted. The response amplitudes of (b) DC and (c) IC are plotted against the visual field MD according to the visual field quadrants. The box plots at the right of each graph show normal values: middle line, the mean; top and bottom box edges, one SD; top and bottom bars, the range; solid lines, the best-fit line of the points showing the relationship between the mfERG amplitude and the visual field MD. (*) Correlation coefficients are statistically significance, but both are negative and of little clinical significance.

Although the subjects with glaucoma show significant reductions in both DC and IC amplitudes in quadrant analysis compared with the normal group (one-way repeated-measures ANOVA; $p < 0.05$, for all four stimulus conditions), none of the responses shows any correlation between mfERG amplitudes and visual field defect at any luminance-difference level (Figure 7.5). However subjects with glaucoma showed a specific change in the DC luminance-modulated response function. We have developed an adaptive index, by calculating the area indicating the degree of saturation of the DC luminance-modulated response. This index is calculated by subtracting the area under the line joining the responses from 0.62 to 2.12 $\text{cd}\cdot\text{s}/\text{m}^2$ luminance-difference from the area under the luminance-modulated response function fitted with a second-order best-fit line in this region (Figure 7.6a). The loss of dependence on the luminance-difference in the luminance-modulated response function in those glaucoma subjects is shown in a reduction of the adaptive index. Figure 7.6b shows a plot of the adaptive index against the MD of the visual field defect in every quadrant. The normal values of the adaptive indices for all four quadrants were similar (one-way repeated-measures ANOVA; $p = 0.19$); the normal range is shown by a box plot at the right of the graph. The adaptive indices among quadrants from the subjects with glaucoma show statistically significant reductions (unpaired t-test; $p < 0.0001$) from the normal values.

Adaptive index = Area under curve – Area under line

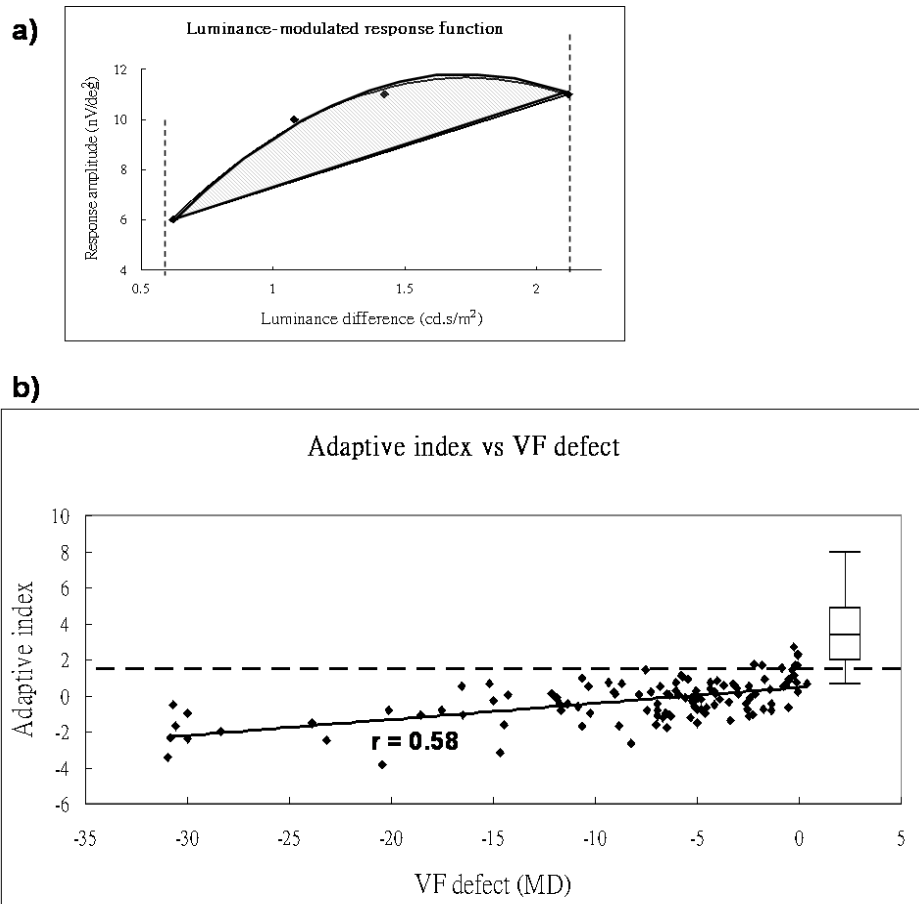


Figure 7.6 (a) Shaded area: the adaptive index of the DC response. It is calculated as the difference between the area under the curve (plotted using the second-order best-fit curve of the responses) and the area under the line (plotted joining the two values at the points at 2.12 and 0.62 $\text{cd}\cdot\text{s}/\text{m}^2$ luminance-difference). (b) The adaptive indices from all quadrants plotted against the visual field MD in corresponding visual field quadrants. Box plot at the right: normal values; solid line: the best-fit line of the points showing a statistically significant correlation ($r = 0.58$) between the adaptive index and the visual field MD and this correlation is also clinically significant; dotted line: the cutoff value of the adaptive index based on the ROC curve in Figure 7.7 (adaptive index = 1.5).

The adaptive index shows good differentiation between the two groups. **Figure 7.7** shows the ROC curve based on different cutoff values of the adaptive index. This ROC curve illustrates the balance between sensitivity and specificity for the discrimination of subjects with glaucoma from normal subjects. The area under the ROC curve provides an index for quantifying the accuracy of the test (where 1.0 is a perfect result). The area under this ROC curve is 0.986, which is close to a perfect test. The sensitivity would be 93% with a specificity of 95% using the best cutoff adaptive index value of 1.5 based on this ROC curve. Correlation of the adaptive index with the visual field defect is statistically significant ($r = 0.58$, $p < 0.0001$), whereas the mfERG amplitude measures do not correlate with the visual field measures. Differentiation of glaucoma from normal subjects using the adaptive index is shown in **Figure 7.6b**, where the horizontal dotted line shows an adaptive index of 1.5.

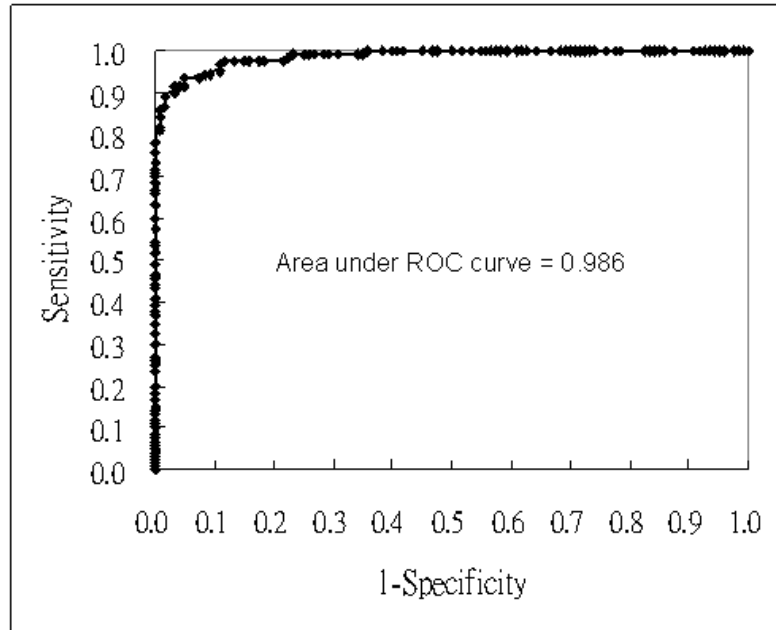


Figure 7.7 ROC plot derived from different cutoffs of the adaptive index. The adaptive index cutoff of 1.5 provides the best differentiation between the normal and glaucoma groups, and gives a sensitivity of 93% with specificity of 95%.

Discussion

This modified global flash paradigm with luminance-modulation is designed to measure the adaptive changes in the retina. Inserting a global flash in the m-sequence stimulus adjusts the overall adaptation level, so that these adaptation effects add to the higher-order kernels of the m-sequence response (Shimada et al., 2005). The DC is the response of the local flashes influenced to a degree by the global flash in the prior m-sequence stimulation, and the IC is the change to the response of the global flash produced by the current m-sequence stimulation (Sutter et al., 1999). Both components reflect interaction between the m-sequence stimulus and the global flash (Shimada et al., 2005) and are likely to be affected by the luminance-modulation of the multifocal flashes.

For high luminance-difference m-sequence stimulation, we have shown the different characteristics of the DC in the central (within 10°) and peripheral (beyond 19°) regions of the retina. The difference of the central response seems to be made by the overlapping of a component that is relatively larger and later than that in periphery, just before P1 (Figure 7.2a). The ascending edge of the central P1 waveforms appears to have been combined by this component, whereas separation of this component from the P1 seems to have occurred in the peripheral responses. The variations of the DC waveform with eccentricity may reflect different adaptive mechanisms across the

retina, and this phenomenon is not shown in the first-order response with conventional flickering stimulation (Sutter and Tran, 1992), where there is no constant adaptive flash. This regional change in responsiveness may be caused by variation in the rod/cone mix with eccentricity, change in the ways in which receptors and receptive fields are connected, and different responsiveness to changes in overall luminance.

The first-order response of the conventional m-sequence stimulation appears to be linearly dependent on the changes of luminance-difference in the response (Brown and Yap, 1996). However, in a more complex interaction with the global flash stimulus, only the peripheral DC response appears to be independent of the luminance-difference changes, where the DC response seems to remain steady at high luminance-difference levels. This implies that this nonlinear response function curve is altered by the adaptive mechanism that was induced by the global flash. The different nature of the luminance-modulated response function between the central and peripheral retina suggests that the global flash adaptive effect may have different cellular bases in these regions, as relatively pure P1 without an overlapped prior component can be obtained in the peripheral regions.

In this experiment, the IC response was also influenced by the luminance-modulation of the multifocal flashes. The response decreased with decreasing luminance-difference of the multifocal flashes, even though the mean

luminance was constant. This result is not surprising, because each local flash of the multifocal frame not only elicited a particular response, it also affects the following global flash response at the same location. The IC response thus depends on the adaptive effect elicited by the luminance intensity of the local flashes (Shimada et al., 2005), but not the mean focal luminance.

The fast-adapting mechanisms that induce the IC are thought to be located predominantly in the inner retinal layers because of its nonlinear characteristics (Sutter et al., 1999; Shimada et al., 2001; Fortune et al., 2002a; Palmowski et al., 2002), and probably have contributions from the ONHC (Sutter et al., 1999; Bearse et al., 2001a; Sutter et al., 2001b). Results of previous studies have suggested that the reduction of the IC in subjects with glaucoma seems indicative of impaired adaptive effects due to inner retinal damage (Palmowski et al., 2002), even though the variations of the IC amplitudes do not show any spatial correspondence to visual field sensitivity (Fortune et al., 2002a). Similar results have been shown for all luminance-difference levels in this experiment. However, as mentioned earlier, the DC should still have a certain adaptive effect while it contains contribution(s) from the ONHC (Sutter et al., 1999).

Impaired adaptive effects due to inner retinal damage may also affect the DC response, and the changes of the DC have been reported in diabetic patients (Shimada

et al., 2001). However, no previous study has shown any relationship between the DC response and glaucoma. It was speculated that this may be related to the different characteristics between the luminance-modulated response function of the DC and IC. The normal DC responses remain steady at high luminance-difference levels, but in subjects with glaucoma, the DC responses show less reduction in amplitude at high stimulus luminance-difference conditions than at mid stimulus luminance-difference conditions. In contrast, the IC responses show a larger reduction in amplitude under high stimulus luminance-difference conditions. Because most previous studies have only used a high stimulus luminance-difference condition for global flash stimulation (Bears et al., 2001a; Palmowski et al., 2002), this may explain why the amplitude changes of the DC responses from those glaucoma subjects were difficult to observe when compared with the IC response.

In this experiment, the reduction of the DC amplitude at the mid luminance-difference level enhances the loss of the luminance-difference saturation of the DC luminance-modulated response function in subjects with glaucoma. To enhance differentiation between normal and glaucomatous eyes, previous studies have suggested that decreased stimulus contrast increases the relative contribution of the inner retina to the mfERG signal (Bears and Sutter, 1998), and stimuli of reduced stimulus contrast have been used in an attempt to detect glaucoma (Hood et

al., 2000a; Bearse et al., 2001a; Palmowski et al., 2002; Raz et al., 2002). However, in this experiment, the DC response amplitudes even at the mid luminance-difference level still did not demonstrate any good correlation with visual field defect; hence, the mfERG response amplitude alone is not likely to be a useful measure.

Alternatively, the mfERG response is a measurement related to rapid adaptive processing, and any dysfunction of this processing can provide an early indication of disease (Hood et al., 1998). The inner retinal layer is believed to be damaged early in glaucoma (Glovinsky et al., 1991; Desatnik et al., 1996; Anderson and O'Brien, 1997; Klistorner and Graham, 1999a); Morgan (2002) also showed that the M ganglion cells do undergo shrinkage before cell death. The widespread morphological changes affect the physiological behavior of these neurons and thus may affect short-term retinal adaptive mechanisms (Bearse et al., 2001b; Sutter et al., 2001b; Fortune et al., 2002a; Palmowski et al., 2002). Besides mfERG amplitude reduction, subjects with glaucoma in this experiment also showed a loss of luminance-difference saturation in the DC luminance-modulated response function. This feature most likely depends on the short-term fast-adaptation mechanism due to the interaction of global flashes. However, the loss of this feature may also be due to a generalized loss of function of the neurons which respond to these input signals; thus, the abnormal changes that occur in

glaucoma probably reflect a combination of factors.

Nevertheless, it is intriguing that these patients showed a specific loss for the luminance-modulated response function, across a wide range of luminance-difference levels. Quantifying this loss by calculating the adaptive index showed good differentiation between the normal subjects and those with glaucoma and also showed a good correlation to the glaucomatous visual field defect.

The ROC curve shows that this method provides good sensitivity and specificity in differentiating normal subjects and those with suspected glaucoma. The adaptive index in some normal field quadrants from subjects with glaucoma shows an apparent reduction in value, and this may be due to the loss of nerve fibers or neural activity before the appearance of visual field defects (Quigley et al., 1989). This raises the possibility that electrophysiological measurements with special stimulation protocols may detect early functional changes. Because this functional change can be tested and localized objectively, development of this test together with appropriate norms could form the basis of a new test for glaucoma and other retinal dysfunctions with abnormal adaptive mechanisms.

Chapter 8

Experiment II

Luminance-Modulated Adaptation of Global Flash mfERG:

Fellow Eye Losses in Unilateral Glaucoma

(Invest Ophthalmol Vis Sci. 2007; 48 (6):2626-33)

Abstract

Purpose

To use the global flash mfERG in subjects with unilateral glaucoma to determine whether retinal function is affected in fellow eyes that have no glaucomatous visual field defects.

Methods

Forty normal subjects and 12 subjects with unilateral glaucoma were recruited for visual field and mfERG measurement. The mfERG was assessed by using a global flash stimulation paradigm with four video frames: 103 scaled hexagonal elements followed by a dark frame, a global flash frame, and a dark frame. The localized luminance-difference was set at 96%, 65%, 49%, and 29% display contrast during the four different test conditions, respectively. The first-order kernel response was measured, and the “adaptive index” which has been used previously was calculated.

Results

In fellow eyes with normal visual fields, the amplitude of the IC was significantly reduced, and the adaptive index was also reduced by a factor of almost 10 ($p < 0.0001$), as it was in the glaucomatous eyes. Although the adaptive index in the better (fellow) eye of the subjects with glaucoma was slightly higher than in the eyes with diagnosed glaucoma, these differences were not statistically significant.

Conclusions

The significant reduction of the adaptive index in the better eyes in subjects with unilateral glaucoma shows that the fast adaptive mechanism(s) were reduced in these eyes. This implies that these eyes with functionally normal VA and visual fields have abnormal fast-adaptive mechanisms.

Introduction

The POAG is the second leading cause of blindness worldwide (Quigley, 1996). It primarily affects the inner retina (Quigley et al., 1989; Glovinsky et al., 1991) and has unremarkable symptoms in the early stages, but damage to the inner retina results in visual field constriction and ultimately in loss of central vision (Wilson, 2002). POAG is generally a bilateral disease, although its severity is not necessarily symmetrical, and subjects with unilateral glaucomatous visual field loss are believed to constitute a group at high risk for the development of glaucomatous visual field abnormalities in the fellow eye (Harbin et al., 1976; Kass et al., 1976; Olivius and Thorburn, 1978; Susanna et al., 1978; Poinosawmy et al., 1998).

Standard perimetry (white-on-white automated threshold testing) is essential for diagnosis and evaluation of glaucoma. However, the relationship between losses in visual sensitivity and loss of retinal ganglion cells has been considered to lack precision (Quigley et al., 1989; Harwerth et al., 1999; Kerrigan-Baumrind et al., 2000), because a large amount of ganglion cell loss may occur before standard perimetry detects significant visual field defects. The development of the GHT for the evaluation of visual field test results in glaucoma has been based on the symmetry of sensitivity across the horizontal meridian and on the anatomical arrangement of the retinal nerve fibers (Asman and Heijl, 1992a). Incorporation of the GHT into the

automated perimeter has allowed significant improvement in differentiation of normal subjects from those with glaucoma (Asman and Heijl, 1992b). Interest in the functional capacity of the fellow eye in subjects with unilateral glaucoma has prompted the current investigation.

The mfERG allows recording of multiple local retinal responses within a short period (Sutter and Tran, 1992). The topographical distribution of responses reflects retinal function, and the first-order kernel mfERG responses are derived predominantly from distal retinal layers (photoreceptors and bipolar cells) (Hare and Ton, 2002; Hood et al., 2002). Higher-order responses are derived from more proximal retinal layers and primarily reflect inner retinal function (Frishman et al., 2000). The global flash paradigm, a new stimulation mode of the mfERG, is thought to elicit a relatively enhanced inner retinal response by emphasizing retinal fast-adaptive mechanisms (Sutter et al., 1999). The DC from the global flash paradigm was found to be sensitive to early changes in retinal function in diabetes (Shimada et al., 2001) and age-related maculopathy (Feigl et al., 2005); while the IC was found to be an indicator of glaucoma (Fortune et al., 2002a; Palmowski et al., 2002).

A sophisticated stimulation mode which combined the global flash and luminance-modulation of the multifocal flashes (luminance-modulated global flash

mfERG stimulation) for glaucoma detection was used in experiment 1. The nonlinearity of the DC induced with this stimulation mode was quantified and a derived adaptive index showed significant reduction and relatively good correlation with the visual field defect in subjects with glaucoma. From experiment 1, it was believed that the reduction of the adaptive index was related to abnormal retinal adaptive mechanisms, presumably resulting from inner retinal damage (Chu et al., 2006a).

In experiment 2, the fast-adaptive mechanisms in the fellow eye in subjects with unilateral glaucoma, where there is no evidence of field defects with conventional perimetry, were investigated.

Methods

Subjects

Twelve Chinese subjects with POAG age ranged from 23 to 59 years (mean, 44.8 ± 12.1 years), with corrected VA 0.1 logMAR or better (Range of refractive errors: between +1.0 and -4.0 DS and less than -1.0 DC) but with unilateral glaucomatous visual field defects were recruited for this study (Table 8.1). All subjects had unilateral glaucoma of more than 1 year's duration as diagnosed by their ophthalmologists. Their eyes were being treated with either latanoprost (Pfizer Corp., New York) or timolol maleate (Alcon, Ltd., Fort Worth, TX) in both eyes which were prescribed by their own ophthalmologists. An eye examination was performed to exclude ocular abnormalities in addition to glaucoma. Visual field measurements were conducted twice on all subjects, with the 30-2 threshold (SITA) program of the visual field perimeter (Humphrey Visual Field Analyzer; Carl Zeiss Meditec, Inc., Dublin, CA). Subjects with an abnormal GHT index in the affected eye, and normal visual fields plus a normal GHT index in the fellow eye were accepted into the study. IOP in the fellow eyes was less than 21 mmHg (Goldmann tonometer: Haag-Streit AG, Bern, Switzerland), and there was no significant glaucomatous reduction of the RNFL thickness measured by optical coherence tomography (Carl Zeiss Meditec, Inc., Dublin, CA).

Forty age-matched Chinese control subjects age ranged from 23 from 58 years (mean, 41.5 ± 13.2 years) were also recruited. All control subjects were required to have corrected VA of 0.0 (logMAR) or better (Range of refractive errors: between +1.0 and -4.0 DS and less than -1.0 DC) and IOP less than 21 mmHg (Goldmann tonometer: Haag-Streit AG, Bern, Switzerland). All control subjects had open anterior angles, normal visual field (GHT index within normal range) and normal appearance of the optic disc in both eyes. One eye of each control subject was randomly selected for testing.

All research procedures adhered to the tenets of the Declaration of Helsinki and were approved by the Ethics Committee of The Hong Kong Polytechnic University. All subjects were fully informed of the possible risks and gave written, voluntary consent.

<i>Subject</i>	<i>Eye</i>	<i>Mean Deviation</i>	<i>Significance level</i>	<i>Pattern Standard Deviation</i>	<i>Significance level</i>	<i>Visual Acuity</i>
1*	OD	-3.32	p < 2%	3.22	p < 5%	0.00
	OS	-17.84	p < 0.5%	13.32	p < 0.5%	0.04
2	OD	-5.30	p < 1%	4.23	p < 0.5%	0.02
	OS	-1.05	p > 5%	1.84	p > 5%	0.02
3*	OD	-12.51	p < 0.5%	16.31	p < 0.5%	0.00
	OS	-3.28	p < 2%	3.13	p < 5%	0.00
4	OD	-0.02	p > 5%	1.51	p > 5%	0.00
	OS	-10.81	p < 0.5%	11.55	p < 0.5%	0.00
5	OD	-3.53	p < 1%	4.60	p < 0.5%	0.00
	OS	-1.98	p < 5%	1.77	p > 5%	0.00
6	OD	-0.53	p > 5%	1.38	p > 5%	0.00
	OS	-14.05	p < 0.5%	15.83	p < 0.5%	0.08
7	OD	-2.56	p < 5%	2.24	p > 5%	0.02
	OS	-6.70	p < 0.5%	7.35	p < 0.5%	0.04
8	OD	-4.89	p < 0.5%	5.18	p < 0.5%	0.00
	OS	1.08	p > 5%	1.31	p > 5%	0.00
9	OD	-9.07	p < 0.5%	12.73	p < 0.5%	0.08
	OS	-1.19	p > 5%	1.64	p > 5%	0.02
10	OD	-0.92	p > 5%	1.41	p > 5%	0.02
	OS	-11.84	p < 0.5%	14.76	p < 0.5%	0.04
11	OD	-2.46	p < 5%	1.58	p > 5%	0.00
	OS	-13.47	p < 0.5%	13.26	p < 0.5%	0.04
12	OD	-0.37	p > 5%	1.63	p > 5%	0.00
	OS	-10.00	p < 0.5%	8.25	p < 0.5%	0.00

Table 8.1 Clinical data of unilateral glaucoma subjects. The eyes shaded in grey are glaucoma eyes with abnormal GHT values; GHT index of fellow eyes were normal except for borderline GHT values found in fellow eyes of subjects 1 and 3 (*).

Stimulus conditions

The mfERG stimulus pattern was presented on a 19-inch RGB (red-green-blue) monitor (model GDM-500PS; Sony, Tokyo, Japan), and the mfERG program (VERIS 4.1; EDI, San Mateo, CA) was run on a computer (Macintosh G3; Apple Computer, Cupertino, CA). The mfERG was measured by using the luminance-modulated global flash mfERG paradigm as in experiment 1 (Chu et al., 2006a) (Figure 7.1).

Recordings were divided into 16 slightly overlapping recording segments. The recording time for each stimulation cycle was approximately 8 minutes, with a $2^{13} - 1$ binary m-sequence. Four different stimulus contrast conditions under the global flash paradigm were performed, and the luminance-difference of the multifocal flashes were set at 2.12, 1.42, 1.08 and 0.62 $\text{cd}\cdot\text{s}/\text{m}^2$ (Figure 7.1b). The order of the four stimulus conditions was randomised across subjects.

Recording conditions

A DTL electrode was used, as active and gold-cup surface electrodes were used for both the reference and the ground. Before testing, the pupil of the tested eye was fully dilated to at least 7 mm diameter, with 1% tropicamide (Alcon, Ltd.). During the mfERG recording, the untested eye was occluded. The refractive error of the tested eye was fully corrected for the viewing distance of 30 cm with a 70mm diameter

uncut ophthalmic lens, where the optical center of the lens was aligned with the pupil center. The signal was amplified (Grass P511K amplifier; bandpass: 10-300 Hz; gain: x100,000). The recording was monitored using the online signals shown by the mfERG program (VERIS; EDI). Any recording segments contaminated with blinks or small eye movements were rejected and immediately rerecorded.

Data analysis

First-order kernels were analysed using the mfERG system (VERIS 4.1). The mfERG findings were represented by peak-to-peak response amplitude measurement (Figure 7.2a) and the responses from different stimulus conditions were plotted as a function of the luminance-difference value of the stimulus. The way in which these functions varied from the normal response in subjects with unilateral glaucoma were observed, and the adaptive index was calculated for comparison (Figure 7.6a).

Results

The traces in [Figure 8.1](#) are typical grouped responses from three normal subjects and three with unilateral glaucoma (both affected and fellow eye). The waveforms were similar in appearance in control subjects and those with glaucoma; the DC amplitudes from both the affected and fellow eyes were reduced to a similar degree, but the reduction of IC amplitude was greater in the glaucomatous eye. Peripheral mfERG responses were of interest in this study because glaucomatous visual field defects first occur in the Bjerrum area. Based on experiment 1 (Chu et al., 2006a), responses from the four peripheral rings of the mfERG responses were grouped as shown in [Figure 7.5a](#), because of their similarities in waveform and latency and their similar characteristics in the luminance-modulated response function.

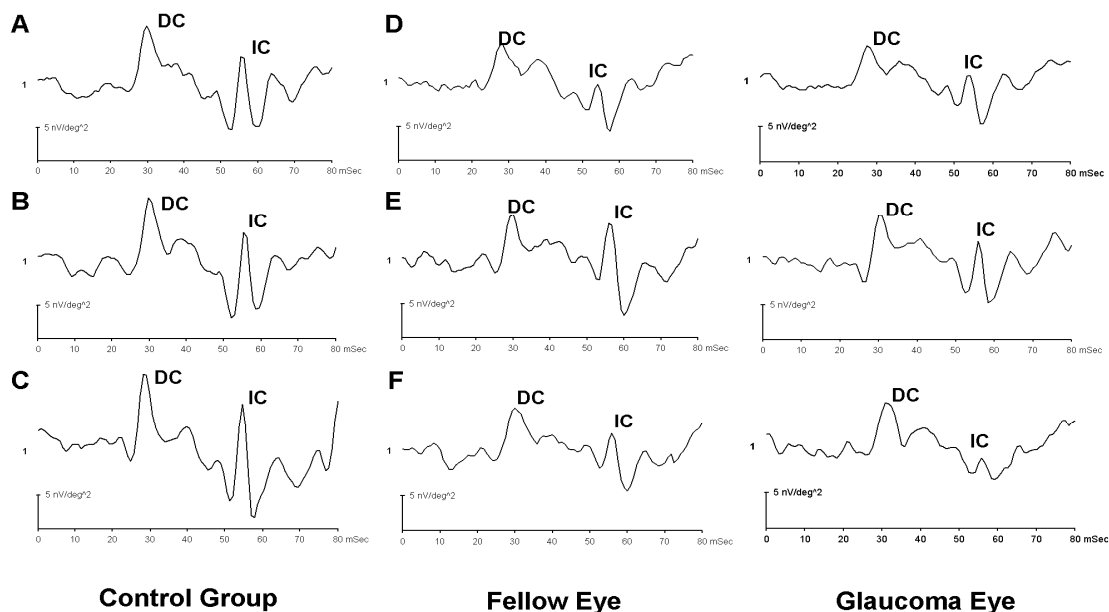


Figure 8.1 Typical grouped responses from three normal (A-C) and three subjects with unilateral glaucoma (D-F) for the $2.12 \text{ cd}\cdot\text{s}/\text{m}^2$ luminance-difference of the multifocal flashes.

Figure 8.2 shows the luminance-modulated response function obtained from control, affected, and fellow eyes. In the control group, the grouped peripheral DC responses are independent of the luminance-difference beyond $1.1 \text{ cd}\cdot\text{s}/\text{m}^2$ and became relatively unchanged in their responses. In affected and fellow eyes, however, the grouped peripheral DC amplitudes were reduced overall, but continued to increase as luminance-difference levels increase. The response functions for both affected and fellow eyes maintained dependence of response amplitude on the luminance-difference characteristic, mainly because of the reduction in response amplitudes at the mid luminance-difference levels. The DC amplitudes of the control

group were significantly larger than those of both eyes of the subjects with unilateral glaucoma in all stimulus contrast conditions, except at the lowest luminance-difference level (Table 8.2). Slightly larger DC amplitudes at all luminance-difference levels were observed in fellow eyes compared with affected eyes, but there was no statistically significant difference between these two groups at any luminance-difference.

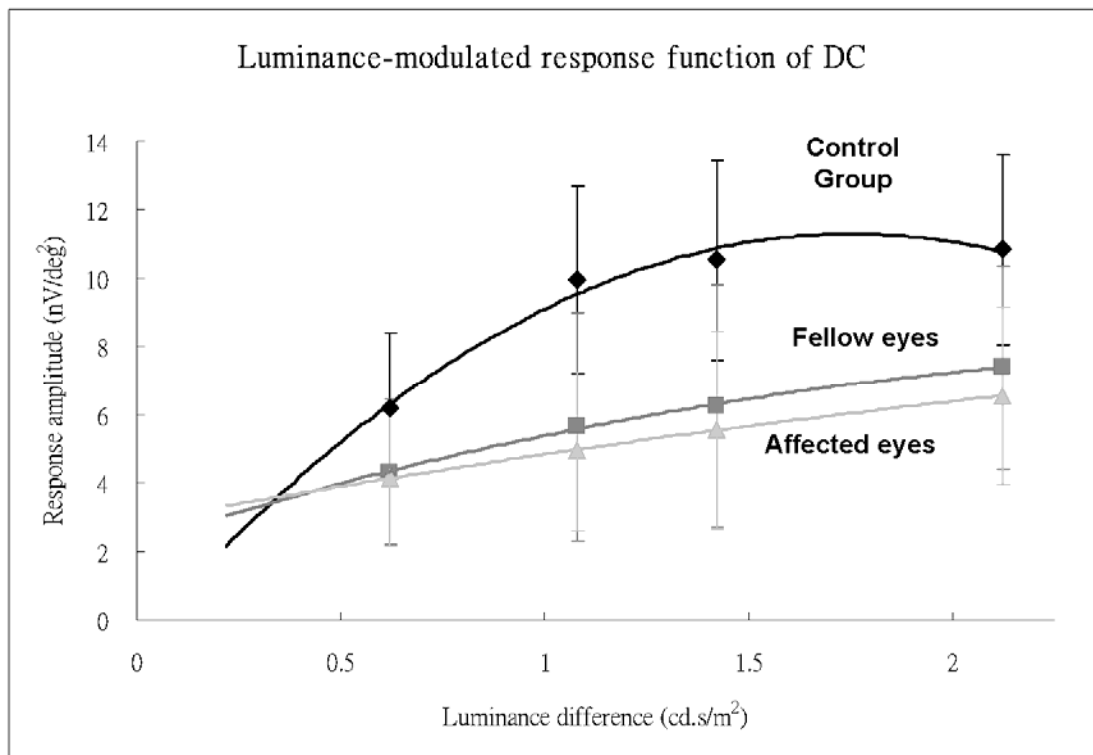


Figure 8.2 The luminance-modulated response function of the peripheral grouped DC responses (rings 4 - 7) from the normal eyes of the control subjects and the affected and fellow eyes of the subjects with glaucoma. Lines represent the second-order, best fitting curves. Error bars, ± 1 SD.

Luminance-difference level		2.12 cd·s/m ²	1.42 cd·s/m ²	1.08 cd·s/m ²	0.62 cd·s/m ²
Control Group (nV/deg ²)		10.83 ± 2.78	10.53 ± 2.93	9.95 ± 2.74	6.18 ± 2.21
Affected Eyes (nV/deg ²)		6.55 ± 2.58	5.57 ± 2.90	4.93 ± 2.33	4.14 ± 1.99
Fellow Eyes (nV/deg ²)		7.39 ± 2.98	6.26 ± 3.55	5.63 ± 3.35	4.33 ± 2.14
One-way ANOVA		F = 18.741			
		df = (11, 244)			
		p < 0.0001			
<i>Post-hoc</i> test (Bonferroni corrected)	Control Vs Affected Eyes	t = 4.789	t = 5.557	t = 5.614	t = 2.275
		p < 0.001	p < 0.001	p < 0.001	p > 0.05
	Control Vs Fellow Eyes	t = 3.848	t = 4.783	t = 4.830	t = 2.070
		p < 0.01	p < 0.001	p < 0.001	p > 0.05
	Affected Eyes Vs Fellow Eyes	t = 0.759	t = 0.624	t = 0.632	t = 0.165
		p > 0.05	p > 0.05	p > 0.05	p > 0.05

Table 8.2 Grouped peripheral response (peak-to-peak) amplitudes of DC for the three groups at four luminance-difference levels, with statistical comparisons.

We calculated the adaptive index, indicating the degree of saturation of the DC luminance-modulated response, by subtracting the area under the line joining the responses from 0.62 to 2.12 cd·s/m² luminance-difference from the area under the luminance-modulated response function fitted with a second-order, best-fit line in this region (Figure 7.6a). There is a reduction of the adaptive index in glaucoma. The mean adaptive index decreases by a factor of nearly 10 in the fellow eyes of subjects with unilateral glaucoma (Figure 8.3). The control group had the largest adaptive

index with a mean of 3.28 ± 1.61 , but the fellow eyes from subjects with glaucoma shows a significant reduction, with a mean of 0.36 ± 1.45 (unpaired t-test; $p < 0.0001$), and the affected eyes show a further reduction with a mean of 0.11 ± 1.21 (unpaired t-test; $p < 0.0001$). There was no significant difference between the affected and fellow eyes (paired t-test; $p > 0.05$).

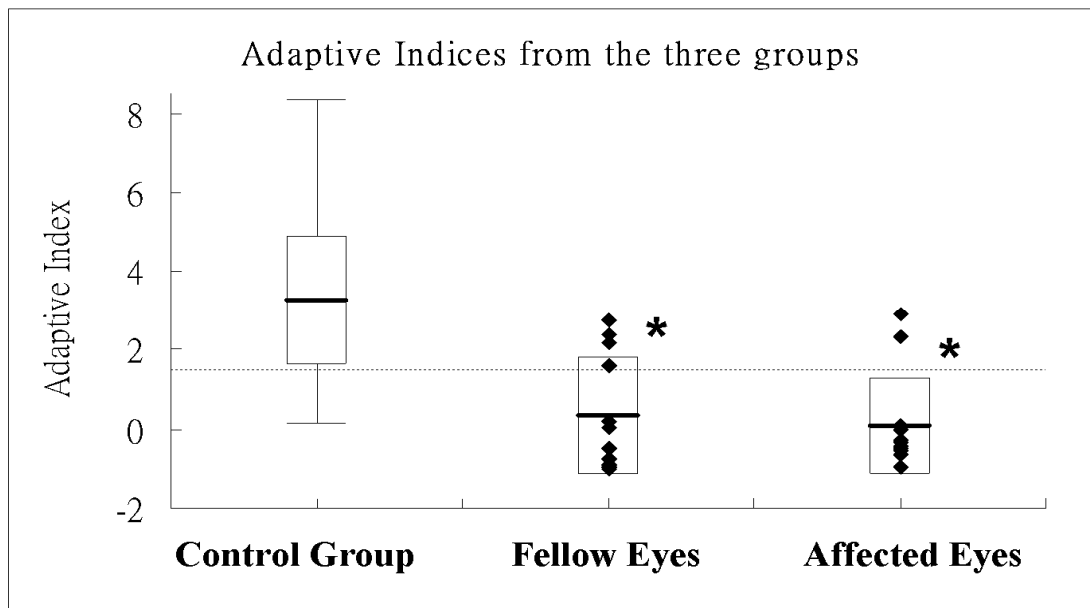


Figure 8.3 Statistical results of the adaptive index from the three groups shown as box plots. There was a statistically significant reduction (*) of the adaptive index in both the affected and fellow eyes of the subjects with glaucoma when compared with the control group ($p < 0.05$). Dotted line: best cutoff point of the adaptive index (1.5) for glaucoma differentiation; middle line: the mean; top and bottom box edges: ± 1 SD; top and bottom bars: the range. (♦) The individual values from fellow and affected eyes of subjects with unilateral glaucoma.

The peripheral mfERG response amplitudes in fellow and affected eyes were averaged in corresponding visual field quadrants (Figure 7.5a), to calculate the adaptive index to compare with visual field data. The mean value of the adaptive index is 0.37 ± 1.59 and -0.07 ± 1.65 across all four quadrants in the fellow eyes and affected eyes, respectively. There are no significant differences between the mean quadrantal peripheral adaptive index and the grouped peripheral adaptive index (paired t-test; $p > 0.05$) in fellow or affected eyes. Figure 8.4 shows the plots of the adaptive index against the MD of the visual field in all quadrants. Because there was no glaucomatous field defect with normal GHT index in the fellow eyes, the mean MD for all field quadrants was -1.56 dB. The correlation of the adaptive index with the MD is statistically significant ($r = 0.37$; $p < 0.01$). However, there is a higher correlation of the adaptive index with the MD in the affected eye of the subjects with unilateral glaucoma ($r = 0.44$; $p < 0.01$), and the mean MD was approximately -10.15 dB.

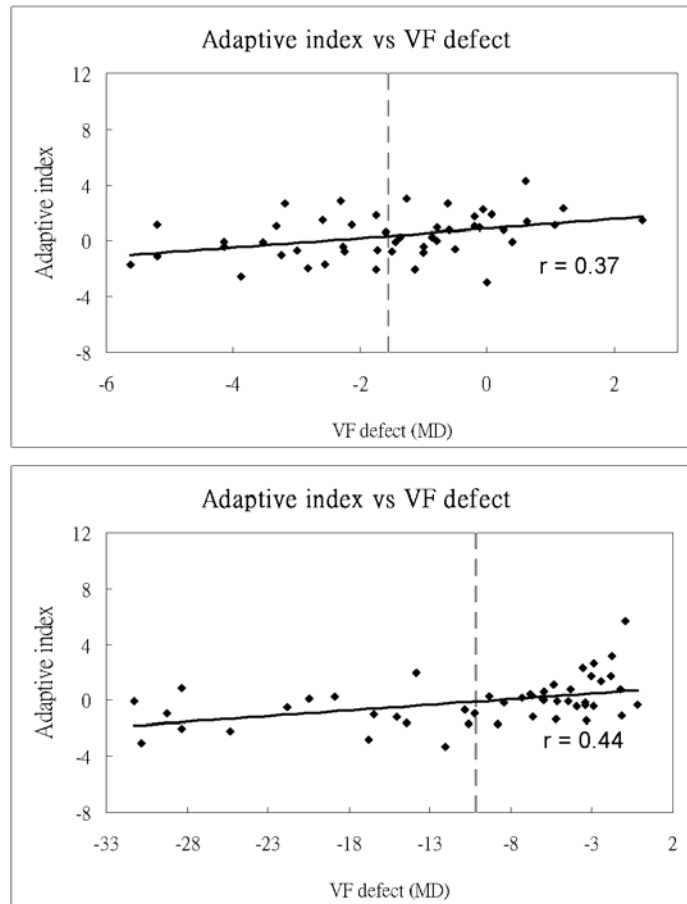


Figure 8.4 The adaptive indices from all quadrants from fellow (upper panel) and affected (lower panel) eyes of the subjects with unilateral glaucoma plotted against visual field MD values in corresponding visual field quadrants. Vertical dotted lines: mean MD for each group. Solid line: the best-fitting line of the points showing a statistically significant correlation ($r = 0.37$ and $r = 0.44$) between adaptive index and visual field MD of fellow eyes (top) and affected eyes (bottom).

IC amplitude has also been reported to be a sensitive indicator of glaucoma (Palmowski et al., 2002). Grouped central IC amplitudes from the highest luminance-difference stimulation level in the fellow eyes were evaluated, and the mean amplitude was 19.50 ± 8.08 nV/deg², but there is no significant difference from the grouped central IC amplitudes of the control group (20.05 ± 7.10 nV/deg²; **Figure 8.5 (top)**; unpaired t-test; $p > 0.05$). The mean amplitude of the grouped peripheral IC amplitudes from the highest luminance-difference stimulation level in the fellow eyes was 10.28 ± 4.25 nV/deg², which is significantly lower than the grouped peripheral IC amplitudes (15.86 ± 3.74 nV/deg²) of the control group (**Figure 8.5 (bottom)**; unpaired t-test; $p < 0.0001$).

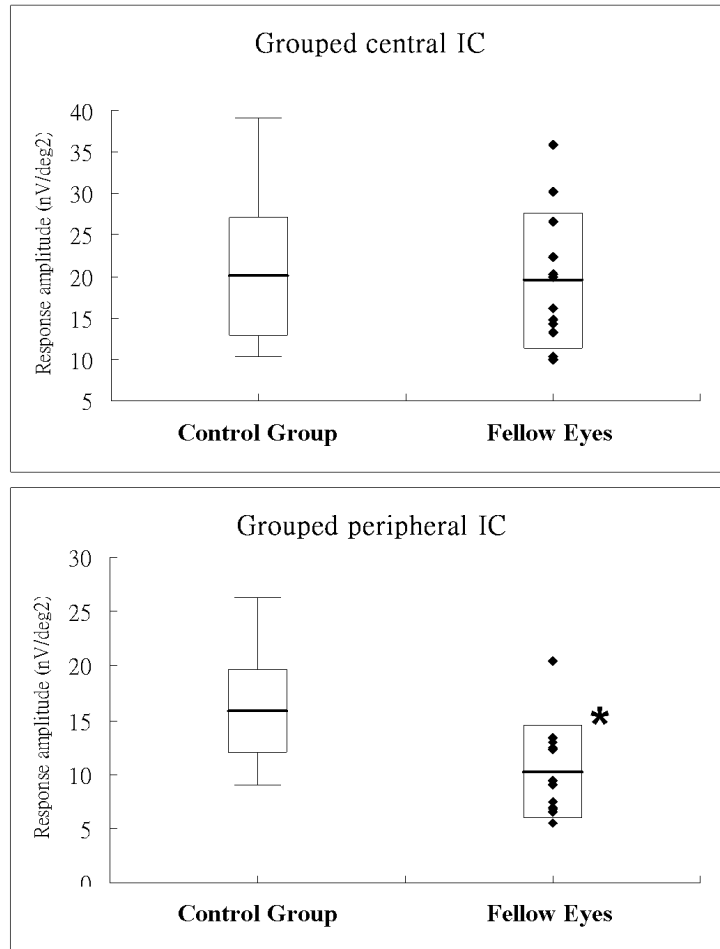


Figure 8.5 The IC response amplitude elicited for the 2.12 cd·s/m² luminance-difference of the multifocal flashes. **Top:** Central IC in the control group and the fellow eyes of subjects with glaucoma. No statistically significant difference was found. **Bottom:** Peripheral IC in the control group and the fellow eyes of subjects with glaucoma. There was a statistically significant reduction (*) in the peripheral IC amplitude in the fellow eyes when compared with the control group ($p < 0.05$). The box plot indications are as in Figure 8.4. (♦) Individual values from fellow eye; the mean and ± 1 SD are shown.

Figure 8.2 suggests that the rate of change of the luminance-modulated response function may be another indicator of variation of retinal adaptation. In addition, this may offer a way to reduce the testing time for this paradigm, allowing only two luminance-modulation levels to be tested, rather than four. Therefore, the slope of the DC response between the two lowest luminance-difference levels ($1.08 \text{ cd}\cdot\text{s}/\text{m}^2$ and $0.62 \text{ cd}\cdot\text{s}/\text{m}^2$) was calculated. The grouped central region and peripheral regions were compared. In **Figure 8.6**, the control group had the highest slope values, whether from the central or from the peripheral region, with mean slopes of 11.10 ± 5.58 and 8.21 ± 5.58 , respectively. The central region of the fellow eyes of subjects with unilateral glaucoma had a mean slope of 7.97 ± 5.96 , a small, insignificant reduction (unpaired t-test; $p > 0.05$). However affected eyes show a significant reduction of the slope value (mean, 4.57 ± 4.18 ; unpaired t-test; $p = 0.00005$).

In the peripheral region, there was a significant reduction of the slope value in both eyes of subjects with unilateral glaucoma. Slopes in affected and fellow eyes were 1.72 ± 2.84 (unpaired t-test; $p = 0.0003$) and 2.84 ± 3.67 (unpaired t-test; $p = 0.003$), respectively (**Figure 8.6**).

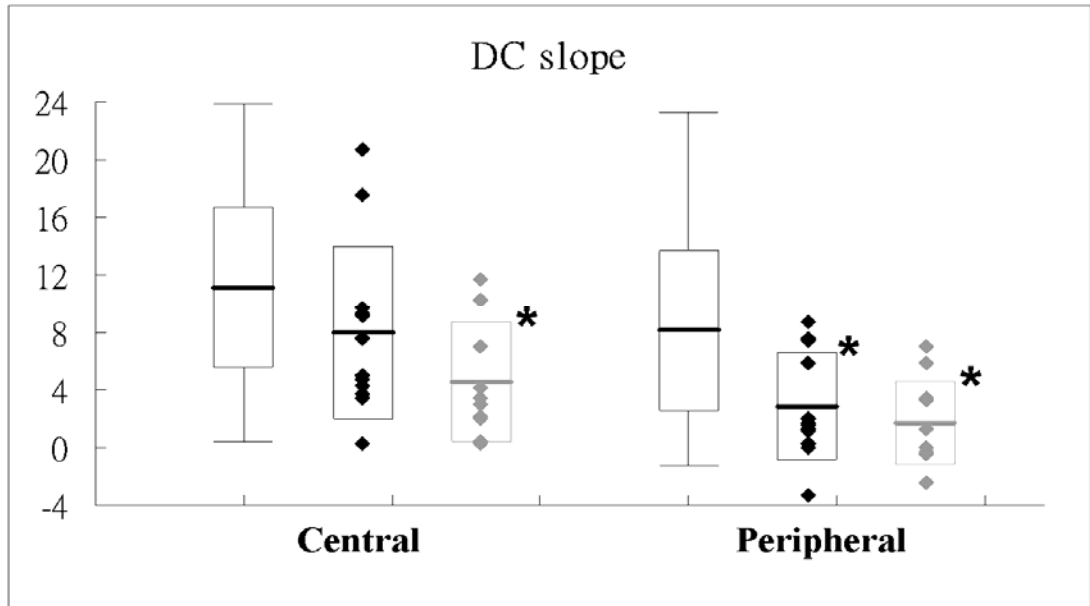


Figure 8.6 Statistical results of the DC slope grouped in central and peripheral region from the three groups (Control, Fellow eye, Glaucomatous eye). The DC slope is calculated as the slope of the DC response amplitude at the two lowest luminance-difference levels. Black diamonds: individual values from fellow eyes; Grey diamonds: individual values from glaucomatous eyes. The box plot is as described in [Figure 8.3](#). (*) represents statistically significant differences compared with the appropriate control group.

[Figure 8.7](#) (top) shows the ROC curve based on different cutoff values of the peripheral slope for the discrimination of subjects with glaucoma from normal subjects. These data are derived from all eyes in the study. The area under this ROC curve is 0.822; the sensitivity is 75% with a specificity of 80% when the best slope cutoff value of 4.7 is used. However, four fellow eyes and two affected eyes were

considered as normal, based on this cutoff value. When the ROC is based on the luminance-modulated response (adaptive index) in these eyes and derived from quadrant responses as in experiment 1 (Chu et al., 2006a), the area under the curve increased to 0.922 (Figure 8.7, bottom), and sensitivity and specificity increased to 82% and 91%, respectively. The cutoff for the adaptive index in this case is 1.5, confirming our findings in experiment 1 (Chu et al., 2006a). As expected, better discrimination between the control subjects and those with glaucoma was obtained when more information was used.

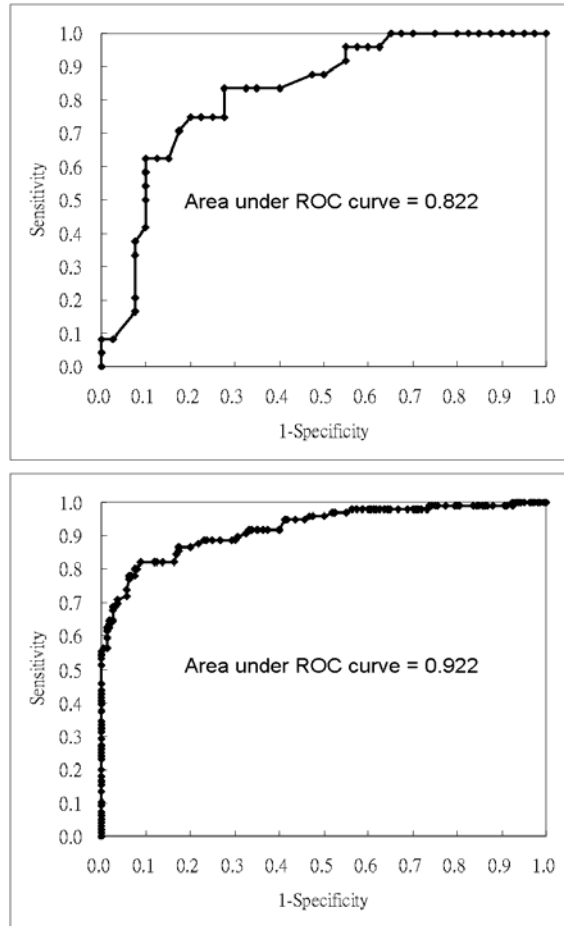


Figure 8.7 ROC plot derived from different cutoff values of the peripheral DC slope (**top**). The peripheral slope cutoff of 4.7 provides the best differentiation between the normal and glaucoma groups and gives a sensitivity of 75% with specificity of 80%. The ROC plot of the adaptive index (**bottom**) shows that the cutoff of 1.5 provides the best differentiation between the normal and glaucoma groups and gives a sensitivity of 82% with specificity of 91%.

Discussion

The findings with the global flash paradigm with luminance-modulation in this experiment have shown that fellow eyes of patients with unilateral glaucoma are similar to glaucomatous eyes that have impaired retinal adaptive changes shown in experiment 1 (Chu et al., 2006a). Patients with POAG who had unilateral glaucomatous visual field defects were used in the present study because Harbin and co-workers (1976) reported that 43% of fellow eyes of patients with POAG with monocular field loss developed visual field losses within 4.4 years.

Previous studies have reported that there may be retinal changes before any defined visual field loss is present in the fellow eyes of patients with unilateral glaucoma. Neuroretinal rim thinning has been reported after tomography analysis (HRT; Heidelberg Engineering, Heidelberg, Germany) (Wollstein et al., 2000). A report of a study in which OCT was used also noted that RNFL changes can be detected before any reduction in visual field sensitivity (Kim et al., 2005). The PERG in patients with unilateral glaucoma has shown significant differences between eyes, but these early amplitude reductions in fellow eyes were not compared with a normal control group (Wanger and Persson, 1983). The PERG has been reported to be an early indicator of dysfunction preceding glaucoma (Bach et al., 2006) and can help to predict stability or progression to OHT glaucoma at least 1 year ahead of conversion.

The mfERG provides an objective measurement of retinal function (Sutter and Tran, 1992), and the second-order kernel is believed to be effective in assessing nonlinear retinal responses, mainly reflecting the adaptation activity of inner retinal layers (Sutter and Tran, 1992; Palmowski et al., 1997; Chan and Brown, 1999; Palmowski and Ruprecht, 2004). However, Sakemi and colleagues (2002) found that the second-order kernel of the mfERG does not correlate with glaucomatous visual field abnormalities, and they questioned its relationship with inner retinal responses. In fact, outer retinal activity also makes a contribution to second-order responses (Hare and Ton, 2002), and this contribution may complicate interpretation of any retinal changes in subjects with glaucoma. Sakemi and colleagues (2002) also reported a non-significant difference in the second-order kernel of the mfERG between eyes in the same subject with glaucoma who had unilateral visual field abnormalities. Their result is not surprising if inner retinal function of eyes with normal visual fields from subjects with unilateral glaucoma is compromised. It suggests that the retinal function of the fellow eye in patients with unilateral glaucoma should be further investigated.

The global flash paradigm with luminance-modulation used in this study is designed for measuring retinal adaptive changes. Previous studies have reported that IC amplitudes reduce in subjects with glaucoma (Palmowski et al., 2002) and that

reduction of the IC seems indicative of impaired adaptive effects due to inner retinal damage (Palmowski et al., 2002). In experiment 2, the peripheral, but not the central, was also reduced before visual field abnormalities were apparent, which suggests that there are impaired fast-adaptive effects in the periphery of the fellow eyes of patients with unilateral glaucoma. However, experiment 1 has showed that the IC amplitude does not correlate with the MD of the Humphrey visual field analysis (Chu et al., 2006a).

The DC luminance-modulated response function showed a similar characteristic in eyes of patients with glaucoma, with and without field defects. In these patients, the largest reduction of the DC amplitude at the mid luminance-difference level produces a loss of luminance-difference saturation of the response function. Glaucomatous damage may actually cause a depression of responses at the mid luminance-difference level and may produce an inverted luminance-modulated response function (Chu et al., 2006a). Quantifying this loss by calculating the adaptive index showed a significant reduction in subjects with unilateral glaucoma in eyes with glaucomatous visual field defects and in fellow eyes with normal visual fields. The significant reduction of the adaptive index in the fellow eyes of patients with unilateral glaucoma further confirms that an impaired fast-adaptive mechanism occurs before observed visual field abnormalities in patients at high risk for glaucoma.

Caution may be needed in interpreting the data because the samples were not precisely age-matched (44.8 ± 12.1 years for the subjects with unilateral glaucoma and 41.5 ± 13.2 years for the control subjects), and the DC may be age dependent (Shimada et al., 2001).

The adaptive index, however, can only be used for responses obtained outside the macular region. A simple comparison of DC response amplitude at the two lowest luminance-difference levels may be another important parameter to allow monitoring of macular and peripheral retinal function. Although the DC slope was only been measured with the two luminance-difference levels, it provides similar information to that provided by the adaptive index. The reduction of the slope value is likely to represent directly the depression of responses at the mid luminance-difference level caused by glaucomatous damage. Therefore, both central IC amplitude and central DC slope showing the non-significant differences between the control and the fellow eyes indicate that the central retinal function may not be obviously affected in the early stage. This conclusion agrees with the progression of glaucomatous damage that initially affects the Bjerrum area.

The significant reduction of both the adaptive index and the DC slope in unilateral glaucoma shows that the fast adaptive mechanism of both eyes is compromised. Experiment 1 demonstrated that the best cutoff point of the adaptive

index for glaucoma differentiation is 1.5 (Chu et al., 2006a). This value works well in experiment 2, since only 8.7% of field quadrants from the normal subjects were classified as abnormal based upon this level, and the mean level, even in fellow eyes, was still below the cutoff point. Thus, even eyes that were functionally normal in VA or visual field had abnormal changes in the fast-adaptive mechanism, which allows differentiating them from normal by pre-established criteria. The ROC curve for the peripheral DC slope shows that this method provides reasonable sensitivity and specificity in differentiating the normal subjects from those with suspected glaucoma, although it does not work as well as the adaptive index. However, care must be exercised in interpreting the ROC data derived herein, and the values obtained should only be used as a rough guide; both eyes from the subjects with unilateral glaucoma have been included (and these cannot be regarded as independent), and the number of glaucomatous eyes included is small.

The measurement of the adaptive index or DC slope using this luminance-modulated global flash mfERG stimulation can provide additional information for diagnosis. The DC slope can be used as a screening tool for detection of glaucomatous damage, but for more detailed monitoring of regional changes of retinal function, use of the adaptive index is suggested because of its relatively lower variability which gives better differentiation between the normal subjects and those

with glaucoma.

Chapter 9

Experiment III

**Luminance-modulated adaptation of global flash mfERG: A
potential indicator of early changes in high risk glaucoma
patients**

Abstract

Purpose

To investigate the association of the luminance-modulation global flash mfERG and other retinal assessments for subsets of subjects at high risk of developing glaucomatous damage.

Methods

Forty-two subjects (75 eyes) with unilateral glaucoma, OHT, family history of glaucoma and large optic disc cupping were assessed in this experiment using visual field, OCT and mfERG measurements. Ophthalmic examinations were scheduled every 12 months for three years. The mfERG was assessed using a luminance-modulated global flash stimulation paradigm. The adaptive index which has been applied in experiment 1 and 2 was calculated.

Results

There was significant thinning of the parapapillary RNFL thickness over the course of the experiment for the fellow eyes with unilateral glaucoma and the eyes with OHT which initially had an abnormal adaptive index; these eyes showed a thinning rate of -3.02 and -3.54 $\mu\text{m}/\text{year}$ respectively. However, thinning was not found in eyes which initially had a normal adaptive index.

Conclusions

The adaptive index calculated from the measurement of the luminance-modulated global flash mfERG may be useful for predicting glaucomatous

progression, especially in high risk groups. The abnormal adaptive index follows from change in fast-adaptive mechanisms and may indicate the risk of developing glaucoma.

Introduction

The POAG is a chronic eye disease with progressive loss of retinal ganglion cells (Quigley, 1993), and patients with POAG are usually asymptomatic in the early stage of this slowly progressive condition. However, there are a number of risk factors for developing POAG and the prevalence of glaucoma is higher in some subsets of the population. Patients with unilateral glaucomatous visual field loss are believed to constitute a high risk group for developing glaucomatous damage in the fellow eye (Harbin et al., 1976; Kass et al., 1976; Olivius and Thorburn, 1978; Susanna et al., 1978; Poinoosawmy et al., 1998), since POAG is generally a bilateral but asymmetric disease. OHT is defined as elevated IOP without the visual field abnormalities which characterize glaucoma. Although elevated IOP is not always an indicator of glaucoma, it is a major risk factor in glaucomatous optic neuropathy (Kass et al., 2002; Keltner et al., 2006). The risk of developing glaucoma is approximately 1% in those with IOP below 20 mmHg, and may be six times higher in those with IOP greater than 24 mmHg (Leske, 1983). Family history studies of POAG are consistent with the notion of genetic determinants of this condition (Wirtz et al., 1999), and a higher risk of glaucoma has been reported in siblings than in parents or children of known glaucoma patients (Tielsch et al., 1994; Nemesure et al., 1996).

Automated perimetry is the commonly accepted clinical test of visual sensitivity

and reduction of visual sensitivity results from loss of retinal ganglion cells in glaucoma (Harwerth et al., 2002). However, the relationship between losses in visual sensitivity and losses in retinal ganglion cells has not been precisely defined. It has been reported that an initial 5 dB loss in visual field sensitivity occurs only after 25% of retinal ganglion cells have been lost (Kerrigan-Baumrind et al., 2000). To optimize early diagnosis and evaluation of the progression of glaucoma, a functional test that can detect glaucomatous damage earlier than the currently available assessment tools is essential, as visual functional loss can be minimized through timely therapy.

The mfERG has been used as a retinal functional assessment tool for some years (Sutter and Tran, 1992; Chan and Brown, 1998; Chan and Brown, 1999; Chan and Brown, 2000; Kretschmann et al., 2000), and the new stimulation paradigm, the global-flash mfERG, was developed to enhance inner retinal response contributions by emphasizing retinal fast-adaptive mechanisms (Sutter et al., 1999). The global-flash paradigm consists of a periodic global flash interleaved with the pseudorandom binary m-sequence multifocal stimulation. It produces two components, a DC and an IC; the IC has been found to show changes in glaucoma (Fortune et al., 2002a; Palmowski et al., 2002; Chu et al., 2006a; Chu et al., 2007). Naso-temporal response asymmetries across the retina are reported in the IC of the human global flash mfERG, which is a nonlinear response component predominantly

from the inner retina (Sutter et al., 1999), and the IC can reflect impaired adaptive effects due to damage from glaucoma (Palmowski et al., 2002; Palmowski-Wolfe et al., 2007). However, its sensitivity in the localized assessment of glaucomatous damage in individual patients is reported to be limited (Shimada et al., 2001).

To quantify retinal adaptation, an index derived from the DC induced by the luminance-modulated global flash mfERG has been developed and it was described in experiment 1 (Chu et al., 2006a). This adaptive index was demonstrated to be sensitive to glaucomatous damage and correlated well with the visual field defect. It was assumed that reduction of this index was related to abnormal retinal adaptive mechanisms, presumably resulting from inner retinal damage (Chu et al., 2006a; Chu et al., 2008). Moreover, the index is reduced in fellow eyes in subjects with unilateral glaucoma even when VA and visual fields are normal (Chu et al., 2007). Hence, the adaptive index appears likely to predict impairment of visual function and it may be a potential indicator in diagnosis of early glaucoma.

In experiment 3, the co-variation of factors which are known to be associated with glaucoma over a limited time period has been tested. The OCT measures retinal thickness (and can indicate any thinning of the retina), and it is known that the adaptive index is associated with visual field losses; this experiment has therefore been conducted (over a three year period) to determine if these factors co-vary in

populations known to be at risk of developing glaucoma. This experiment will give us additional data on reliability of these tests over this time period, which will also indicate their clinical utility.

Methods

Subjects

Fifty-six Chinese subjects with unilateral glaucoma, OHT, family history of glaucoma and abnormal optic disc cupping were enrolled in this experiment. Ten unilateral POAG patients had unilateral glaucomatous visual field defects; they were aged from 29 to 59 years (mean 48.1 ± 9.7 years), with corrected VA 0.1 logMAR or better. All of these subjects had visual field loss of the affected eye indicating glaucoma, and normal visual field in the fellow eye (Table 9.1); the fellow eyes with normal visual field were selected for testing. All had unilateral glaucoma of more than one year duration as diagnosed by their ophthalmologists and were being treated with either Latanoprost (Pfizer) or Timolol Maleate (Alcon) in both eyes.

<i>Subject</i>	<i>Eye</i>	<i>Mean Deviation</i>	<i>Significance level</i>	<i>Pattern Standard Deviation</i>	<i>Significance level</i>	<i>Visual Acuity</i>
1	OD	-0.92	p > 5%	1.41	p > 5%	0.02
	OS	-11.84	p < 0.5%	14.76	p < 0.5%	0.04
2	OD	-9.07	p < 0.5%	12.73	p < 0.5%	0.08
	OS	-1.19	p > 5%	1.64	p > 5%	0.02
3	OD	-2.56	p < 5%	2.24	p > 5%	0.02
	OS	-6.70	p < 0.5%	7.35	p < 0.5%	0.04
4	OD	-0.53	p > 5%	1.38	p > 5%	0.00
	OS	-14.05	p < 0.5%	15.83	p < 0.5%	0.08
5	OD	-3.53	p < 1%	4.60	p < 0.5%	0.00
	OS	-1.98	p < 5%	1.77	p > 5%	0.00
6	OD	-0.02	p > 5%	1.51	p > 5%	0.00
	OS	-10.81	p < 0.5%	11.55	p < 0.5%	0.00
7	OD	-4.89	p < 0.5%	5.18	p < 0.5%	0.00
	OS	1.08	p > 5%	1.31	p > 5%	0.00
8*	OD	-12.51	p < 0.5%	16.31	p < 0.5%	0.00
	OS	-3.28	p < 2%	3.13	p < 5%	0.00
9	OD	-5.30	p < 1%	4.23	p < 0.5%	0.02
	OS	-1.05	p > 5%	1.84	p > 5%	0.02
10*	OD	-3.32	p < 2%	3.22	p < 5%	0.00
	OS	-17.84	p < 0.5%	13.32	p < 0.5%	0.04

Table 9.1 Clinical data of unilateral glaucoma subjects. The eyes shaded in grey are glaucoma eyes with abnormal GHT values; GHT index of fellow eyes were normal except for borderline GHT values found in fellow eyes of subjects 8 and 10 (*).

Eighteen OHT subjects with IOP \geq 22 mmHg (measured by Goldmann tonometry), aged from 16 to 59 years (mean 43.1 \pm 14.4 years), with corrected VA 0.0 logMAR or better were included. Corneal thickness was measured using the

Orbscan II optical pachometry system (Orbtek, Inc., Salt Lake City, UT) to account for the effect of central corneal thickness on tonometry. All IOP values were corrected to account for variation in corneal thickness. The mean IOP of all eyes measured by Goldmann tonometer (Haag-Streit AG, Bern, Switzerland) was 23.3 ± 0.86 mmHg with compensation for the central corneal thickness (using the formula: $P = A + (550 - T) / X$, where $P =$ IOP in mmHg, $A =$ Goldmann applanation reading in mmHg, $T =$ central corneal thickness in μm , $X =$ the correction ratio) (Shimmyo et al., 2003).

Fifteen subjects with family history of glaucoma, aged from 22 to 61 years (mean 44.9 ± 10.2 years), with corrected VA 0.0 logMAR or better were included. One or more of their siblings or parents had a confirmed diagnosis of POAG. Finally, thirteen subjects, aged from 21 to 71 years (mean 46.5 ± 15.8 years), with abnormal optic disc cupping (mean cup-to-disc ratio of 0.71 ± 0.06), and corrected VA 0.1 logMAR or better were recruited. Subjects with suspicious appearance of the optic nerve head (cup-to-disc ratio equal to or more than 0.6) or asymmetry of the cup-to-disc ratio between eyes (more than 0.2) were included.

All participants underwent an eye examination before the experiment to exclude ocular abnormalities in addition to the inclusion criteria. All subjects had open anterior angles. Visual field measurements were conducted on all subjects using the central 30-2 threshold (SITA) test of the Humphrey Visual Field Analyzer (Carl Zeiss

Meditec, Inc., Dublin, CA). No tested eye showed a glaucomatous visual field defect. Apart from the unilateral glaucoma group, all other tested eyes had normal mean deviation and pattern standard deviation ($p > 0.05$). In addition, all tested eyes had normal parapapillary RNFL thickness (within the age-matched normal range limits provided with the instrument, which is compatible with Chinese population (Mok et al., 2002), and one of the subjects younger than 18 years old was compared with the normogram obtained from Chinese children (Leung et al., 2009)) as measured by OCT (Carl Zeiss Meditec, Inc., Dublin, CA) using fast parapapillary RNFL circular scan. The results consisted of the average of three concentric scans of the optic disc at a single measurement, at a diameter of 3.46 mm, and 360° around the optic nerve head. The average of the three scans was then calculated automatically, and only the results with signal greater than the value of 7 were used. Scans were further analyzed using the RNFL thickness average analysis protocol; the protocol quantifies the average RNFL thickness in 12 different clock-hour sectors (30°)

Stimulus and recording conditions:

The mfERG program (VERIS 4.1; EDI, San Mateo, CA) was run on a Macintosh G3 computer (Apple Computer, Cupertino, CA) and the mfERG stimulus pattern was presented on a 19-inch RGB monitor (model GDM-500PS; Sony, Tokyo,

Japan). The mfERG was measured using the luminance-modulated global flash mfERG paradigm as in experiment 1 (Chu et al., 2006a) (Figure 7.1). The presentation order of the four stimulus conditions was randomised across subjects.

A DTL electrode was used as the active electrode and gold-cup surface electrodes were used for both reference and ground. Before testing, the pupil of the tested eye was fully dilated to at least 7 mm diameter, with 1% Tropicamide (Alcon). During the mfERG recording, the refractive error of the tested eye was fully corrected for the viewing distance of 30 cm with a 70mm diameter uncut ophthalmic lens, where the optical center of the lens was aligned with the pupil center. The size of the stimulus pattern was 42° vertically and 48° horizontally. The signal was amplified using a Grass P511K amplifier (bandpass: 10 to 300 Hz; gain: x100,000). The recording was monitored using the real time signals shown by the VERIS program; any recording segments contaminated with blinks or small eye movements were rejected and immediately re-recorded. Recordings were divided into 16 slightly overlapping recording segments and the recording time for each stimulation cycle was approximately 8 minutes with the binary m-sequence ($2^{13} - 1$) which was used.

Follow up visits

Four complete ophthalmic examinations with visual field, OCT and the mfERG

recordings were scheduled every 12 months in a three-year period. After the first visit, eight subjects withdrew, and at subsequent visits two and four more subjects withdrew. Forty-two subjects subsequently completed all the examinations, including nine unilateral glaucoma patients (9 eyes), 12 subjects with family history of glaucoma (24 eyes), 10 subjects with OHT (20 eyes) and 11 subjects with abnormal optic disc cupping (22 eyes).

Subject consent

All research procedures adhered to the tenets of the Declaration of Helsinki and were approved by the Ethics Committee of The Hong Kong Polytechnic University. All subjects were fully informed of the possible risks and gave written, voluntary consent.

Data analysis

Only data from eyes with measurements from all four visits were used for analysis. Peripheral mfERG responses were of interest in this experiment because glaucomatous visual field defects first occur in the Bjerrum area. Based on our previous experiments (Chu et al., 2006a; Chu et al., 2007), responses from the four peripheral rings of the mfERG responses were grouped in quadrants (Figure 9.1a).

These responses have similarities in waveform and latency, as well as similar characteristics in the luminance-modulated response function. The mfERG findings in different quadrants of the field were represented by calculating the adaptive index where the DC responses from different stimulus conditions were plotted as a function of the luminance-difference value of the stimulus. The way in which these functions varied over time in the subjects with high risk of glaucoma were indicated by the adaptive index value, indicating the degree of saturation of the DC luminance-modulated response (Chu et al., 2006a; Chu et al., 2007). The index was calculated by subtracting the area under the line joining the DC responses from 0.62 cd·s/m² to 2.12 cd·s/m² luminance-difference from the area under the DC luminance-modulated response function fitted with a second-order best-fit line.

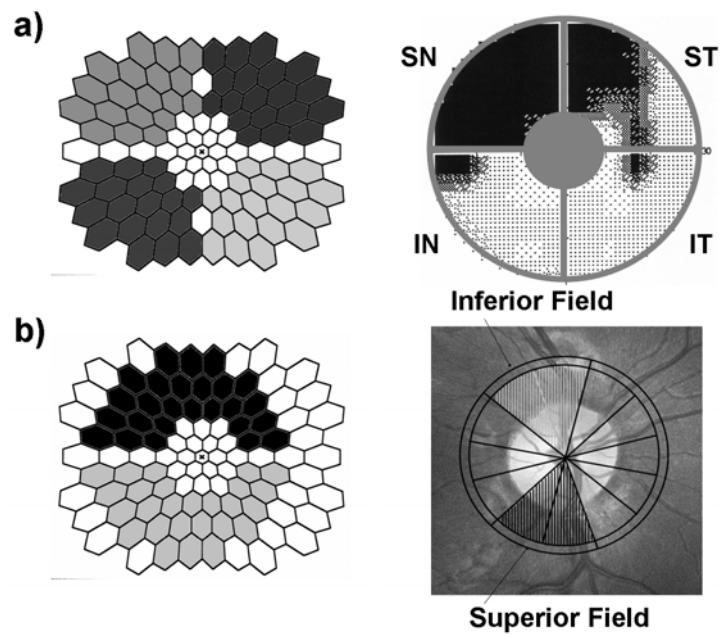


Figure 9.1 (a) The global flash mfERG responses from the four peripheral rings were grouped as the peripheral responses, which were further averaged into visual field quadrants shown for analysis. (b) The peripheral global flash mfERG responses were divided into superior and inferior field for comparison with the corresponding optic nerve head sectors from the OCT assessment.

To examine the co-variation of the adaptive index associated with glaucoma, the corresponding field regions with abnormal (lower than 1.5) and normal (more than 1.5) initial adaptive indices (Chu et al., 2006a) were grouped separately, so as to assess the changes of visual field test and OCT over the course of the study. The relationship between the peripheral mfERG response and the visual field MD was evaluated by comparing the measurements averaged within each quadrant. In order to

compare with the OCT values, the mfERG responses were regrouped in an arcuate area (Hood et al., 2007) and compared with the corresponding sectors of the OCT results (Figure 9.1b).

For all high risk groups, other than unilateral glaucoma, both eyes from all subjects were analyzed. The statistical method of generalized estimating equations (GEE) in SPSS 16.0 was applied to account for the possible correlation of measurements from both eyes of the same subjects (Horn et al., 2007). The GEE method allows estimates models that account for any correlations found in the input data sets (e.g. from right and left eyes); these models correct the variance-covariance matrix on a weighted scale and thus account for related measurements from right and left eyes of the same patient. Highly correlated data thus have reduced influence on the final results. A criterion significant level of 0.05 was used in all statistical tests and Bonferroni *post-hoc* correction was used for analysis of repeated measurements.

Results

Seventy-five eyes of 42 subjects with high risk of developing glaucoma completed the four visits. There was a range of values of adaptive index among the four groups of subjects in the first visit (Figure 9.2); the fellow eyes from unilateral glaucoma subjects had the lowest value (0.23 ± 1.47), while eyes with abnormal optic nerve cupping had the highest value (2.62 ± 2.40). Even though different values of adaptive index were shown between groups, and the adaptive index of the fellow eyes from unilateral glaucoma subjects are known to be compromised (Chu et al., 2007), the visual field and the OCT results were still clinically normal (within the age-matched normal limits) in all subjects. Among the subjects in all four groups, some of the field quadrants already had an abnormal value of adaptive index (below 1.5) as defined in our previous experiment (Chu et al., 2006a). There were 83% abnormal field quadrants in the fellow eye from unilateral glaucoma subjects and 48% abnormal field quadrants in subjects with OHT. In addition, abnormal adaptive index was also found in 31% and 34% field quadrants in subjects with abnormal optic disc cupping and with family history of glaucoma, respectively (Table 9.2).

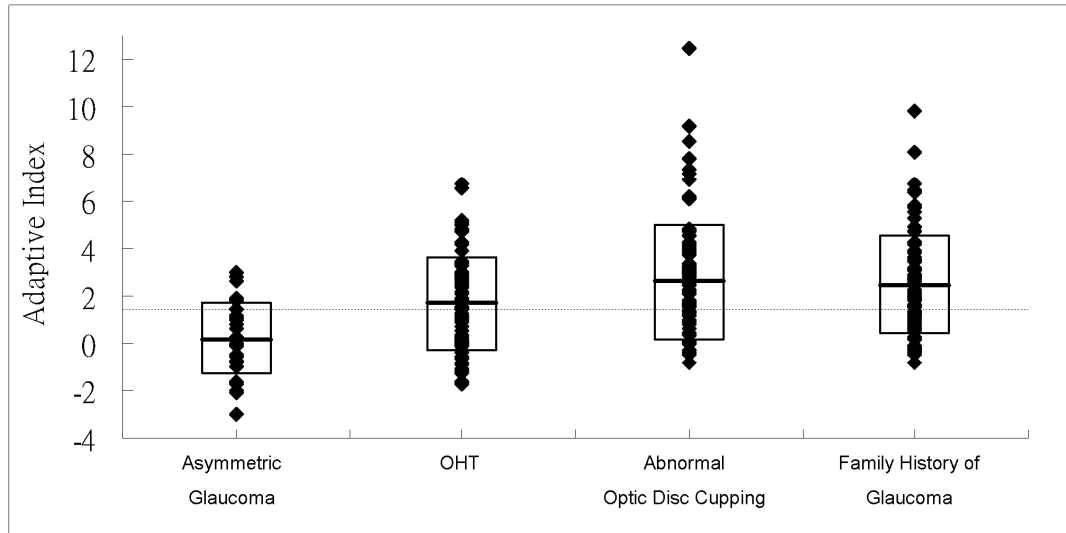


Figure 9.2 The adaptive index for different high risk groups in the first visit. Dotted line: best cutoff point of the adaptive index (1.5) for glaucoma differentiation; middle line: the mean; top and bottom box edges: ± 1 SD. (♦) The individual values from subjects with different high risk groups.

		<i>Unilateral Glaucoma</i>	<i>OHT</i>	<i>Abnormal Optic Disc Cupping</i>	<i>Family History of Glaucoma</i>
<i>Adaptive Index Value</i>	<i>Normal (Above 1.5)</i>	2.46 ± 0.56 (6 field quadrants)	3.16 ± 1.29 (42 field quadrants)	3.66 ± 2.13 (61 field quadrants)	3.55 ± 1.79 (63 field quadrants)
	<i>Abnormal (Below 1.5)</i>	-0.23 ± 1.13 (30 field quadrants)	0.07 ± 0.93 (38 field quadrants)	0.27 ± 0.68 (27 field quadrants)	0.50 ± 0.65 (33 field quadrants)
<i>Visual Field (dB)</i>	<i>Normal Adaptive Index</i>	-1.18 ± 0.56	-0.70 ± 1.23	-0.42 ± 1.11	-0.61 ± 0.83
	<i>Abnormal Adaptive Index</i>	-2.04 ± 1.70	-1.22 ± 1.21	-1.12 ± 0.96	-0.87 ± 0.70
<i>OCT (um)</i>	<i>Normal Adaptive Index</i>	127.67 ± 5.69	142.48 ± 19.69	140.17 ± 17.40	145.16 ± 15.47
	<i>Abnormal Adaptive Index</i>	122.57 ± 25.74	133.50 ± 26.49	134.07 ± 26.26	142.91 ± 24.42

Table 9.2 The visual field and the OCT data for different high risk groups in the first visit were divided into two categories according to whether the initial adaptive index was above or below 1.5. Quadrants in the field with adaptive index below 1.5 were considered as abnormal.

Since the four high risk groups may differ in their potential for developing glaucoma, they were analyzed separately. Quadrants in the field with adaptive index below 1.5 at the first visit were considered as abnormal (Chu et al., 2006a; Chu et al., 2007). The subjects with unilateral glaucoma had over 80% of field quadrants with abnormal initial adaptive index which was the lowest value among the four high risk groups (Table 9.2) and there was a significant reduction of the adaptive index over the period of this study (GEE with *post-hoc* Bonferroni: $p < 0.05$) (Figure 9.3a). The field quadrants with initially normal adaptive index did not show any significant reduction of value (GEE with *post-hoc* Bonferroni: $p > 0.05$) although it was the lowest normal quadrant value among all four groups. For the subjects in other three groups, the field quadrants with initially normal index were usually above 3; while the field quadrants with initially abnormal index were usually below 1 (Table 9.2). There was no significant reduction of adaptive index over visits in these three groups, even in those field quadrants with an abnormal adaptive index among these three high risk groups (GEE with *post-hoc* Bonferroni: $p > 0.05$).

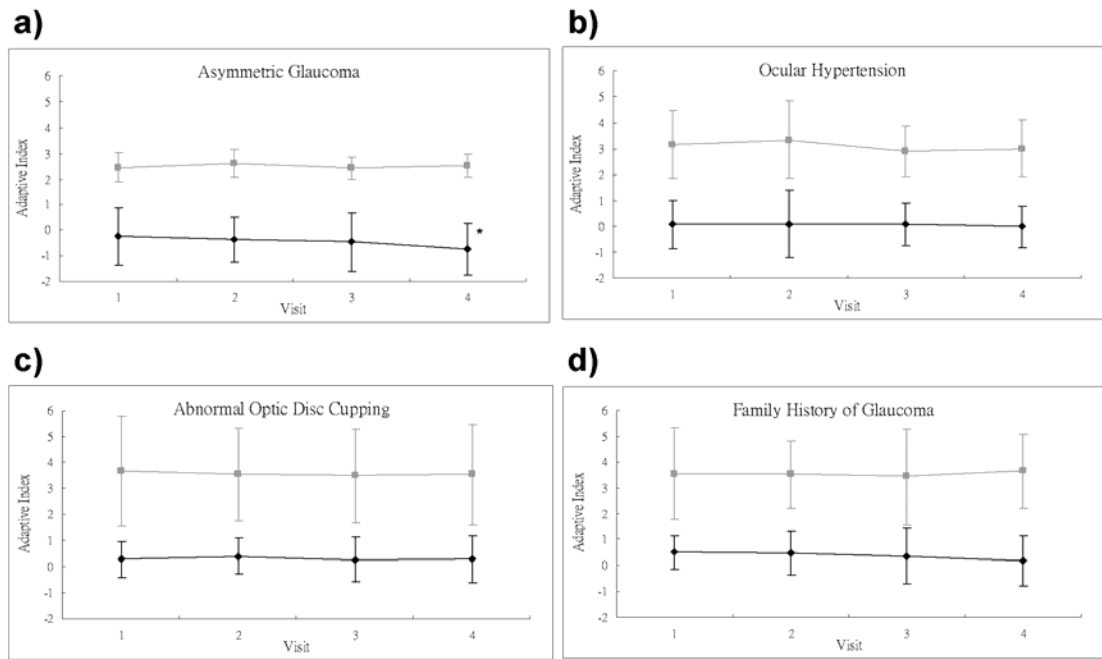


Figure 9.3 The variations of adaptive index with the grouped initially normal adaptive index (grey) and the grouped initially abnormal adaptive index (black) among different high risk groups were plotted over the four visits. Bars indicate ± 1 SD and result marked with (*) showed significant reduction.

In order to observe the changes of visual sensitivity in the field in corresponding to the mfERG response, the quadrantal visual field data from each high risk group was divided into two categories according to whether the initial adaptive index was above or below 1.5. Generally, the visual fields in the category with abnormal adaptive index had lower MDs than those with normal adaptive index. Nevertheless, none of the four groups showed significant reduction of the visual field MD over time when compared with the initial visual field MD (GEE with *post-hoc* Bonferroni: $p >$

0.05) despite the field quadrants with adaptive index being in the abnormal range. However, in those field quadrants with abnormal adaptive index, unilateral glaucoma subjects and OHT subjects had lower initial MD values (Table 9.2), and both groups showed larger reduction rates (-0.19 dB/year and -0.06 dB/year, respectively) among all four groups (Figure 9.4a and b). In contrast, subjects with abnormal optic disc cupping and subjects with family history of glaucoma had larger initial MD values for field quadrants with abnormal adaptive index (Table 9.2), thus both groups showed a lower reduction rates of -0.02 dB/year and -0.01 dB/year, respectively (Figure 9.4c and d).

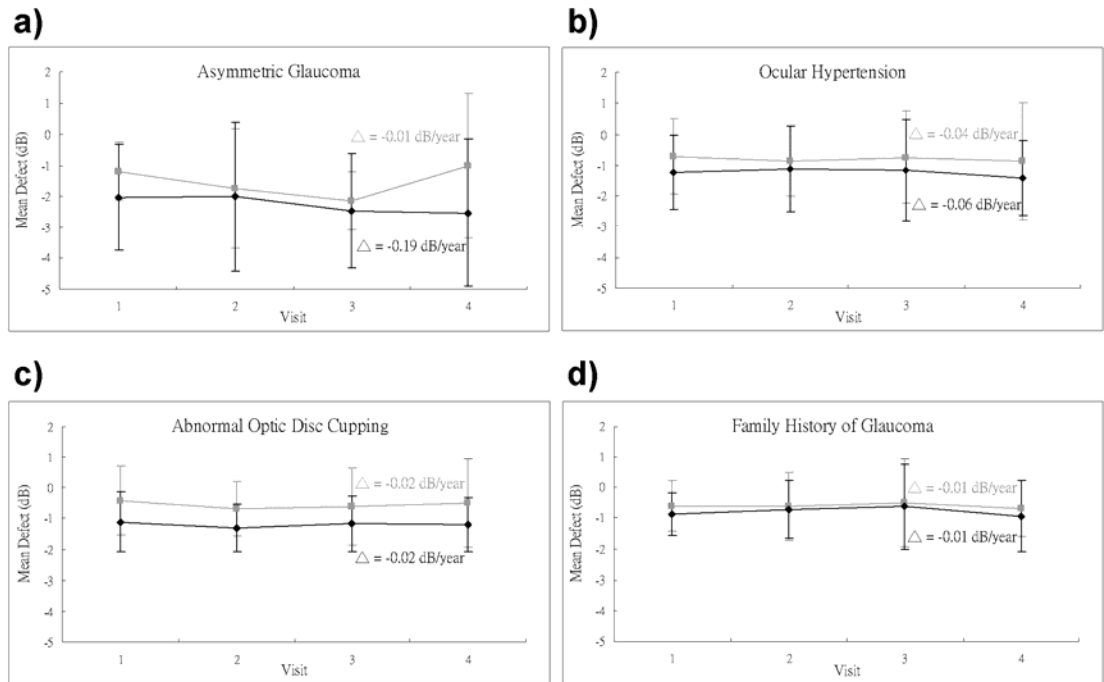


Figure 9.4 The visual field MD from subjects in different high risk groups were divided into two groups based on the initial adaptive index value. Both the MD with abnormal initial adaptive index value (black) and those with initially normal adaptive index (grey) revealed no significant changes over the course of the study. Bars indicate ± 1 SD and Δ indicate rate of change.

The parapapillary RNFL thickness revealed by OCT was also evaluated (Figure 9.5). Since the OCT values represent sectoral regions of the optic disc, rather than field quadrants, mfERG responses were regrouped into arcuate regions according to the arrangement of the OCT setting. Arcuate regions with adaptive index above and below 1.5 in the first visit were extracted separately for comparison with the OCT data. As with the visual field results, the RNFL was generally thinner in those regions

with abnormal adaptive index than those with normal adaptive index among groups. Subjects with unilateral glaucoma (Figure 9.5a) or OHT (Figure 9.5b), who had initial abnormal adaptive index, showed thinner RNFL than the other two high risk groups (Table 9.2). A significant thinning of the RNFL thickness was found over the period of this experiment with a reduction rate of -3.02 (GEE with *post-hoc* Bonferroni: $p < 0.001$) and -3.54 $\mu\text{m}/\text{year}$ (GEE with *post-hoc* Bonferroni: $p < 0.05$), respectively. In contrast, in subjects with unilateral glaucoma or with OHT who initially had a normal adaptive index, there was no significant thinning of the RNFL thickness over time (GEE with *post-hoc* Bonferroni: $p > 0.05$). On the other hand, neither the subjects with abnormal optic disc cupping nor with family history of glaucoma showed significant thinning of the RNFL thickness over the period of this study (GEE with *post-hoc* Bonferroni: $p > 0.05$) even though the adaptive index was in the abnormal range. As compared with other two groups, their initial RNFL thicknesses were thicker (Table 9.2), and the reduction rates were lower with only -0.85 and -1.03 $\mu\text{m}/\text{year}$, respectively (Figure 9.5c and d).

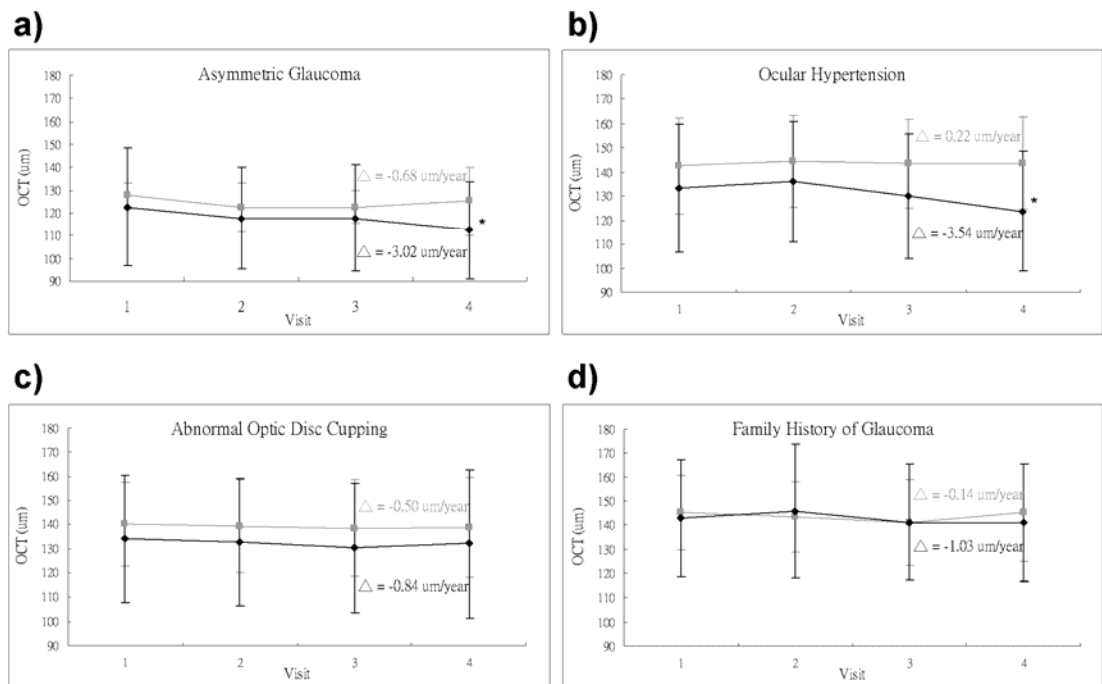


Figure 9.5 The RNFL thickness measured by OCT from subjects with (a) unilateral glaucoma; (b) OHT; (c) abnormal optic disc cupping; and (d) family history of glaucoma were divided into two groups based on the initial adaptive index value. The RNFL thickness with abnormal initial adaptive index value (black) showed a significant thinning (*) at the last visit in both OHT and unilateral glaucoma groups, while there was no significant thinning of the RNFL thickness for subjects with normal initial adaptive index value (grey). Bars indicate ± 1 SD and Δ indicate rate of change.

Discussion

Different initial adaptive indices were found among groups in this experiment, but the different subjects may be at different points of the timeline of glaucoma progression, and this would complicate the interpretation, making it difficult to decide whether any group has higher potential to develop glaucoma than any others. However, among the four groups, some of the field quadrants already had an abnormal value of adaptive index demonstrating that some subjects have functional changes in mfERG, even though they had no visual field or OCT abnormalities. The global flash paradigm with luminance-modulation is designed to measure retinal adaptive changes (Chu et al., 2006a; Chu et al., 2007), and the adaptive index which is significantly reduced in glaucoma subjects has shown good correlation with glaucomatous visual field defects (Chu et al., 2006a). Moreover, our previous experiment demonstrated that the best cutoff point of the adaptive index for glaucoma differentiation is 1.5, which optimized the sensitivity/specificity relationship (Chu et al., 2006a).

Subjects with unilateral glaucoma show impairment of the fast-adaptive mechanism before any visual field defect becomes apparent in the fellow eye (Chu et al., 2007), which initially has an abnormal adaptive index. In addition, subjects with OHT also had abnormal mfERG responses (Chan and Brown, 2000) and the pattern

ERG predicts the progression to glaucoma at least one year prior to conversion (Bach et al., 2006). The current experiment confirms that eyes of OHT and unilateral glaucoma subjects have low adaptive indices and that these eyes have a higher percentage of field quadrants with an abnormal initial adaptive index. On the other hand, physiological cupping of the optic disc may be classed as “abnormal” and may not be due to glaucomatous changes. This can help to explain why the highest adaptive index values and the smallest percentage of field quadrants with initially abnormal adaptive index were found in this group.

POAG is a chronic eye disease with slowly progressive loss of retinal ganglion cells. In order to investigate the co-variation of the adaptive index in retinal functional/structural changes for subsets of subjects at high risk of developing glaucoma damage, it would be preferable to observe the progression of glaucomatous changes. Thus, a comparison between the field quadrants with the initially obtained normal or abnormal adaptive index was performed in order to focus on those particular field regions for functional and structural changes, by analysis of the visual field and the OCT results. Generally, those regions with abnormal adaptive index had lower visual field MD and thinner RNFL thickness than those with normal adaptive index. But, in this study, there was no significant reduction in the visual field sensitivity over the study period although the fast-adaptive mechanism was initially

shown to be impaired. This may relate to the poor sensitivity of perimetry in detecting visual field changes in the early stages of glaucoma (Kerrigan-Baumrind et al., 2000). Although static white-on-white threshold perimetry, which shows the reduction of visual sensitivity as a result of retinal ganglion cells loss, has become the standard procedure for assessment of glaucoma (Johnson, 1996; Harwerth et al., 2002), a certain level of ganglion cell loss must occur before standard perimetry will detect significant visual field defects (Quigley et al., 1989; Harwerth et al., 1999; Kerrigan-Baumrind et al., 2000). Indeed, about 7.2% of fellow eyes in patients with unilateral POAG progress to glaucomatous visual field loss five years after initial diagnosis (Chen and Park, 2000). Other studies have reported that 24 – 43% of fellow eyes in patients with unilateral POAG develop glaucomatous visual field loss over 3 to 7 years (Harbin et al., 1976; Kass et al., 1976; Olivius and Thorburn, 1978; Susanna et al., 1978). In addition, the conversion rate from untreated OHT to glaucoma is only about 1% per year and the conversion rate possibly decreases to half for treated OHT (Kass et al., 2002). The current experiment is in its first three year phase, and is probably not long enough to show the development of glaucomatous visual field defects, even for subjects at high risk.

OCT is a recently developed technology that provides an *in-vivo* objective measurement of the parapapillary RNFL thickness. The RNFL thickness measured by

OCT has been demonstrated to have high diagnostic value in eyes with early glaucoma (Kanamori et al., 2003; Hess et al., 2005; Medeiros et al., 2005; Sihota et al., 2006), and it provides higher sensitivity than conventional visual field testing (Kim et al., 2007). A loss of 10 μm in RNFL thickness from baseline has been shown to predict glaucomatous change (Lalezary et al., 2006). Moreover, the association between OCT findings and visual field loss is strong (Wollstein et al., 2004; Sihota et al., 2006) with good reproducibility in both normal and glaucomatous eyes (Blumenthal et al., 2000b; Budenz et al., 2008). These studies clearly demonstrate that OCT can be used in the diagnosis and monitoring of glaucoma.

In relating visual function in visual field sectors to structure in optic nerve head sectors, arcuate nerve fiber bundles in Bjerrum's area were analysed because the arcuate fibers entering the optic nerve head at the 12 and 6 o'clock positions are the most sensitive sectors for glaucoma differentiation (Kanamori et al., 2003). Thus the mfERG responses in this experiment were regrouped in the same regions for comparison with the corresponding sectors of the OCT results. When the adaptive index was initially abnormal, significant reductions of the RNFL thickness were observed over the study period in both the unilateral glaucoma and OHT groups. However there were no changes in OCT results for subjects with abnormal optic disc cupping or with family history of glaucoma. Despite the fact that no significant

glaucoma was developed over the study period, thinning of the RNFL is one of the indicators of glaucomatous changes (Lalezary et al., 2006). There is a significant negative correlation reported in RNFL thickness with increasing age, but the loss of retinal thickness with age is only 3.3 μm per decade (Mok et al., 2002), which is only one tenth of the loss observed in this study (-3.02 and -3.54 $\mu\text{m}/\text{year}$ for the unilateral glaucoma and OHT groups respectively). On the other hand, reductions in thickness were not observed in corresponding sectors with normal initial adaptive indices; hence, the thinning of the RNFL indicates a progression of glaucomatous change.

These findings further support the hypothesis that early retinal nerve fiber loss shown in the OCT precedes visual field defects shown in standard perimetry (Kim et al., 2007). Furthermore, since the adaptive index is based on interaction of local and global flashes and represents the retinal fast-adaptive mechanism, the abnormal index appears to support the estimation of increased glaucoma risk and the fast-adaptive mechanism seems to be impaired before structural changes can be measured in the retina. With the RNFL beginning to reduce in thickness, both unilateral glaucoma and OHT groups in this experiment seem to have increased risk of developing glaucoma.

In conclusion, the adaptive index deduced from the modified global flash mfERG paradigm has demonstrated good sensitivity for differentiating subjects with real risk of glaucoma development and may assist in predicting progression of

glaucoma. This raises the possibility of using the modified global flash mfERG paradigm as a potential indicator for early detection of glaucomatous dysfunction.

Chapter 10

Experiment IV

**Porcine Global Flash mfERG: Possible Mechanisms for the
Glaucomatous Changes in Luminance-Modulated Response
Function**

(Vision Res. 2008; 48 (16):1726-34)

Abstract

Purpose

The aim of this experiment was to obtain a better understanding of the cellular contributions to the porcine global flash mfERG by using a pharmacologic dissection method, together with the luminance-modulation method which has been used to demonstrate mfERG changes in human glaucoma.

Methods

Global flash mfERGs with luminance-modulation, where the localized luminance-difference was set as 96%, 65%, 49% or 29% stimulus contrast, were recorded from 14 eyes of 10 six-week-old Yorkshire pigs in control conditions and after suppression of inner retinal responses with inhalation of isoflurane (ISO), and injections of TTX and NMDA. ON- and OFF-pathway responses were isolated by injection of 2-amino-4-phosphonobutyric acid (APB) and cis-2,3-piperidinedicarboxylic acid (PDA).

Results

The porcine global flash mfERG consisted of an early DC and a late IC. ISO and TTX removed inner retinal contributions to the IC; NMDA application further abolished the oscillatory wavelets in the DC and removed the residual IC waveform. The inner retina contributed regular oscillation-like wavelets (W1, W2 and W3) to the

DC and shaped the IC. After removing the inner retinal contributions, the porcine global flash mfERG waveform becomes comparable to that obtained with conventional mfERG stimulation. The remaining waveform (smoothed DC) was mainly contributed by the ON- and OFF-bipolar cells as revealed after APB or PDA injection. Photoreceptors contributed a small signal to the leading edge of N1. The characteristic of luminance-modulated response function of DC was demonstrated to be contributed by the inner retinal oscillation-like wavelets.

Conclusions

We believe that the DC of the porcine global flash mfERG is mainly composed of contributions from photoreceptors, and ON- and OFF-bipolar cells, where inner retinal activity partially shaped the DC with superimposed regular wavelets. However, the IC is dominated by inner retinal activity. The luminance-modulated response functions of DC consisted of both outer retinal response and oscillation-like wavelets of the inner retinal response. Both contain different characteristics during luminance-modulation of the stimulus, where the changes of W2 of the inner retinal response seem independent of luminance-modulation. The DC luminance-modulated response feature depends mainly on the relative contribution of inner retinal activities; the loss of inner retinal cells may alter the DC luminance-modulated response function, making it tend toward linearity.

Introduction

The mfERG allows for objective assessment of multiple localized retinal functions simultaneously in a brief recording session (Sutter and Tran, 1992). Investigation of the cellular contributions to the conventional mfERG in primates, has advanced the application of this technique in responses from normal and diseased eyes (Hare and Ton, 2002; Hood et al., 2002). Application of pharmacological dissection methods has suggested that human first-order kernel mfERG responses are mainly generated from distal retinal layers with contributions from photoreceptors, and ON- and OFF-bipolar cells (Hood et al., 2002). This finding supports application of the mfERG to a range of outer retinal dysfunctions (Huang et al., 2000; Vajaranant et al., 2002). In addition, non-linear components of retinal responses, which are generated by interactions between responses to successive flashes, are shown as higher-order kernels (Sutter, 2000). Although much clinical data has already demonstrated that these responses are affected in retinal diseases which are largely restricted to the inner retinal layers (Chan and Brown, 1999; Chan and Brown, 2000; Palmowski and Ruprecht, 2004), the relatively poor signal-to-noise ratio and the contributions from both inner and outer retinal neurons to the higher-order responses have limited their further utility.

To enhance the contribution of the inner retinal response to the human mfERG,

an alternative stimulus mode, with temporal interposition of global flashes, has been introduced to evoke a large non-linear component that is thought to reflect activity from inner retinal cells (Palmowski et al., 1999). This global flash paradigm provides an interaction between the multifocal flashes and the periodic global flash (Shimada et al., 2005), and has been widely reported to assess retinal adaptive mechanism (Fortune et al., 2002a; Palmowski et al., 2002; Chen et al., 2006; Chu et al., 2006a; Chu et al., 2007; Palmowski-Wolfe et al., 2007). Thus, it is important to understand further the related changes of the global flash mfERG waveform to particular retinal cells.

The important work of Hood and colleagues has shown that there is a larger contribution of the inner retina to the rhesus monkey's conventional mfERG than to the human mfERG (Hood et al., 2002). The waveform of the human first-order mfERG response and the rhesus monkey mfERG show close similarity only after removal of the inner retinal influences (Hood et al., 1999a; Hood et al., 1999b; Hood et al., 2002). Therefore, we used another animal model which is also structurally close to the human for our investigation. The porcine eye model has recently been used in studies of retinal transplantation (Ghosh and Arner, 2002), photoreceptor degeneration (Li et al., 1998) and glaucoma (Ruiz-Ederra et al., 2005). The porcine retina is cone photoreceptor-rich (Beauchemin, 1974; Chandler et al., 1999;

Hendrickson and Hicks, 2002). Moreover, the pig retina consists of the same layers as the human retina and the vascular anatomy, histology and physiology of the pig eye are very similar to the human eye (Stefansson et al., 2005). The waveform of the conventional mfERG response from the porcine eye and human eye are also similar (Voss Kyhn et al., 2007; Ng et al., 2008). The response is shaped by large contributions from ON- and OFF-bipolar cells (Ng et al., 2008); thus we expect comparable retinal physiology in human and porcine eyes, and we expect that the porcine eye will be suitable for studying the global flash paradigm, presumably because of similar inner retinal contribution to the mfERG reported from a recent study on the porcine eye (Ng et al., 2008).

The aim of this experiment was to examine the cellular contributions of the porcine global flash mfERG and hence, with this information, to gain a better understanding of the cellular basis of the human global flash mfERG and the characterization of luminance-modulated dependency on both DC and IC responses. It is possible to examine various aspects of retinal response in isolation using pharmacological dissection: ISO depresses NMDA receptor-mediated responses and TTX blocks spiking activity, such that inner retinal responses can be suppressed. APB and PDA block ON- and OFF-pathway responses, respectively. We used the simplest global flash mfERG stimulation sequence (Chu et al., 2006a; Chu et al., 2007) to

produce the mfERG waveform, and used pharmacologic agents, alone and in combination, to block the activity of particular retinal cell types or circuits of the porcine retina.

Methods

Animals

The mfERG recordings were obtained from 14 eyes of 10, normal, six-week-old Yorkshire pigs. Animals were anesthetized initially with ketamine (20 mg/kg IM), xylazine (2 mg/kg IV) and were treated with propofol (14-20 mg/kg/hr IV). Lactated Ringer's solution was administered by intravenous perfusion and artificial ventilation following orotracheal intubation was used to maintain the blood SpO₂ level at 95-100% throughout anesthesia. Rectal temperature was maintained at 38-39°C using a circulating hot water heating pad and blanket. Heart rate and SpO₂ levels were monitored throughout the experiment. Pupils were fully dilated with 1% tropicamide and 10% phenylephrine, and the ocular surface was anesthetized with 1% proparacaine HCl. After obtaining control recordings from all eyes, inhalation of ISO (4%) with 100% oxygen supply was used to replace propofol in order to facilitate prolonged anesthesia recommended by the animal care guidelines of veterinary medicine, as hypotension and transient apnea are experienced in long-term usage of propofol. All experimental and animal care procedures adhered to the ARVO Statement for the Use of Animals in Ophthalmic and Vision Research and were approved by the North Carolina State University Institutional Animal Care and Use Committees and the Animal Ethics-subcommittee of The Hong Kong Polytechnic

University.

Stimulus conditions

The stimulus pattern was presented on a Hewlett-Packard 17-inch CRT monitor (Model No: s7540), and an Apple Macintosh G4 computer was used to run the mfERG program (VERIS 5.01, EDI, San Mateo, CA, USA). The working distance from the screen to the tested eye was 20 cm, so the stimulus pattern subtends the visual angle close to 60° . The mfERG was measured using the simplest global flash paradigm with the pattern consisting of 103 non-scaled hexagons; each m-sequence of the stimulus contained four video frames (each frame lasts 11.8 ms with a frame rate of 85 Hz). During stimulation with multifocal flashes, each hexagon was either flashed (160 cd/m^2) or dark (1 cd/m^2) according to the selected $2^{12}-1$ pseudo-random binary m-sequence. In addition to the multifocal flashes, the global flash paradigm contains a dark frame (1 cd/m^2), a full screen global flash (160 cd/m^2) and a second dark frame (1 cd/m^2) between successive m-sequence stimulations (Figure 10.1a). The average luminance of the multifocal flash frame was about 80 cd/m^2 and the background was set to this value. The recording time for each stimulation cycle was approximately 3.2 minutes.

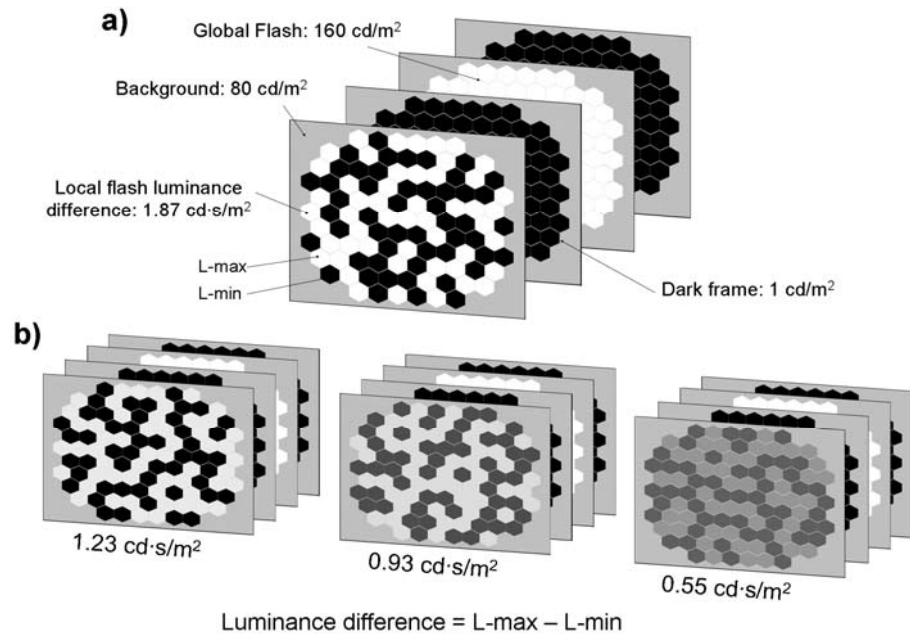


Figure 10.1 (a) Each stimulus sequence contains four frames. The initial frame (multifocal flash) alternated between bright and dark according to a pseudo-random binary m-sequence with a preset stimulus contrast level. (b) The luminance-difference between the brighter hexagons and the dimmer hexagons ($L_{\max} - L_{\min}$) of the multifocal flashes in four stimulus contrast settings are denoted 1.87, 1.23, 0.93 and 0.55 $\text{cd}\cdot\text{s}/\text{m}^2$.

Recording conditions

Conjunctival sutures were inserted 2 mm from superior and inferior limbus, respectively to prevent the drift of ocular orientation during recording. The eyelids of the tested eye were held by an eye speculum. A monopolar ERG-jet contact lens electrode (Universal SA, La Chaux-de-Fons, Switzerland) was used as an active electrode. It was placed on the cornea with ocular lubricant (Lacryvisc gel 0.3%,

Alcon Cleveland, OH, USA) and Grass subdermal F-E7 electrodes (Astro-med, Inc., West Warwick) were applied subcutaneously at the rostrum and the temporal canthus of the tested eye as ground and reference electrodes, respectively. The refractive error shown by retinoscopy at 20 cm viewing distance with the contact lens electrode in place was fully corrected by a 70 mm diameter ophthalmic lens placed in front of the porcine eye.

ERG signals were amplified by a Grass amplifier (band pass: 1 to 300 Hz; gain: x20,000; model CP122 bench-top style amplifier; Grass Instruments, Inc., Quincy, MA, USA). Before each recording, in order to maintain the same alignment between the eye and the stimulator, a short conventional mfERG recording was performed and the three-dimensional topography was used to locate and to align the positions of the optic nerve head and the visual streak (Figure 10.2a).

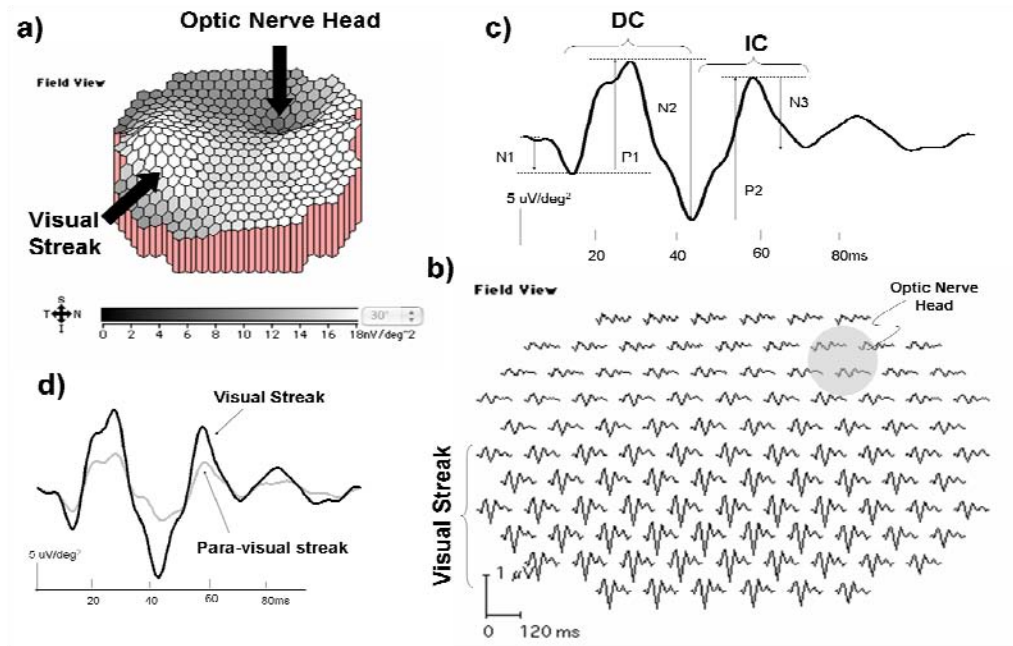


Figure 10.2 A typical mfERG result from a porcine eye. **(a)** Three-dimensional field-view topography across the retina from a left porcine eye at 99% stimulus contrast level, where the optic nerve head and the visual streak are shown. **(b)** Localized responses of 103 traces are also demonstrated. **(c)** The typical global flash mfERG response of first-order kernel (K1) contains two components: the DC and the IC. The measurements of peak-to-peak amplitudes of the two components are illustrated (P1 represents the DC amplitude and N3 represents the IC amplitude). **(d)** Superimposed comparisons of the averaged responses grouped from the visual streak (dark trace) and the para-visual streak region (grey trace).

Intravitreal injections

Intravitreal injections (25 μL) were made 3 mm posterior to the superior limbus with a sterile 27-gauge needle inserted through the pars plana. Assuming that the

vitreal volume is 2.0 mL, the intravitreal concentrations of the pharmacologic agents (Sigma-Aldrich, Missouri, USA) used were: Tetrodotoxin (TTX: 5 μ M), N-methyl-D-aspartic acid (NMDA: 4 mM), 2-amino-4-phosphonobutyric acid (APB: 1 mM) and cis-2,3-piperidinedicarboxylic acid (PDA: 3.5 mM). These concentrations are sufficient to have the desired effects on the flash ERG and mfERG in primates (Hare and Ton, 2002; Hood et al., 2002; Ueno et al., 2004) and pigs (Lalonde et al., 2006). The specific actions of the above individual drugs in pig eyes had been reported in a recent study (Ng et al., 2008). Treatment of TTX and NMDA was applied for all eyes, while eyes were randomly divided into two groups to investigate the effects of APB or PDA. Recordings were made at least one and half hours after each drug administration for the stabilization of the effect. Binocular indirect ophthalmoscopy was performed just after each intravitreal injection and conjunctival suturing to ensure the retinal integrity.

In all cases, the consecutive porcine mfERGs for each pig were measured in two different days in order to minimize the effect of prolonged anesthesia. The mfERG measurements up to the treatment of TTX were performed on the first day, while the treatments of TTX+NMDA, APB or PDA and APB+PDA were performed on the day after next. The total length of the period of anesthesia for each pig was around 6 hours per day.

Data analysis

First-order kernels were analyzed using the VERIS 5.01 software. The 103 individual mfERG responses from each pig eye were grouped differently into two regions according to the regional DC response amplitude; region with responses with amplitudes within the top 25 percentile were grouped to represent the visual streak, while the other regions were grouped as the area outside the visual streak except the optic disc area (Figure 10.2b) (Ng et al., 2008). The grouping criterion was based on the assumption that the amplitude would be proportional to the cone and ganglion cell density of the porcine retina, where the densities of cone and ganglion cell in porcine peripheral retina are less than about 70% from those of the visual streak (Chandler et al., 1999; Garca et al., 2005). The mfERG findings were represented by peak-to-peak response amplitude measurements of the relevant component (DC, IC or wavelets) and the effects of various drug administrations to the mfERG responses were compared using ANOVA with Bonferroni *post-hoc* correction.

Results

Control recordings

The array in [Figure 10.2b](#) shows typical localized global flash mfERG responses (control data) from one of the porcine eyes at 99% stimulus contrast level and the grouped response is shown in [Figure 10.2c](#). As with the human global flash mfERG response, the waveform contains two components, the DC and IC. The DC consists of an initial major trough (N1) at 14 ms followed by a major positive component (P1) at 30 ms, and there are two small wavelets overlaying the leading edge and the trailing edge of P1. The IC waveform contains a P2 peak at 65 ms. The responses were grouped into two regions, the visual streak and the para-retina (outside the visual streak), apart from larger responses obtained from the visual streak, there were no obvious differences in waveform between the two regions ([Figure 10.2b](#)). Because of the invariant global flash mfERG response across the retina, the visual streak responses were used to investigate the cellular contributions of the global flash mfERG response.

Effects of ISO, TTX and NMDA

The amplitudes and implicit times of the grouped responses from the visual streak before and after the application of ISO, TTX and NMDA are summarized in

Table 10.1. Figure 10.3a shows the averaged mfERG responses from the visual streak from one of the porcine eyes before and after inhalation of 4% ISO. After application of ISO, there was no remarkable change in the waveform; however the P2 and N3 of the IC showed a small reduction in amplitude, although these were not statistically significant and there was no change in implicit time (Table 10.1).

Application of TTX together with ISO made the oscillatory wavelets during both DC and IC phases of the response merely become more visible, but the general shape of the response remained essentially unchanged (Figure 10.3b). The ISO+TTX application further reduced the response of N2 in the DC and P2 and N3 of the IC, but only the amplitude reduction of P2 in the IC ($p < 0.01$) was statistically significant (Table 10.1).

Implicit time					
	DC			IC	
	N1	P1	N2	P2	N3
Control (14 eyes)	13.33 (0.40)	29.54 (0.31)	46.46 (0.37)	63.87 (0.37)	78.9 (0.54)
ISO (14 eyes)	13.86 (0.27)	30.81 (0.24)	46.68 (0.23)	63.89 (0.29)	79.54 (0.53)
ISO+TTX (14 eyes)	14.27 (0.42)	31.07 (0.50)	47.37 (0.57)	64.70 (0.65)	78.89 (0.52)
ISO+TTX+NMDA (14 eyes)	12.14 (0.63)	28.91 (0.66)	44.94 (0.33)	69.25 (0.67) ***	74.93 (1.18) ***
Amplitude					
	DC			IC	
	N1	P1	N2	P2	N3
Control (14 eyes)	8.45 (1.78)	20.89 (2.36)	31.45 (3.18)	29.57 (3.79)	13.92 (2.01)
ISO (14 eyes)	7.04 (0.71)	23.62 (1.98)	30.05 (2.68)	22.12 (2.76)	10.76 (1.80)
ISO+TTX (14 eyes)	8.74 (1.33)	22.04 (3.60)	22.90 (3.90)	15.84 (2.67) **	6.19 (1.07)
ISO+TTX+NMDA (14 eyes)	3.60 (0.82)	19.23 (2.63)	24.85 (3.52)	12.11 (1.35) ***	1.85 (0.41) **

Table 10.1 Mean of amplitude and implicit time with ± 1 SEM of the global flash mfERG features from the visual streak area. Statistical comparisons (ANOVA with Bonferroni *post-hoc* test) were done with the control data; ** (p<0.01) and *** (p<0.001) indicate levels of significant difference from the control group.

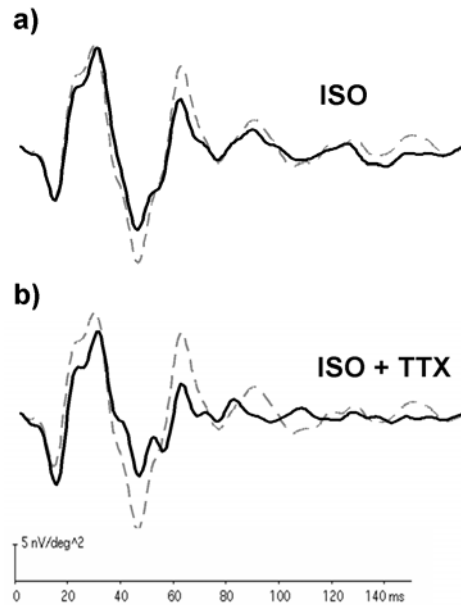


Figure 10.3 Superimposed comparisons of the typical averaged responses from the visual streak of one porcine eye. **(a)** The K1 waveforms of global flash mfERG under the influence of ISO (dark trace) and the control response (grey dotted trace). **(b)** The K1 waveforms of global flash mfERG under the effect of ISO+TTX (dark trace) and the control response (grey dotted trace).

However, the shape of the global flash mfERG waveform changed prominently after NMDA had been added (Figure 10.4a). NMDA removed nearly all the higher frequency components of the early DC, which now showed smooth leading and trailing edges. It also modified the shape of the IC, producing a significant delay ($p < 0.001$) in the P2 and a shift of N3 to an earlier implicit time; the amplitude of P2 ($p < 0.001$) and N3 ($p < 0.01$) of the IC were also reduced significantly (Table 10.1).

By subtraction of the post-ISO+TTX+NMDA response from the control

response, the component removed by ISO+TTX+NMDA can be obtained. This ISO+TTX+NMDA sensitive component contained a series of regular oscillation-like wavelets (W1, W2 and W3) superimposed on a sloping gradient before 50 ms. A prominent corneal-positive component with peak at 65 ms composed the rest of the waveform (Figure 10.4b), and this late prominent peak was consistent with the original IC waveform.

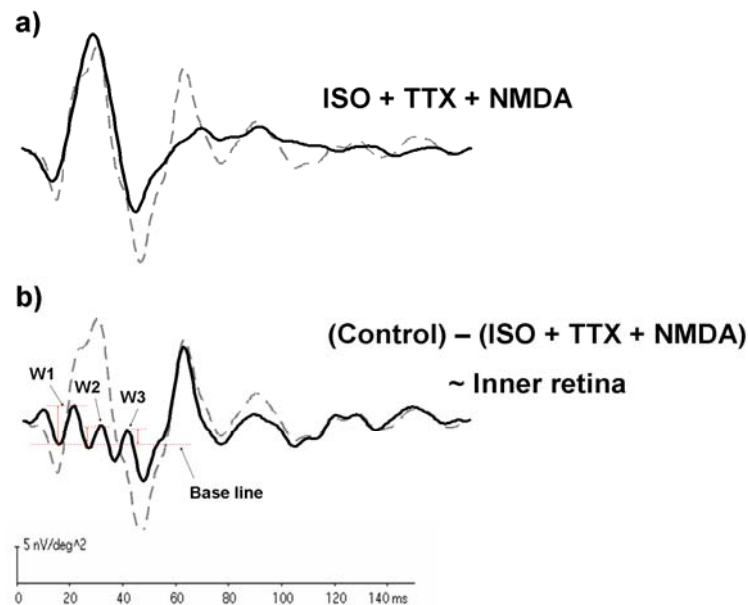


Figure 10.4 Superimposed comparisons of the typical averaged responses from the visual streak of one of the porcine eyes. (a) The K1 waveforms of global flash mfERG under the influence of ISO+TTX+NMDA (dark trace) and the control response (grey dotted trace). (b) The dark trace is an estimation of inner retinal activity suppressed by ISO+TTX+NMDA. (The amplitude of the oscillation-like wavelets indicated by the red lines was measured from the first trough (base line) to the peak of W1, W2 and W3, respectively.)

Effects of PDA and APB

To investigate the effects of PDA and APB on the residual mfERG response, responses were recorded after injection of PDA on 7 porcine eyes and APB was applied to another 7 porcine eyes. Amplitudes and implicit times of the resultant waveforms after the application of APB and PDA are summarized in [Table 10.2](#). PDA significantly reduced the implicit time of N1 ($p < 0.05$), while APB significantly reduced the amplitude of P1 ($p < 0.01$) and N2 ($p < 0.001$) with a significantly delay of N1, P1 and N2 responses ($p < 0.001$) ([Table 10.2](#)). [Figure 10.5](#) shows the responses from two different porcine eyes which received an injection of PDA or APB after ISO+TTX+NMDA. Application of PDA produced no statistically significant change in the waveform, but a small cornea negative-positive component (which shows a close resemblance to the response after application of APB) was removed. The estimated components from ON- and OFF-bipolar cells were extracted by subtraction of post-APB and post-PDA responses, respectively, from the preceding response. The application of APB+PDA significantly reduced both P1 and N2 amplitudes ($p < 0.001$), and all the implicit times were significantly increased ($p < 0.001$) ([Table 10.2](#)).

Implicit time					
	DC			IC	
	N1	P1	N2	P2	N3
ISO+TTX+NMDA (14 eyes)	12.14 (0.63)	28.91 (0.66)	44.94 (0.33)	69.25 (0.67)	74.93 (1.18)
Plus APB (7 eyes)	23.10 (0.56) ***	39.99 (0.53) ***	49.26 (1.42) ***	Nil	Nil
Plus PDA (7 eyes)	9.30 (0.53) *	26.47 (0.79)	45.22 (0.92)	68.98 (1.40)	Nil
Plus APB+PDA (14 eyes)	25.66 (0.43) ***	42.79 (0.56) ***	48.63 (0.74) ***	Nil	Nil
Amplitude					
	DC			IC	
	N1	P1	N2	P2	N3
ISO+TTX+NMDA (14 eyes)	3.60 (0.82)	19.23 (2.63)	24.85 (3.52)	12.11 (1.35)	1.85 (0.41)
Plus APB (7 eyes)	5.64 (0.66)	8.30 (1.26) **	6.03 (0.95) ***	Nil	Nil
Plus PDA (7 eyes)	1.17 (0.42)	21.97 (3.24)	34.03 (4.33)	18.57 (2.47)	Nil
Plus APB+PDA (7 eyes)	3.45 (0.35)	4.18 (0.81) ***	1.80 (0.44) ***	Nil	Nil

Table 10.2 Mean of amplitude and implicit time with ± 1 SEM of the global flash mfERG features from the visual streak area. Statistical comparisons (ANOVA with Bonferroni *post-hoc* test) were done with the data under ISO+TTX+NMDA; * ($p < 0.05$), ** ($p < 0.01$) and *** ($p < 0.001$) indicate levels of significant difference from the control group. Values marked with (Nil) represent no such parameters could be measured.

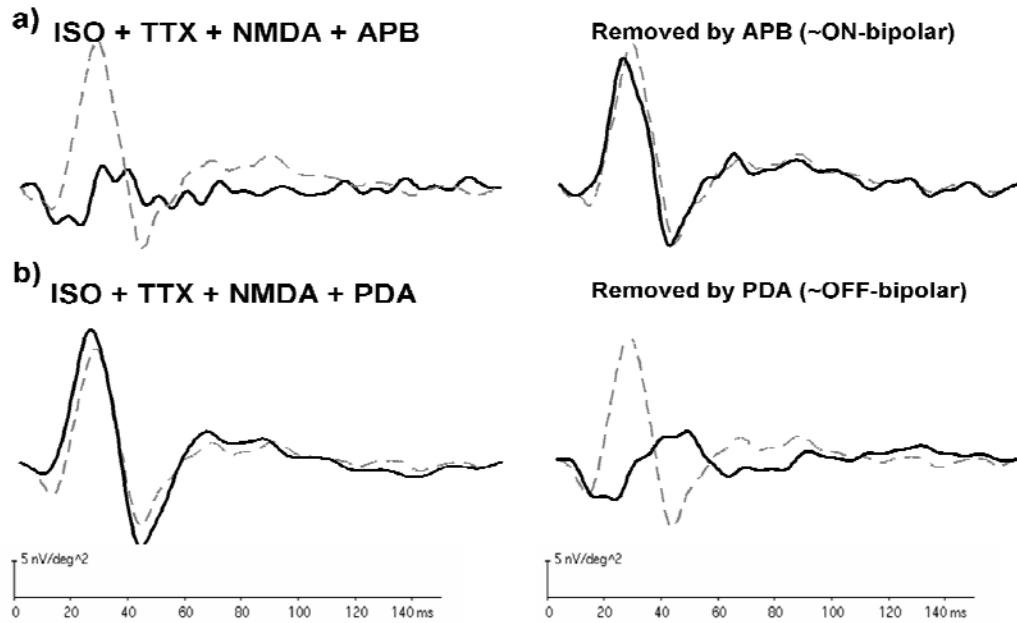


Figure 10.5 The grey dotted traces are the mfERG waveforms under effect of ISO+TTX+NMDA from two different porcine eyes. **(a)** The left dark trace shows the typical effect of APB on the global flash mfERG from one eye and the right dark trace estimates the ON-bipolar contributions isolated by APB. **(b)** The left dark trace shows the typical effect of PDA on the global flash mfERG from another eye and the right dark trace estimates the OFF-bipolar contributions isolated by PDA.

Figure 10.6 illustrates the possible contributions to the porcine global flash mfERG; they are mainly divided into outer and inner retinal contributions. Both the DC and IC contain inner retinal response, but the IC is mainly composed of the inner retinal contribution. Although the DC is shaped partly by the oscillation-like wavelets, it is largely composed of the responses generated from the ON- and OFF-bipolar cells.

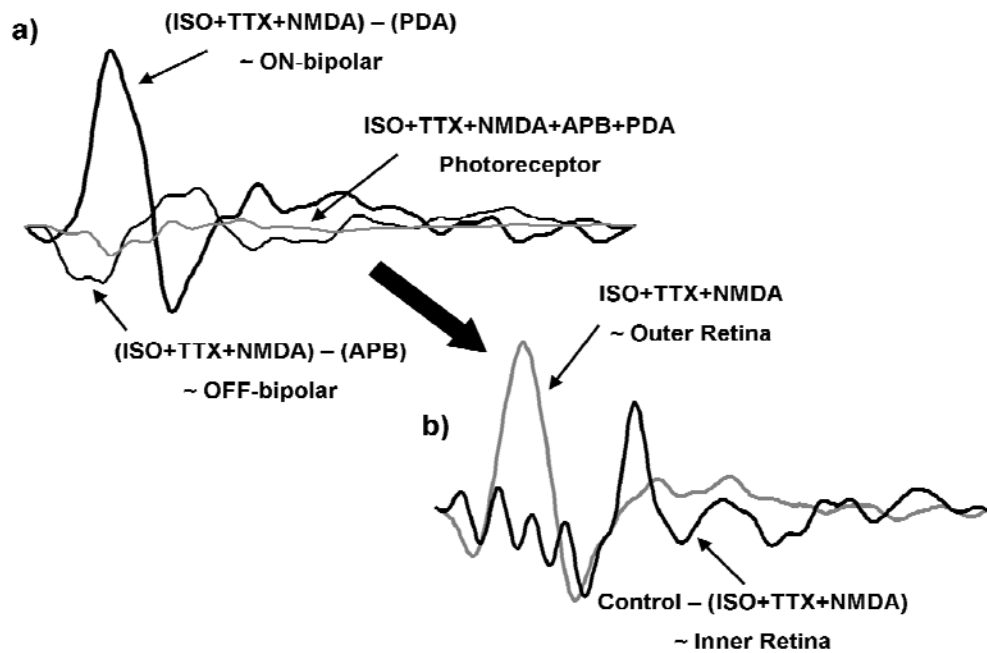


Figure 10.6 (a) The main contributions of the outer retinal response to the global flash mfERG are demonstrated, where the photoreceptor response (grey trace) obtained after APB+PDA is injected, the estimated ON-bipolar response (thick dark trace) and the estimated OFF-bipolar response (thin dark trace). (b) The approximate outer retinal response (grey trace) and the estimated inner retinal response (dark trace) are believed to shape the porcine global flash mfERG response.

Effect of luminance-modulation

In order to examine the porcine luminance-modulated response function of the global flash mfERG, the luminance-differences of the multifocal flashes were altered in the same way as the one from our previous experiments (Figure 10.1b) (Chu et al., 2006a; Chu et al., 2007). Figure 10.7 shows the DC and IC luminance-modulated

response functions obtained from the visual streak and the area beyond it from the control data. The porcine IC luminance-modulated response functions from both areas show a nearly constant (but low) rate of amplitude increase with the luminance-difference levels. Besides, the DC luminance-modulated response functions from both areas show a similar characteristic of approximate fixed rate of amplitude increase with luminance-difference levels.

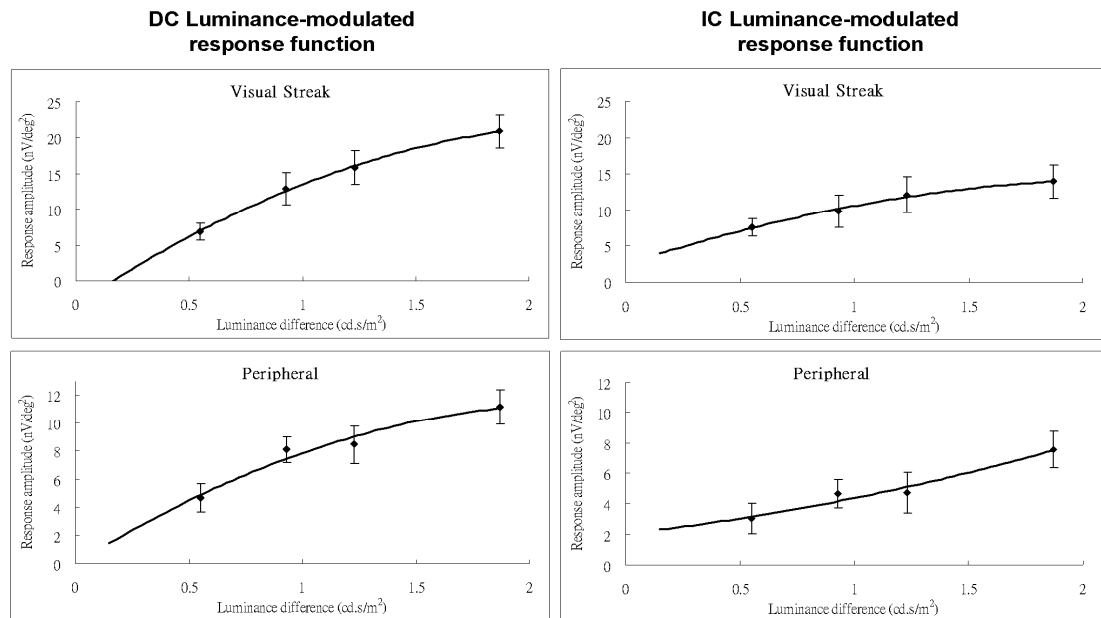


Figure 10.7 The luminance-modulated response functions of the grouped DC responses (P1) and the grouped IC responses (N3) from the visual streak (upper panels) and the para-visual streak area (lower panels) for control data. Lines represent the second-order best-fitting curves which provide better fit with higher value of R^2 than straight lines (Error bars = ± 1 SEM).

For better understanding of this characteristic, the mfERG waveform at the visual streak under different luminance-difference levels of post-ISO+TTX+NMDA and the component removed by ISO+TTX+NMDA were further investigated (Figure 10.8). Both the DC amplitude of post-ISO+TTX+NMDA and the IC amplitude of the component removed by ISO+TTX+NMDA generally increased with increasing luminance-difference levels. The luminance-modulated response function of the DC under ISO+TTX+NMDA in Figure 10.9a shows a nearly linear function with increasing luminance-difference levels.

The luminance-modulated response function of each component involved in the DC was also investigated (Figure 10.9b and 10.9c). The luminance-modulated response functions from the estimated ON-bipolar cell, OFF-bipolar cell and photoreceptor also showed an approximately linear function with increasing luminance-difference levels (Figure 10.9b). The amplitude of W1 increased with increasing luminance-difference levels, while the amplitude of W3 did not change significantly with variation of the luminance-difference levels. However, W2 showed an obvious independence of luminance-modulation for higher luminance-difference levels.

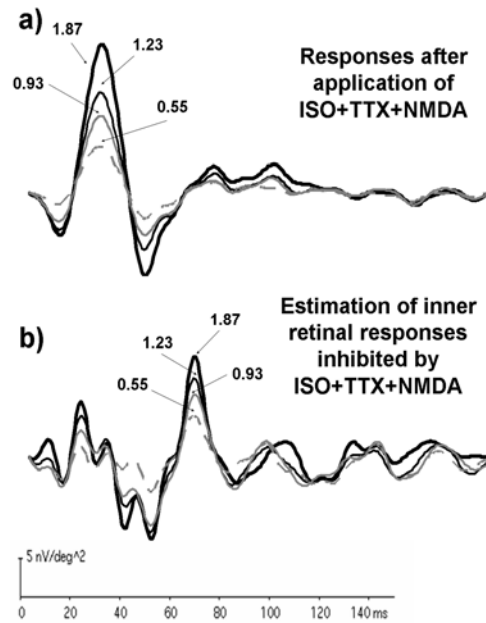


Figure 10.8 The typical mfERG waveform at the visual streak under different luminance-difference levels from one of the porcine eyes (**a**) Estimated outer retinal responses isolated with ISO+TTX+NMDA under different luminance-difference levels of the multifocal flash. (**b**) Estimated inner retinal responses obtained by subtraction of responses under ISO+TTX+NMDA from the control response with four different luminance-difference levels of the multifocal flash. (1.87 cd·s/m²: thick dark trace, 1.23 cd·s/m²: thin dark trace, 0.93 cd·s/m²: grey trace and 0.55 cd·s/m²: grey dotted trace)

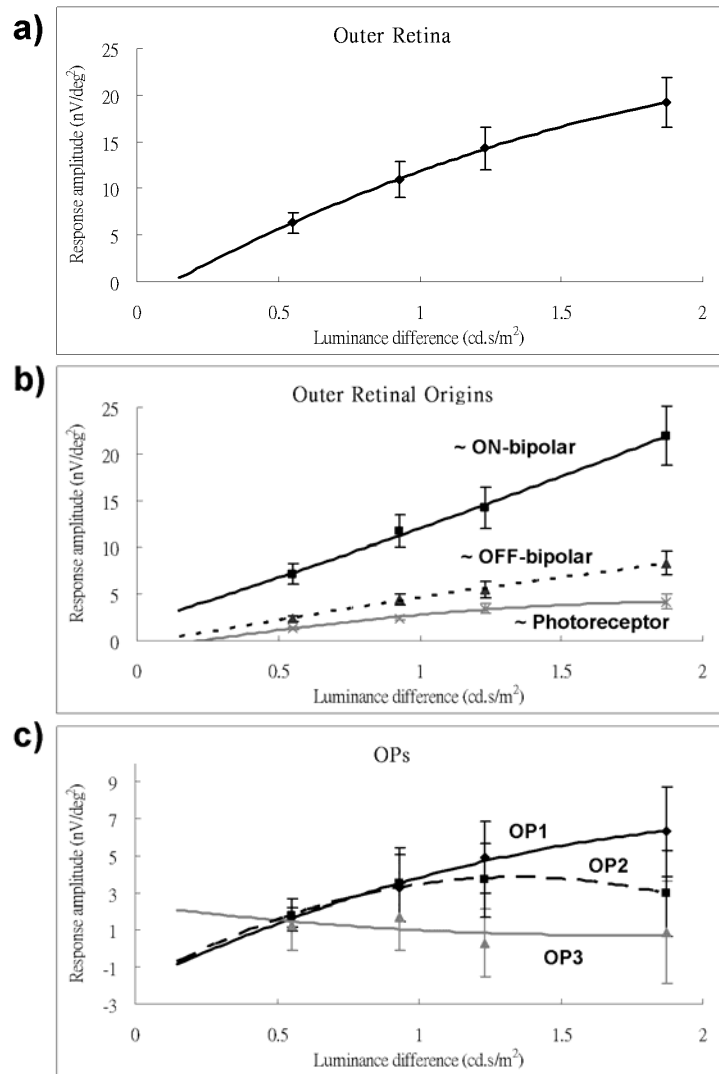


Figure 10.9 (a) The luminance-modulated response functions of the P1 amplitude of the DC from the estimated outer retinal response. (b) The estimated luminance-modulated response functions of the P1 amplitude of the ON-bipolar, OFF-bipolar and photoreceptors and (c) the estimated luminance-modulated response functions of W1, W2 and W3 amplitudes from the inner retinal response. Fitted lines are the best-fitting second-order curves that provide better fit with higher value of R^2 than straight lines (Error bars = ± 1 SEM).

Discussion

This experiment demonstrated the cellular origins of the porcine global flash mfERG using an established pharmacological dissection method for isolating particular contributions to the mfERG (Hood et al., 2002; Viswanathan et al., 2002; Ueno et al., 2004). As with the human retina, the porcine retina is cone-rich and the cone-to-rod ratio is close to that found in the para-macular region of the human retina (Curcio et al., 1990; Chandler et al., 1999). Although the porcine retina lacks a defined macular region, the cone cells as well as the ganglion cells are localized in a broad region in the central retina forming the visual streak. The densities of cone and ganglion cell gradually decrease towards the peripheral retina where both are less than about 70% in density in the visual streak (Chandler et al., 1999; Garca et al., 2005). Apart from the amplitude reduction, there are no remarkable differences between the porcine global flash mfERG responses at the visual streak and the peripheral retina. This suggests that these two retinal regions are very similar.

The porcine mfERG waveform from this global flash paradigm contains mainly two components (DC and IC), and this mirrors the response in humans. It has been suggested that the IC is affected in glaucoma (Fortune et al., 2002a; Palmowski et al., 2002), similar results have also been reported in our previous experiments (Chu et al., 2006a; Chu et al., 2007) and thus the IC is thought to be originated predominantly

from the inner retina (Palmowski et al., 1999). However, the large intersubject variability of the IC (Shimada et al., 2001) and the poor correlation between the localized IC responses and the visual field defect (Fortune et al., 2002a) limited so far the validity in using IC for the assessment of localized glaucomatous damage in individual patients. The DC is thought to be analogous to the conventional mfERG flicker response, but it is also believed to reflect the level of light adaptation because of the effects of periodic global flashes (Shimada et al., 2005). It shows certain optic nerve head response contributions (Palmowski et al., 1999), and it may show early changes in diabetic retinopathy (Shimada et al., 2001) and age-related maculopathy (Feigl et al., 2005). As shown in the luminance-modulation paradigm in our previous experiments, the DC can be used for detecting response change in glaucoma patients and it demonstrates good correlation with the visual field defect (Chu et al., 2006a; Chu et al., 2007). Cellular contributions of the porcine global flash mfERG provide additional information regarding the DC and IC, which assist in interpretation of particular changes with different eye diseases, and extend our knowledge of the basis of the human global flash mfERG.

Contributions from the inner retina

The volatile gas ISO is used commonly as an anesthetic agent in surgery.

However, ISO may affect the inner retinal signal (Fortune et al., 2002b), including depression of NMDA receptor mediated responses (Harada et al., 1999) and suppression up to 50% of voltage-gated sodium channel activity (Duch et al., 1998). In addition, the porcine mfERG with ISO anesthesia shows similar effects to that obtained by optic nerve section (Lalonde et al., 2006). Thus in our control recording, propofol instead of ISO as the anesthetic agent was used, because propofol has been reported to have minimal influence on human evoked potentials (Hans and Bonhomme, 2006), and to give identical porcine mfERG response to those recorded under ketamine anesthesia (Lalonde et al., 2006).

However, ISO had only little effect on the porcine global flash mfERG, producing only a slight reduction of the IC amplitudes. The further administration of TTX, significantly reduced P2 amplitude of the IC; TTX was conventionally used to eliminate inner retinal activities in animal studies (Hood et al., 1999a; Lalonde et al., 2006). TTX inhibits the voltage-gated sodium channel in the ganglion cells and some amacrine cells, where the voltage-gated sodium channel is used to trigger action potentials. Although retinal bipolar cells do not fire action potentials, the voltage-gated sodium channel has also been found in mammalian retinal bipolar cells (Ichinose et al., 2005). Therefore, TTX effectively isolates the spiking activities of the ganglion and amacrine cells and may have little effect on the outer retina, but

is powerful in removing a large inner retinal contribution of the primate mfERG (Hood et al., 1999a; Hood et al., 1999b; Hare and Ton, 2002; Hood et al., 2002). NMDA (an ionotropic glutamate agonist) was used to remove the remaining inner retinal activity that was not suppressed by TTX (Hood, 2000).

In an attempt to further suppress inner retinal activity, ISO+TTX+NMDA was applied. The use of TTX+NMDA has been reported to suppress most inner retinal activity with less influence on the outer retinal response in the primate mfERG (Hood et al., 2002). Both NMDA and TTX were also reported to influence the first- and second-order responses from the conventional porcine mfERG and were useful in suppressing the inner retinal activities for the porcine retina (Ng et al., 2008). The results in this experiment demonstrated that further use of NMDA abolished the oscillations on the leading and trailing edges of the DC of the porcine global flash mfERG, and the IC was completely removed.

After the inner retina was suppressed, the residual component of the porcine global flash mfERG is mainly generated by the outer retinal cells, where by subtraction of the post-ISO+TTX+NMDA response from the control response, the difference (the component inhibited by ISO+TTX+NMDA) is mainly generated by the inner retina. Results show that inner retinal activity partially shaped the DC with superimposed regular oscillation-like wavelets, where W1 and W3 shaped the

leading and trailing edges of the DC, respectively, and W2 overlapped with the prominent positive peak of the DC. In addition, the sloping gradient of the oscillation-like wavelets demonstrates an underneath low-frequency component which also contributes to the DC amplitude. The IC is dominated by inner retinal activity which supports Sutter and colleagues' (1999) early hypothesis that the IC of the human global flash mfERG is generated primarily within the inner retina (Sutter et al., 1999). Since ISO+TTX only partially affected the IC amplitude, the action potentials from inner retinal cells contribute little to the global flash mfERG and are mainly limited to the IC waveform. The remaining inner retinal contribution after ISO+TTX, that is the NMDA sensitive component, is likely to be generated by local potentials of the inner retinal cells. Although this NMDA sensitive component mainly contributed to the IC waveform, it also shaped the edges of the DC and contributed to the P1 amplitude.

Contributions from the outer retina

After the inner retinal influences have been essentially removed, the porcine global flash mfERG waveform is comparable to that obtained from conventional mfERG stimulation (Voss Kyhn et al., 2007; Ng et al., 2008). It was believed that the remaining DC of the global flash mfERG is mainly composed of contributions from

photoreceptors, and ON- and OFF-bipolar cells, and the findings in this experiment are consistent with previous findings (Tremblay et al., 2005; Ng et al., 2008). To isolate these contributions, responses were recorded after injection of APB or PDA. APB is a glutamate analogue that inhibits signal transmission from the photoreceptors to the ON-bipolar cells, while PDA is a glutamate analogue that blocks transmission from photoreceptors to OFF-bipolar cells and horizontal cells (Slaughter and Miller, 1983), and to the third-order neurons. Both APB and PDA were reported to be effective on the porcine retina (Tremblay et al., 2005), and previous studies demonstrated some common influences in both porcine and primate conventional mfERG (Hare and Ton, 2002; Tremblay et al., 2005).

By subtraction of post-APB and post-PDA responses from the ISO+TTX+NMDA response, the contributions of ON- and OFF-pathways in the remaining mfERG response can be estimated. The component removed by APB is the contribution mainly from ON-bipolar cells, and the component removed by PDA is mainly from OFF-bipolar cells; these ON- and OFF-responses which have recorded in this experiment are very similar to those from primates (Hood et al., 2002) and pigs (Ng et al., 2008).

The onset (hyperpolarization) of the OFF-bipolar cell starts just before the depolarization of the ON-bipolar cell and thus shapes the leading edge of the N1

component. Then the large ON-response (depolarization of the ON-bipolar cell) covers the effect of the OFF-response and shapes the leading edge of the P1 component. Recovery of the OFF-response occurs slightly before the peak of P1 and the recovery of the ON-response mainly forms the trailing edge of P1. The photoreceptor response shows a small negative amplitude and may only contribute in shaping the leading edge of N1. However, the large ON-response magnitude mainly influences the shape of the DC response.

Luminance-modulated response function

The general trend of porcine DC luminance-modulated response function looks similar to that obtained from the human para-macular region, but the DC luminance-modulated response function from the porcine global flash mfERG did not show obvious variations with retinal eccentricity (as occurs in humans (Chu et al., 2006a; Chu et al., 2007)), and the DC luminance-modulated response function, either from visual streak or para-visual streak region failed to show an obvious saturation characteristic which was characteristic of the DC luminance-modulated response function from human peripheral retina.

It was concluded that the DC amplitude is likely to be composed of the outer retinal response and the oscillation-like wavelets which are directly related to the

contribution of the inner retinal response; it appears that luminance-modulated stimulation produces different response characteristics in these responses in the porcine eye than in humans. The resultant feature of the DC luminance-modulated response function likely depends on the ratios of these two components. In the porcine global flash mfERG, the relatively small contribution of the oscillation-like wavelets, as compared to the large outer retinal response, may contribute to a linear DC luminance-modulated response function; on the other hand, if there is a larger contribution of the oscillation-like wavelets to the global flash mfERG, this may produce a saturation characteristic as seen in the DC luminance-modulated response function of the human mfERG (Chu et al., 2006a).

This experiment has provided an insight into the global flash mfERG and evidence that the DC is not produced purely by outer retinal activity. It further confirms that the IC is predominately produced by inner retinal activity. These findings confirm that better assessment of inner retinal function can be obtained by the global flash mfERG (Fortune et al., 2002a; Palmowski et al., 2002; Chu et al., 2006a; Chu et al., 2007; Palmowski-Wolfe et al., 2007) than the standard mfERG paradigm. Eye diseases involving damage of inner retinal layers may reduce oscillation-like wavelets; the contribution of W2 to the DC amplitude in the mid luminance-difference levels may play an important role in the decrease in DC

response amplitude which glaucoma patients obviously show at these luminance-difference levels (Chu et al., 2006a; Chu et al., 2007). Therefore, it was proposed that glaucoma patients are likely to have a loss of W2 which alters the saturation characteristic of DC luminance-modulated response function. The similarity of the porcine and human global flash mfERG waveforms suggests that the retinal physiology may be comparable. However, some care should be taken in this interpretation since the different rod/cone mix across the retina and different photoreceptor or ganglion cell distribution between human eye and porcine eye may cause different responsiveness to fast adaptation that makes the different luminance-modulated response characteristics from the porcine eye. Nevertheless, the W2 showed an obvious independence of luminance-modulation for higher luminance-difference levels which may be sensitive to glaucomatous changes, thus provides the possibility of the porcine eye as the experimental glaucoma model for further investigation.

Chapter 11 - Conclusions and Suggestions for Future Research

Glaucoma is well known to cause blindness when it reaches its most severe stage. The loss of ganglion cells due to glaucomatous damage cannot be reversed, but early and appropriate treatment is effective for preventing further retinal ganglion cell death. Early recognition and accurate assessment of glaucomatous functional loss is a major goal for clinicians and researchers since this will prevent the progression of glaucomatous damage; thus a sensitive diagnostic technique is very important as it will lead to early treatment. Visual field analysis has been the basis of current standards for glaucoma diagnosis; however, early diagnosis is not possible because visual field loss is detected only once a significant loss of ganglion cell fibers has already occurred (Harwerth et al., 1999). In recent years, glaucoma diagnostic techniques have shown rapid progress and many new instruments have been developed to assist in the early diagnosis of glaucoma. The latest method applied in the diagnosis of OAG is to measure the RNFL thickness as an indication of ganglion cell fiber loss (Sihota et al., 2006). Despite the diagnostic value of RNFL thickness measurement in glaucoma, imaging instruments with quantitative outputs including the confocal scanning laser ophthalmoscope, the SLP and the OCT provide only structural assessment for glaucoma diagnosis, and these methods can only detect pathological changes once an irreversible loss of nerve fibers has already occurred.

Functional changes in glaucoma should also be considered because the loss of retinal ganglion cells is characterized by specific patterns of progressively decreasing retinal sensitivity which reflect the patient's visual performance and indicate visual malfunction.

The current study has demonstrated a new approach in early detection of glaucomatous dysfunction by using the mfERG which objectively measures topographical retinal responses. Although a number of studies have used the mfERG to assess the physiological response of the ganglion cells in order to look for signs of glaucomatous damage, the usefulness of the mfERG in assessing glaucomatous damage has remained uncertain. Application of the mfERG has been limited mostly due to lack of correlation with visual field sensitivity. In an attempt to improve the efficacy of the mfERG in detecting inner retinal activity, a stimulus protocol previously employed by Fortune and his colleagues (Fortune et al., 2002a) was used in this study with the modification of the stimulation pattern to produce a new mfERG protocol in order to achieve the purpose of early detection of glaucoma.

This modified global flash paradigm with luminance-modulation is designed to measure retinal adaptive changes. Inserting a global flash in the m-sequence stimulus adjusts the overall adaptation level of the retina, so that rapid adaptation effects add to the m-sequence response. The DC is the response of the local flashes influenced to a

degree by the global flash in the prior m-sequence stimulation, and the IC is the change to the response of the global flash produced by the current m-sequence stimulation (Sutter et al., 1999). Both components reflect interaction between the m-sequence stimulus and the global flash (Shimada et al., 2005) and are likely to be affected by the luminance-modulation of the multifocal flashes.

Results of previous studies have suggested that the reduction of the IC in subjects with glaucoma seem to indicate impaired adaptive effects due to inner retinal damage (Palmowski et al., 2002). However, no study has shown any relationship between the DC response and glaucoma. The DC and IC luminance-modulated response function showed different characteristics as discussed in Chapter 7. The normal DC responses remain steady at high luminance-difference levels, but in subjects with glaucoma, the DC responses show less reduction in amplitude at high stimulus luminance-difference conditions than at mid stimulus luminance-difference conditions. In contrast, the IC responses show a larger reduction in amplitude under high stimulus luminance-difference conditions. Since most previous studies have only used the high stimulus luminance-difference condition for global flash stimulation (Bears et al., 2001a; Palmowski et al., 2002), this may explain why the amplitude changes of DC responses from glaucoma subjects were difficult to observe when compared with the changes of IC responses.

DC response amplitudes even for the mid luminance-difference level still did not demonstrate good correlation with the changes of visual field sensitivity in glaucoma (see Chapter 7); hence, the mfERG response amplitude alone is not likely to be a useful measure as previously discussed (Fortune et al., 2002a). In addition to mfERG amplitude reduction, subjects with glaucoma also showed a loss of luminance-difference saturation in the DC luminance-modulated response function. The loss of this feature in glaucoma is most likely caused by impairment of the fast-adaptation mechanism in retina. Quantifying this loss by calculating the adaptive index provides a measure of the intrinsic response changes with luminance-modulation; the adaptive index neglects the baseline response amplitude, and minimises the effect of intersubject variation of the response amplitude.

In order to be able to introduce a more timely therapy for glaucoma, tests with a higher sensitivity are needed for early detection of glaucoma and for monitoring the success of early treatment. The results of Chapter 7 show that the adaptive index provides good differentiation between normal subjects and those with glaucoma (the sensitivity is 93% with a specificity of 95% using the best cutoff adaptive index value of 1.5 based on the ROC curve). The adaptive index also shows good correlation ($r = 0.58$) with the glaucomatous visual field defect.

The adaptive index gives very good sensitivity and specificity in detection of

glaucoma; its usefulness in detecting functional changes in patients at high risk of having glaucoma was also evaluated. The findings with the global flash paradigm with luminance-modulation in Chapter 8 have shown that fellow eyes of patients with unilateral glaucoma are similar to glaucomatous eyes that have impaired retinal adaptive changes. The adaptive index in fellow eyes was also reduced by a factor of almost 10 and the mean level was below the best cutoff point demonstrated in Chapter 7. Thus, fellow eyes that were functionally normal in VA and visual field had already shown abnormal changes in the fast-adaptive mechanism; this allows these fellow eyes to be differentiated from normal by the pre-established criteria. Previous studies have reported that certain retinal changes before any defined visual field loss may be present in the fellow eyes of patients with unilateral glaucoma (Kim et al., 2005). The significant reduction of the adaptive index in the fellow eyes of patients with unilateral glaucoma further confirms that an impaired fast-adaptive mechanism occurs before observed visual field abnormalities in patients at high risk of glaucoma.

Due to the different characteristics of the DC luminance-modulated response function in the central (within 10°) and peripheral (beyond 19°) regions of the retina as discussed in Chapter 7, the adaptive index can only be used for responses obtained outside the macular region. However, from the result of experiment 2, the rate of change of the luminance-modulated response function is suggested to be another

indicator of the variation of retinal adaptation. This may offer a way to reduce the testing time for this paradigm, allowing only two luminance-modulation levels to be tested, rather than four. In Chapter 8, a simple comparison of the rate of change in DC response amplitude at the two lowest luminance-difference levels (the slope) was discussed, and slope may be another important parameter to allow monitoring of macular and peripheral retinal function. Although the DC slope has only been measured using two luminance-difference levels, it provides similar information to that provided by the adaptive index. The reduction of the slope value is likely to directly represent the depression of responses at the mid luminance-difference level caused by glaucomatous damage. However, based on the data in Chapter 8, both central IC amplitude and central DC slope showing non-significant differences between the control and the fellow eyes indicate that the central retinal function may not be obviously affected in the early stage of glaucoma. This conclusion agrees with the progression of glaucomatous damage that initially affects the Bjerrum area. The ROC curve for the peripheral DC slope shows that this method provides reasonable sensitivity (75%) and specificity (80%) (when the best slope cutoff value of 4.7 is used) in differentiating normal subjects from those with suspected glaucoma, although it does not work as good as the adaptive index. The measurement of the adaptive index or DC slope using this luminance-modulated global-flash mfERG

stimulation can provide additional information for diagnosis. The DC slope suggested in Chapter 8 can be used as a screening tool for detection of glaucomatous damage, but for more detailed monitoring of regional changes of retinal function, use of the adaptive index is suggested because of its lower variability which gives better differentiation between the normal subjects and those with glaucoma.

In Chapter 9, a three-year study was performed to investigate the association of the luminance-modulated global flash mfERG and other visual/retinal assessments for subsets of subjects at high risk of developing glaucomatous damage. Among the high risk groups, some of the field quadrants already having an initial abnormal value of adaptive index below 1.5 demonstrate that some subjects have already shown functional changes (revealed by the mfERG), even though no abnormalities were revealed by visual field or OCT. In order to observe the changes of visual sensitivity and parapapillary RNFL thickness in the field corresponding to the mfERG response, the visual field and OCT data from each high risk group was divided into two categories according to whether the initial adaptive index was above or below 1.5. Generally, those regions with abnormal adaptive index had lower visual field MD and thinner parapapillary RNFL thickness than those with normal adaptive index. But, in this experiment, there was no significant reduction in the visual field sensitivity over the study period although the fast-adaptive mechanism was initially shown to be

impaired. This may relate to the poor sensitivity of perimetry to detect visual field changes in the early stages of glaucoma (Kerrigan-Baumrind et al., 2000). Indeed, only 7.2% of fellow eyes in patients with unilateral POAG progress to glaucomatous visual field loss five years after initial diagnosis (Chen and Park, 2000). Other studies have reported that 24 – 43% of fellow eyes in patients with unilateral POAG develop glaucomatous visual field loss over 3 to 7 years (Harbin et al., 1976; Kass et al., 1976; Olivius and Thorburn, 1978; Susanna et al., 1978). In addition, the conversion rate from untreated OHT to glaucoma is only about 1% per year and the conversion rate possibly decreases to half for treated OHT (Kass et al., 2002). The current experiment is in its first three year phase, and thus is probably not long enough to show the development of glaucomatous visual field defects, even for subjects at high risk. However, this 3-year study demonstrates that the functional impairment in glaucoma should be at least 3 years earlier than the structural changes in the retina.

Meanwhile, significant reductions of the parapapillary RNFL thickness were observed over the study period in both the unilateral glaucoma and OHT groups, and these reductions in thickness were not observed in field regions with initially normal adaptive index. Despite the fact that no significant glaucoma developed over the study period, thinning of the nerve fiber layer is one of the indicators of glaucomatous changes (Lalezary et al., 2006) and a loss of 10 μm in RNFL thickness from baseline

has been shown to predict glaucomatous change (Lalezary et al., 2006). Hence, the thinning of the RNFL indicates a progression of glaucomatous change, and this further supports the hypothesis that early retinal nerve fiber loss shown in the OCT precedes visual field defects shown in standard perimetry (Kim et al., 2007). Furthermore, since the adaptive index is based on interaction of local and global flashes and represents the retinal fast-adaptive mechanism, the abnormal index appears to support the estimation of increased glaucoma risk and the fast-adaptive mechanism seems to be impaired before structural changes can be measured in the retina. With the RNFL beginning to reduce in thickness, both unilateral glaucoma and OHT groups in this study seem to have increased risk of developing glaucoma.

The experiment described in Chapter 10 helps to obtain a better understanding of the cellular contributions to the porcine global flash mfERG by using a pharmacologic dissection method, together with the method using variation of stimulus contrast which has demonstrated mfERG changes in human glaucoma. The porcine mfERG waveform from this global flash paradigm also contains mainly two components (DC and IC), and this mirrors the response in humans. Results show that inner retinal activity partially shaped the DC with superimposed regular oscillation-like wavelets, where W1 and W3 shaped the leading and trailing edges of the DC, respectively and W2 overlapped with the prominent positive peak of the DC.

The IC is dominated by inner retinal activity, which supports Sutter and colleagues' early hypothesis that the IC of the human global flash mfERG is generated primarily within the inner retina (Palmowski et al., 1999; Sutter et al., 1999).

The DC response is likely to be composed of the outer retinal response, and the oscillation-like wavelets which are directly related to the contribution of the inner retinal response; the resultant feature of the DC luminance-modulated response function likely depends on the ratios of these two components. A larger contribution of the oscillation-like wavelets to the global flash mfERG may produce a saturation characteristic as seen in the DC luminance-modulated response function of the human mfERG. This study has provided an insight into the global flash mfERG, where eye diseases involving damage of inner retinal layers may reduce oscillation-like wavelets; the contribution of the second wavelets (W2) to the DC amplitude in the mid luminance-modulation levels may play an important role in the decrease in DC response amplitude which glaucoma patients obviously show at these luminance-modulation levels. Therefore, we propose that glaucoma patients are likely to have a loss of W2 which alters the saturation characteristic of DC luminance-modulated response function.

11.1 Possible glaucoma retinal mechanism(s)

From the results of the experiment described in Chapter 10, the oscillation-like wavelets along the DC is the NMDA sensitive component, which is likely to be generated by local potentials of the inner retinal cells. Specifically, the special characteristic of luminance-modulated response function from the W2 is quite similar to that presented from the M-type of ganglion cell, which has a high gain at low contrast levels and starts to saturate at mid contrast levels (Lee et al., 1990); a similar response function generated by the multifocal VEP was speculated to arise from the M-ganglion cells (Klistorner et al., 1997). However, the first-order kernel mfERG response produces a waveform that represents the difference between responses to "bright" and "dark" local flashes; the DC luminance-modulated response function is not a contrast response, it is the difference between the waveforms of the local responses evoked by flashes of two different luminance levels. The apparent saturation of the DC amplitude at high luminance-difference levels is, therefore, actually an indication that the "bright" and "dark" luminance responses reached some sort of equilibrium, but not that the response generators have necessarily reached saturation. The saturation feature of the DC luminance-modulated response function is based on the temporal interaction of the global adaptive frame related to the fast-adaptation mechanism. The first-order response of the conventional m-sequence

stimulation appears to be linearly dependent on the changes of luminance-difference in the response (Brown and Yap, 1996). However, in a more complex interaction with the global flash stimulus, only the peripheral DC response appears to be independent of the luminance-difference changes, where the DC response seems to remain steady at high luminance-difference levels. This implies that this nonlinear response function curve is altered by the adaptive mechanism that was induced by the global flash. The loss of this feature in glaucoma is most likely caused by impairment of the short-term fast-adaptation activity produced by the interaction of global flashes. However, this change may also be due to a generalized loss of function of the neurons which respond to these input signals; thus, the abnormal changes that occur in glaucoma probably reflect a combination of factors and most likely refer to inner retinal dysfunction. These findings support the conjecture that the response components due to fast-adapting mechanisms are located predominantly in the inner retinal layers because of its nonlinear characteristics (Sutter et al., 1999; Shimada et al., 2001; Fortune et al., 2002a; Palmowski et al., 2002),

Recently, Morgan (2002) showed that retinal ganglion cells do undergo shrinkage, including body size reduction and axon diameter reduction, prior to cell death (Morgan, 2002). The widespread morphologic changes of the ganglion cell population are likely to accompany changes in normal function and thus affect the

physiological behavior of these cells, which may include a loss of temporal interaction function. Nevertheless, the different nature of the luminance-modulated response function between the central and peripheral retina suggests that the fast-adapting mechanism may have different cellular bases in these regions, or the cellular bases to control this mechanism are distributed differently in these regions.

Although it is speculated glaucoma patients have a loss of the oscillation-like wavelets, especially W2, which alters the saturation characteristic of DC luminance-modulated response function, its definite generator still remains unclear. However, this oscillation does not resemble the ONHC, since the oscillation-like wavelets found in this study were hardly affected by TTX, which inhibits the ganglion cell responses that compose the ONHC response. The OPs of the full-field flash ERG are believed to be generated from the inner plexiform layer, and the swelling and retraction of the ganglion cell dendrites in the inner plexiform layer in early glaucoma are thought to result in abnormal OPs (Fortune et al., 2002a). Alternatively, the origins of the oscillation-like wavelets found in this study can be explained on the basis of the low-frequency OPs of the slow-sequence mfERG. This hypothesis is initially driven by the match in frequency between our oscillation-like wavelets (around 85 Hz) and the low-frequency (80 Hz) oscillation component found by Zhou and co-workers ((Zhou et al., 2007). In addition, Zhou and co-workers

demonstrated that the low-frequency OPs partly originate from inner retina, primarily from the non-spiking activity of amacrine cells and partly contributed from more distal retinal activity (second-order neurons), since only part of the low-frequency OPs were removed by TTX+NMDA (Zhou et al., 2007). However, in this study of pharmacological blockage characteristics of the oscillation-like wavelets, TTX+NMDA seems to remove all the oscillatory components of the DC, but these components were not significantly affected by TTX. The oscillation-like wavelets found in this study are speculated to be mainly generated from the inner plexiform layer. Nevertheless, OP component is not likely to derive from a single generator, but derives from activity of local inner plexiform layer circuitry in the retina. Furthermore, this inferred that glaucomatous damage is not localized in the ganglion cells, but that more widespread retinal damage has occurred. This demonstrates that the functional impairment in the inner plexiform layer circuitry seems to be the first physiological change in glaucoma.

In addition, the specific loss of the luminance-modulated response function across a wide range of luminance-difference levels in glaucoma is also likely to be related to malfunction of the M-pathway. This pathway responds to high frequency stimuli and would be expected to be driven by the mfERG stimulus used in this study, which provides a high temporal frequency (75 Hz frame rate and short duration) and low

spatial frequency (hexagon sizes from 2.5° to 5°), achromatic pattern stimuli (Keating et al., 2000). The M-pathway responds to high temporal and low spatial frequency information as well as to luminance information and is involved in the processing of motion and high frequency flicker information (Livingstone and Hubel, 1987; Livingstone and Hubel, 1988). The M-pathway is also more dominant in the peripheral retina (Bauer et al., 1999), and this also supports our findings that the independence of the luminance-difference changes in the DC response is more obvious in the peripheral retina. Furthermore, the above two hypotheses may have close relationship since it is also speculated that the inner plexiform layer circuitry in the retina may be the location of starter of the M-pathway in the visual system.

11.2 Suggestions for future research

In conclusion, the adaptive index calculated from the mfERG responses assists in predicting progression of glaucoma. Since this functional change in retina can be tested objectively and localized, this raises the possibility of objective measurement of glaucomatous dysfunction. Moreover, the adaptive index deduced from the modified global flash mfERG paradigm has demonstrated good sensitivity for differentiating patients with real risk of glaucoma development. This raises the possibility of using the modified global flash mfERG paradigm as a potential

indicator for early detection of glaucomatous dysfunction; another longitudinal study including more high risk glaucoma patients and over a longer time period would be more informative. Such a study (if the study period is long enough for monitoring eyes until they converted to glaucoma) would improve the accuracy of the assessment to classify high risk patients into those who remain stable and those who develop glaucoma. According to the previous long-term studies of untreated OHT and unilateral POAG, a conversion rate to glaucoma of 5 to 7% over 5 years were shown (Chen and Park, 2000; Kass et al., 2002). Hence, one would expect 14 conversions among 120 patients in these two groups after a mean follow-up period of 10 years.

The new assessment described in this thesis can be applied in conjunction with existing assessment methods to enhance accuracy and sensitivity in diagnosis of glaucoma, especially in the early stages of the condition. The aging population requires a more cost-effective allocation of the social resources in the treatment and management of glaucoma. This suggests that identification of glaucoma suspects will limit the overall costs and the social burden for glaucoma management. Treatment should therefore be considered for those who are at moderate to high risk of progression, while widespread treatment for low-risk glaucoma suspects is likely not recommended. Therefore, this new assessment will help to differentiate the moderate to high risk glaucoma suspects from those with low risk and this would benefit to

make the management of glaucoma more cost-effective.

Since the comprehensive measurement of the adaptive index reflects inner retinal adaptation function, application of this measurement may not be limited only to glaucoma. The use of this protocol may also enable monitoring of the development of other inner retinal diseases, such as diabetic retinopathy. Further investigation of this technique in various diseases may help to consolidate the new luminance-modulation global flash mfERG technique and broaden its usage in clinical practice. However, modification of the measurement protocol is necessary in order to shorten the measuring period for clinical purposes.

The similarity of the porcine and human global flash mfERG waveforms suggests that the retinal physiology of these species may be comparable. The W2 component showed an obvious independence of luminance-modulation for higher luminance-difference levels and this independence probably explains the saturation characteristic of DC luminance-modulation function in humans which is sensitive to glaucomatous changes. Thus it provides the possibility that the porcine eye can be developed as an experimental glaucoma model for future investigations. Additionally, further study in isolating and assessing the oscillation-like wavelets using the luminance-modulation global flash mfERG paradigm in human subjects with a proper band-pass filtering may help the future development in glaucoma assessment.

The available treatment of glaucoma in the past is IOP reduction, while longitudinal clinical evaluation from the Collaborative Initial Glaucoma Treatment Study (CIGTS) showed that, under IOP reduction treatment, substantial worsening of visual field from baseline was found in about 20% of glaucoma patients (Musch et al., 2009). The IOP reduction is no longer regarded as the only therapy for glaucoma, the focus of research is now shifting toward other strategies, such as neuroprotection (Cheung et al., 2008). This experimental glaucoma model can provide a platform for testing and developing different strategies in glaucomatous treatment.

PART III – APPENDIX

Chapter 12

Appendix I

Effects of Unsteady Fixation on the mfERG

(Graefes Arch Clin Exp Ophthalmol. 2006; 224 (10):1273-82)

Abstract

Purpose

To investigate the effect of unsteady fixation on the mfERG measurement.

Methods

The mfERGs of 20 subjects with normal vision (mean age = 23.5 years) were recorded with different levels of voluntary eye movements made to mimic unsteady fixation. Subjects were required to move their fixation regularly every 2 s between the center and the ends of a fixation cross, so that 51.2% of the time fixation was at the center and 12.2% of the time it was at each end of the fixation cross. Four different conditions were performed: central fixation (without voluntary eye movements) and with 2°, 4° and 6° magnitude of unsteady fixation. First-order kernel mfERG findings are presented.

Results

Analysis of the ring responses indicated that the central mfERG amplitude was most affected by unsteady fixation. There was significantly reduced amplitude for 4° unsteady fixation and as expected, this reduction became larger with 6° unstable fixation. However, there was no significant effect on the center hexagon amplitude for 2° unsteady fixation. The amplitudes of the ring-2 responses were only affected in the 6° unsteady fixation condition. No significant change in implicit time was found

for any level of unsteady fixation.

Conclusions

These results suggest that mfERG amplitude is not substantially affected if fixation is maintained within the central stimulus hexagon. It was concluded that, for patients with poor fixation, the accuracy of mfERG results may be difficult to interpret and the use of a fixation-monitoring system is desirable for ideal measurement. The depth of depression at the blind spot area may be another useful parameter to interpret the accuracy of mfERG results in patients with poor fixation.

Introduction

The mfERG technique was developed in 1992 (Sutter and Tran, 1992) and although the complex multifocal responses obtained by this technique have advantages over the standard Ganzfeld ERG, the signal-to-noise ratio is smaller and it is more prone to be influenced by recording conditions, such as unsteady fixation (Keating et al., 2000). Steady fixation is a major issue for collecting good quality mfERG responses (Jiang et al., 2001), but it is difficult for subjects, especially those with poor VA, to maintain steady fixation for the duration of recording. The guidelines from the International Society for Clinical Electrophysiology of Vision (ISCEV) for recording mfERG suggest that fixation should be monitored either by direct observation or by fundus monitoring instruments (Marmor et al., 2003), and another device to monitor fixation is the use of a scanning laser ophthalmoscope (Poloschek et al., 2003; Rudolph et al., 2003).

Most studies, however, have divided the total recording time into short segments in order to reduce the chance of involuntary eye movements. After recording with the VERIS system, each segment is checked for the presence of eye movements, blinks and/or noise, by the consideration of the distribution of sampling values for that entire segment and the consistency across the whole recording, and any segments which are contaminated can be re-recorded.

Nevertheless, Chisholm et al. (2001) showed that, even for the subjects with normal central vision, small eye movements which are hard to be observed do occur in the measuring period and only about 51% of fixation time would be within 1.2° from the fixation target. They also noted that the mfERG flicker stimulus does not adversely affect fixation quality. They suggested that the scaled stimulus where the central hexagon subtends 2.4° or more is adequate for this fixation quality. However, subjects with retinal diseases, especially with poor central vision, may have severe involuntary unsteady fixation that will make the mfERG measurements inaccurate. The stimulus hexagons, especially the central smallest hexagon, will project on inappropriate retinal locations under large eye movements and hence the stimulus elements will stimulate other parts of the retina and thus contaminate the recording and analysis of the data.

In this experiment, the effects of unsteady fixation on the mfERG in normal subjects was investigated in order to elucidate whether unsteady fixation of larger extent than the central hexagon will decrease mfERG responses.

Methods

Subjects

Twenty normal subjects, experienced mfERG observers and who have been tested prior to mfERG recording for precise fixation during the fast flickering stimulation using a goggle-like infra-red eye movement recording system (Visagraph II, Compevo AB, Sweden), aged from 20 to 25 years (mean age = 23.5), were recruited from the Optometry Clinic at The Hong Kong Polytechnic University. All had corrected VA of 0.0 (logMAR) or better. Refractive errors were from plano to -3.00 D and with less than -0.75 D astigmatism. A standard eye examination was performed prior to the mfERG measurement to exclude the presence of any ocular abnormalities. All research procedures followed the tenets of the Declaration of Helsinki and were approved by the ethics committee of The Hong Kong Polytechnic University. All subjects were fully informed of the possible risks and gave voluntary written consent.

Stimulus conditions

The stimulus pattern was presented on a Philips FIMI high resolution 21" monitor (Model no: MGD 403, Italy), and an Apple Macintosh G4 computer was used to run the mfERG program (VERIS 5, EDI, San Mateo, CA, USA). The working

distance from the screen to the subject was 30 cm, so that the angle subtended by the full hexagon stimulus pattern were 42° (vertical) and 48° (horizontal) (Hood et al., 2003a). The stimulus matrix consisted of 103 scaled hexagonal elements; the central hexagon subtended about 2.4° , and the sizes of hexagons in ring-2 and ring-3 subtended about 3.2° and 4° respectively (the size of hexagons increases with eccentricity). Bright hexagons were about 200 cd/m^2 while dark presentations were 1 cd/m^2 . Thus the average luminance of the stimulus matrix was about 100 cd/m^2 and the background was set to this luminance. The room illuminance was about 100 lux.

The stimulus presentation followed a pseudo-random binary m-sequence (each frame lasts 13.3 ms with 75 Hz frame rate). The recording time for each fixation experiment was approximately 8 minutes in using a 2^{15} binary m-sequence. The recording process was divided into 32 slightly overlapping recording segments of 14.65 s (with 1 s pre-exposure time), with rest intervals of about 5 s between segments.

Recording conditions

The pupil of the tested eye (chosen randomly) was fully dilated, to at least 7 mm diameter, with 1% Tropicamide (Alcon) before testing. Subjects were fully corrected for the working distance. The DTL electrode was used as an active electrode and

gold-cup surface electrodes were used for both reference (located 1 cm away from the outer canthus of the tested eye) and ground (located at the central forehead). During the mfERG recording, the untested eye was occluded. The mfERGs were recorded with voluntary eye movements to mimic involuntary unsteady fixations. Subjects were asked to shift their fixation every 2 s (using a pre-set auditory timer control) between the center and one end of the fixation cross, and the fixation shifting pattern was shown in [Figure 12.1](#). Since there was about 0.35 s recording time less at the last ends of the fixation cross in each recording segment, 51.2% of the fixation time was at the center and about 12.2% of the time was at each end of the fixation cross. Four different conditions were performed: central fixation (no eye movements) and with different fixation crosses resulting in 2°, 4° and 6° of unsteady fixation. To distribute the effect of fatigue equally across the conditions, the order of the four fixation conditions across the subjects was randomized. The width of the strokes of the target cross was adjusted to be the same in all conditions. The fixation target would have no effect on the mfERG results since it is a stationary, non-flickering target and the VERIS software compensates for the percentage of each hexagon covered by a part of the fixation cross (Jurklies et al., 2002).

The electrical signals were amplified using a Grass P511K amplifier with band pass filter setting from 10 to 300 Hz and gain of x100,000. Any recording segments

contaminated with blinks were rejected and repeated immediately.

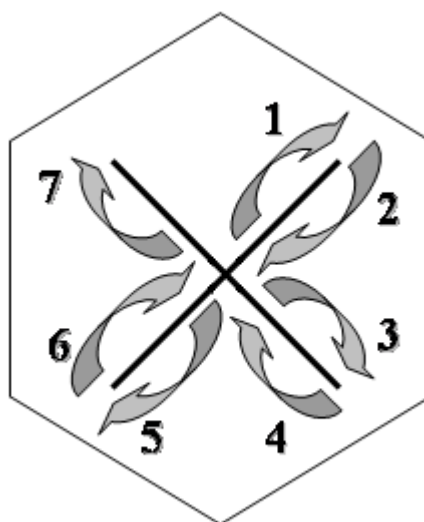


Figure 12.1 Pattern of voluntary eye movements used to mimic involuntary unsteady fixation. Subjects were required to shift their fixation every 2s starting from the center and following the fixation sequence shown. A pre-set timer was used to remind the subjects to move their fixations. Subjects were asked to shift the whole pattern as clockwise (from 1 to 7) for every segment. This pattern of fixation was used (about 15 s), but with clockwise 90° phase shift for each recording segment in order to distribute the different recording time at different ends of the fixation cross equally.

Data analysis

Data were analyzed using the VERIS 5 software. The artefact removal algorithm in the VERIS system was applied once without any spatial averaging. The data were then grouped by rings according to eccentricity from the macular response (central

hexagon, i.e. ring-1) and this would help to investigate the effect of unsteady fixation on the mfERG responses at different eccentricities. As well as the central macular response, it was expected that the localized responses from the ring-2 hexagons might also be severely influenced by the unsteady fixation. The individual responses from each hexagon of ring-2 were also investigated in order to evaluate the influence of unsteady fixation of varied magnitudes (Figure 12.2). In this experiment, the first-order kernel analysis was used. The effect of different unsteady fixation conditions was evaluated by using one-way repeated measures ANOVA and Bonferroni test was used as a *post-hoc* test.

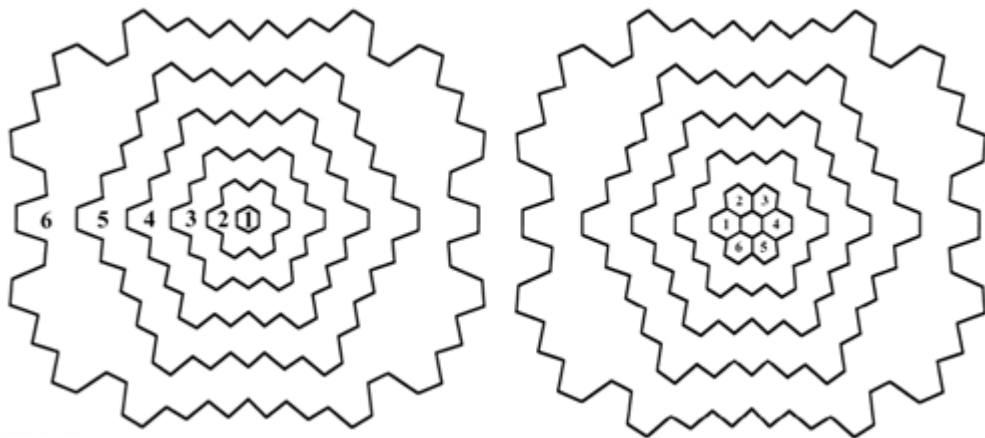


Figure 12.2 Responses from 103 stimulus hexagons were grouped into six concentric rings (left) for analysis and localized responses from the ring-2 hexagons (right) were also investigated.

Results

Responses from six concentric rings

The first negative trough and first positive peak of the multifocal waveform were defined as N1 and P1, respectively. The amplitude of N1 was measured from the baseline to the first major negative trough and the P1 amplitude was measured from the first major negative trough to the first major positive peak. The time periods from the stimulus onset to the peak of N1 and P1 were defined as their implicit times. The implicit times of N1 and P1 were about 19 ms and 35 ms, respectively. There were no statistically significant effects for implicit times (both N1 and P1) for any conditions for any eccentricities (rings) (repeated measures ANOVA, $p > 0.05$) (Figure 12.3a and 12.3b).

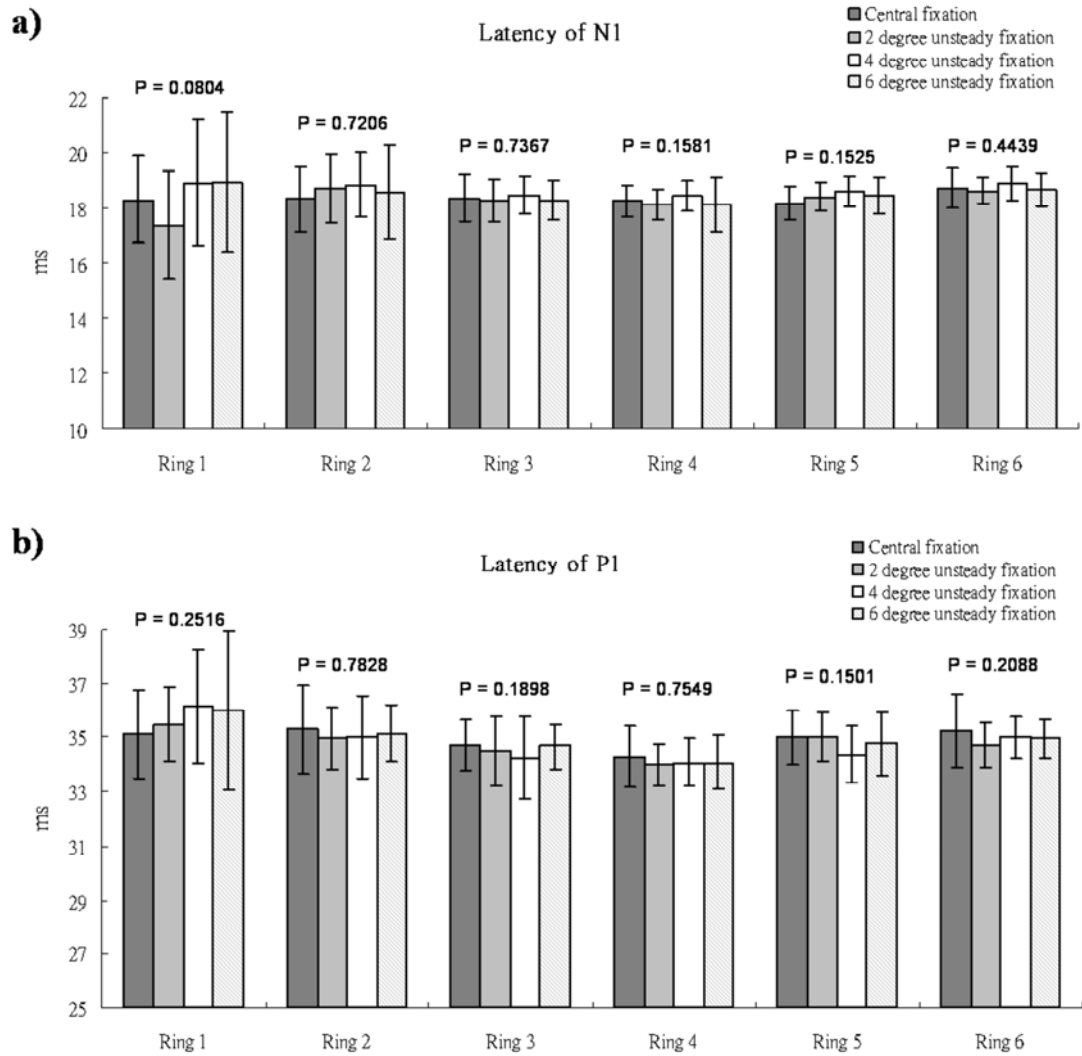


Figure 12.3 Statistical results of N1 and P1 implicit times (ms) in ring response under four conditions: steady fixation, 2° unsteady fixation, 4° unsteady fixation and 6° unsteady fixation. There was no statistically significant difference ($p > 0.05$) between the central fixation and any unsteady fixation conditions at any eccentricity. Error bars indicate \pm 1 SD of means.

Repeated measures ANOVA for amplitude (N1 and P1) values demonstrated that there was a statistically significant effect on the fixation condition at the central and the ring-2 response. *Post-hoc* analysis showed that with 2° of unsteady fixation condition, there was no significant effect on the central hexagon responses and the amplitudes of N1 and P1 did not change significantly at any eccentricities compared with the responses from the steady fixation condition (Figure 12.4). However, the responses from the central hexagon were significantly reduced in both the 4° and 6° unsteady fixation conditions, with 27% and 49% reduction, respectively, of the P1 amplitude, and 27% reduction for 6° unsteady fixation for the N1 amplitude. The amplitudes from ring-2 were only significantly reduced in the 6° unsteady fixation condition (18% reduction for the N1 amplitude and 15% reduction for the P1 amplitude), but they were not significantly different in the 4° unsteady fixation condition. From ring-3 to ring-6, there was no statistically significant difference for the N1 and P1 amplitudes in any of the unsteady fixation conditions, compared with steady fixation.

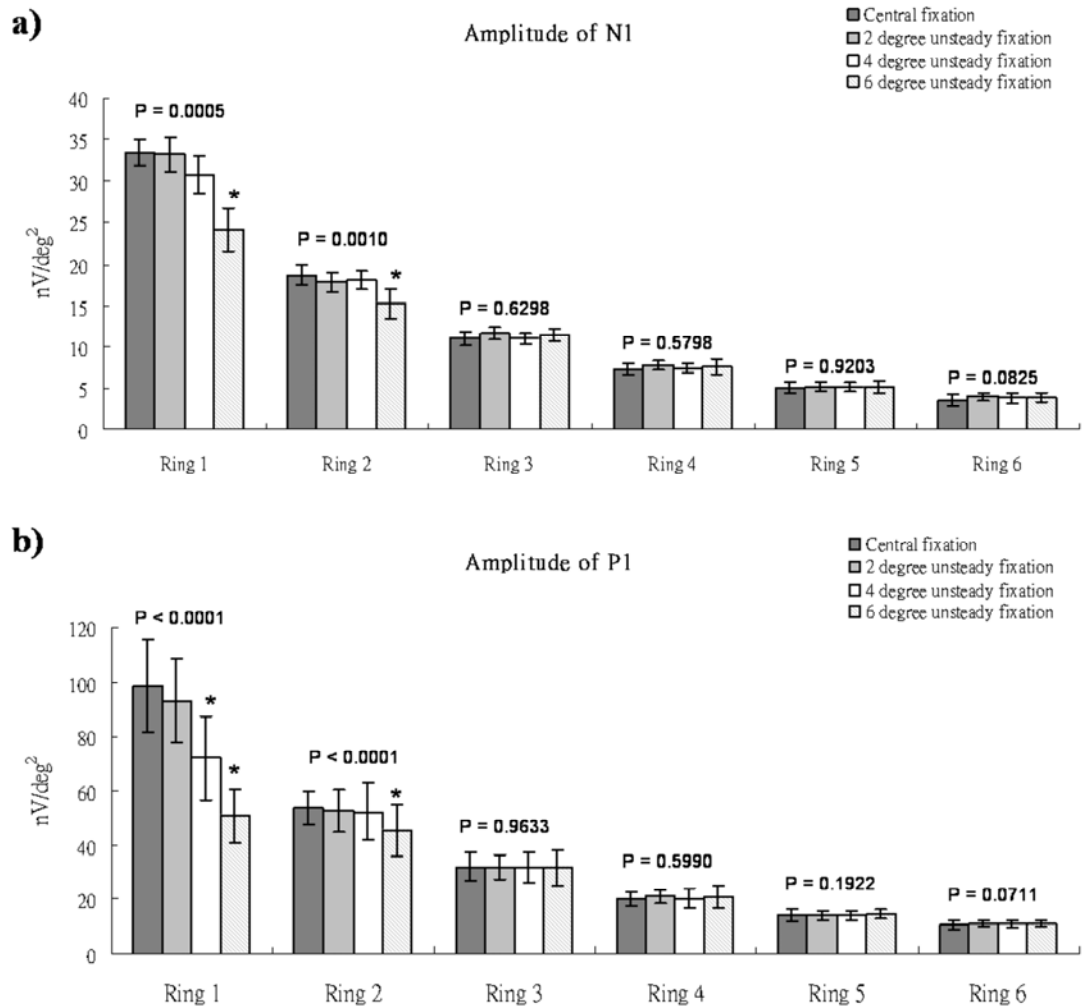


Figure 12.4 Amplitude values (nV/deg^2) in ring responses of N1 and P1 under four conditions: steady fixation, 2° unsteady fixation, 4° unsteady fixation and 6° unsteady fixation. (*) indicates statistical significantly difference ($p < 0.05$) compared with the steady fixation condition at the particular eccentricity. Error bars indicate ± 1 SD of means.

Localized responses from the ring-2 hexagons

Six localized responses from the ring-2 hexagons were also evaluated with different unsteady fixation conditions. All the localized responses from ring-2 showed an obvious reduction in magnitude for the 6° unsteady fixation condition. There was a statistically significant effect for amplitude (N1 and P1) values on the fixation condition at the six ring-2 responses (repeated measures ANOVA, $p < 0.05$). *Post-hoc* analysis showed that the amplitudes from the six ring-2 hexagons were only significantly reduced in the 6° unsteady fixation condition but was not significantly changed in 2° or 4° unsteady fixation condition (Figure 12.5).

There were no statistically significant effects for implicit times (N1 or P1) on the fixation condition for the six ring-2 responses (repeated measures ANOVA, $p > 0.05$) (Figure 12.6a and 12.6b).

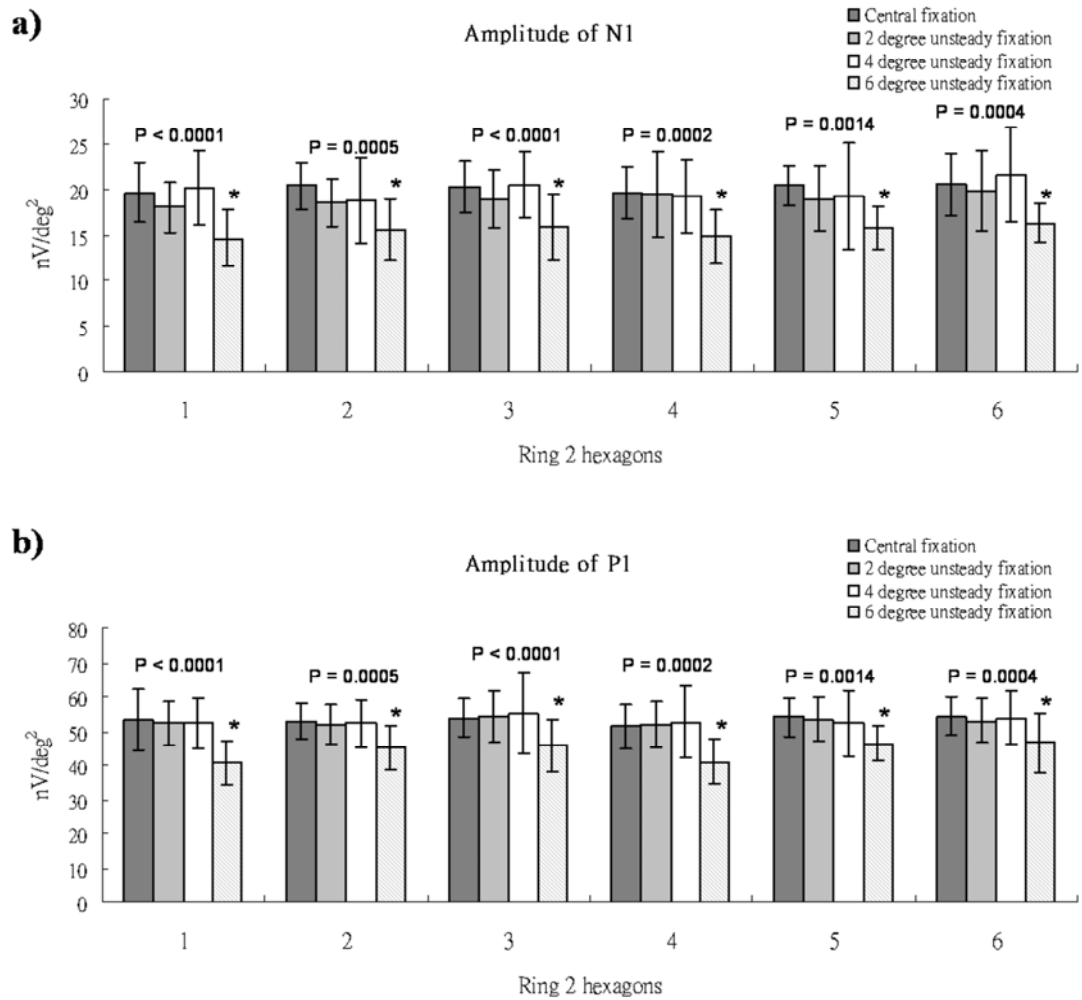


Figure 12.5 Amplitude values (nV/deg^2) of ring-2 hexagons responses of N1 and P1 under four conditions: steady fixation, 2° unsteady fixation, 4° unsteady fixation and 6° unsteady fixation. (*) indicates statistical significantly difference ($p < 0.05$) compared with the steady fixation condition at ring-2. Error bars indicate ± 1 SD of means.

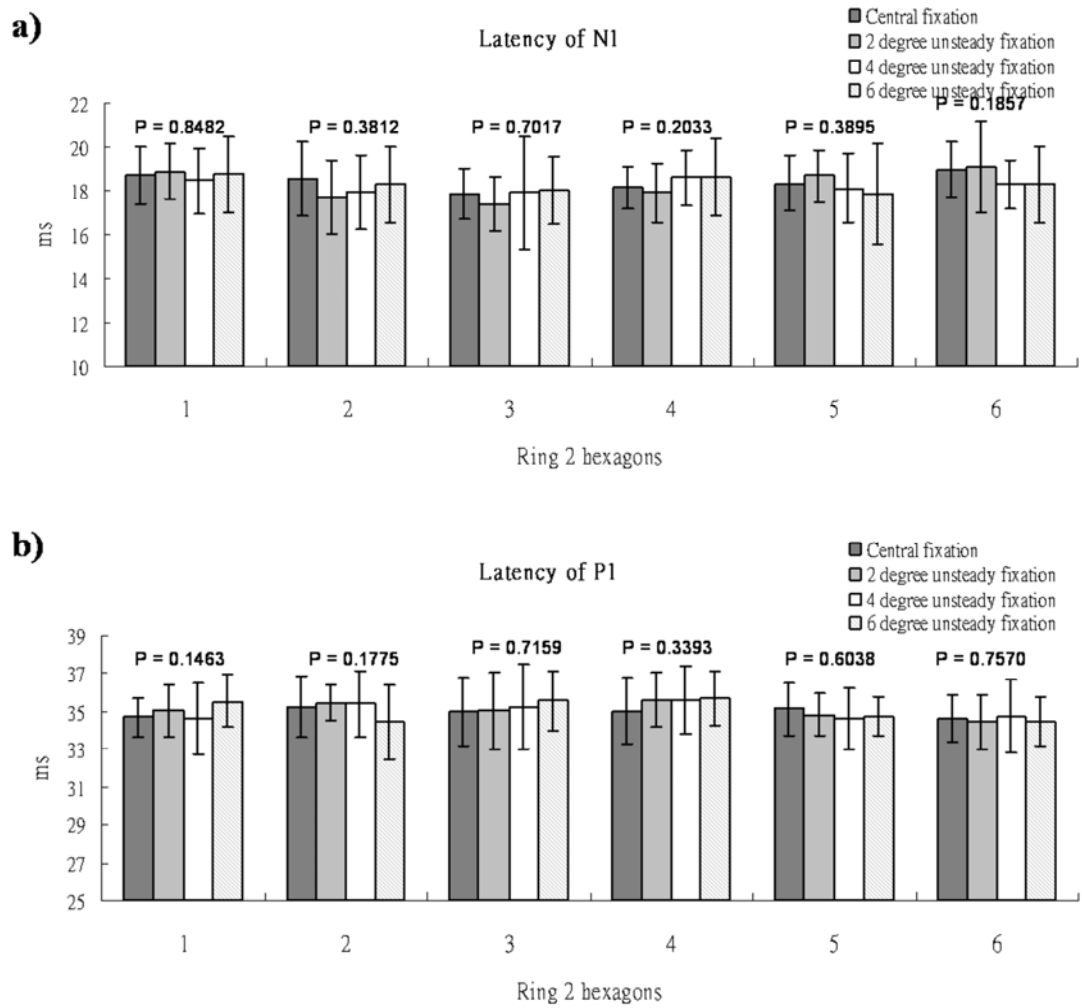


Figure 12.6 Implicit time (ms) of ring-2 hexagons responses of N1 and P1 under four conditions: steady fixation, 2° unsteady fixation, 4° unsteady fixation and 6° unsteady fixation. There was no statistically significant difference ($p > 0.05$) between the central fixation and any unsteady fixation conditions at ring-2. Error bars indicate ± 1 SD of means.

Depth of depression at the blind spot region

Typical mfERG results from one of the subjects are illustrated in [Figure 12.7](#). The waveforms from the four different fixation conditions seemed to be similar, although noisier waveforms were observed centrally in 4° or 6° unsteady fixation conditions. However, there is an obvious reduction of the central response amplitude (ring-1) with increasing magnitude of unsteady fixation. By 6° of unsteady fixation, there is a decrease in the central peak and a dome-shape central peak is observed to replace a sharp peak. However, the topographical map did not show any remarkable changes in the peripheral responses and the optic nerve head depression can still be observed even in the 6° unsteady fixation condition, although its depth is clearly reduced.

Effects of unsteady fixation on the depth of depression at the blind spot region are shown in [Figure 12.8](#). The depth ratio of the blind spot was obtained as the ratio of the averaged P1 amplitude of the six hexagons surrounding the blind spot region to the P1 amplitude of the most depressed hexagon (blind spot region) which is determined from the three-dimensional plots. The depth of depression in this region decreases as the magnitude of unsteady fixation increases. Repeated measures ANOVA with *post-hoc* analysis demonstrated that the depth ratio of the blind spot only significantly reduced in 4° and 6° unsteady fixation condition but was not

reduced for the 2° unsteady fixation.

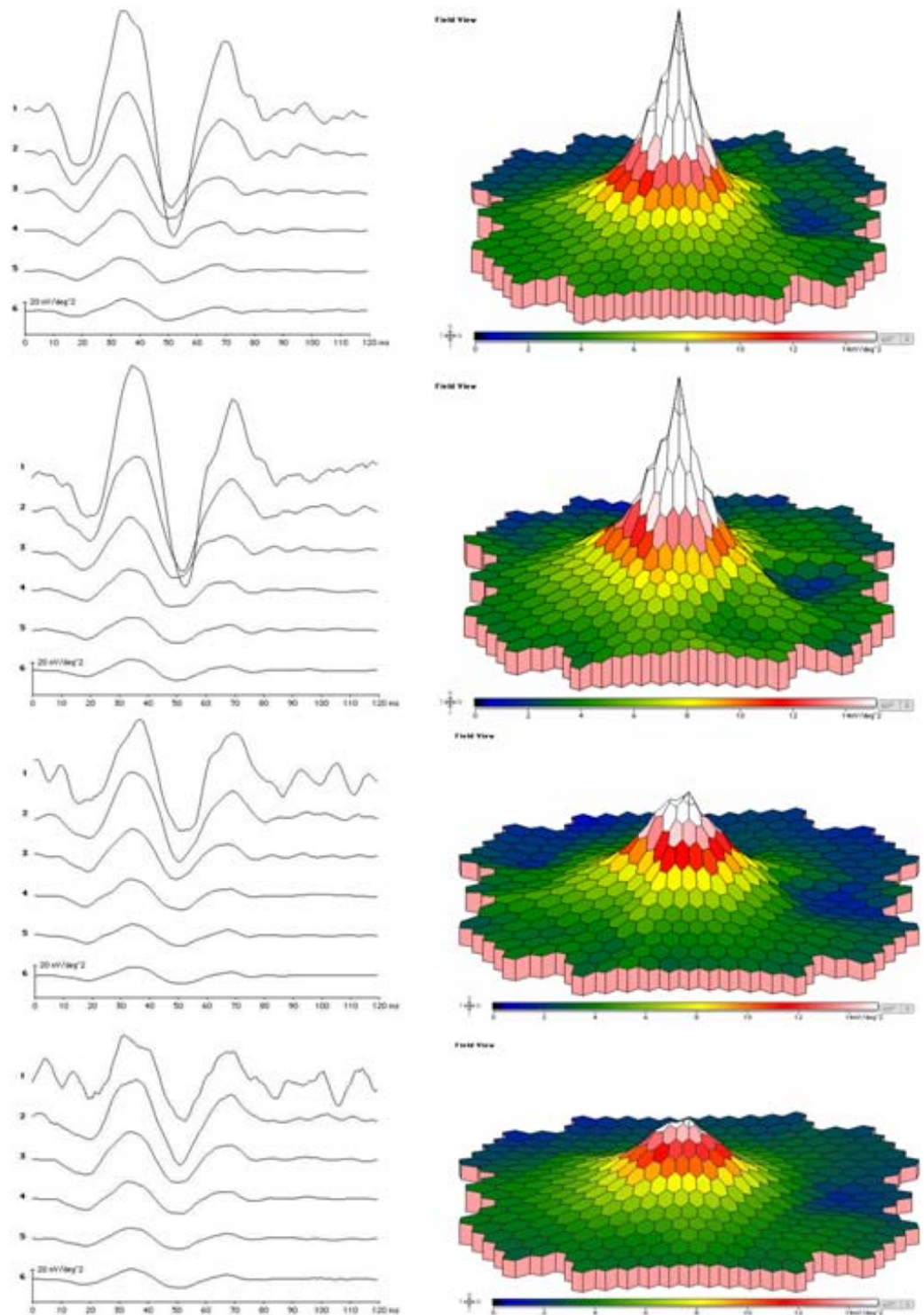


Figure 12.7 Concentric ring responses (left) and three-dimensional plots (right) under four conditions from a typical subject: steady fixation, 2° unsteady fixation, 4° unsteady fixation and 6° unsteady fixation (top to bottom, respectively).

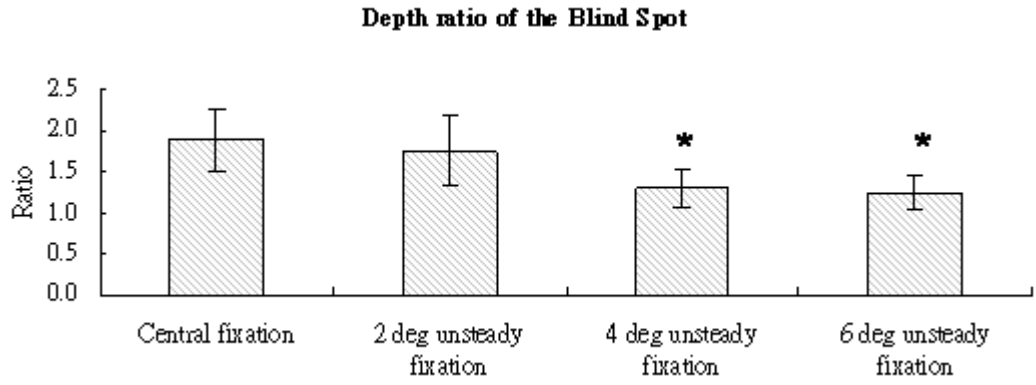


Figure 12.8 Effects of unsteady fixation on the depth of depression at the blind spot region by calculating the depth ratio of the blind spot were shown. (*) indicates there was statistical significantly difference ($p < 0.05$) compared with the steady fixation condition. Error bars indicate ± 1 SD of means.

Discussion

The mfERG has been shown to be affected by inattention, unsteady fixation and poor focus (Vrabec et al., 2004). This experiment also demonstrates that unsteady fixation will suppress the amplitude of the central mfERG responses even with a healthy retina and good concentration, thus demonstrating that fixation is an important issue that must be considered in clinical diagnosis using the mfERG.

However, patients with macular problems, such as those with age-related maculopathy (ARM) will usually choose an eccentric preferred retinal locus (PRL) instead of the fovea for visual tasks. The size of the PRL varies among patients and visual tasks are performed by placing the image of the visual target within the PRL. Schuchard and co-workers (1999) found that 41% ARM patients do develop a PRL larger than 2° in diameter and 19% still have wandering fixation eye movement within the PRL. Large involuntary unsteady eye movements that are larger than the size of central mfERG hexagon provide a challenge for interpretation of mfERG measurements.

There are various factors which may cause a reduction in the mfERG response with unsteady fixation. Small eye movements during the mfERG measurement, although not saturating the input amplifiers will generate noise and contaminate the input signals. This noise, however, can be minimised by the artifact rejection process

in the VERIS program, which replaces the traces at specified locations by the best prediction based on the entire record (Sutter and Tran, 1992).

Under poor fixation conditions, the stimulus hexagons project onto the retinal positions other than the intended ones, and the surrounding retinal responses will contribute to the response from the intended location. The reduction of amplitude with poor fixation may be mainly due to the recording from unintended and variable retinal locations.

The central mfERG response (ring-1) was most affected by unsteady fixation and the ring-2 response was also affected when the magnitude of unsteady fixation increased. The central response is most prone to this effect because the central hexagon is the smallest in the scaled stimulus (scaled for retinal cone densities) which was used in this study, and this is the most common format in the mfERG measurement. For the 103-scaled stimulation as used in this study, the central hexagon subtends about 2.4° , the hexagons in rings-2 and ring-3 subtend about 3.2° and 4° , respectively, and the size of the hexagons increases with eccentricity. In addition, the fovea gives the largest response amplitude. If the central hexagon is displaced eccentrically, for some of the recording time, there will be a significant decrease in the amplitude of the recorded central response.

The lack of effect under the 2° unsteady fixation condition suggests that the

overall mfERG topography is not influenced significantly if the unsteady fixation is maintained within the central hexagon (Menz and Sutter, 2004). However, greater magnitude of fixation instability influences the result more, for example, in the 4° unsteady fixation condition, the eye movements pass beyond the boundary of the central hexagon. Para-macular responses then contribute to the response from the central hexagon. The mfERG responses are mainly generated by the cone bipolar cells (Hood et al., 2002) and the central macular region contains the highest density of the cone cells while in surrounding areas there is a steep drop off in gradient in the cone cell density (Curcio et al., 1990). Thus when the fixation is unsteady, the para-macular response contributes to and reduces the response from the central hexagon.

Imagine if each retinal element is undergoing the same amount of movement as the macula does, there is less relative change of the intended retinal stimulated area with eccentricity during unsteady fixation. With small eye movements, especially within 2° changes, significant changes in the peripheral response could not be measured. For a relative large eye movement, such as 4° unsteady fixation, the decrease in amplitude only occurs at the central region but not at ring-2 or more eccentric rings. The central response and the localized six ring-2 responses were significantly reduced under measurement with 6° unsteady fixation, but the responses

from ring-3 to ring-6 are not substantially affected. At the more eccentric rings, because of a relative large retinal area giving rise to the response, a large portion of area in each hexagon remains over the intended retinal area, and thus the response is less affected.

While the results from this experiment do not show a significant effect of poor fixation on the mfERG responses in the peripheral rings, primarily also because of the relatively uniform structure of the peripheral retina, there is some evidence that the peripheral responses are altered. In the 4° condition, the blind spot (in the three-dimensional plot) can still be observed, while in the 6° condition, the depth of depression from the blind spot was reduced although its relative position was unchanged. This reduction of depth occurs because the surrounding retinal signals contribute to the response that is expected from the hexagon at the position of the optic nerve head. Therefore, the monitoring of the relative position of the blind spot in the three-dimensional plot of the mfERG results may not be accurate enough to determine the quality of fixation. However, the depth of depression at the blind spot area is suggested to be another important parameter to monitor the fixation quality.

Results also demonstrate that poor fixation does not alter N1 or P1 implicit time. Therefore, in patients with unsteady fixation, implicit times are the most suitable parameters for diagnosis (Huang et al., 2000; Li et al., 2001). In addition, during the

interpretation of the results, attention should be paid to those cases with unsteady fixation which would mask the real result (Heinemann-Vernaleken et al., 2001).

A previous study suggested that fixation quality during the recording process is more important for high resolution stimuli (more than 103 hexagons) (Chisholm et al., 2001). Ensuring that the subject maintains stable fixation throughout a recording process is thus necessary for obtaining a reliable mfERG record. The use of a fixation monitoring system, e.g. fundus camera, infra-red eye gaze monitoring system, is desirable, so that segments with unstable fixation can be re-recorded. It has been suggested that a real time stimulus-tracking system in response to any eye movements can be developed to minimize fixation losses (Keating et al., 2000), and such a system should, on the basis of our findings, have a resolution of about 2 degrees for the standard 103 VERIS stimulus array.

In summary, poor fixation which is greater than the visual angle subtended by the central hexagon during the mfERG measurement reduces the recorded mfERG amplitudes, especially the central response. Since the implicit time is unaffected, it has practical implications for subjects with age-related macular degeneration or other eye diseases with a central scotoma. It was concluded that for patients with poor fixation, the mfERG results would be difficult to interpret and the use of a proper fixation monitoring system is desirable for accurate measurement. Any measured

segments with larger eye movement than the size of central hexagon should be repeated. The presence of a clearly defined 'blind spot' also permits fixation control and the depth of depression at the blind spot area may be considered as a useful guide to the quality of fixation control.

REFERENCES

- Anderson, R. S. and O'Brien, C. (1997). Psychophysical evidence for a selective loss of M ganglion cells in glaucoma. *Vision Res*, 37 (8), 1079-83.
- Ansari, E. A., Morgan, J. E. and Snowden, R. J. (2002). Psychophysical characterisation of early functional loss in glaucoma and ocular hypertension. *Br J Ophthalmol*, 86 (10), 1131-5.
- Asman, P. and Heijl, A. (1992a). Glaucoma Hemifield Test. Automated visual field evaluation. *Arch Ophthalmol*, 110 (6), 812-9.
- Asman, P. and Heijl, A. (1992b). Evaluation of methods for automated Hemifield analysis in perimetry. *Arch Ophthalmol*, 110 (6), 820-6.
- Azuara-Blanco, A., Katz, L. J., Spaeth, G. L., Vernon, S. A., Spencer, F. and Lanzl, I. M. (2003). Clinical agreement among glaucoma experts in the detection of glaucomatous changes of the optic disk using simultaneous stereoscopic photographs. *Am J Ophthalmol*, 136 (5), 949-50.
- Bach, M., Hawlina, M., Holder, G. E., Marmor, M. F., Meigen, T., Vaegan and Miyake, Y. (2000). Standard for pattern electroretinography. International Society for Clinical Electrophysiology of Vision. *Doc Ophthalmol*, 101 (1), 11-8.
- Bach, M. (2001). Electrophysiological approaches for early detection of glaucoma. *Eur J Ophthalmol*, 11 Suppl 2 S41-9.
- Bach, M., Unsoeld, A. S., Philipppin, H., Staubach, F., Maier, P., Walter, H. S., Bommer, T. G. and Funk, J. (2006). Pattern ERG as an early glaucoma indicator in ocular hypertension: a long-term, prospective study. *Invest Ophthalmol Vis Sci*, 47 (11), 4881-7.
- Bathija, R. (2000). Optic nerve blood flow in glaucoma. *Clin Exp Optom*, 83 (3), 180-184.
- Bauer, U., Scholz, M., Levitt, J. B., Obermayer, K. and Lund, J. S. (1999). A model for the depth-dependence of receptive field size and contrast sensitivity of cells in layer 4C of macaque striate cortex. *Vision Res*, 39 (3), 613-29.

- Bearse, M. A., Sutter, E. E., Sim, D. and Stamper, R. (1996). Glaucomatous dysfunction revealed in higher order components of the electroretinogram. In: *Vision Science and Its Applications, 1996 OSA Technical Digest Series, Vol. 1, Washington, D.C.: Optical Society of America*, 104-7.
- Bearse, M. A. and Sutter, E. E. (1998). Contrast dependence of multifocal ERG components. In: *Vision Science and Its Applications, 1998 OSA Technical Digest Series, Vol. 1, Washington, D.C.: Optical Society of America*, 24-7.
- Bearse, M. A., Stamper, R. L. and Sutter, E. E. (2001a). Detection of functional abnormalities in glaucoma using a new multifocal ERG paradigm. *Invest Ophthalmol Vis Sci*, 41 (4), ARVO Abstract S103.
- Bearse, M. A., Sutter, E. E. and Stamper, R. L. (2001b). Detection of glaucomatous dysfunction using a global flash multifocal electroretinogram (mERG) paradigm. In: *Vision Science and Its Applications, 2001 OSA Technical Digest Series, Vol. 1, Washington, D.C.: Optical Society of America*, 14-7.
- Bearse, M. A., Jr. and Sutter, E. E. (1996). Imaging localized retinal dysfunction with the multifocal electroretinogram. *J Opt Soc Am A Opt Image Sci Vis*, 13 (3), 634-40.
- Bearse, M. A., Jr., Shimada, Y. and Sutter, E. E. (2000). Distribution of oscillatory components in the central retina. *Doc Ophthalmol*, 100 (2-3), 185-205.
- Beauchemin, M. L. (1974). The fine structure of the pig's retina. *Albrecht Von Graefes Arch Klin Exp Ophthalmol*, 190 (1), 27-45.
- Becker, B. (1971). Diabetes mellitus and primary open-angle glaucoma. The XXVII Edward Jackson Memorial Lecture. *Am J Ophthalmol*, 1 (1 Part 1), 1-16.
- Becquet, F., Courtois, Y. and Goureau, O. (1997). Nitric oxide in the eye: multifaceted roles and diverse outcomes. *Surv Ophthalmol*, 42 (1), 71-82.
- Bengtsson, B. (1981). The prevalence of glaucoma. *Br J Ophthalmol*, 65 (1), 46-9.
- Biro, I. (1951). Notes upon the question of hereditary glaucoma. *Ophthalmologica*, 122 (4), 228.

Blessing, E. M., Solomon, S. G., Hashemi-Nezhad, M., Morris, B. J. and Martin, P. R. (2004). Chromatic and spatial properties of parvocellular cells in the lateral geniculate nucleus of the marmoset (*Callithrix jacchus*). *J Physiol*, 557 (Pt 1), 229-45.

Blumenthal, E. Z., Sample, P. A., Zangwill, L., Lee, A. C., Kono, Y. and Weinreb, R. N. (2000a). Comparison of long-term variability for standard and short-wavelength automated perimetry in stable glaucoma patients. *Am J Ophthalmol*, 129 (3), 309-13.

Blumenthal, E. Z., Williams, J. M., Weinreb, R. N., Girkin, C. A., Berry, C. C. and Zangwill, L. M. (2000b). Reproducibility of nerve fiber layer thickness measurements by use of optical coherence tomography. *Ophthalmology*, 107 (12), 2278-82.

Bowd, C., Zangwill, L. M., Berry, C. C., Blumenthal, E. Z., Vasile, C., Sanchez-Galeana, C., Bosworth, C. F., Sample, P. A. and Weinreb, R. N. (2001). Detecting early glaucoma by assessment of retinal nerve fiber layer thickness and visual function. *Invest Ophthalmol Vis Sci*, 42 (9), 1993-2003.

Bozkurt, B., Irkeç, M., Gedik, S., Orhan, M., Erdener, U., Tatlipinar, S. and Karaagaoglu, E. (2002). Effect of peripapillary chorioretinal atrophy on GDx parameters in patients with degenerative myopia. *Clin Experiment Ophthalmol*, 30 (6), 411-4.

Brown, B. and Yap, M. K. (1996). Contrast and luminance as parameters defining the output of the VERIS topographical ERG. *Ophthalmic Physiol Opt*, 16 (1), 42-8.

Budenz, D. L., Fredette, M. J., Feuer, W. J. and Anderson, D. R. (2008). Reproducibility of peripapillary retinal nerve fiber thickness measurements with stratus OCT in glaucomatous eyes. *Ophthalmology*, 115 (4), 661-6.

Bui, B. V. and Fortune, B. (2004). Ganglion cell contributions to the rat full-field electroretinogram. *J Physiol*, 555 (Pt 1), 153-73.

Caprioli, J. and Spaeth, G. L. (1985). Static threshold examination of the peripheral nasal visual field in glaucoma. *Arch Ophthalmol*, 103 (8), 1150-4.

- Carpineto, P., Ciancaglini, M., Zuppari, E., Falconio, G., Doronzo, E. and Mastropasqua, L. (2003). Reliability of nerve fiber layer thickness measurements using optical coherence tomography in normal and glaucomatous eyes. *Ophthalmology*, 110 (1), 190-5.
- Chan, H. H. and Brown, B. (2000). Pilot study of the multifocal electroretinogram in ocular hypertension. *Br J Ophthalmol*, 84 (10), 1147-53.
- Chan, H. H. (2005). Detection of glaucomatous damage using multifocal ERG. *Clin Exp Optom*, 88 (6), 410-4.
- Chan, H. L. and Brown, B. (1998). Investigation of retinitis pigmentosa using the multifocal electroretinogram. *Ophthalmic Physiol Opt*, 18 (4), 335-50.
- Chan, H. L. and Brown, B. (1999). Multifocal ERG changes in glaucoma. *Ophthalmic Physiol Opt*, 19 (4), 306-16.
- Chan, H. L., Tam, W. K., Chen, C. L. and Ng, N. C. (2003). The detection of small simulated field defects using multifocal VEPs. *Ophthalmic Physiol Opt*, 23 (3), 205-12.
- Chandler, M. J., Smith, P. J., Samuelson, D. A. and MacKay, E. O. (1999). Photoreceptor density of the domestic pig retina. *Vet Ophthalmol*, 2 (3), 179-184.
- Chaturvedi, N., Hedley-Whyte, E. T. and Dreyer, E. B. (1993). Lateral geniculate nucleus in glaucoma. *Am J Ophthalmol*, 116 (2), 182-8.
- Chauhan, B. C. and Johnson, C. A. (1999). Test-retest variability of frequency-doubling perimetry and conventional perimetry in glaucoma patients and normal subjects. *Invest Ophthalmol Vis Sci*, 40 (3), 648-56.
- Chauhan, B. C., McCormick, T. A., Nicolela, M. T. and LeBlanc, R. P. (2001). Optic disc and visual field changes in a prospective longitudinal study of patients with glaucoma: comparison of scanning laser tomography with conventional perimetry and optic disc photography. *Arch Ophthalmol*, 119 (10), 1492-9.

Chen, J. C., Brown, B. and Schmid, K. L. (2006). Retinal adaptation responses revealed by global flash multifocal electroretinogram are dependent on the degree of myopic refractive error. *Vision Res*, 46 (20), 3413-21.

Chen, P. P. and Park, R. J. (2000). Visual field progression in patients with initially unilateral visual field loss from chronic open-angle glaucoma. *Ophthalmology*, 107 (9), 1688-92.

Cheung, W., Guo, L. and Cordeiro, M. F. (2008). Neuroprotection in glaucoma: drug-based approaches. *Optom Vis Sci*, 85 (6), 406-16.

Chisholm, J. A., Keating, D., Parks, S. and Evans, A. L. (2001). The impact of fixation on the multifocal electroretinogram. *Doc Ophthalmol*, 102 (2), 131-9.

Chou, S. L., Misajon, R., Gallo, J. and Keeffe, J. E. (2003). Measurement of indirect costs for people with vision impairment. *Clin Experiment Ophthalmol*, 31 (4), 336-40.

Chu, P. H., Chan, H. H. and Brown, B. (2006a). Glaucoma detection is facilitated by luminance modulation of the global flash multifocal electroretinogram. *Invest Ophthalmol Vis Sci*, 47 (3), 929-37.

Chu, P. H., Chan, H. H. and Leat, S. J. (2006b). Effects of unsteady fixation on multifocal electroretinogram (mfERG). *Graefes Arch Clin Exp Ophthalmol*, 244 (10), 1273-82.

Chu, P. H., Chan, H. H. and Brown, B. (2007). Luminance-modulated adaptation of global flash mfERG: fellow eye losses in asymmetric glaucoma. *Invest Ophthalmol Vis Sci*, 48 (6), 2626-33.

Chu, P. H., Chan, H. H., Ng, Y. F., Brown, B., Siu, A. W., Beale, B. A., Gilger, B. C. and Wong, F. (2008). Porcine Global Flash Multifocal Electroretinogram: Possible Mechanisms for the Glaucomatous Changes in Contrast Response Function. *Vision Res*, 48 (16), 1726-34.

Chung, H. S., Harris, A., Evans, D. W., Kagemann, L., Garzozzi, H. J. and Martin, B. (1999). Vascular aspects in the pathophysiology of glaucomatous optic neuropathy. *Surv Ophthalmol*, 43 Suppl 1 S43-50.

Corbett, M. C., Shilling, J. S. and Holder, G. E. (1995). The assessment of clinical investigations: the Greenwich Grading System and its application to electrodiagnostic testing in ophthalmology. *Eye*, 9 (Pt 6 Su) 59-64.

Curcio, C. A. and Allen, K. A. (1990). Topography of ganglion cells in human retina. *J Comp Neurol*, 300 (1), 5-25.

Curcio, C. A., Sloan, K. R., Kalina, R. E. and Hendrickson, A. E. (1990). Human photoreceptor topography. *J Comp Neurol*, 292 (4), 497-523.

Dandona, L., Hendrickson, A. and Quigley, H. A. (1991). Selective effects of experimental glaucoma on axonal transport by retinal ganglion cells to the dorsal lateral geniculate nucleus. *Invest Ophthalmol Vis Sci*, 32 (5), 1593-9.

Delgado, M. F., Nguyen, N. T., Cox, T. A., Singh, K., Lee, D. A., Dueker, D. K., Fechtner, R. D., Juzych, M. S., Lin, S. C., Netland, P. A., Pastor, S. A., Schuman, J. S. and Samples, J. R. (2002). Automated perimetry: a report by the American Academy of Ophthalmology. *Ophthalmology*, 109 (12), 2362-74.

Desatnik, H., Quigley, H. A. and Glovinsky, Y. (1996). Study of central retinal ganglion cell loss in experimental glaucoma in monkey eyes. *J Glaucoma*, 5 (1), 46-53.

Drasdo, N., Aldebasi, Y. H., Mortlock, K. E., Chiti, Z., Morgan, J. E., North, R. V. and Wild, J. M. (2002). Ocular optics, electroretinography and primary open angle glaucoma. *Ophthalmic Physiol Opt*, 22 (5), 455-62.

Dreyer, E. B., Zurakowski, D., Schumer, R. A., Podos, S. M. and Lipton, S. A. (1996). Elevated glutamate levels in the vitreous body of humans and monkeys with glaucoma. *Arch Ophthalmol*, 114 (3), 299-305.

Duch, D. S., Rehberg, B. and Vysotskaya, T. N. (1998). Volatile anesthetics significantly suppress central and peripheral mammalian sodium channels. *Toxicol Lett*, 100-101 255-63.

Dumskyj, M. J., Eriksen, J. E., Dore, C. J. and Kohner, E. M. (1996). Autoregulation in the human retinal circulation: assessment using isometric exercise, laser Doppler velocimetry, and computer-assisted image analysis. *Microvasc Res*, 51 (3), 378-92.

Fazio, D. T., Heckenlively, J. R., Martin, D. A. and Christensen, R. E. (1986). The electroretinogram in advanced open-angle glaucoma. *Doc Ophthalmol*, 63 (1), 45-54.

Fechtner, R. D. and Weinreb, R. N. (1994). Mechanisms of optic nerve damage in primary open angle glaucoma. *Surv Ophthalmol*, 39 (1), 23-42.

Feigl, B., Brown, B., Lovie-Kitchin, J. and Swann, P. (2005). Adaptation responses in early age-related maculopathy. *Invest Ophthalmol Vis Sci*, 46 (12), 4722-7.

Flammer, J., Orgul, S., Costa, V. P., Orzalesi, N., Krieglstein, G. K., Serra, L. M., Renard, J. P. and Stefansson, E. (2002). The impact of ocular blood flow in glaucoma. *Prog Retin Eye Res*, 21 (4), 359-93.

Fortune, B., Schneck, M. E. and Adams, A. J. (1999). Multifocal electroretinogram delays reveal local retinal dysfunction in early diabetic retinopathy. *Invest Ophthalmol Vis Sci*, 40 (11), 2638-51.

Fortune, B., Johnson, C. A. and Cioffi, G. A. (2001). The topographic relationship between multifocal electroretinographic and behavioral perimetric measures of function in glaucoma. *Optom Vis Sci*, 78 (4), 206-14.

Fortune, B., Bearse, M. A., Jr., Cioffi, G. A. and Johnson, C. A. (2002a). Selective loss of an oscillatory component from temporal retinal multifocal ERG responses in glaucoma. *Invest Ophthalmol Vis Sci*, 43 (8), 2638-47.

Fortune, B., Cull, G., Wang, L., Van Buskirk, E. M. and Cioffi, G. A. (2002b). Factors affecting the use of multifocal electroretinography to monitor function in a primate model of glaucoma. *Doc Ophthalmol*, 105 (2), 151-78.

Fortune, B. and Johnson, C. A. (2002). Decline of photopic multifocal electroretinogram responses with age is due primarily to preretinal optical factors. *J Opt Soc Am A Opt Image Sci Vis*, 19 (1), 173-84.

Fortune, B., Bui, B. V., Morrison, J. C., Johnson, E. C., Dong, J., Cepurna, W. O., Jia, L., Barber, S. and Cioffi, G. A. (2004). Selective ganglion cell functional loss in rats with experimental glaucoma. *Invest Ophthalmol Vis Sci*, 45 (6), 1854-62.

Frishman, L. J., Shen, F. F., Du, L., Robson, J. G., Harwerth, R. S., Smith, E. L., 3rd, Carter-Dawson, L. and Crawford, M. L. (1996). The scotopic electroretinogram of macaque after retinal ganglion cell loss from experimental glaucoma. *Invest Ophthalmol Vis Sci*, 37 (1), 125-41.

Frishman, L. J., Saszik, S., Harwerth, R. S., Viswanathan, S., Li, Y., Smith, E. L., 3rd, Robson, J. G. and Barnes, G. (2000). Effects of experimental glaucoma in macaques on the multifocal ERG. Multifocal ERG in laser-induced glaucoma. *Doc Ophthalmol*, 100 (2-3), 231-51.

Fujimoto, N. and Adachi-Usami, E. (2000). Frequency doubling perimetry in resolved optic neuritis. *Invest Ophthalmol Vis Sci*, 41 (9), 2558-60.

Garca, M., Ruiz-Ederra, J., Hernandez-Barbachano, H. and Vecino, E. (2005). Topography of pig retinal ganglion cells. *J Comp Neurol*, 486 (4), 361-72.

Garway-Heath, D. F., Holder, G. E., Fitzke, F. W. and Hitchings, R. A. (2002). Relationship between electrophysiological, psychophysical, and anatomical measurements in glaucoma. *Invest Ophthalmol Vis Sci*, 43 (7), 2213-20.

Gerth, C., Garcia, S. M., Ma, L., Keltner, J. L. and Werner, J. S. (2002). Multifocal electroretinogram: age-related changes for different luminance levels. *Graefes Arch Clin Exp Ophthalmol*, 240 (3), 202-8.

Ghosh, F. and Arner, K. (2002). Transplantation of full-thickness retina in the normal porcine eye: surgical and morphologic aspects. *Retina*, 22 (4), 478-86.

Girkin, C. A., Emdadi, A., Sample, P. A., Blumenthal, E. Z., Lee, A. C., Zangwill, L. M. and Weinreb, R. N. (2000). Short-wavelength automated perimetry and standard perimetry in the detection of progressive optic disc cupping. *Arch Ophthalmol*, 118 (9), 1231-6.

Glovinsky, Y., Quigley, H. A. and Dunkelberger, G. R. (1991). Retinal ganglion cell loss is size dependent in experimental glaucoma. *Invest Ophthalmol Vis Sci*, 32 (3), 484-91.

Glovinsky, Y., Quigley, H. A. and Pease, M. E. (1993). Foveal ganglion cell loss is size dependent in experimental glaucoma. *Invest Ophthalmol Vis Sci*, 34 (2), 395-400.

Graham, S. L., Drance, S. M., Chauhan, B. C., Swindale, N. V., Hnik, P., Mikelberg, F. S. and Douglas, G. R. (1996). Comparison of psychophysical and electrophysiological testing in early glaucoma. *Invest Ophthalmol Vis Sci*, 37 (13), 2651-62.

Graham, S. L., Klistorner, A. I., Grigg, J. R. and Billson, F. A. (2000). Objective VEP perimetry in glaucoma: asymmetry analysis to identify early deficits. *J Glaucoma*, 9 (1), 10-9.

Grant, W. M. and Burke, J. F., Jr. (1982). Why do some people go blind from glaucoma? *Ophthalmology*, 89 (9), 991-8.

Greenfield, D. S., Knighton, R. W. and Huang, X. R. (2000). Effect of corneal polarization axis on assessment of retinal nerve fiber layer thickness by scanning laser polarimetry. *Am J Ophthalmol*, 129 (6), 715-22.

Greenfield, D. S., Knighton, R. W., Feuer, W. J., Schiffman, J. C., Zangwill, L. and Weinreb, R. N. (2002). Correction for corneal polarization axis improves the discriminating power of scanning laser polarimetry. *Am J Ophthalmol*, 134 (1), 27-33.

Gur, M., Zeevi, Y. Y., Bielik, M. and Neumann, E. (1987). Changes in the oscillatory potentials of the electroretinogram in glaucoma. *Curr Eye Res*, 6 (3), 457-66.

Haefliger, I. O., Flammer, J. and Luscher, T. F. (1992). Nitric oxide and endothelin-1 are important regulators of human ophthalmic artery. *Invest Ophthalmol Vis Sci*, 33 (7), 2340-3.

Haefliger, I. O., Flammer, J., Beny, J. L. and Luscher, T. F. (2001). Endothelium-dependent vasoactive modulation in the ophthalmic circulation. *Prog Retin Eye Res*, 20 (2), 209-25.

Hans, P. and Bonhomme, V. (2006). Why we still use intravenous drugs as the basic regimen for neurosurgical anaesthesia. *Curr Opin Anaesthesiol*, 19 (5), 498-503.

Harada, H., Kelly, P. J., Cole, D. J., Drummond, J. C. and Patel, P. M. (1999). Isoflurane reduces N-methyl-D-aspartate toxicity in vivo in the rat cerebral cortex. *Anesth Analg*, 89 (6), 1442-7.

Harbin, T. S., Jr., Podos, S. M., Kolker, A. E. and Becker, B. (1976). Visual field progression in open-angle glaucoma patients presenting with monocular field loss. *Trans Sect Ophthalmol Am Acad Ophthalmol Otolaryngol*, 81 (2), 253-7.

Hare, W., Ton, H., Woldemussie, E., Ruiz, G., Feldmann, B. and Wijono, M. (1999). Electrophysiological and histological measures of retinal injury in chronic ocular hypertensive monkeys. *Eur J Ophthalmol*, 9 Suppl 1 S30-3.

Hare, W. A., Ton, H., Ruiz, G., Feldmann, B., Wijono, M. and WoldeMussie, E. (2001). Characterization of retinal injury using ERG measures obtained with both conventional and multifocal methods in chronic ocular hypertensive primates. *Invest Ophthalmol Vis Sci*, 42 (1), 127-36.

Hare, W. A. and Ton, H. (2002). Effects of APB, PDA, and TTX on ERG responses recorded using both multifocal and conventional methods in monkey. Effects of APB, PDA, and TTX on monkey ERG responses. *Doc Ophthalmol*, 105 (2), 189-222.

Harwerth, R. S., Carter-Dawson, L., Shen, F., Smith, E. L., 3rd and Crawford, M. L. (1999). Ganglion cell losses underlying visual field defects from experimental glaucoma. *Invest Ophthalmol Vis Sci*, 40 (10), 2242-50.

Harwerth, R. S., Crawford, M. L., Frishman, L. J., Viswanathan, S., Smith, E. L., 3rd and Carter-Dawson, L. (2002). Visual field defects and neural losses from experimental glaucoma. *Prog Retin Eye Res*, 21 (1), 91-125.

Hasegawa, S., Takagi, M., Usui, T., Takada, R. and Abe, H. (2000). Waveform changes of the first-order multifocal electroretinogram in patients with glaucoma. *Invest Ophthalmol Vis Sci*, 41 (6), 1597-603.

Heijl, A., Leske, M. C., Bengtsson, B., Hyman, L. and Hussein, M. (2002). Reduction of intraocular pressure and glaucoma progression: results from the Early Manifest Glaucoma Trial. *Arch Ophthalmol*, 120 (10), 1268-79.

Heinemann-Vernaleken, B., Palmowski, A. M., Allgayer, R. and Ruprecht, K. W. (2001). Comparison of different high resolution multifocal electroretinogram recordings in patients with age-related maculopathy. *Graefes Arch Clin Exp Ophthalmol*, 239 (8), 556-61.

Hendrickson, A. and Hicks, D. (2002). Distribution and density of medium- and short-wavelength selective cones in the domestic pig retina. *Exp Eye Res*, 74 (4), 435-44.

Hernandez, M. R. (2000). The optic nerve head in glaucoma: role of astrocytes in tissue remodeling. *Prog Retin Eye Res*, 19 (3), 297-321.

Hess, D. B., Asrani, S. G., Bhide, M. G., Enyedi, L. B., Stinnett, S. S. and Freedman, S. F. (2005). Macular and retinal nerve fiber layer analysis of normal and glaucomatous eyes in children using optical coherence tomography. *Am J Ophthalmol*, 139 (3), 509-17.

Hiller, R. and Kahn, H. A. (1975). Blindness from glaucoma. *Am J Ophthalmol*, 80 (1), 62-9.

Hitchings, R. A. (1997). Glaucoma. *Eye*, 11 (Pt 6) 900-3.

Holder, G. E. (1987). Significance of abnormal pattern electroretinography in anterior visual pathway dysfunction. *Br J Ophthalmol*, 71 (3), 166-71.

Holopigian, K., Greenstein, V. C., Seiple, W., Hood, D. C. and Ritch, R. (2000). Electrophysiologic assessment of photoreceptor function in patients with primary open-angle glaucoma. *J Glaucoma*, 9 (2), 163-8.

Honkanen, R. A., Baruah, S., Zimmerman, M. B., Khanna, C. L., Weaver, Y. K., Narkiewicz, J., Waziri, R., Gehrs, K. M., Weingeist, T. A., Boldt, H. C., Folk, J. C., Russell, S. R. and Kwon, Y. H. (2003). Vitreous amino acid concentrations in patients with glaucoma undergoing vitrectomy. *Arch Ophthalmol*, 121 (2), 183-8.

Hood, D. C., Seiple, W., Holopigian, K. and Greenstein, V. (1997). A comparison of the components of the multifocal and full-field ERGs. *Vis Neurosci*, 14 (3), 533-44.

Hood, D. C., Holopigian, K., Greenstein, V., Seiple, W., Li, J., Sutter, E. E. and Carr, R. E. (1998). Assessment of local retinal function in patients with retinitis pigmentosa using the multi-focal ERG technique. *Vision Res*, 38 (1), 163-79.

Hood, D. C., Frishman, L. J., Viswanathan, S., Robson, J. G. and Ahmed, J. (1999a). Evidence for a ganglion cell contribution to the primate electroretinogram (ERG): effects of TTX on the multifocal ERG in macaque. *Vis Neurosci*, *16* (3), 411-6.

Hood, D. C., Greenstein, V., Frishman, L., Holopigian, K., Viswanathan, S., Seiple, W., Ahmed, J. and Robson, J. G. (1999b). Identifying inner retinal contributions to the human multifocal ERG. *Vision Res*, *39* (13), 2285-91.

Hood, D. C. (2000). Assessing retinal function with the multifocal technique. *Prog Retin Eye Res*, *19* (5), 607-46.

Hood, D. C., Greenstein, V. C., Holopigian, K., Bauer, R., Firoz, B., Liebmann, J. M., Odel, J. G. and Ritch, R. (2000a). An attempt to detect glaucomatous damage to the inner retina with the multifocal ERG. *Invest Ophthalmol Vis Sci*, *41* (6), 1570-9.

Hood, D. C., Zhang, X., Greenstein, V. C., Kangovi, S., Odel, J. G., Liebmann, J. M. and Ritch, R. (2000b). An interocular comparison of the multifocal VEP: a possible technique for detecting local damage to the optic nerve. *Invest Ophthalmol Vis Sci*, *41* (6), 1580-7.

Hood, D. C., Bearse, M. A., Jr., Sutter, E. E., Viswanathan, S. and Frishman, L. J. (2001). The optic nerve head component of the monkey's (*Macaca mulatta*) multifocal electroretinogram (mERG). *Vision Res*, *41* (16), 2029-41.

Hood, D. C., Frishman, L. J., Saszik, S. and Viswanathan, S. (2002). Retinal origins of the primate multifocal ERG: implications for the human response. *Invest Ophthalmol Vis Sci*, *43* (5), 1673-85.

Hood, D. C., Odel, J. G., Chen, C. S. and Winn, B. J. (2003a). The multifocal electroretinogram. *J Neuroophthalmol*, *23* (3), 225-35.

Hood, D. C., Zhang, X. and Winn, B. J. (2003b). Detecting glaucomatous damage with multifocal visual evoked potentials: how can a monocular test work? *J Glaucoma*, *12* (1), 3-15.

Hood, D. C., Anderson, S. C., Wall, M. and Kardon, R. H. (2007). Structure versus function in glaucoma: an application of a linear model. *Invest Ophthalmol Vis Sci*, *48* (8), 3662-8.

Horn, F. K., Nguyen, N. X., Mardin, C. Y. and Junemann, A. G. (2003). Combined use of frequency doubling perimetry and polarimetric measurements of retinal nerve fiber layer in glaucoma detection. *Am J Ophthalmol*, 135 (2), 160-8.

Horn, F. K., Link, B., Mardin, C. Y., Junemann, A. G. and Martus, P. (2007). Long-term reproducibility of screening for glaucoma with FDT-perimetry. *J Glaucoma*, 16 (5), 448-55.

Huang, S., Wu, D., Jiang, F., Ma, J., Wu, L., Liang, J. and Luo, G. (2000). The multifocal electroretinogram in age-related maculopathies. *Doc Ophthalmol*, 101 (2), 115-24.

Ichinose, T., Shields, C. R. and Lukasiewicz, P. D. (2005). Sodium channels in transient retinal bipolar cells enhance visual responses in ganglion cells. *J Neurosci*, 25 (7), 1856-65.

Iester, M., Mikelberg, F. S., Courtright, P., Burk, R. O., Caprioli, J., Jonas, J. B., Weinreb, R. N. and Zangwill, L. (2001). Interobserver variability of optic disk variables measured by confocal scanning laser tomography. *Am J Ophthalmol*, 132 (1), 57-62.

Jackson, G. R., Ortega, J., Girkin, C., Rosenstiel, C. E. and Owsley, C. (2002). Aging-related changes in the multifocal electroretinogram. *J Opt Soc Am A Opt Image Sci Vis*, 19 (1), 185-9.

Jiang, F., Huang, S., Luo, G., Wu, D., Liang, J. and Liu, C. (2001). [The measurement of multifocal electroretinography]. *Yan Ke Xue Bao*, 17 (4), 217-9.

Johnson, C. A. (1996). Standardizing the measurement of visual fields for clinical research: Guidelines from the Eye Care Technology Forum. *Ophthalmology*, 103 (1), 186-9.

Johnson, M. A., Drum, B. A., Quigley, H. A., Sanchez, R. M. and Dunkelberger, G. R. (1989). Pattern-evoked potentials and optic nerve fiber loss in monocular laser-induced glaucoma. *Invest Ophthalmol Vis Sci*, 30 (5), 897-907.

Jones, A. L., Sheen, N. J., North, R. V. and Morgan, J. E. (2001). The Humphrey optical coherence tomography scanner: quantitative analysis and reproducibility study of the normal human retinal nerve fibre layer. *Br J Ophthalmol*, 85 (6), 673-7.

Jurklies, B., Weismann, M., Husing, J., Sutter, E. E. and Bornfeld, N. (2002). Monitoring retinal function in neovascular maculopathy using multifocal electroretinography - early and long-term correlation with clinical findings. *Graefes Arch Clin Exp Ophthalmol*, 240 (4), 244-64.

Kanamori, A., Nakamura, M., Escano, M. F., Seya, R., Maeda, H. and Negi, A. (2003). Evaluation of the glaucomatous damage on retinal nerve fiber layer thickness measured by optical coherence tomography. *Am J Ophthalmol*, 135 (4), 513-20.

Kass, M. A., Kolker, A. E. and Becker, B. (1976). Prognostic factors in glaucomatous visual field loss. *Arch Ophthalmol*, 94 (8), 1274-6.

Kass, M. A., Heuer, D. K., Higginbotham, E. J., Johnson, C. A., Keltner, J. L., Miller, J. P., Parrish, R. K., 2nd, Wilson, M. R. and Gordon, M. O. (2002). The Ocular Hypertension Treatment Study: a randomized trial determines that topical ocular hypotensive medication delays or prevents the onset of primary open-angle glaucoma. *Arch Ophthalmol*, 120 (6), 701-13; discussion 829-30.

Keating, D., Parks, S. and Evans, A. (2000). Technical aspects of multifocal ERG recording. *Doc Ophthalmol*, 100 (2-3), 77-98.

Kellerman, L. and Posner, A. (1955). The value of heredity in the detection and study of glaucoma. *Am J Ophthalmol*, 40 (5 Part 1), 681-5.

Kelly, D. H. (1981). Nonlinear visual responses to flickering sinusoidal gratings. *J Opt Soc Am*, 71 (9), 1051-5.

Keltner, J. L., Johnson, C. A., Anderson, D. R., Levine, R. A., Fan, J., Cello, K. E., Quigley, H. A., Budenz, D. L., Parrish, R. K., Kass, M. A. and Gordon, M. O. (2006). The association between glaucomatous visual fields and optic nerve head features in the Ocular Hypertension Treatment Study. *Ophthalmology*, 113 (9), 1603-12.

Kerrigan-Baumrind, L. A., Quigley, H. A., Pease, M. E., Kerrigan, D. F. and Mitchell, R. S. (2000). Number of ganglion cells in glaucoma eyes compared with threshold visual field tests in the same persons. *Invest Ophthalmol Vis Sci*, 41 (3), 741-8.

Khaw, P. T., Shah, P. and Elkington, A. R. (2004). Glaucoma--1: diagnosis. *Bmj*, 328 (7431), 97-9.

Kielczewski, J. L., Pease, M. E. and Quigley, H. A. (2005). The effect of experimental glaucoma and optic nerve transection on amacrine cells in the rat retina. *Invest Ophthalmol Vis Sci*, 46 (9), 3188-96.

Kim, D. M., Hwang, U. S., Park, K. H. and Kim, S. H. (2005). Retinal nerve fiber layer thickness in the fellow eyes of normal-tension glaucoma patients with unilateral visual field defect. *Am J Ophthalmol*, 140 (1), 165-6.

Kim, T. W., Zangwill, L. M., Bowd, C., Sample, P. A., Shah, N. and Weinreb, R. N. (2007). Retinal nerve fiber layer damage as assessed by optical coherence tomography in eyes with a visual field defect detected by frequency doubling technology perimetry but not by standard automated perimetry. *Ophthalmology*, 114 (6), 1053-7.

Klistorner, A., Crewther, D. P. and Crewther, S. G. (1997). Separate magnocellular and parvocellular contributions from temporal analysis of the multifocal VEP. *Vision Res*, 37 (15), 2161-9.

Klistorner, A., Graham, S. L., Martins, A., Grigg, J. R., Arvind, H., Kumar, R. S., James, A. C. and Billson, F. A. (2007). Multifocal blue-on-yellow visual evoked potentials in early glaucoma. *Ophthalmology*, 114 (9), 1613-21.

Klistorner, A. I., Graham, S. L., Grigg, J. R. and Billson, F. A. (1998). Multifocal topographic visual evoked potential: improving objective detection of local visual field defects. *Invest Ophthalmol Vis Sci*, 39 (6), 937-50.

Klistorner, A. I. and Graham, S. L. (1999a). Early magnocellular loss in glaucoma demonstrated using the pseudorandomly stimulated flash visual evoked potential. *J Glaucoma*, 8 (2), 140-8.

Klistorner, A. I. and Graham, S. L. (1999b). Multifocal pattern VEP perimetry: analysis of sectoral waveforms. *Doc Ophthalmol*, 98 (2), 183-96.

Klistorner, A. I., Graham, S. L. and Martins, A. (2000). Multifocal pattern electroretinogram does not demonstrate localised field defects in glaucoma. *Doc Ophthalmol*, 100 (2-3), 155-65.

Ko, M. L., Hu, D. N., Ritch, R., Sharma, S. C. and Chen, C. F. (2001). Patterns of retinal ganglion cell survival after brain-derived neurotrophic factor administration in hypertensive eyes of rats. *Neurosci Lett*, 305 (2), 139-42.

Korth, M., Nguyen, N. X., Horn, F. and Martus, P. (1994). Scotopic threshold response and scotopic PII in glaucoma. *Invest Ophthalmol Vis Sci*, 35 (2), 619-25.

Kretschmann, U., Bock, M., Gockeln, R. and Zrenner, E. (2000). Clinical applications of multifocal electroretinography. *Doc Ophthalmol*, 100 (2-3), 99-113.

Kwong, J. M. and Lam, T. T. (2000). N -methyl- D -aspartate (NMDA) induced apoptosis in adult rabbit retinas. *Exp Eye Res*, 71 (4), 437-44.

Kymes, S. M., Kass, M. A., Anderson, D. R., Miller, J. P. and Gordon, M. O. (2006). Management of ocular hypertension: a cost-effectiveness approach from the Ocular Hypertension Treatment Study. *Am J Ophthalmol*, 141 (6), 997-1008.

Lalezary, M., Medeiros, F. A., Weinreb, R. N., Bowd, C., Sample, P. A., Tavares, I. M., Tafreshi, A. and Zangwill, L. M. (2006). Baseline optical coherence tomography predicts the development of glaucomatous change in glaucoma suspects. *Am J Ophthalmol*, 142 (4), 576-82.

Lalonde, M. R., Chauhan, B. C. and Tremblay, F. (2006). Retinal ganglion cell activity from the multifocal electroretinogram in pig: optic nerve section, anesthesia and intravitreal tetrodotoxin. *J Physiol*, 570 (Pt 2), 325-38.

Larrosa, J. M., Polo, V., Pablo, L., Pinilla, I., Fernandez, F. J. and Honrubia, F. M. (2000). Short-wavelength automated perimetry and neuroretinal rim area. *Eur J Ophthalmol*, 10 (2), 116-20.

Lau, J. T., Lee, V., Fan, D., Lau, M. and Michon, J. (2002). Knowledge about cataract, glaucoma, and age related macular degeneration in the Hong Kong Chinese population. *Br J Ophthalmol*, 86 (10), 1080-4.

Lee, B. B., Pokorny, J., Smith, V. C., Martin, P. R. and Valberg, A. (1990). Luminance and chromatic modulation sensitivity of macaque ganglion cells and human observers. *J Opt Soc Am A*, 7 (12), 2223-36.

Lee, P. P., Walt, J. G., Doyle, J. J., Kotak, S. V., Evans, S. J., Budenz, D. L., Chen, P. P., Coleman, A. L., Feldman, R. M., Jampel, H. D., Katz, L. J., Mills, R. P., Myers, J. S., Noecker, R. J., Piltz-Seymour, J. R., Ritch, R. R., Schacknow, P. N., Serle, J. B. and Trick, G. L. (2006). A multicenter, retrospective pilot study of resource use and costs associated with severity of disease in glaucoma. *Arch Ophthalmol*, 124 (1), 12-9.

Lee, V. W. and Mok, K. H. (1999). Retinal nerve fiber layer measurement by nerve fiber analyzer in normal subjects and patients with glaucoma. *Ophthalmology*, 106 (5), 1006-8.

Leighton, D. A. and Phillips, C. I. (1972). Systemic blood pressure in open-angle glaucoma, low tension glaucoma, and the normal eye. *Br J Ophthalmol*, 56 (6), 447-53.

Leske, M. C. (1983). The epidemiology of open-angle glaucoma: a review. *Am J Epidemiol*, 118 (2), 166-91.

Leske, M. C., Connell, A. M., Wu, S. Y., Hyman, L. G. and Schachat, A. P. (1995). Risk factors for open-angle glaucoma. The Barbados Eye Study. *Arch Ophthalmol*, 113 (7), 918-24.

Leung, M., Huang, R. and Lam, A. (2009). Retinal Nerve Fiber Layer Thickness in Normal Hong Kong Chinese Children Measured with Optical Coherence Tomography. *J Glaucoma*, In Press.

Li, J., Tso, M. O. and Lam, T. T. (2001). Reduced amplitude and delayed latency in foveal response of multifocal electroretinogram in early age related macular degeneration. *Br J Ophthalmol*, 85 (3), 287-90.

Li, R. S., Tay, D. K., Chan, H. H. and So, K. F. (2006). Changes of retinal functions following the induction of ocular hypertension in rats using argon laser photocoagulation. *Clin Experiment Ophthalmol*, 34 (6), 575-83.

Li, Z. Y., Wong, F., Chang, J. H., Possin, D. E., Hao, Y., Petters, R. M. and Milam, A. H. (1998). Rhodopsin transgenic pigs as a model for human retinitis pigmentosa. *Invest Ophthalmol Vis Sci*, 39 (5), 808-19.

Livingston, P. M., McCarty, C. A. and Taylor, H. R. (1998). Knowledge, attitudes, and self care practices associated with age related eye disease in Australia. *Br J Ophthalmol*, 82 (7), 780-5.

Livingstone, M. and Hubel, D. (1987). Psychophysical evidence for separate channels for the perception of form,color, movement, and depth. *J Neurosci*, 7 3418-68.

Livingstone, M. and Hubel, D. (1988). Segregation of form, color, movement, and depth: anatomy, physiology, and perception. *Science*, 240 (4853), 740-9.

Maddess, T., Hemmi, J. M. and James, A. C. (1998). Evidence for spatial aliasing effects in the Y-like cells of the magnocellular visual pathway. *Vision Res*, 38 (12), 1843-59.

Marmor, M. F. (1998). Standardization notice: EOG standard reapproved. Electro-oculogram. *Doc Ophthalmol*, 95 (1), 91-2.

Marmor, M. F., Chappelow, A. V. and Luo, G. (2002). Recognition of small stimulus screen masks using the multifocal ERG. *Doc Ophthalmol*, 104 (3), 277-86.

Marmor, M. F., Hood, D. C., Keating, D., Kondo, M., Seeliger, M. W. and Miyake, Y. (2003). Guidelines for basic multifocal electroretinography (mfERG). *Doc Ophthalmol*, 106 (2), 105-15.

Martin, P. R., White, A. J., Goodchild, A. K., Wilder, H. D. and Sefton, A. E. (1997). Evidence that blue-on cells are part of the third geniculocortical pathway in primates. *Eur J Neurosci*, 9 (7), 1536-41.

Marx, M. S., Podos, S. M., Bodis-Wollner, I., Howard-Williams, J. R., Siegel, M. J., Teitelbaum, C. S., Maclin, E. L. and Severin, C. (1986). Flash and pattern electroretinograms in normal and laser-induced glaucomatous primate eyes. *Invest Ophthalmol Vis Sci*, 27 (3), 378-86.

Mastropasqua, L., Lobefalo, L., Mancini, A., Ciancaglini, M. and Palma, S. (1992). Prevalence of myopia in open angle glaucoma. *Eur J Ophthalmol*, 2 (1), 33-5.

Matsumoto, C., Shirato, S., Haneda, M., Yamashiro, H. and Saito, M. (2003). Study of retinal nerve fiber layer thickness within normal hemivisual field in primary open-angle glaucoma and normal-tension glaucoma. *Jpn J Ophthalmol*, 47 (1), 22-7.

Medeiros, F. A., Zangwill, L. M., Bowd, C., Vessani, R. M., Susanna, R., Jr. and Weinreb, R. N. (2005). Evaluation of retinal nerve fiber layer, optic nerve head, and macular thickness measurements for glaucoma detection using optical coherence tomography. *Am J Ophthalmol*, 139 (1), 44-55.

Menz, M. and Sutter, E. (2004). The effect of fixation instability on the multifocal VEP. *Doc Ophthalmol*, 109 (2), 147-56.

Michon, J. J., Lau, J., Chan, W. S. and Ellwein, L. B. (2002). Prevalence of visual impairment, blindness, and cataract surgery in the Hong Kong elderly. *Br J Ophthalmol*, 86 (2), 133-9.

Minckler, D. S., Bunt, A. H. and Johanson, G. W. (1977). Orthograde and retrograde axoplasmic transport during acute ocular hypertension in the monkey. *Invest Ophthalmol Vis Sci*, 16 (5), 426-41.

Mok, K. H., Lee, V. W. and So, K. F. (2002). Retinal nerve fiber layer measurement of the Hong Kong chinese population by optical coherence tomography. *J Glaucoma*, 11 (6), 481-3.

Morgan, J. E., Uchida, H. and Caprioli, J. (2000). Retinal ganglion cell death in experimental glaucoma. *Br J Ophthalmol*, 84 (3), 303-10.

Morgan, J. E. (2002). Retinal ganglion cell shrinkage in glaucoma. *J Glaucoma*, 11 (4), 365-70.

Munoz, B., West, S. K., Rubin, G. S., Schein, O. D., Quigley, H. A., Bressler, S. B. and Bandeen-Roche, K. (2000). Causes of blindness and visual impairment in a population of older Americans: The Salisbury Eye Evaluation Study. *Arch Ophthalmol*, 118 (6), 819-25.

Musch, D. C., Gillespie, B. W., Lichter, P. R., Niziol, L. M. and Janz, N. K. (2009). Visual field progression in the Collaborative Initial Glaucoma Treatment Study the impact of treatment and other baseline factors. *Ophthalmology*, 116 (2), 200-7.

Nabeshima, T., Tazawa, Y., Mita, M. and Sano, M. (2002). Effects of aging on the first and second-order kernels of multifocal electroretinogram. *Jpn J Ophthalmol*, 46 (3), 261-9.

Nemesure, B., Leske, M. C., He, Q. and Mendell, N. (1996). Analyses of reported family history of glaucoma: a preliminary investigation. The Barbados Eye Study Group. *Ophthalmic Epidemiol*, 3 (3), 135-41.

Neufeld, A. H., Das, S., Vora, S., Gachie, E., Kawai, S., Manning, P. T. and Connor, J. R. (2002). A prodrug of a selective inhibitor of inducible nitric oxide synthase is neuroprotective in the rat model of glaucoma. *J Glaucoma*, 11 (3), 221-5.

Ng, Y. F., Chan, H. H., Chu, P. H., Siu, A. W., To, C. H., Beale, B. A., Gilger, B. C. and Wong, F. (2008). Pharmacologically defined components of the normal porcine multifocal ERG. *Doc Ophthalmol*, 116 (3), 165-76.

Odom, J. V., Bach, M., Barber, C., Brigell, M., Marmor, M. F., Tormene, A. P., Holder, G. E. and Vaegan (2004). Visual evoked potentials standard (2004). *Doc Ophthalmol*, 108 (2), 115-23.

O'Donoghue, E., Arden, G. B., O'Sullivan, F., Falcao-Reis, F., Moriarty, B., Hitchings, R. A., Spilleers, W., Hogg, C. and Weinstein, G. (1992). The pattern electroretinogram in glaucoma and ocular hypertension. *Br J Ophthalmol*, 76 (7), 387-94.

Olivius, E. and Thorburn, W. (1978). Prognosis of glaucoma simplex and glaucoma capsulare. A comparative study. *Acta Ophthalmol (Copenh)*, 56 (6), 921-34.

Paczka, J. A., Friedman, D. S., Quigley, H. A., Barron, Y. and Vitale, S. (2001). Diagnostic capabilities of frequency-doubling technology, scanning laser polarimetry, and nerve fiber layer photographs to distinguish glaucomatous damage. *Am J Ophthalmol*, 131 (2), 188-97.

Palmowski, A. M., Sutter, E. E., Bearnse, M. A., Jr. and Fung, W. (1997). Mapping of retinal function in diabetic retinopathy using the multifocal electroretinogram. *Invest Ophthalmol Vis Sci*, 38 (12), 2586-96.

Palmowski, A. M., Sutter, E. E., Bearnse, M. A., Jr. and Fung, W. (1999). Multifocal electroretinogram (MF-ERG) in diagnosis of macular changes. Example: senile macular degeneration. *Ophthalmologie*, 96 (3), 166-73.

Palmowski, A. M., Allgayer, R. and Heinemann-Vernaleken, B. (2000). The multifocal ERG in open angle glaucoma--a comparison of high and low contrast recordings in high- and low-tension open angle glaucoma. *Doc Ophthalmol*, 101 (1), 35-49.

Palmowski, A. M., Allgayer, R., Heinemann-Vernaleken, B. and Ruprecht, K. W. (2002). Multifocal electroretinogram with a multiflash stimulation technique in open-angle glaucoma. *Ophthalmic Res*, 34 (2), 83-9.

Palmowski, A. M. and Ruprecht, K. W. (2004). Follow up in open angle glaucoma. A comparison of static perimetry and the fast stimulation mfERG. Multifocal ERG follow up in open angle glaucoma. *Doc Ophthalmol*, 108 (1), 55-60.

Palmowski-Wolfe, A. M., Allgayer, R. J., Vernaleken, B., Schotzau, A. and Ruprecht, K. W. (2006). Slow-stimulated multifocal ERG in high- and normal-tension glaucoma. *Doc Ophthalmol*, 112 (3), 157-68.

Palmowski-Wolfe, A. M., Todorova, M. G., Orguel, S., Flammer, J. and Brigell, M. (2007). The 'two global flash' mfERG in high and normal tension primary open-angle glaucoma. *Doc Ophthalmol*, 114 (1), 9-19.

Peeters, A., Schouten, J. S., Webers, C. A., Prins, M. H., Hendrikse, F. and Severens, J. L. (2008). Cost-effectiveness of early detection and treatment of ocular hypertension and primary open-angle glaucoma by the ophthalmologist. *Eye*, 22 (3), 354-62.

Perry, V. H., Oehler, R. and Cowey, A. (1984). Retinal ganglion cells that project to the dorsal lateral geniculate nucleus in the macaque monkey. *Neuroscience*, 12 (4), 1101-23.

Perry, V. H. and Cowey, A. (1985). The ganglion cell and cone distributions in the monkey's retina: implications for central magnification factors. *Vision Res*, 25 (12), 1795-810.

Pfeiffer, N. and Krieglstein, G. K. (1993). Knowledge about glaucoma in the population. *Invest Ophthalmol Vis Sci*, 34 (suppl) 1192.

Poinoosawmy, D., Fontana, L., Wu, J. X., Bunce, C. V. and Hitchings, R. A. (1998). Frequency of asymmetric visual field defects in normal-tension and high-tension glaucoma. *Ophthalmology*, 105 (6), 988-91.

Poloschek, C. M., Rupp, V., Krastel, H. and Holz, F. G. (2003). Multifocal ERG recording with simultaneous fundus monitoring using a confocal scanning laser ophthalmoscope. *Eye*, 17 (2), 159-66.

Porciatti, V., Di Bartolo, E., Nardi, N. and Fiorentini, A. (1997). Responses to chromatic and luminance contrast in glaucoma: a psychophysical and electrophysiological study. *Vision Res*, 37 (14), 1975-87.

Qi, S. and Jiang, Y. (2002). [Short-wavelength perimetry in diagnosis of early glaucoma: comparison with standard automated perimetry]. *Zhonghua Yan Ke Za Zhi*, 38 (1), 31-5.

Quigley, H. and Anderson, D. R. (1976). The dynamics and location of axonal transport blockade by acute intraocular pressure elevation in primate optic nerve. *Invest Ophthalmol*, 15 (8), 606-16.

Quigley, H. A. (1985). Early detection of glaucomatous damage. II. Changes in the appearance of the optic disk. *Surv Ophthalmol*, 30 (2), 111, 117-26.

Quigley, H. A., Sanchez, R. M., Dunkelberger, G. R., L'Hernault, N. L. and Baginski, T. A. (1987). Chronic glaucoma selectively damages large optic nerve fibers. *Invest Ophthalmol Vis Sci*, 28 (6), 913-20.

Quigley, H. A., Dunkelberger, G. R. and Green, W. R. (1989). Retinal ganglion cell atrophy correlated with automated perimetry in human eyes with glaucoma. *Am J Ophthalmol*, 107 (5), 453-64.

Quigley, H. A. (1993). Open-angle glaucoma. *N Engl J Med*, 328 (15), 1097-106.

Quigley, H. A. (1996). Number of people with glaucoma worldwide. *Br J Ophthalmol*, 80 (5), 389-93.

Quigley, H. A., Tielsch, J. M., Katz, J. and Sommer, A. (1996). Rate of progression in open-angle glaucoma estimated from cross-sectional prevalence of visual field damage. *Am J Ophthalmol*, 122 (3), 355-63.

Quigley, H. A. and Broman, A. T. (2006). The number of people with glaucoma worldwide in 2010 and 2020. *Br J Ophthalmol*, 90 (3), 262-7.

Rangaswamy, N. V., Hood, D. C. and Frishman, L. J. (2003). Regional variations in local contributions to the primate photopic flash ERG: revealed using the slow-sequence mfERG. *Invest Ophthalmol Vis Sci*, 44 (7), 3233-47.

Rangaswamy, N. V., Zhou, W., Harwerth, R. S. and Frishman, L. J. (2006). Effect of experimental glaucoma in primates on oscillatory potentials of the slow-sequence mfERG. *Invest Ophthalmol Vis Sci*, 47 (2), 753-67.

Raz, D., Seeliger, M. W., Geva, A. B., Percicot, C. L., Lambrou, G. N. and Ofri, R. (2002). The effect of contrast and luminance on mfERG responses in a monkey model of glaucoma. *Invest Ophthalmol Vis Sci*, 43 (6), 2027-35.

Raz, D., Perlman, I., Percicot, C. L., Lambrou, G. N. and Ofri, R. (2003). Functional damage to inner and outer retinal cells in experimental glaucoma. *Invest Ophthalmol Vis Sci*, 44 (8), 3675-84.

Resnikoff, S., Pascolini, D., Etya'ale, D., Kocur, I., Pararajasegaram, R., Pokharel, G. P. and Mariotti, S. P. (2004). Global data on visual impairment in the year 2002. *Bull World Health Organ*, 82 (11), 844-51.

- Rohrschneider, K., Burk, R. O., Kruse, F. E. and Volcker, H. E. (1994). Reproducibility of the optic nerve head topography with a new laser tomographic scanning device. *Ophthalmology*, 101 (6), 1044-9.
- Rudolph, G., Kalpadakis, P., Bechmann, M., Haritoglou, C. and Kampik, A. (2003). Scanning laser ophthalmoscope-evoked multifocal ERG (SLO-mfERG) in patients with macular holes and normal individuals. *Eye*, 17 (7), 801-8.
- Ruiz-Ederra, J., Garcia, M., Hernandez, M., Urcola, H., Hernandez-Barbachano, E., Araiz, J. and Vecino, E. (2005). The pig eye as a novel model of glaucoma. *Exp Eye Res*, 81 (5), 561-9.
- Sakemi, F., Yoshii, M. and Okisaka, S. (2002). Multifocal electroretinograms in early primary open-angle glaucoma. *Jpn J Ophthalmol*, 46 (4), 443-50.
- Sample, P. A. (2000). Short-wavelength automated perimetry: its role in the clinic and for understanding ganglion cell function. *Prog Retin Eye Res*, 19 (4), 369-83.
- Sample, P. A., Bosworth, C. F., Blumenthal, E. Z., Girkin, C. and Weinreb, R. N. (2000). Visual function-specific perimetry for indirect comparison of different ganglion cell populations in glaucoma. *Invest Ophthalmol Vis Sci*, 41 (7), 1783-90.
- Sano, M., Tazawa, Y., Nabeshima, T. and Mita, M. (2002). A new wavelet in the multifocal electroretinogram, probably originating from ganglion cells. *Invest Ophthalmol Vis Sci*, 43 (5), 1666-72.
- Sasoh, M., Yoshida, S., Kuze, M. and Uji, Y. (1998). The multifocal electroretinogram in retinal detachment. *Doc Ophthalmol*, 94 (3), 239-52.
- Schuchard, R. A., Naseer, S. and de Castro, K. (1999). Characteristics of AMD patients with low vision receiving visual rehabilitation. *J Rehabil Res Dev*, 36 (4), 294-302.
- Seeliger, M. W., Kretschmann, U. H., Apfelstedt-Sylla, E. and Zrenner, E. (1998). Implicit time topography of multifocal electroretinograms. *Invest Ophthalmol Vis Sci*, 39 (5), 718-23.

Seiple, W., Vajaranant, T. S., Szlyk, J. P., Clemens, C., Holopigian, K., Paliga, J., Badawi, D. and Carr, R. E. (2003). Multifocal electroretinography as a function of age: the importance of normative values for older adults. *Invest Ophthalmol Vis Sci*, 44 (4), 1783-92.

Shabana, N., Peres, V. C., Carkeet, A. and Chew, P. T. (2003). Motion perception in glaucoma patients: a review. *Surv Ophthalmol*, 48 (1), 92-106.

Shah, N. N., Bowd, C., Medeiros, F. A., Weinreb, R. N., Sample, P. A., Hoffmann, E. M. and Zangwill, L. M. (2006). Combining structural and functional testing for detection of glaucoma. *Ophthalmology*, 113 (9), 1593-602.

Shimada, Y., Li, Y., Bearse, M. A., Jr., Sutter, E. E. and Fung, W. (2001). Assessment of early retinal changes in diabetes using a new multifocal ERG protocol. *Br J Ophthalmol*, 85 (4), 414-9.

Shimada, Y., Bearse, M. A., Jr. and Sutter, E. E. (2005). Multifocal electroretinograms combined with periodic flashes: direct responses and induced components. *Graefes Arch Clin Exp Ophthalmol*, 243 (2), 132-41.

Shimmyo, M., Ross, A. J., Moy, A. and Mostafavi, R. (2003). Intraocular pressure, Goldmann applanation tension, corneal thickness, and corneal curvature in Caucasians, Asians, Hispanics, and African Americans. *Am J Ophthalmol*, 136 (4), 603-13.

Sihota, R., Sony, P., Gupta, V., Dada, T. and Singh, R. (2006). Diagnostic capability of optical coherence tomography in evaluating the degree of glaucomatous retinal nerve fiber damage. *Invest Ophthalmol Vis Sci*, 47 (5), 2006-10.

Silverman, S. E., Trick, G. L. and Hart, W. M., Jr. (1990). Motion perception is abnormal in primary open-angle glaucoma and ocular hypertension. *Invest Ophthalmol Vis Sci*, 31 (4), 722-9.

Siu, A. W., Leung, M. C., To, C. H., Siu, F. K., Ji, J. Z. and So, K. F. (2002). Total retinal nitric oxide production is increased in intraocular pressure-elevated rats. *Exp Eye Res*, 75 (4), 401-6.

Slaughter, M. M. and Miller, R. F. (1983). An excitatory amino acid antagonist blocks cone input to sign-conserving second-order retinal neurons. *Science*, 219 (4589), 1230-2.

Smith, D. C., Keating, D., Parks, S. and Evans, A. L. (2002). An instrument to investigate temporal processing mechanisms with the multifocal ERG. *J Med Eng Technol*, 26 (4), 147-51.

Spry, P. G., Johnson, C. A., McKendrick, A. M. and Turpin, A. (2003). Measurement error of visual field tests in glaucoma. *Br J Ophthalmol*, 87 (1), 107-12.

Stefansson, E., Pedersen, D. B., Jensen, P. K., la Cour, M., Kiilgaard, J. F., Bang, K. and Eysteinnsson, T. (2005). Optic nerve oxygenation. *Prog Retin Eye Res*, 24 (3), 307-32.

Stewart, W. C., Stewart, J. A., Nasser, Q. J. and Mychaskiw, M. A. (2008). Cost-effectiveness of treating ocular hypertension. *Ophthalmology*, 115 (1), 94-8.

Susanna, R., Drance, S. M. and Douglas, G. R. (1978). The visual prognosis of the fellow eye in uniocular chronic open-angle glaucoma. *Br J Ophthalmol*, 62 (5), 327-9.

Sutter, E. (2000). The interpretation of multifocal binary kernels. *Doc Ophthalmol*, 100 (2-3), 49-75.

Sutter, E. E. and Tran, D. (1992). The field topography of ERG components in man--I. The photopic luminance response. *Vision Res*, 32 (3), 433-46.

Sutter, E. E. and Bearnse, M. A. (1995). Extraction of a ganglion cell component from the corneal response. In: *Vision Science and Its Applications, 1995 OSA Technical Digest Series, Vol. 1, Washington, D.C.: Optical Society of America*, 310-3.

Sutter, E. E. and Bearnse, M. A., Jr. (1999). The optic nerve head component of the human ERG. *Vision Res*, 39 (3), 419-36.

Sutter, E. E., Shimada, Y., Li, Y. and Bearse, M. A. (1999). Mapping inner retinal function through enhancement of adaptation components in the M-ERG. In: *Vision Science and Its Applications, 1999 OSA Technical Digest Series, Vol. 1, Washington, D.C.: Optical Society of America*, 52-5.

Sutter, E. E. (2001). Imaging visual function with the multifocal m-sequence technique. *Vision Res*, 41 (10-11), 1241-55.

Sutter, E. E., Bearse, M. A., Stamper, R. L., Lambrou, G. N., Percicot, C. L., Ofri, R. and Raz, D. (2001a). Monitoring retinal ganglion cell function with the MERG. In: *Vision Science and Its Applications, 2001 OSA Technical Digest Series, Vol. 1, Washington, D.C.: Optical Society of America*, 10-3.

Sutter, E. E., Bearse, M. A., Stamper, R. L., Lambrou, G. N., Percicot, C. L., Ofri, R. and Raz, D. (2001b). Monitoring retinal ganglion cell function with the MERG: recent advances. In: *Vision Science and Its Applications, 2001 OSA Technical Digest Series, Vol. 1, Washington, D.C.: Optical Society of America*, 10-3.

Tam, W. K., Chan, H., Brown, B., Leung, K. W., Woo, V. and Yap, M. (2006). Aging and mfERG topography. *Eye*, 20 (1), 18-24.

The AGIS Investigators (2000). The Advanced Glaucoma Intervention Study (AGIS): 7. The relationship between control of intraocular pressure and visual field deterioration. The AGIS Investigators. *Am J Ophthalmol*, 130 (4), 429-40.

Tielsch, J. M., Sommer, A., Katz, J., Royall, R. M., Quigley, H. A. and Javitt, J. (1991). Racial variations in the prevalence of primary open-angle glaucoma. The Baltimore Eye Survey. *Jama*, 266 (3), 369-74.

Tielsch, J. M., Katz, J., Sommer, A., Quigley, H. A. and Javitt, J. C. (1994). Family history and risk of primary open angle glaucoma. The Baltimore Eye Survey. *Arch Ophthalmol*, 112 (1), 69-73.

Tielsch, J. M., Katz, J., Sommer, A., Quigley, H. A. and Javitt, J. C. (1995). Hypertension, perfusion pressure, and primary open-angle glaucoma. A population-based assessment. *Arch Ophthalmol*, 113 (2), 216-21.

Toffoli, G., Vattovani, O., Cecchini, P., Pastori, G., Rinaldi, G. and Ravalico, G. (2002). Correlation between the retinal nerve fiber layer thickness and the pattern electroretinogram amplitude. *Ophthalmologica*, 216 (3), 159-63.

Towle, V. L., Moskowitz, A., Sokol, S. and Schwartz, B. (1983). The visual evoked potential in glaucoma and ocular hypertension: effects of check size, field size, and stimulation rate. *Invest Ophthalmol Vis Sci*, 24 (2), 175-83.

Tremblay, F., Nason, J. and Maleki, B. (2005). Shaping of GERG, PERG and MFERG by APB- and PDA-sensitive cells in the pig retina. *Invest Ophthalmol Vis Sci*, 46 ARVO E-Abstract 2247.

Trick, G. L., Calotti, F. Y. and Skarf, B. (2006). Advances in imaging of the optic disc and retinal nerve fiber layer. *J Neuroophthalmol*, 26 (4), 284-95.

Uchida, H., Brigatti, L. and Caprioli, J. (1996). Detection of structural damage from glaucoma with confocal laser image analysis. *Invest Ophthalmol Vis Sci*, 37 (12), 2393-401.

Ueno, S., Kondo, M., Niwa, Y., Terasaki, H. and Miyake, Y. (2004). Luminance dependence of neural components that underlies the primate photopic electroretinogram. *Invest Ophthalmol Vis Sci*, 45 (3), 1033-40.

Vaegan, Graham, S. L., Goldberg, I. and Millar, T. J. (1991). Selective reduction of oscillatory potentials and pattern electroretinograms after retinal ganglion cell damage by disease in humans or by kainic acid toxicity in cats. *Doc Ophthalmol*, 77 (3), 237-53.

Vaegan and Sanderson, G. (1997). Absence of ganglion cell subcomponents in multifocal luminance electroretinograms. *Aust N Z J Ophthalmol*, 25 Suppl 1 S87-90.

Vajaranant, T. S., Szlyk, J. P., Fishman, G. A., Gieser, J. P. and Seiple, W. (2002). Localized retinal dysfunction in central serous chorioretinopathy as measured using the multifocal electroretinogram. *Ophthalmology*, 109 (7), 1243-50.

Viswanathan, S., Frishman, L. J., Robson, J. G., Harwerth, R. S. and Smith, E. L., 3rd (1999). The photopic negative response of the macaque electroretinogram: reduction by experimental glaucoma. *Invest Ophthalmol Vis Sci*, 40 (6), 1124-36.

Viswanathan, S., Frishman, L. J., Robson, J. G. and Walters, J. W. (2001). The photopic negative response of the flash electroretinogram in primary open angle glaucoma. *Invest Ophthalmol Vis Sci*, 42 (2), 514-22.

Viswanathan, S., Frishman, L. J. and Robson, J. G. (2002). Inner-retinal contributions to the photopic sinusoidal flicker electroretinogram of macaques. Macaque photopic sinusoidal flicker ERG. *Doc Ophthalmol*, 105 (2), 223-42.

Vorwerk, C. K., Lipton, S. A., Zurakowski, D., Hyman, B. T., Sabel, B. A. and Dreyer, E. B. (1996). Chronic low-dose glutamate is toxic to retinal ganglion cells. Toxicity blocked by memantine. *Invest Ophthalmol Vis Sci*, 37 (8), 1618-24.

Voss Kyhn, M., Kiilgaard, J. F., Lopez, A. G., Scherfig, E., Prause, J. U. and la Cour, M. (2007). The multifocal electroretinogram (mfERG) in the pig. *Acta Ophthalmol Scand*, 85 (4), 438-44.

Vrabec, T. R., Affel, E. L., Gaughan, J. P., Foroozan, R., Tennant, M. T., Klancnik, J. M., Jr., Jordan, C. S. and Savino, P. J. (2004). Voluntary suppression of the multifocal electroretinogram. *Ophthalmology*, 111 (1), 169-76.

Wall, M., Neahring, R. K. and Woodward, K. R. (2002). Sensitivity and specificity of frequency doubling perimetry in neuro-ophthalmic disorders: a comparison with conventional automated perimetry. *Invest Ophthalmol Vis Sci*, 43 (4), 1277-83.

Wamsley, S., Gabelt, B. T., Dahl, D. B., Case, G. L., Sherwood, R. W., May, C. A., Hernandez, M. R. and Kaufman, P. L. (2005). Vitreous glutamate concentration and axon loss in monkeys with experimental glaucoma. *Arch Ophthalmol*, 123 (1), 64-70.

Wang, X. Y., Huynh, S. C., Burlutsky, G., Ip, J., Stapleton, F. and Mitchell, P. (2007). Reproducibility of and effect of magnification on optical coherence tomography measurements in children. *Am J Ophthalmol*, 143 (3), 484-8.

Wanger, P. and Persson, H. E. (1983). Pattern-reversal electroretinograms in unilateral glaucoma. *Invest Ophthalmol Vis Sci*, 24 (6), 749-53.

Weinstein, G. W., Arden, G. B., Hitchings, R. A., Ryan, S., Calthorpe, C. M. and Odom, J. V. (1988). The pattern electroretinogram (PERG) in ocular hypertension and glaucoma. *Arch Ophthalmol*, 106 (7), 923-8.

Whitaker, R., Jr., Whitaker, V. B. and Dill, C. (1999). Glaucoma: what the ophthalmic nurse should know. *Insight*, 24 (3), 86-91.

WHO (1997). Blindness and visual disability. Part II of VII: major causes worldwide. Geneva, World Health Organization.

Wildberger, H. and Junghardt, A. (2002). Local visual field defects correlate with the multifocal electroretinogram (mfERG) in retinal vascular branch occlusion. *Klin Monatsbl Augenheilkd*, 219 (4), 254-8.

Wilson, M. R. (2002). Progression of visual field loss in untreated glaucoma patients and suspects in St Lucia, West Indies. *Trans Am Ophthalmol Soc*, 100 365-410.

Wilson, M. R., Kosoko, O., Cowan, C. L., Jr., Sample, P. A., Johnson, C. A., Haynatzki, G., Enger, C. and Crandall, D. (2002). Progression of visual field loss in untreated glaucoma patients and glaucoma suspects in St. Lucia, West Indies. *Am J Ophthalmol*, 134 (3), 399-405.

Wilson, R., Richardson, T. M., Hertzmark, E. and Grant, W. M. (1985). Race as a risk factor for progressive glaucomatous damage. *Ann Ophthalmol*, 17 (10), 653-9.

Wirtz, M. K., Samples, J. R., Rust, K., Lie, J., Nordling, L., Schilling, K., Acott, T. S. and Kramer, P. L. (1999). GLC1F, a new primary open-angle glaucoma locus, maps to 7q35-q36. *Arch Ophthalmol*, 117 (2), 237-41.

Wollstein, G., Garway-Heath, D. F., Poinoosawmy, D. and Hitchings, R. A. (2000). Glaucomatous optic disc changes in the contralateral eye of unilateral normal pressure glaucoma patients. *Ophthalmology*, 107 (12), 2267-71.

Wollstein, G., Schuman, J. S., Price, L. L., Aydin, A., Beaton, S. A., Stark, P. C., Fujimoto, J. G. and Ishikawa, H. (2004). Optical coherence tomography (OCT) macular and peripapillary retinal nerve fiber layer measurements and automated visual fields. *Am J Ophthalmol*, 138 (2), 218-25.

Yoshii, M., Yanashima, K., Matsuno, K., Wakaguri, T., Kikuchi, Y. and Okisaka, S. (1998). Relationship between visual field defect and multifocal electroretinogram. *Jpn J Ophthalmol*, 42 (2), 136-41.

Yoshii, M., Yanashima, K., Wada, H., Sakemi, F., Enoki, T. and Okisaka, S. (2001). Analysis of second-order kernel response components of multifocal electroretinograms elicited from normal subjects. *Jpn J Ophthalmol*, 45 (3), 247-51.

Yucel, Y. H., Zhang, Q., Gupta, N., Kaufman, P. L. and Weinreb, R. N. (2000). Loss of neurons in magnocellular and parvocellular layers of the lateral geniculate nucleus in glaucoma. *Arch Ophthalmol*, 118 (3), 378-84.

Yucel, Y. H., Zhang, Q., Weinreb, R. N., Kaufman, P. L. and Gupta, N. (2001). Atrophy of relay neurons in magno- and parvocellular layers in the lateral geniculate nucleus in experimental glaucoma. *Invest Ophthalmol Vis Sci*, 42 (13), 3216-22.

Zhou, W., Rangaswamy, N., Ktonas, P. and Frishman, L. J. (2007). Oscillatory potentials of the slow-sequence multifocal ERG in primates extracted using the Matching Pursuit method. *Vision Res*, 47 (15), 2021-36.